

Decision-making under uncertainty in short-term electricity markets

Zur Erlangung des akademischen Grades eines

Doktors der Wirtschaftswissenschaften
(Dr. rer. pol.)

von der KIT-Fakultät für Wirtschaftswissenschaften
des Karlsruher Instituts für Technologie (KIT)

genehmigte

DISSERTATION

von

Emil Kraft, M.Sc.

Tag der mündlichen Prüfung: 31. März 2022
Referent: Prof. Dr. Wolf Fichtner
Korreferent: Prof. Dr. Steffen Rebennack

Acknowledgments

This dissertation was prepared during my time at the Chair of Energy Economics at Karlsruhe Institute of Technology (KIT). In this time, I had the privilege to contribute to research projects funded by the German Federal Ministry for Economic Affairs and Energy (now: Federal Ministry for Economic Affairs and Climate Action) and the German Federal Ministry of Education and Research. I had the opportunity to receive a Research Travel Grant by the Karlsruhe House for Young Scientists (KHYS), and was able to prepare parts of this thesis while being hosted by the Norwegian University of Science and Technology (NTNU) in Trondheim, Norway. I am very thankful to these institutions for providing me the environment to pursue my research interests. Further, I experienced the support and trust of many people, for which I want to express my gratitude.

First and most importantly, I want to thank my supervisor Wolf Fichtner for his guidance, his trust and support, and his empathic nature. I could not have imagined a better supervisor for my dissertation. I also want to thank Steffen Rebennack, who took over the role as co-reviewer, as well as Karl-Martin Ehrhart and Hagen Lindstädt for serving as members of the committee.

Moreover, I want to thank the senior researchers and professors I had the chance to collaborate with or who kindly agreed to discuss my work with them. Here, I would like to give special thanks to Armin Ardone, Christoph Fraunholz, Christoph Weber, Dogan Keles, Fabian Ocker, Marianna Russo, Stein-Erik Fleten, and Valentin Bertsch.

I also want to direct my deepest gratitude towards all my colleagues and friends at KIT for all the discussions, the support, the coffee breaks, and the remarkable conference and doctoral seminar experiences. In particular, I want to mention Andreas Bublitz, Andreas Rudi, Anthony Britto, Christian Füllner, Christoph Fraunholz, Daniel Fett, Dogan Keles, Elias Naber, Farnaz Mahdavian, Felix Hübner, Florian Zimmermann, Hans Schermeyer, Jann M. Weinand, Joris Dehler-Holland, Kim K. Miskiw, Max Kleinebrahm, Manuel Ruppert, Nico Lehmann, Rafael Finck, Richard C. Müller, and Viktor Slednev. I am sorry if anybody misses her or his name in the list and am sure she or he deserved to be mentioned.

Most of the time, academic discussions are terminated abruptly, due to next appointments or conference slots that are ridiculously short. In my experience

however, discussions become more interesting just after the coffee cup is empty. And, as empirical evidence shows, sometimes the discussions reach their peak and are the most insightful not before the discussants have decided to move on to different drinks. I am very grateful to have colleagues who are intrinsically curious and not willing to accept superficial answers to complex questions. Even if the shortcut sometimes appears tempting, for important and complex questions it sometimes requires some more effort to approach them. It will be worth it, although sometimes the journey needs to be glorified in hindsight. It is important to bear in mind what was the initial motivation behind joining in this journey. Maybe it's not even reaching the end goal, but the act of getting there and the lessons along the way that matter most. Sometimes asking the right questions is more important than finding the right answers.

I also want to direct my thanks to my helping hands in several projects throughout the years: Benedikt Krieger, Hannah Heimpel, Hans Wilhelm, Kim K. Miskiw, and Philipp Heidinger.

At last, I want to appreciate the role of my beloved family and friends outside the university context. The time I spend with you and your support are the key to any success I ever have achieved and I ever will achieve. So many thanks to my mother Ingrid, to my father Dieter, to my grandparents, and to my brother Hagen.

Karlsruhe, April 2022

Emil Kraft

Abstract

In the course of the energy transition, the share of electricity generation from renewable energy sources in Germany has increased significantly in recent years and will continue to rise. Particularly fluctuating renewables like wind and solar bring more uncertainty and volatility to the electricity system. As markets determine the unit commitment in systems with self-dispatch, many changes have been made to the design of electricity markets to meet the new challenges. Thereby, a trend towards real-time can be observed. Short-term electricity markets are becoming more important and are seen as suitable for efficient resource allocation. Therefore, it is inevitable for market participants to develop strategies for trading electricity and flexibility in these segments.

The research conducted in this thesis aims to enable better decisions in short-term electricity markets. To achieve this, a multitude of quantitative methods is developed and applied: (a) forecasting methods based on econometrics and machine learning, (b) methods for stochastic modeling of time series, (c) scenario generation and reduction methods, as well as (d) stochastic programming methods. Most significantly, two- and three-stage stochastic optimization problems are formulated to derive optimal trading decisions and unit commitment in the context of short-term electricity markets. The problem formulations adequately account for the sequential structure, the characteristics and the technical requirements of the different market segments, as well as the available information regarding uncertain generation volumes and prices. The thesis contains three case studies focusing on the German electricity markets.

Results confirm that, based on appropriate representations of the uncertainty of market prices and renewable generation, the optimization approaches allow to derive sound trading strategies across multiple revenue streams, with which market participants can effectively balance the inevitable trade-off between expected profit and associated risk. By considering coherent risk metrics and flexibly adaptable risk attitudes, the trading strategies allow to substantially reduce risk with only moderate expected profit losses. These results are significant, as improving trading decisions that determine the allocation of resources in the electricity system plays a key role in coping with the uncertainty from renewables and hence contributes to the ultimate success of the energy transition.

Contents

I	Framework	1
1	Introduction	3
1.1	Motivation	3
1.2	Objective and overall research question	5
1.3	Structure of the thesis	6
2	Background	9
2.1	Institutional framework of the German electricity market	9
2.1.1	The German electricity system	9
2.1.2	Design and development of the electricity wholesale markets	12
2.1.3	Design and development of the balancing reserve markets . .	19
2.1.4	Supply flexibility and technical provision of balancing services	26
2.1.5	Further system services	30
2.2	Uncertainty and risk in electricity markets	33
2.2.1	Definitions of uncertainty and risk	33
2.2.2	Taxonomy of risks and key uncertainties in the energy sector	39
2.2.3	Categorization and allocation of the thesis in the taxonomy of risks	41
3	Methodology	45
3.1	Modeling of time series and forecasting	45
3.1.1	Categorization of time series modeling approaches	45
3.1.2	Finance and econometric time series models	47
3.1.3	Machine learning models	52
3.1.4	Limitations and extensions of forecasting	56
3.2	Scenario tree generation and reduction	57

3.3	Stochastic optimization approaches	60
3.3.1	Optimization under uncertainty in the energy context	60
3.3.2	Replacement of stochastic optimization models with deterministic models	62
3.3.3	Exact stochastic optimization techniques	63
3.3.4	Sampling-based stochastic optimization methods	64
4	Case studies	67
4.1	Paper A: Modeling of frequency containment reserve prices with econometrics and artificial intelligence	67
4.1.1	Background information	67
4.1.2	Motivation and research question	68
4.1.3	Methodology	68
4.1.4	Results and conclusions	70
4.2	Paper B: Short-term risk management of electricity retailers under rising shares of decentralized solar generation	71
4.2.1	Background information	71
4.2.2	Motivation and research question	72
4.2.3	Methodology	73
4.2.4	Results and conclusions	76
4.3	Paper C: Stochastic optimization of trading strategies in sequential electricity markets	77
4.3.1	Background information	77
4.3.2	Motivation and research question	77
4.3.3	Methodology	78
4.3.4	Results and conclusions	81
5	Critical reflection and outlook	85
6	Summary and conclusion	91
	References	95

II	Research papers	115
A	Modeling of frequency containment reserve prices with econometrics and artificial intelligence	117
B	Short-term risk management of electricity retailers under rising shares of decentralized solar generation	137
C	Stochastic optimization of trading strategies in sequential electricity markets	239

Part I

Framework

Chapter 1

Introduction

1.1 Motivation

Historically, the German energy sector is characterized by a strong dependency on primary energy carrier imports and a large demand of industry. The German electricity sector was traditionally dominated by the primary energy carriers hard coal, lignite, natural gas, and uranium. The locations of power plants and the structure of the transmission grid followed the needs of the demand and were expanded accordingly by regional monopoly companies, which also operated the electricity system and set the prices. The heritage of conventional generation technologies can still be observed by looking at the generation mix or the installed generation capacity by technologies¹.

However, recent and current developments consist in a nuclear phase-out combined with the aim for decarbonization of the electricity sector in order to meet ambitious climate targets. Figure 1.1 illustrates the effect on installed conventional capacity in Germany that comes with these phase-out plans. In the future, this development shall ultimately result in a full decarbonization not only of the electricity sector but also of the entire energy sector, including the energy demand for transportation and heating. Complying to these developments means a fundamental shift in the organization of the electricity system and requires a new approach to supply the electricity demand. This approach is based on large shares

¹As these figures are reported in many public sources and may outdate fast after the publication of this thesis, the reader is referred to the annual monitoring reports provided by Germany's Federal Network Agency *Bundesnetzagentur* (cf. *Bundesnetzagentur*, 2021, for the latest version).

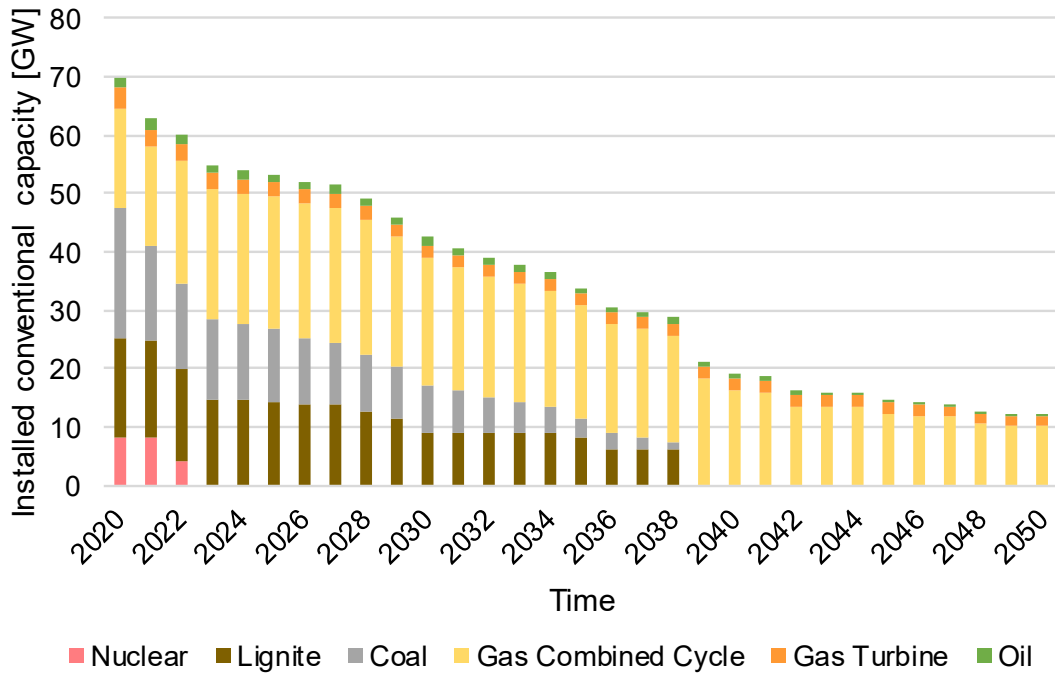


Figure 1.1: Conventional power plant capacities in Germany following the nuclear and coal phase-out plans without additional investments (own illustration based on data from S&P Global Platts, 2015, and own assumptions regarding technical lifetimes).

of renewable energy sources (RES), and in particular volatile renewable energy sources (vRES) such as solar photovoltaic (PV) and wind energy, resulting in a fundamentally different environment for market participants.

The phase-out of nuclear, which is completed by the end of 2022, the phase-out of coal, expected the latest to take place by 2038, the increasing age of the existing conventional power plant fleet and the continuous expansion of vRES in Germany raise fundamental questions about the future of electricity markets and the linked economics that market participants face. A key characteristic of these new economics is that market participants face more uncertainty and more volatility. Market participants are used to the fact that strategic decisions are subject to large uncertainty. However, these developments primarily affect the short-term electricity markets, which prevents the use of established methods to hedge risk, and require appropriate approaches to respond to them.

1.2 Objective and overall research question

On an overarching level, the outlined development leads to one major research question that will be pursued in this paper-based thesis. For each of the contained papers, more specific research questions are developed. These are presented in the respective sections in Chapter 4.

The overall research question is how to optimally operate and trade assets on short-term electricity markets in the presence of uncertainty. This general question can be precised with two questions: (a) How to model the uncertainty and (b) how to make optimal trading decisions under uncertainty in the short-term electricity markets. Compared to traditional trading, the market participants face a new market structure with market segments such as intraday trading and complex reserve products. In such a market design setting and with increasing uncertainties, multiple uncertain revenue streams need to be assessed for an optimal operational planning.

Based on the market environment and associated operational revenues of the recent past, market participants build expectations about the market circumstances in near future and the development of profitability as well as risk exposure of their assets. Therefore, answering the research question not only derives a set of optimal trading decisions, but also serves as a basis to asset valuation.

Almost naturally, question (a) translates into a need to model the uncertainty of renewable generation, its effects on market prices and its impact on the risk exposure for market participants as well as to investigate risk management strategies. An essential element of this consists in developing forecasting methods and stochastic models to characterize the interrelated uncertainties.

For question (b), it is inevitable to thoroughly understand the market design setting. To be able to formulate the mathematical problem for an optimal trading decision on short-term electricity markets, both the temporal organization of the competing market segments and the particularities of the market segments themselves need to be taken into account. Compared to the market design in the beginning of liberalization of power markets, substantial changes were implemented to arrive at today's market design.

However, up to now this is not done in a thorough and scientifically sound manner in the scientific literature, and practitioners base their decisions mostly on

simpler information and decision support tools, experience, and gut feelings. The thesis hence contributes to this research gap by developing methods and providing insights to risk management that take into account both, buying and selling parties of the market. Furthermore, the risk implications of different customer tariff designs for retailers are investigated.

1.3 Structure of the thesis

This thesis is organized in two parts. Part I provides the framework and the theoretical background as well as summaries of the three papers included in the thesis, Part II contains the manuscript versions of the Papers A, B, and C. In Part I, Chapter 2 first wraps up the institutional framework and its developments in Section 2.1. It presents the market design setting, for which the mathematical problems are developed and applied in the case studies. Further, in Section 2.2 it introduces relevant definitions as well as a risk taxonomy to categorize the uncertainties that affect participants in the short-term electricity markets.

Chapter 3 provides the methodological background to this thesis. As several quantitative methods are applied and developed in this thesis, it contains three subsections covering stochastic modeling of time series and forecasting (3.1), scenario tree generation and reduction (3.2), as well as stochastic optimization approaches (3.3).

In Chapter 4, the three papers and case studies are presented and summarized (4.1, 4.2, 4.3). Chapter 5 critically reflects the developed approaches and the underlying assumptions. It discusses limitations of the results and provides directions of future research based on this thesis. Finally, Chapter 6 summarizes the main findings and concludes the thesis.

The full manuscript versions of the three papers can be found in Part II of this thesis. Paper A is published in the *Journal of Forecasting*. Paper B is published as a working paper and submitted to the journal *Energy Economics*. Paper C is published as a working paper and submitted to the *European Journal of Operational Research*. The suggested citation for the papers is as follows:

Paper A

Kraft, E.; Keles, D.; Fichtner, W. (2020): Modeling of frequency containment reserve prices with econometrics and artificial intelligence. In: Journal of Forecasting, 39 (8), S. 1179–1197. <http://dx.doi.org/10.1002/for.2693>.

Paper B

Russo, M.; Kraft, E.; Bertsch, V.; Keles, D. (2021): Short-term Risk Management for Electricity Retailers Under Rising Shares of Decentralized Solar Generation. In: KIT Working Paper in Production and Energy No. 57, Karlsruhe Institute of Technology (KIT), Karlsruhe. <http://dx.doi.org/10.5445/IR/1000134345>.

Paper C

Kraft, E.; Russo, M.; Keles, D.; Bertsch, V. (2021): Stochastic Optimization of Trading Strategies in Sequential Electricity Markets. In: KIT Working Paper in Production and Energy No. 58, Karlsruhe Institute of Technology (KIT), Karlsruhe. <http://dx.doi.org/10.5445/IR/1000134346>.

Chapter 2

Background

2.1 Institutional framework of the German electricity market

2.1.1 The German electricity system

As previously mentioned, the German electricity system has a heritage with a large industrial demand. In the old days, the electricity generation by the conventional thermal power plant fleet followed the relatively inelastic demand. In recent years, due to several developments taking place in parallel, this paradigm was shifted towards increasing shares of inelastic supply from renewable generation, and continues to do so. The main driver behind this development is the promise of the *Energiewende*, a term that refers to the shift of the entire German energy supply from the unsustainable use of fossil and nuclear energy sources to a sustainable use of carbon-free and renewable energy sources.

Hence, one of the cornerstones of the *Energiewende* is a continuous expansion of renewable electricity generation. For this purpose, expansion paths for the renewable technologies onshore wind, offshore wind, solar and biomass have been legally anchored in Germany's Renewable Energy Act *Erneuerbare-Energien-Gesetz* (EEG). To remunerate renewable energy expansion and provide economic incentives as well as a stable investment environment to investors, a multitude of remuneration schemes are implemented across the world. In Germany, feed-in-tariff schemes and one-sided contracts for difference, the so-called market premium,

are implemented to foster the expansion of RES. To remain concise, the interested reader is referred to Kitzing et al. (2012) and Newbery et al. (2018) for an overview and a discussion of different mechanisms.

It is relevant to point out in the context of this thesis that the overarching trend is the (exogenously given) fundamental change in the technology mix of electricity generation away from a large share of dispatchable thermal generation to increasing shares of volatile renewable generation. Further, an overarching element relevant to this thesis is the consequence of this development to decision takers in energy economics. For market participants, new challenges arise and the exposure to uncertainties and associated risks requires new modeling approaches and optimization methods to determine optimal decisions.

A prominent example for this is the market premium and the directly linked obligation for direct marketing of renewable generation in the spot markets. Whereas operators of newly installed renewable energy systems with a capacity below 100 kW (i.e., sizes typical for PV rooftop installations) can still receive a feed-in tariff under the EEG without having to worry about trading the electricity, all operators with plants larger than 100 kW are obliged to trade the electricity produced by the plant themselves or via a service provider. They also bear the balancing responsibility for deviations and are obliged to develop strategies for managing renewable feed-in uncertainty, such as participation in intraday trading. According to the monitoring report for energy provided by the Bundesnetzagentur (2021), the majority (81 percent) of the renewable electricity produced in Germany in 2019 was marketed directly either by the operator or by a service provider.

According to the political agenda, in the near future new generation capacities will most likely consist of only vRES and flexible gas-fired power plants². Further, utility-scale storages, such as lithium-ion and redox-flow batteries, appear as mature technologies and available investment options for market participants. Whereas the capacity expansion of vRES involves a tight interaction with the policy targets and the associated regulatory measures to achieve them, the investment in new firm capacity, such as gas power plants but also utility-scale storages, shall take place based on expected profitability in the electricity market setting. Their

²Moreover, the obligation to make arrangements for a future fuel switch from natural gas to hydrogen is under discussion at the time of writing.

profitability is however subject to a large set of uncertainties, such as commodity and carbon prices, overall demand level, or future weather years.

In other countries, to ensure generation adequacy, capacity remuneration mechanisms (CRMs) are in place and shall provide security for investments in firm capacity. In this context, firm capacity refers to capacity that is dispatchable upon request in a scarcity situation. For a thorough investigation of CRMs and the impacts of different market designs on a national and international system level, the reader is referred to Cramton and Ockenfels (2012), Cramton et al. (2013), Newbery (2016), Bublitz et al. (2019), Bublitz (2019), and Fraunholz (2021).

It is common sense that the expansion of vRES combined with the stable or decreasing level of firm generation capacity and a relatively inelastic demand will lead to a more volatile electricity system. This volatility is particularly pronounced when steep load gradients occur, e.g., in the morning (evening) hours when solar PV generation increases (decreases) simultaneously as well as at the beginning (end) of stormy weather situations with steep increase (decrease) of overall wind generation within a short period of time.

In a market-based dispatch system, the volatility of the electricity system will also reflect on the situation on the electricity markets. Already today, “sudden” price increases and drops can be observed in the spot markets. Updates of vRES generation forecasts create significant price spreads between the day-ahead and the intraday markets. Finally, the balancing reserve markets (BRMs), for which market participants consider the electricity spot markets as opportunities, are also linked to the volatility and price levels of the electricity spot markets.

For a thorough understanding of how the German electricity system is operated, one must bear in mind that the generation dispatch and reserve capacity reservation as well as their pricing are not centrally decided upon, as e.g. in parts of the US, but follow the trading decisions of the market participants. Eventually, the aggregation of these individual trading decisions emerges as the overall dispatch of the electricity system and its costs. Therefore, with inherent short-term uncertainty in the system that is likely to further increase in the future, the question on how to derive optimal trading decisions becomes increasingly important, but turns out to be a challenging one. Besides the aim of maximizing profit or minimizing costs, another important aspect for market participants in the light of uncertainty consists in the exposure to risk that is linked to the trading decisions.

To provide a background with regard to the market structure, the next section outlines the market design setting that market participants face. It also aims at providing the institutional context for the developed methods and case studies of this thesis.

2.1.2 Design and development of the electricity wholesale markets

The structure of liberalized electricity markets with self-dispatch³ is similar across the world. The two main dimensions in which trading with electricity and flexibility can be distinguished are the geographical and the temporal dimension. The geographical dimension implies the definition of market areas and the interaction between connected market areas. In Europe, the market areas are typically defined by the national country borders⁴. This stands in opposition to the locational or nodal pricing approach, in which each node in the transmission grid is assigned a single price that reflects the marginal costs and the grid situation in that particular node (cf. Stoft, 1997).

However, European electricity markets are designed to have market areas that cover a larger geographical and grid-topological scope. Within one market area, the assumption of a copper plate (i.e., there are no grid congestions) leads to a single market price for the entire market area. This is the main take-away regarding the geographical dimension of trade for the remainder of this thesis. All market participants in one market area face the same market signals, be it the prices on the wholesale electricity market or the prices on the BRMs.

In the case of sufficient transmission capacity, multiple market areas are coupled to be operated as a single market area. The rationale behind market coupling is the maximization of economic welfare within the European internal market. As this is not in the main scope of this work, the reader is referred to literature on flow-based market coupling and market splitting for more information on the

³This thesis does not discuss market structures with central dispatch. However, the developed approaches could in principle be adapted to a system with central dispatch.

⁴However, there are a few exceptions, such as Luxembourg and Germany forming one market area and Italy as well as the Scandinavian countries being divided in several market areas. These particularities are driven by the topology of the grid and the occurrence or absence of grid congestions within a market area.

geographical dimension of electricity markets (cf., e.g., van den Bergh et al., 2016; Felling et al., 2019; Ringler, 2017; Bublitz, 2019; Fraunholz, 2021).

In the following, the focus is set on the temporal dimension of electricity trading. The market participants on the supply side as well as those on the demand side face the electricity market as a sequence of distinct market segments. Figure 2.1 illustrates this market sequence and distinguishes between *energy markets*, *balancing reserve markets*, and *capacity remuneration mechanisms*.

The time axis represents the market design setting with gate closure times (GCTs) in force as of January 2022 in Germany. The exact GCTs may differ from one country to another, yet the general setting is representative for liberalized electricity markets with self-dispatch across the world. Even though there is no explicit CRM in place in Germany⁵, it is featured in the illustration for two reasons. Firstly, because it is a market design element in many countries in Europe as well as across the world (see Bublitz, 2019, for an overview) and by European regulation, asset owners in the German market area must be allowed to participate in the CRMs that are in place in connected market areas. Secondly and more important, because the implementation of CRMs is still under discussion in Germany and at the time of writing it cannot be excluded that CRMs will play a key role for market participants' economics in the near future. However, CRMs will not be discussed in detail in the following.

The core elements of the electricity market are the *energy market* segments, also referred to as wholesale electricity markets. These segments have by far the highest trading volumes and determine the economics of market participants to the largest extent. For 2020, the European Commission reports a total of 7,000 TWh of traded volume from OTC- and exchange-based electricity trading in Germany, which corresponds to more than fourteen times the net electricity production for the same year (European Commission, 2021; Fraunhofer ISE, 2021). The energy markets can be distinguished into future and spot markets by their lead time until realisation⁶. On future markets, contracts have lead times ranging from one day over several weeks and months up to several years. These contracts are

⁵However, the existing reserves such as the so-called strategic reserve and the grid reserve can be considered as capacity remuneration.

⁶One could also distinguish by contracts with financial and physical fulfillment. However, this goes mainly hand in hand with the lead time, as contracts on the future market are typically financially fulfilled and contracts on the spot markets are subject to physical fulfillment.

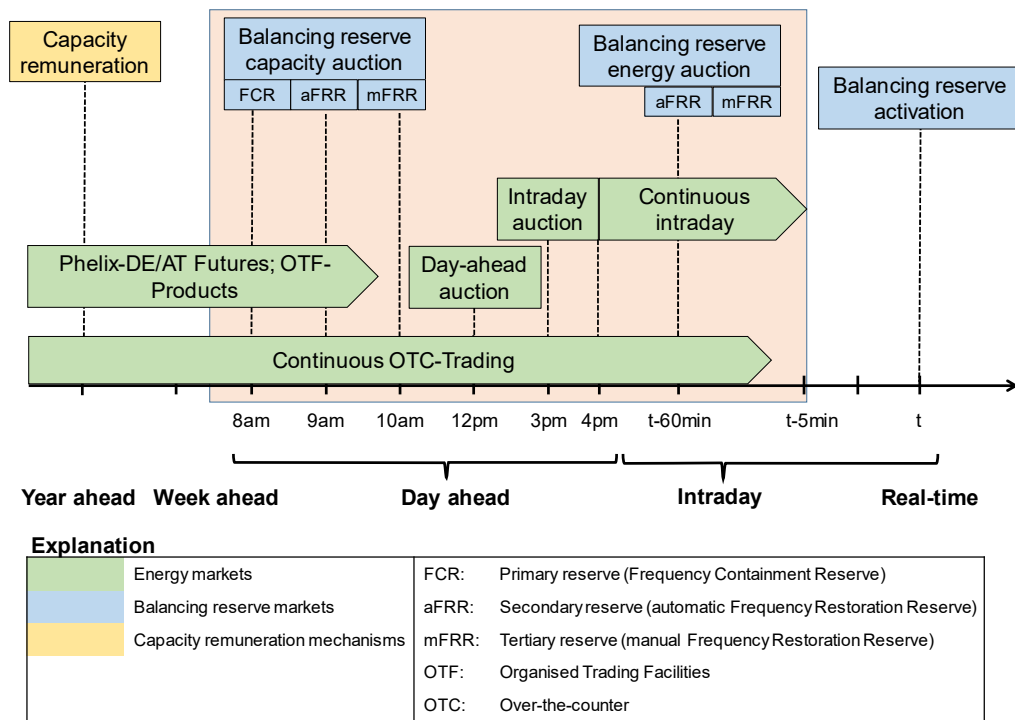


Figure 2.1: Electricity market design in Germany as a sequence of market segments. The red box indicates the day-ahead and intraday decisions this thesis puts the main focus on. (Status: January 2022, own illustration)

mainly traded to hedge mid- and long-term risks with regard to prices and volumes. Historically, mainly generation from conventional power plants is sold in the future markets with precisely defined base and peak load products. In recent years, also renewable generation, particularly from large wind and PV parks, became the underlying of trades several years into the future in so-called power purchase agreement (PPA) contracts. These PPAs are a key measure to stabilize revenues for vRES investments that take place outside of support schemes.

An additional feature of the future market is the distinction into trades agreed over-the-counter (OTC) via so-called forward contracts and exchange-based trades via future contracts. Forward contracts are bilateral contracts and can as well last for several years. Among energy supply companies and large consumers, they are typically complemented with other commodity futures or forwards (e.g., for fuels) in order to derisk the cash flows for the assets or future electricity costs. On the other hand, the exchange-based future market allows for liquid trading typically only for the year ahead and shorter lead times. To remain concise, strategies for trading electricity and hedging risk in the mid- and long-term will not be further detailed. The key insight with regard to the scope of the thesis is that there are several strategies and market segments to hedge price and volume risks until the spot market stage. However, although the settlement of financial contracts is organized with the spot market as the reference point, the spot market itself is due to substantial uncertainty for market participants. As presented in Chapter 2.2 in more detail, this short-term uncertainty is mainly introduced by vRES generation⁷.

The spot market can be distinguished into the day-ahead market and the intraday market. In Europe, only nominated electricity market operators (NEMOs) are allowed to operate electricity markets. In Germany, as in most countries in continental Europe, these markets are operated by the European Power Exchange (EPEX Spot). Hence, the following paragraphs base on the market description provided by EPEX Spot (2021). Note, that the market operator which traditionally operated the electricity exchanges in the Scandinavian countries, Nord Pool, is also a NEMO for the German market area and operates spot markets. However,

⁷There are also power plant outages, line outages, and short-term demand fluctuations as sources of short-term uncertainty in the electricity system. However, balancing reserves in acceptable amounts can cope with these.

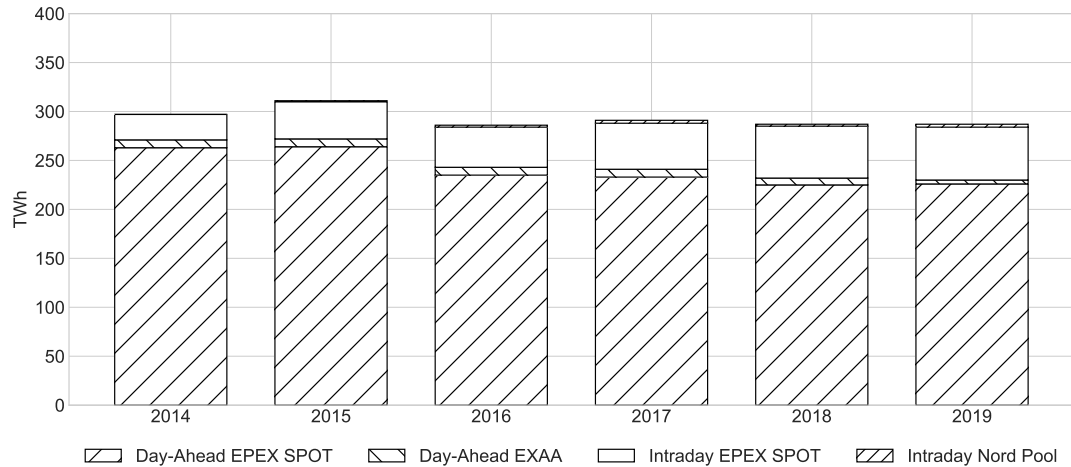


Figure 2.2: Spot market volumes of EPEX Spot, the Austrian Energy Exchange (EXAA), and Nord Pool for the German market area. The EPEX Spot has the main share and is therefore the reference in this thesis (own illustration based on data from Bundesnetzagentur, 2021). After the split of the German-Austrian market area in 2019, EXAA has lost its relevance for the German market area.

as illustrated in Figure 2.2, the EPEX Spot markets have a higher liquidity and are therefore considered as the reference for market prices in this thesis.

The day-ahead market consists of an auction for the 24 hourly products of the next day and takes place at 12 p.m. on the day ahead. The auction is a first-price auction with uniform pricing, thus the volume (“market clearing volume”) is determined at the intersect of the demand and the supply curve and the marginal power plant sets the price (“market clearing price”) that is paid for all accepted bids in an hour. The day-ahead market auction is followed by the so-called intraday auction that – despite its name – takes place at 3 p.m. on the day ahead. It is organized as a first-price auction with uniform pricing, in which the 96 quarter-hourly contracts of the day ahead are traded. The main difference compared to the day-ahead auction is the quarter-hourly resolution and that market participants may have better information available with regard to the next day. Further, the intraday auction works as a reference auction for the continuous intraday trading that starts after 4 p.m. on the day ahead (EPEX Spot, 2021).

The importance of intraday trading has increased substantially in recent years, mainly due to increasing shares of vRES, the linked economic opportunities, and new duties for market participants, as can be seen in Figure 2.3. In particular, the

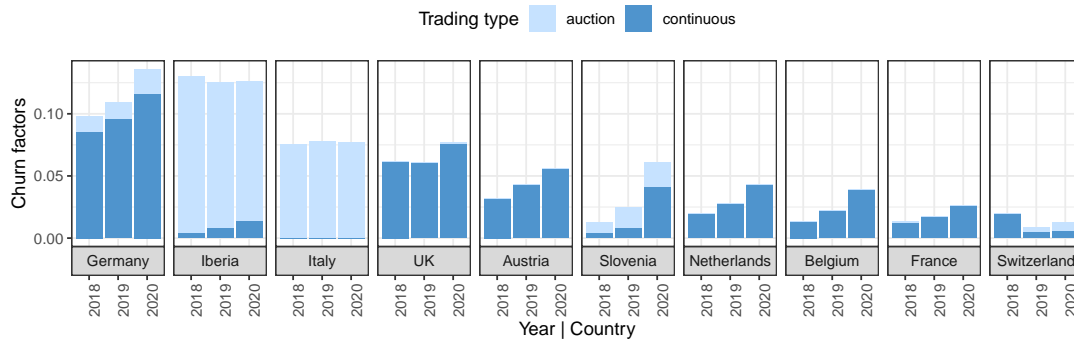


Figure 2.3: Liquidity of intraday trading in Germany and other European market areas, measured by the Churn factor. The Churn factor is defined as the volume of all trades in a market segment divided by the overall electricity consumption (own illustration based on data from ACER and CEER, 2021).

intraday market in Germany is very liquid compared to other European market areas. As reported in the market monitoring report by ACER and CEER (2021), for each consumed MWh in the German market area, roughly 0.13 MWh were traded in the intraday market (cf. also Figure 2.3).

In opposition to the two previous auctions, in intraday trading market participants fill order books with their sell and ask bids and the market is cleared continuously, 24 hours per day and seven days per week. Therefore, prices for a certain quarter hour contract change over time with new information becoming available to the market. However, in reality, the continuous intraday trading turns out to be liquid mostly in the last three hours before delivery and the most liquid in the last hour before delivery. At the time of writing, intraday trading is possible until five minutes before delivery in the German market area (i.e., a lead time of five minutes) (EPEX Spot, 2021).

To find representative indices for the price level, besides to the overall volume-weighted average price, the indices ID3 and ID1 are defined⁸. They are defined as the volume-weighted average of all completed trades for a quarter hour contract in the last three hours and in the last hour before delivery, respectively. In markets of other countries, particularly in those with less intraday liquidity than the German market, the intraday market is organized as a sequence of intraday auctions. Ocker and Jaenisch (2020) present an overview over the current organization of different

⁸In Paper B and C, the ID3 index is used as representative for the intraday price.

intraday markets in Europe and discuss advantages and disadvantages of auction-based versus continuous intraday trading. They point out that the auction-based design has advantages in terms of bundling of liquidity, resilience against market power, and static allocation efficiency. Further, the auction-based design allows for a more efficient use of cross-border transmission capacities.

However, the main disadvantage and the striking argument in favor of continuous trading lies in the information efficiency, meaning that information should be reflected in market signals as soon as it becomes available. In consequence, this means that the value of the speed to have new information available, such as having the fastest vRES generation updates, becomes more important and can be a key to success over market participants with less advanced forecasts and trading processes. Thus, assuming sufficient liquidity and perfect competition, as well as taking into consideration that cross-border capacities are typically allocated in the day-ahead market coupling, continuous trading is in theory a suitable and efficient market design for the intraday market. It is successfully implemented in the German and many other market areas, whereas e.g. in Italy and the Iberian peninsula the intraday market is organized auction-based.

Since June 2018, the geographical scope of continuous trading has been expanded within Europe, under the name cross-border intraday (XBID) market. At the time of writing, the geographical scope of the intraday market coupling covers 23 countries in Europe (ENTSO-E, 2021b). However, this integration is mainly implemented in terms of information technology. The physical grid situation rarely allows trading from Northern Norway to Portugal or Sicily in the intraday market, as cross-border capacities are mainly assigned by the market coupling of the day-ahead market.

Apart from exchange-based intraday trading, in theory OTC trades would be possible also in the intraday time frame. Due to liquidity, the short time to find counterparts and to agree deals with them, this appears economically unreasonable and is therefore not institutionalized.

For the remainder of this thesis the following is worth stressing. There is a multitude of *energy markets* to trade electricity on, with different scopes, different products and different market designs. The spot market with day-ahead and intraday trading is the key market for trading electricity and flexibility. Further, the *balancing reserve market* segments (blue boxes in Figure 2.1) are a second

considerable revenue stream for market participants to trade the flexible capacity of their assets and thus competes with the spot market for the available flexibility. Yet, the purpose of the balancing reserve market is not to balance out potential imbalances⁹ that are already known to market participants during intraday trading – it is a duty for each balancing responsible party (BRP) to balance these by trading actions. Therefore, although competing for the same product (flexibility) and being an economical opportunity to market participants, the two markets are not redundant and have their own purpose.

The challenge for market participants is therefore to make optimal decisions in the presented sequence of markets. In this thesis and in the included papers, the focus is set on decisions the market participants have to take on the day ahead and during the day until shortly before delivery. These are hence highlighted with the red box in Figure 2.1. With regard to the trading sequence, please note, that the bids for the capacity auctions in the BRM segments must be submitted before the GCT of the day-ahead wholesale market. Likewise, the bids for the energy auctions in the BRMs must be submitted before the GCTs of intraday trading for the respective time steps.

In the next paragraphs, the principles of balancing reserves, its technical requirements, and the particularities of the different segments of the BRM are presented. These rather complex product definitions stand in opposition to the straightforward definition of scheduled energy that is traded on the wholesale markets.

2.1.3 Design and development of the balancing reserve markets

After spot market trading has finished, the resulting schedule commitments are forwarded to the transmission system operators (TSOs) that are responsible for the system operation in the respective control zone of physical fulfillment. In order to ensure the stable operation of the electricity system at the frequency of 50 Hz, the

⁹In the context of electricity and balancing markets, the term imbalance is defined as the deviation of a balancing group's (German: Bilanzkreis) announced feed-in or withdrawal commitment (German: Fahrplan) from the actual feed-in or withdrawal from the grid. BRPs are responsible to balance their balancing groups. In imbalance settlement, each BRP must match the actual feed-in or withdrawal for each of his balancing groups with respective contracts for each imbalance settlement period (in Europe typically 15 minutes). Imbalances are then charged with the imbalance price, see Section 2.1.3.

power balance of feed-in and withdrawal must be ensured at all time. The power balance must be monitored continuously and corrective action must be taken if necessary in the event of fluctuations or outages in feed-in and withdrawal.

In a self-dispatch market like the German electricity market, the task of balancing the system is carried out by the responsible TSOs. In terms of procurement and activation of reserve capacities to fulfill this task, the TSOs distinguish the three qualities Frequency Containment Reserve (FCR), automatic Frequency Restoration Reserve (aFRR), and manual Frequency Restoration Reserve (mFRR). These are also referred to as primary, secondary, and tertiary reserve. In case of an event disturbing the system frequency, reserve activation takes place in three stages, though not each event requires the application of all three stages. The following description and Figure 2.4 present this procedure for the case of a shortage in the system, caused e.g. by the unplanned outage of a power plant, and a resulting frequency drop. For the reverse imbalance direction of a surplus in the system and a rising frequency, the activation of reserves takes place in the same sequence, but in the other direction.

Firstly, the FCR is activated within 30 seconds to stop the frequency drop and stabilize the frequency at the lower level as quickly as possible. The FCR is activated non-selectively among all contracted providers, not only in the German control zones, but also in the entire International Grid Control Cooperation (IGCC). The IGCC covers 24 control zones in continental Europe¹⁰. In the technical process of FCR activation, it is worth noting that no explicit control signal is sent by the TSOs. Instead, the providers monitor and translate the deviation from the set point of 50 Hz directly into their respective control signal via proportional control with full activation at ± 200 mHz frequency deviation (pro rata activation).

To make the FCR available for another disturbing event and to restore the frequency to the set point, the aFRR replaces the primary reserve. In Germany, the

¹⁰IGCC has 24 member TSOs in 21 countries: Austria (APG), Belgium (Elia), Bulgaria (ESO), Croatia (HOPS), Czech Republic (CEPS), Denmark (Energinet), France (RTE), Germany (50Hertz, Amprion, TenneT DE, TransnetBW), Greece (ADMIE), Hungary (MAVIR), Italy (Terna), Luxembourg (CREOS), the Netherlands (TenneT NL), Poland (PSE), Portugal (REN), Romania (Transelectrica), Serbia (EMS), Slovenia (ELES), Slovak Republic (SEPS), Spain (REE), and Switzerland (Swissgrid). In addition, three TSOs are associated as observer to IGCC: Bosnia and Herzegovina (NOS BiH), Montenegro (CGES) and Republic of North Macedonia (MEPSO) (ENTSO-E, 2021a).

full activation time for aFRR is defined to five minutes. Although full activation times are not fully harmonized in Europe yet, by 2025 aFRR providers throughout Europe shall be able to fully activate the reserve capacity within five minutes (ENTSO-E, 2021c).

The necessary and cost-optimal activation of aFRR is determined by the load-frequency controller of the responsible TSO or network regulation cooperation, such as the so-called *Netzregelverbund* (NRV) in Germany. The determined activation signal is then automatically transmitted to the reserve provider. Like that, the reserve provider receives a set point to ramp up for aFRR provision on a second basis. Hereby, providers are activated according to a merit order list (MOL), i.e. in the order of the cheapest energy prices of bids that were awarded in the aFRR market. More information on the market design will be provided in the following.

Most disturbing events can be resolved by the activation of FCR and aFRR. However, some disturbances have a larger extent or may persist for longer time periods without corrective trading actions on the intraday spot market. To make the secondary reserve available for another disturbing event, the TSOs replace or support the secondary reserve with the tertiary reserve (mFRR). In Germany, the mFRR has a full activation time of 15 minutes, although in the scope of the European harmonization, the European TSOs agreed on a reduction to 12.5 minutes (Consentec, 2020). Like in the case of aFRR activation, the TSOs activate mFRR according to a MOL. The activation is not issued automatically but “manually” by the system control center of the responsible TSO.

As soon as possible, but the latest 60 minutes after the first frequency deviation, the BRP causing the deviation must resolve the schedule imbalance. These corrective measures are typically realized through intraday trading.

Like for the wholesale markets, there is an ongoing process of European harmonization and integration of BRMs. In 2017, regulation 2017/2195/EU establishing a guideline for system balancing in the electricity supply system – often referred to as Electricity Balancing Guideline (EBGL) – was published by the European Commission. The aim of the guideline is to create a functioning and liquid cross-border internal energy market also in the area of system balancing (European Commission, 2017). The regulation sets a European guideline on how to define balancing reserve products and on how to organize their procurement within Europe in the future.

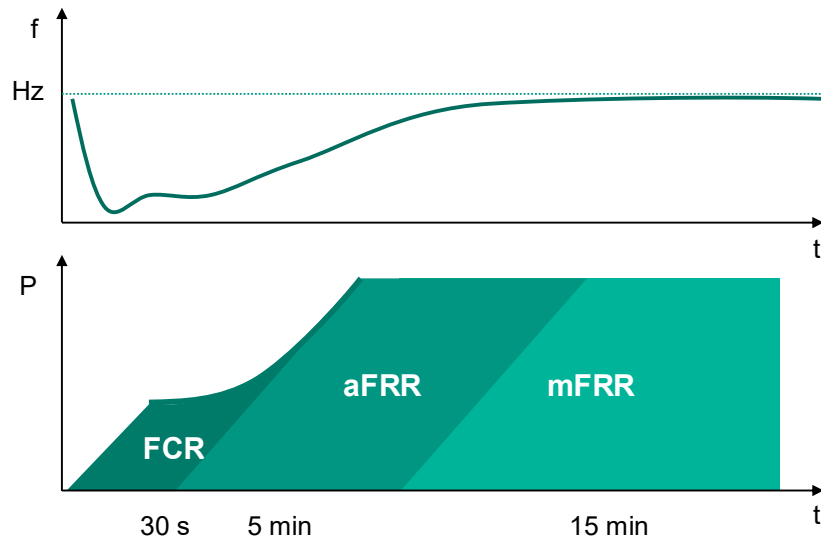


Figure 2.4: Sequence of use of the three reserve qualities in the exemplary case of a frequency disturbing event causing the activation of positive balancing reserve (own illustration).

The German TSOs have already been successfully organized in a network regulation cooperation (NRV) for several years and have been driving forces in the process towards European harmonization. The principle of the NRV is based on the idea that the TSOs cooperate in all steps of procurement and activation of system balancing to realize synergies and to avoid inefficiencies. Between the four German TSOs (50Hertz, Amprion, TenneT, and TransnetBW), there is a joint dimensioning, joint procurement, and a joint cost-optimized activation of balancing reserves. In the same spirit, in the ongoing European projects PICASSO and MARI, the European Network of Transmission System Operators for Electricity (ENTSO-E) members aim at implementing a joint activation process for aFRR and mFRR, with the German NRV as a blueprint.

However, as these project and their proposals are not operative yet, for the works prepared in this thesis, a national scope is sufficient with regard to balancing reserves. As of 2021, the German TSOs procure approximately 600 MW of FCR, 2000 MW of positive and 1800 MW of negative aFRR, as well as 1400 MW of positive and 1000 MW of negative mFRR (Bundesnetzagentur, 2021). Thus, compared to the volumes of the spot market, the size of the BRMs is relatively small.

In the following, the market design for procurement of balancing reserves in Germany as of January 2022 is presented. The official market description is provided by Consentec (2020). The joint procurement is organized in tenders that take place via the platform *regelleistung.net*¹¹. As mentioned before, the three qualities FCR, aFRR, and mFRR are tendered separately. Whereas for the FCR only reserve capacity is auctioned, for the aFRR and the mFRR reserve capacity and reserve energy are distinguished. This serves the purpose to discriminate between the compensation for the reservation of flexible capacity and the compensation for delivery of balancing energy upon request. For FCR, this discrimination does not apply because in expectation there is no delivery of energy for the symmetric definition of the product.

For aFRR and mFRR, this leads to a multi-part auction. The interested reader is referred to e.g. Ocker (2018), Ocker et al. (2018), and Ehrhart and Ocker (2021) for a thorough discussion on BRM design, an investigation of incentives and game-theoretical analyses of this rather unusual multi-part auction setting. The author of the present thesis also contributed to the discussion on the market design and the analysis of bidding strategies in multi-part auctions (Kraft et al., 2018, 2019a).

The insights of these works that are most relevant for this thesis are twofold: (a) The prices on the BRM can deviate from fundamental energy economic concepts such as opportunity-cost-based pricing of reserves (see also Swider and Weber, 2007; Just and Weber, 2008, 2015, for analyses of interactions and equilibria between spot and reserve markets), because they are due to (tacit) collusion and strategic bidding by market participants. (b) The market concentration in the BRM and resulting market power leads to substantial price uncertainty for small market participants and requires a trading approach that can cope with it by considering both profit opportunities and risk exposure.

During the period of preparation of the different papers contained in this thesis, these issues led to several market design adjustments like shorter lead times, shorter product periods and lower minimum bid size to open up the BRMs also for new and smaller reserve providers. During a short period, even the scoring rule was

¹¹This is a difference to exchange-based markets with an independent market operator like EPEX Spot or Nord Pool in the case of spot markets. Tenders are a special form of market-based procurement, since the only market participant on the demand side is the union of TSOs and the volume is defined in advance and not market-based. However, for a better readability, in the context of BRMs the terms market, auction, and tender are used interchangeably.

changed from capacity-price-bid-based scoring to an approach considering a linear combination of capacity price and energy price bid as scoring criterion, which raised major concerns of some market participants. In the end, it even led to a threat to the security of supply of Germany's electricity system and was revoked quickly afterwards (Handelsblatt, 2019). However, the evolutionary process of the BRM is not finished until today.

In November 2020, in accordance to the market design target model provided in the EBGL, a new market segment for balancing reserve energy was introduced to decouple capacity from energy price bids for aFRR and mFRR. In that sense, the balancing energy auction, which is also open to bids that have not been awarded in the balancing capacity¹², takes place 60 minutes before the start of a delivery period and determines the merit order for aFRR and mFRR activation. In the next years, the lead times and product periods are announced to be further reduced to increase competition in and overall efficiency of balancing reserve procurement. In addition, the implementation of the aforementioned PICASSO and MARI initiative will lead to a European market coupling (50Hertz et al., 2020a).

Thus, the market circumstances for balancing reserve providers may again change fundamentally in the near future. In the mean time, balancing reserve providers have become more used to a changing environment rather than a stable one. Against this background, it is particularly important to develop methods that are adaptable to new market designs and do not necessarily require years of historical data¹³ to calibrate. This applies to all the approaches chosen in this thesis, meaning that the contributions and validity of the developed models and findings hold. However, slight adaptations and updates might be necessary when the market designs are changed in future.

In Figure 2.1, the temporal structure valid in the beginning of 2022 is shown. The GCTs for the balancing reserve capacity auctions for FCR, aFRR, and mFRR

¹²This design option is also referred to as the allowance of free or voluntary bids and aims at an increase of competition on the reserve energy price bids. See Ocker (2018); Kraft et al. (2019a); Ehrhart and Ocker (2021); Ehrhart et al. (2021) for more insights into the balancing energy market design.

¹³Market participants in the real world do also only have access to the publicly available data on regelleistung.net and must derive their decisions based on limited information. Although not addressed in the scope of this thesis, this may also be one source of price uncertainty in the BRM, as existing trading models may react sensitively when calibrated to new data and as market participants may explore new market designs with a trial-and-error approach.

are on the day ahead at 8 a.m., 9 a.m., and 10 a.m., respectively, and thus before the electricity spot market begins. In the BRM auctions, six time slices of four hours each are distinguished (0–4 a.m., 4–8 a.m., etc.) in all segments. The temporal interplay with the spot markets is particularly important when modeling trading decisions in competing segments. With its 4-hour-resolution, the BRM has a larger granularity and covers four hourly day-ahead market (DAM) and 16 quarter-hourly intraday market (IDM) products in each time slice.

The minimum bid size and the bid increment are 1 MW for all three qualities. The product for FCR is defined as symmetric, meaning that the offered reserve capacity must be provided in both upward and downward direction. In opposition, the products for aFRR and mFRR are defined as non-symmetric, thus separate products for positive and a negative reserve are auctioned. Furthermore, the FCR auction is cleared with uniform pricing¹⁴. The aFRR and mFRR auctions are cleared with pay-as-bid pricing, both the reserve capacity and the reserve energy segment. Table 2.1 summarizes the key product characteristics of the three qualities valid in the beginning of 2022¹⁵.

The costs occurring for balancing the system are transferred by the TSOs in two ways. The costs linked to the reservation of balancing capacity (i.e., the capacity price payments) are considered inevitable for the provision of the public good security of supply and are settled via the grid charges to connected consumers. On the other hand, the costs linked to the activation of balancing energy (i.e., the energy price payments) are settled according to the cost-by-cause principle. In that sense, for each imbalance settlement period (i.e., 15 minutes), the costs for reserve activation are summed up and then divided by the activation volume to determine the imbalance price, in Germany referred to as *regelzonenübergreifender einheitlicher Ausgleichsenergiepreis* (reBAP). Note, that in the case of negative energy prices, which are common for negative reserves in aFRR and mFRR, also revenues may occur for the TSO. The imbalance price can thus be negative, too.

¹⁴Please note, that the FCR market design to which the forecasting methods in Paper A are applied, is slightly different. The data is based on a market design, in which the lead time as well as the product period is one week, and the auctions are cleared with pay-as-bid pricing. However, this does not affect the general functioning of the developed methodology.

¹⁵For readers that are familiar with older reserve product definitions and want to compare them to the ones presented here, Consentec (2020) provides an overview table with the evolution of product definitions since 2018.

Characteristic	FCR	aFRR	mFRR
Gate closure time (GCT) reserve capacity auction	day ahead, 8 a.m.	day ahead, 9 a.m.	day ahead, 10 a.m.
GCT reserve energy auction	n.a.	60 min before delivery	60 min before delivery
Product resolution	6 x 4 hours	6 x 4 hours	6 x 4 hours
Product directions	symmetric	positive and negative	positive and negative
Minimum bid size	1MW	1MW	1MW
Bid increment size	1MW	1MW	1MW
Scoring rule	capacity price bid	capacity price bid	capacity price bid
Clearing rule	uniform pricing	pay-as-bid	pay-as-bid
Tendered volume (approx.)	+/-600MW	+2000MW, -1800MW	+1400MW, -1000MW

Table 2.1: Key product characteristics of the three balancing reserve qualities FCR, aFRR, and mFRR valid at the time of writing (January 2022).

In imbalance settlement, the TSOs charge BRPs according to the direction of system imbalance and to the deviations from the schedule commitments of their balancing groups. In that way, BRPs are charged or paid the imbalance price for their imbalances.

Although intentional imbalances are prohibited in the German market area, frictions in the economic incentives between the spot market and the imbalance settlement led to intentional imbalances threatening the security of supply in the past (Consentec, 2012; Handelsblatt, 2019). Therefore, a few adjustments to the imbalance price apply to prevent the BRPs from threatening the system by acting economically rational. These are published by the TSOs (50Hertz et al., 2020b).

2.1.4 Supply flexibility and technical provision of balancing services

Other relevant aspects of balancing reserves are the prequalification process, the structure of the supply side, and the technical provision. The technical provision varies for each technology. In general, it can be stated that the feed-in of a generator or the withdrawal of a consumption process must be adjusted quickly, and that in general any generation technology can vary the feed-in to some extent, though not at the same speed and to the same extent. To describe the flexibility of a generation unit of a certain technology and thus its capability to provide bal-

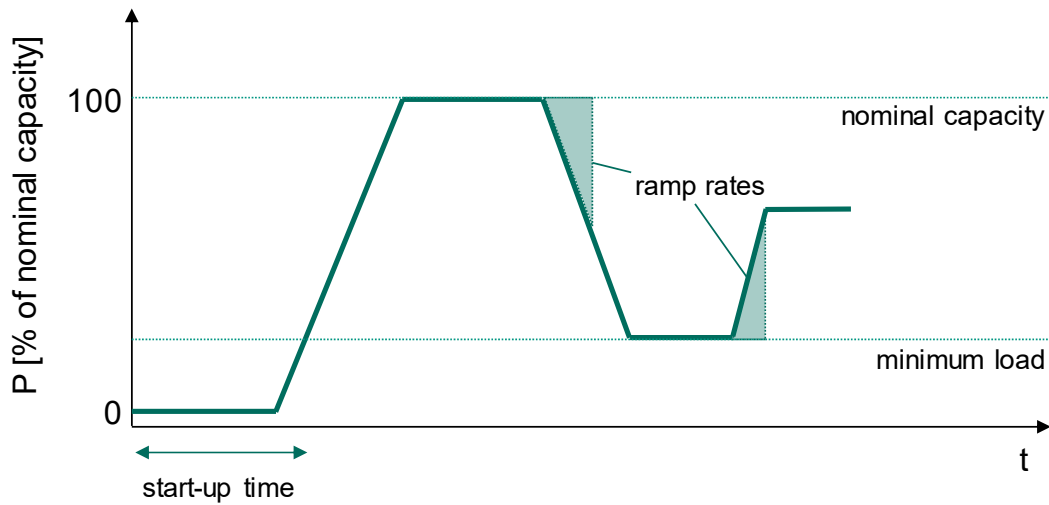


Figure 2.5: Illustration of technical parameters determining the flexibility of a power plant. The start-up time defines the time to reach the minimum load output. Ramp rates are relevant both in upward and downward direction and determine the operational flexibility between minimum load and nominal capacity (own illustration based on Agora Energiewende, 2017).

ancing reserves, the plant parameters minimum load, the ramp rate as well as the start-up time are considered. Figure 2.5 provides an illustration of the technical parameters based on an exemplary load curve.

In addition, Table 2.2 provides an overview of typical ranges for the conventional power plant technologies. It must be noted, that technological developments led to considerable changes in the flexibility of power plants, particularly for coal- and gas-fired power plants. This leads to the distinction between most commonly used power plants, i.e., the existing power plants that dominate the energy system, and state-of-the-art power plants. Overall, it can be observed that large-scale power plants with electricity generation through steam processes – deploying the so-called Rankine cycle – require longer start-up times compared to technologies that use other energy conversion principles. This is mainly due to the thick-walled components in the high-pressure part of the steam process, which can only tolerate limited rates of temperature change and thus limit the start-up speed and ramping rates of the power plant. The limited temperature change rate also explains the difference between hot start-up (i.e., the power plant has been generating within the last 8 hours and components are still hot) and cold start-up times (Albert,

Parameter	Unit(s)	OCGT	CCGT	Hard coal	Lignite	Nuclear
Most commonly used						
Minimum load	[% installed power]	40–50	40–50	25–40	50–60	40–50
Average ramp rate	[% installed power/min]	8–12	2–4	1.5–4	1–2	3.3–10
Hot start-up time	[min] or [h]	5–11 min	1–1.5 h	1.5–3 h	4–6 h	n.a.
Cold start-up time	[min] or [h]	5–11 min	3–4 h	5–10 h	8–10 h	24–50 h
State-of-the-art (2017)						
Minimum load	[% installed power]	20–50	30–40	25–40	35–50	n.a.
Average ramp rate	[% installed power/min]	10–15	4–8	3–6	2–6	n.a.
Hot start-up time	[min] or [h]	5–10 min	30–40 min	1.33–2.5 h	1.25–6 h	n.a.
Cold start-up time	[min] or [h]	5–10 min	2–3 h	4–6 h	5–8 h	n.a.

Table 2.2: Plant parameters determining operational flexibility for different power plant technologies (own compilation based on Agora Energiewende, 2017; Schröder et al., 2013).

1996). Lignite and nuclear power plants are typically dimensioned in the largest scales, leading to the longest start-up times and the slowest ramp rates.

More flexible in terms of start-up and ramping are generation technologies based on the Joule cycle, such as open cycle gas turbines (OCGTs). In the Joule cycle, instead of using steam as transmission medium for the thermal energy, a mixture of compressed air and flue gas is directly expanded in a turbine to generate electrical energy. This simpler process leads to lower start-up times and higher ramp rates, however at the expense of lower process efficiency (Agora Energiewende, 2017). Note, that combined cycle gas turbines (CCGTs) combine a Joule cycle with a subsequent steam-based Rankine cycle, which leads to technical parameters similar to plants deploying the less flexible Rankine cycle.

The technologies used for electricity generation from biogas or biomass are heterogeneous, which also leads to heterogeneous typical plant parameters. Whereas small installations can be based on combustion engines and are thus highly flexible regarding start-up times, minimum load, and ramp rates, larger installations are based on the more efficient Rankine or Joule cycles and hence have technical parameters in the ranges of the respective technologies mentioned in Table 2.2.

Finally, hydro power generation is based on the conversion of mechanical into electrical energy. Hence, there are no limitations directly stemming from the thermodynamics of the energy conversion process, but natural parameters such as inflow, reservoir size, fill levels and ecological restrictions dominate the limitations to operational flexibility. Swider (2006) reports minimum loads of 20 to 30 percent and ramp rates in the range of 1.5 to 2.5 percent per second in terms of nominal capacity for the different turbine types Pelton, Francis, and Kaplan. The differ-

ent types of hydro power plants can be distinguished into run-of-river, reservoir storage, and pumped-storage hydro plants. Whereas run-of-river plants are able to provide flexibility only to limited extent, installations with a reservoir – and particularly those with a pumping operation mode – are able to ramp up within minutes and adapt their output flexibly in order to provide balancing services (Siemonsmeier et al., 2018).

A description of the technical execution of the output adaption according to activation signals for each technology would exceed the scope of this work. The interested reader is referred to, e.g., the dissertation of Swider (2006) for a description of the detailed technical realization of balancing reserve provision. Since the generation output of a turbine is determined by the turbine efficiency, the enthalpy difference between turbine inlet and outlet, and the steam mass flow through the turbine, besides an increase or decrease of the amount of fuel used for combustion, steam process control also provides short-term operational flexibility. With steam process control based on fixed or variable pressure management, the steam mass flow or the thermodynamic state of the steam at the turbine inlet can be modified to control the turbine output. As Swider (2006) mentions, in real-world applications, typically hybrid forms of fixed and variable pressure management are applied.

As balancing services are deployed to ensure the security of supply and are therefore considered part of a critical infrastructure, technical units need to prove reliability and security with regard to the technical provision and the communication architecture in order to be allowed a market participation. In recent years, prequalification requirements were adjusted to lower market entry barriers and to open the BRM to new providers. Today, the BRM segments are open to small technical units, pools of units, and also to storage technologies that can meet the requirements. The valid requirements and a detailed description of the prequalification process are published by the TSOs (50Hertz et al., 2020c).

As mentioned above and as can be observed in the publication of prequalified reserve capacity that is displayed in Figure 2.6 and Table 2.3, various technologies are able to provide balancing reserve (50Hertz et al., 2022). However, despite the market entry of battery storage, biomass, and even vRES such as wind, the majority of the market is still covered by large-scale thermal and hydro power plants. When comparing the prequalified capacities to the tender volumes of the

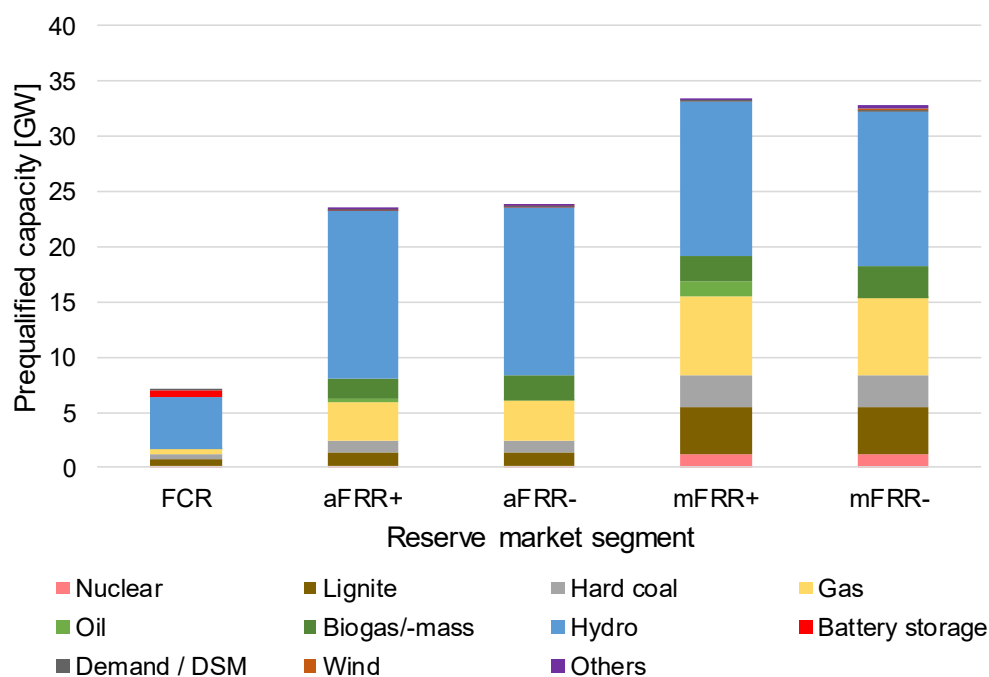


Figure 2.6: Prequalified balancing reserve capacity in Germany as of January 2022, see Table 2.3 for the exact numbers (own illustration based on data from 50Hertz et al., 2022).

BRM, there appears to be sufficient demand coverage, even when subtracting the soon to be phased-out technologies nuclear, hard coal, and lignite. Even though the economics of reserve provision are changing and may further change significantly in the future, it is hence unlikely that there will be a scarcity of reserve capacity from a technical perspective.

2.1.5 Further system services

The scope of this thesis is clearly set on the electricity spot markets and the BRMs. However, besides balancing reserves, further system services or so-called ancillary services are distinguished. These system services are necessary to ensure a safe and stable operation of the electricity grid. As in continental Europe the system services aside balancing energy are nowadays mostly not traded in market-like structures or are limited to special demand groups, they are mentioned here for completeness but will not be further investigated in the thesis. However, for some system services there are markets implemented in other countries. Even though

Technology	FCR	aFRR+	aFRR-	mFRR+	mFRR-
Nuclear	0.22	0.18	0.19	1.27	1.27
Lignite	0.56	1.20	1.21	4.16	4.20
Hard coal	0.48	1.05	1.07	2.98	2.88
Natural gas	0.35	3.53	3.57	7.10	6.94
Oil	0	0.26	0.03	1.28	0.09
Biogas/biomass	0.04	1.84	2.29	2.27	2.75
Hydro	4.79	15.10	15.15	13.99	14.01
Battery storage	0.48	0.08	0.06	0	0
Demand/DSM	0.02	0.12	0.07	0.20	0.14
Wind	0	0	0.03	0	0.22
Others	0	0.01	0.01	0.11	0.3

Table 2.3: Prequalified balancing reserve capacity in GW in Germany as of January 2022 (50Hertz et al., 2022).

these services do not offer a revenue stream for regular market participants as of today, they might become more relevant in the future with less conventional generation capacity in the system.

To guarantee frequency stability and the system balance, besides balancing energy the interruptible loads are contracted by the TSOs. These are typically energy-intensive industrial processes that can be suspended temporarily to support the electricity system. In Germany, quickly (activation within 15 minutes) and immediately (activation within 0.35 seconds) interruptible loads are distinguished, and 750 MW of each are tendered on a weekly basis (50Hertz et al., 2021; TransnetBW, 2021).

Another element of frequency stability is the so-called instantaneous reserve (German: Momentanreserve) that intends to smooth frequency drops without delay and thus limits frequency gradients and deviations. Whereas the other mentioned frequency containment or restoration reserves are based on an increase or decrease of the power feed-in or consumption of a technical unit, the instantaneous reserve is based on the inertia of the technical units in the system. In the current European electricity system, there are sufficient technical units that generate electricity based on masses in rotation with system frequency. These rotating masses provide instantaneous reserve inherently (and could technically also not

avoid to do so) and form a system with sufficient inertia, so that there is no need for the TSOs to procure this service as of today. However, there are studies investigating the need for instantaneous reserve to preserve system inertia in future, vRES-based electricity systems (e.g., dena, 2016, 2020). A prominent example of a system lacking inertia is the United Kingdom, where the TSO National Grid introduced a dynamic containment product. This dynamic containment product with a full activation time of maximum one second corresponds to the provision of instantaneous reserve. Among others, battery storages are technically able to provide this service and generate a significant revenue stream by providing it.

Another ancillary service is the provision of so-called reactive power (German: Blindleistung), and addresses the voltage stability in the alternating-current-based grid. Reactive power is provided by various technical units, such as thermal power plants, decentralized energy resources and even loads, but the effective range of technical units providing reactive power in the grid is limited, leading to the necessity to ensure that sufficient reactive power is available regionally and on each voltage level. This regional and grid-topological scope as well as today's sufficient provision of reactive power makes the setup of a market for it both challenging and not necessary. However, with a higher capacity utilization of power lines, the amount of reactive power required for stable grid operation will increase (dena, 2020).

The last ancillary service to be mentioned in this section is the so-called black-start capability, and describes the ability of an electricity grid to re-establish operation after a blackout. However, this is also rather a future challenge, as today there are sufficient large generation units on the highest voltage level to re-establish grid operation and therefore no economic incentivization is necessary for the market participants to provide black-start capability (dena, 2020).

The fact that the mentioned ancillary services are not part of the current market design does not exclude them from market designs in the future. Particularly providers of instantaneous reserves and reactive power, but also black-start capability will become increasingly important in a decentralized electricity system with a dominant share of non-synchronous generation technologies that feed in inverter-based and are not spinning synchronously with the system frequency. Therefore, in case there is a need for explicit incentives to maintain system security, providers

of these ancillary services will potentially be compensated explicitly in the future. However, in the scope of this thesis, they can be neglected.

After the institutional framework of this thesis and the need for spot and balancing reserve markets are introduced, the next section will summarize essential theoretical concepts and definitions of uncertainty and risk. Further, a taxonomy of risk will be provided to categorize the corporate risks that are addressed in the papers included in this thesis.

2.2 Uncertainty and risk in electricity markets

2.2.1 Definitions of uncertainty and risk

In the previous section, the background with regard to the institutional circumstances of electricity markets was provided. The second basic element of this thesis is uncertainty and the associated risk. On the one hand, these terms are often used intuitively and without scientific claim to precision in daily life, and on the other hand they are used in many scientific and business contexts. Therefore, in the scope of this thesis, it is worth to define them. Further, a typology of risk sources and measures to quantify risk exposure will be introduced to enable the reader to categorize the approaches and models that are developed in this work.

According to the Oxford Learner's Dictionary of Academic English (2021) *uncertainty* is “the state of not knowing [...] exactly” and something *uncertain* is “something that you cannot be sure about”. Ibidem, *risk* is referred to as “the possibility of something bad happening at some time in the future” and “a situation that could [...] have a bad result”. These definitions are fully in line with the intended use in this thesis and the included studies. However, to be able to treat uncertainty and risk quantitatively, further definition of the terms is necessary. The following assumptions and definitions are essential and remain valid in the rest of this thesis.

The following definitions are adapted from and notation-wise in line with Birge and Louveaux (2011) and Chung (2001). Let the future be describable by a finite set of parameters that are relevant to the decision problem (i.e., the space of all potential outcomes for the future). Whereas some of the parameters are deterministic, some others are subject to uncertainty and are represented by random vari-

ables. Let the triplet (Ω, \mathcal{A}, P) be the probability space containing all outcomes of random variables and combinations of them. Ω is the set of all potential outcomes. A single outcome is referred to as an event A , and \mathcal{A} is the set of all events. For each $A \in \mathcal{A}$, a probability $P(A)$ is defined, such that $0 = P(\emptyset) < P(A) \leq P(\Omega) = 1$ and $P(A_1 \cup A_2) = P(A_1) + P(A_2)$, if $A_1 \cap A_2 = \emptyset$.

Based on this definition, an important distinction can be made between uncertainty and ignorance. Ignorance can occur in two ways: (a) It can occur in the form of “unknown unknowns”, as former US Secretary of Defense Donald H. Rumsfeld once put it (Rumsfeld, 2002), i.e., Ω is not completely known or \mathcal{A} is infinite. (b) It can further occur in the form of imprecise probabilities, i.e., even if Ω and \mathcal{A} are known completely and finite, there is no unambiguous representation of the probability distribution of some or all events $A \in \mathcal{A}$ (Bradley, 2019). A famous classic example for a probability space with ambiguous probabilities is the Ellsberg problem (Ellsberg, 1961).

In the scope of this thesis, only decisions under uncertainty and not those under ignorance are considered. A decision problem under uncertainty is hence defined as a decision problem that satisfies the aforementioned probability space characteristics. Where no confusion is expected, such a probability space will be denoted leniently by Ω in the remainder of this thesis.

For a particular random variable ξ and a subset $\omega \subset \Omega$, in accordance with Birge and Louveaux (2011), the following definitions hold. Let

$$F_\xi(x) = P(\{\omega | \xi \leq x\}) \quad (2.1)$$

be the cumulative distribution. This cumulative distribution can either be described with a functional relation or by empirical data, in which cases the terms cumulative distribution function (CDF) and empirical cumulative distribution function (ECDF) are used, respectively.

Further, the two cases of discrete and continuous random variables can be distinguished. A discrete random variable can take a finite number of different values. The probability distribution for a discrete random variable is defined with the list of possible values, ξ^k , $k \in K$, and with associated probabilities, as

$$f(\xi^k) = P(\xi = \xi^k), \quad s.t. \sum_{k \in K} f(\xi^k) = 1. \quad (2.2)$$

On the other hand, a continuous random variable is described with the so-called density function $f(\xi)$. In the density function, the probability of ξ being in an interval $[a, b]$ is defined as (Birge and Louveaux, 2011)

$$P(a \leq \xi \leq b) = \int_a^b f(\xi) d\xi. \quad (2.3)$$

Please note, that the approaches deployed in the papers B and C of this thesis use discrete probability spaces. This is mainly due to algorithmic reasons, as will be outlined in Section 3.3. In discrete probability spaces, the events as realizations of the future are typically referred to as scenarios. If the uncertainty unfolds in multiple stages, the scenarios can be described as paths through a directed graph.

For the special case of a branching-out graph structure (i.e., each successor has a single predecessor, but a predecessor has one or multiple successors), this directed graph is also referred to as a scenario tree. Hereby, the different final states $\omega \in \Omega$ are perceived as the scenario leaves. A second special case of a branching graph structure is the so-called scenario lattice, which is sometimes also referred to as recombining scenario tree. Here, a successor may have several predecessors, and thus a larger number of scenarios can be generated with a fewer number of modelled states for each stage (Heitsch and Römisch, 2009). Both special cases comply to desirable structures of probability spaces and are widely used to model uncertainties in the electricity market context (cf., e.g., Wallace and Fleten, 2003; Plazas et al., 2005; Weber, 2005; Keles, 2013; Löhndorf et al., 2013; Boomsma et al., 2014; Wozabal and Rameseder, 2020, to name just a few). As the generation and reduction of scenario trees is essential to this thesis, a separate section (3.2) is dedicated to it.

Furthermore, in a situation of stochastic decision-making, the set of possible decisions or actions X is defined by the action space \mathcal{X} , which may contain discrete and continuous decision variables. Further we assume a value function $z(x, \Omega)$ that is defined for each decision $x \in X$ and for all states in Ω , and maps them on \mathbb{R} . Note, that as a consequence, z is also a random one-dimensional¹⁶ variable defined in Ω .

¹⁶Generally, a value function could also be multi-dimensional and map \mathcal{X} and Ω on \mathbb{R}^n . However, for the problems in the scope on this thesis, it is sufficient to consider one-dimensional value functions.

To be able to talk about risk in a quantitative and unambiguous way, let the distribution of z , in the papers of this thesis typically a profit distribution, be known in the form of the CDF or the ECDF. The risk exposure of a decision x can then be expressed by measures (a) based on descriptive figures of the entire distribution (e.g., variance), (b) based on predefined threshold values (e.g., the shortfall probability), or (c) by measures based on predefined sections of the distribution (quantiles). In the following these measures will be referred to as risk measures. Please note, that the terms risk metric and risk measure are used interchangeably in this thesis and the papers.

Artzner et al. (1999) define a set of four properties of risk measures that are desirable for financial risk management: monotonicity, sub-additivity, homogeneity, and translational invariance (cf., Artzner et al., 1999, for the mathematical formulation of the properties). A risk measure that satisfies these properties is referred to as a coherent risk measure. In the following, commonly used risk measures are presented. For a more detailed discussion and calculation examples, the interested reader is referred to Conejo et al. (2010).

The variance of z is one representative from group (a) of risk measures. Hereby, the variance of a discrete random variable $z(x, \omega)$ ¹⁷ is defined as

$$\text{Var}(z) = \sum_{i=1}^n p_i (z_i - \mu)^2, \quad (2.4)$$

with p_i being the probability of i and

$$\mu = \sum_{i=1}^n p_i z_i \quad (2.5)$$

being the expected value of z over all n observations in Ω . It provides a measure on how much the values of z typically deviate from the expected value. The square root of the variance is referred to as the standard deviation. The variance is famously used by Markowitz (1968) in modern portfolio theory, in which efficient decisions in mean-variance analysis are defined as non-dominated pairs of expected value and variance of (stock) returns. However, the variance

¹⁷This means, z is dependent on decision x and realization ω . For better readability, the (x, ω) will be dropped in the text in the following.

takes into account both deviations in upward and in downward direction and is sensitive to outliers. Further, the variance is not positively homogeneous and not sub-additive, and thus not a coherent measure of risk. Therefore, different risk measures that are more robust and focus on the risk of loss, have been developed.

An intuitive approach leads to group (b) of risk measures, using threshold values to quantify the risk. The shortfall probability SP is defined as the probability of the random variable $z(x, \omega)$ to fall below a predefined threshold value μ . For the discrete case this translates to

$$SP(\mu, x) = P(\omega | z(x, \omega) < \mu), \quad \forall \mu \in \mathbb{R}. \quad (2.6)$$

Based on the threshold μ , the expected shortage ES is defined as the expected value of z , in case the realization of z is below μ . This leads to the formula

$$ES(\mu, x) = \mu - \frac{1}{SP(\mu, x)} \mathbb{E}_{\omega \in \Omega} \{ \max\{\mu - z(x, \omega), 0\} \}, \quad \forall \mu \in \mathbb{R}. \quad (2.7)$$

However, the use of an arbitrarily fixed threshold can be impractical and further does not comply with the properties of a coherent risk measure. Therefore, the last group (c) of risk measures is based on quantiles of the profit distribution. Firstly, the value-at-risk (VaR), denoted by $\text{VaR}(\alpha, x)$, is defined as the quantile of the distribution of z at $(1 - \alpha)$ -level. Thus, α denotes the probability, with which the z will be lower or equal the VaR. Mathematically, the VaR is defined as

$$\text{VaR}(\alpha, x) = \max \{ \mu : P(\omega | z(x, \omega) < \mu) \leq 1 - \alpha \}, \quad \forall \alpha \in (0, 1). \quad (2.8)$$

As the VaR only captures the quantile (point) value, it does not contain any other information about the distribution of z (e.g., the profit distribution), particularly not about distribution below the quantile. This means, in case of a so-called fat tail (i.e., a large loss with a low probability), the VaR would not be able to capture the risk appropriately. Further, the property of sub-additivity cannot be satisfied, meaning that it violates the diversification principle¹⁸ for some problem structures. Thus, it is also not a coherent risk measure.

¹⁸The diversification principle refers to the intuition, that the risk exposure of a portfolio with two elements is lower or equal than the risk exposure of the two elements considered alone. Mathematically, it is ensured by sub-additivity.

Another quantile-based risk measure that has gained a lot of popularity due to desirable mathematical and computational properties is the conditional value-at-risk (CVaR), denoted by $\text{CVaR}(\alpha, x)$. Based on the definition of the VaR, the CVaR measures the expected value of z in case its value falls below $\text{VaR}(\alpha, x)$. Mathematically, it can be expressed for a discrete distribution as (Conejo et al., 2010)

$$\text{CVaR}(\alpha, x) = \max \left\{ \mu - \frac{1}{1-\alpha} \mathbb{E}_{\omega \in \Omega} \left\{ \max \{ \mu - z(x, \omega), 0 \} \right\} \right\}, \quad \forall \alpha \in (0, 1). \quad (2.9)$$

As the CVaR addresses all the major weaknesses of the other presented risk measures, and also satisfies the properties of coherency defined by Artzner et al. (1999), it is selected for the consideration of risk in Papers B and C. Further, the CVaR is used in several papers handling risk in the electricity market context that are published in prestigious journals (e.g., Morales et al., 2010; Laur et al., 2018; Wozabal and Rameseder, 2020). Thus, it can be considered the state-of-the-art benchmark at the time of preparing this thesis. A detailed formulation of how to integrate the CVaR into stochastic optimization problems is provided in Paper C¹⁹.

There is obviously a trade-off between profitability and risk exposure, meaning that an optimized decision can either sacrifice expected profitability for a lower risk exposure or increase expected profitability at the cost of higher risk exposure. In this thesis, the risk exposure is integrated into the objective function of optimization problems as a linear combination of expected profitability and the risk measure (Eq. 2.10). In that sense, π^* denotes the profitability metric including risk, with α denoting the considered probability level of the CVaR, and λ denoting the weight assigned to the risk measure. λ can hence be interpreted as the risk aversion parameter. $\lambda = 0$ corresponds to risk-neutral decision making, whereas $\lambda = 1$ only considers the risk measure, e.g. the expected value of the worst 5% cases, and therefore corresponds to a high degree of risk aversion.

¹⁹One might expect the CVaR to be computationally very expensive. However interestingly, the supposedly simpler VaR comes with comparably much higher computational expenses in stochastic optimization problems, as many auxiliary binary variables are necessary. The integration of CVaR does not need auxiliary binaries and is therefore not only a mathematically desirable coherent risk measure, but also computationally desirable.

$$\pi^* = (1 - \lambda) \cdot \mathbb{E}(\pi) + \lambda \cdot \text{CVaR}_\alpha(\pi), \quad \forall \alpha \in (0, 1), \lambda \in [0, 1] \quad (2.10)$$

Moreover, the tuple (α, λ) defines the risk attitude of a decision maker. This risk attitude is determined by the share of the distribution to be considered worst cases and the weight that should be given to their expected value in the decision-making. In this logic, by varying α and λ in the problem formulation, efficient decisions can be derived for different risk attitudes. In Papers B and C, the tuples of \mathbb{E} and CVaR of efficient decisions for different (α, λ) -combinations are referred to as efficient frontiers of the decision problem.

Finally, please note that the presented framework generally can only consider quantifiable risks, i.e., the distribution of z must be known. Qualitative risks or hardly quantifiable risks pose a limitation to this decision-making framework. In the next section, a taxonomy of risk as well as the major sources of uncertainty for corporates and decision-makers in electricity markets are presented.

2.2.2 Taxonomy of risks and key uncertainties in the energy sector

When single decisions or a set of interdependent decisions are optimized for profitability and risk exposure, obviously only a small share of the entire corporate risk of an electricity market participant (e.g., an energy supply company) can be captured. To gain an overview over the bigger picture of risks and the main sources of uncertainty, this section presents a taxonomy of the corporate risks a company in the energy sector may be exposed to. For more thorough treatments of this topic, the interested reader is referred to existing literature, e.g., Bergschneider et al. (2001), Pilipović (2007), and Mack (2014). That literature body might in parts appear a little out of date, but still covers the main aspects of risk management in the energy, and in particular the electricity sector. It will therefore serve as a basis for the following paragraphs, and will be complemented by new aspects where necessary.

The corporate risk can be distinguished into internal and external risks (Wolke, 2015). Whereas internal risks are risks that arise from the business strategy and

operational processes, external risks are risks that stem from links to the business environment. The temporal scope of the (internal) decisions is one dimension, along which risks are typically distinguished.

Along the temporal scope, risks can be subdivided into strategic risks that are associated to long-term (strategic) decisions such as mergers and acquisitions, investments, research and development activities, or location planning, and operative risks that are linked to the operative decisions such as staff planning, project development, technical operation of plants, or financing decisions. On the operative level, the risks can be further divided into risks associated with short-term and with mid-term decisions. In particular, the short-term operative decisions also contain the trading activity on electricity markets that is the main scope of the Papers B and C. The main characteristic of internal risks is that they can be actively influenced by the company's business decisions.

Orthogonal to the temporal dimension, the external risks can be subdivided into six subcategories, representing the interfaces to the business environment: (a) market risks, (b) nature risks, (c) legal risks, (d) policy risks, (e) society risks, and (f) other risks. The main characteristic of external risks is that they do not (or hardly) lie in the influence of the company. Please note, that in aforementioned literature (b) and (e) are sometimes included in (f) as *other* risks. However, in the light of weather-dependent electricity generation, natural disasters, climate change, and societal uprising against business activity²⁰, they are listed separately here. An example for other risks may be the counter-party risk.

Whereas the external risk categories cannot be treated completely independent, this thesis sets the focus on decisions and the arising risks associated with markets. However, it appears obvious that policy measures such as the implementation and adaption of emission trading systems, phasing-out or subsidizing of technologies, and European integration have an impact on electricity markets. Further, nature risks such as droughts that impede hydro power generation, but also the logistics and plant operation for conventional power plants and variations in vRES generation have a potentially huge impact on electricity markets, both in the short and in the long term. It must be noted, that market risks do not only contain risks that

²⁰The author wants to avoid subjectivity at this point. Though the motivations for demonstrating against nuclear plants, opencast lignite mining, and emitting greenhouse gases, but also against transmission grid expansion and wind turbines, are acknowledged, from a business perspective these actions pose a risk.

are directly linked to the electricity markets, but also risks linked to other markets, such as resource commodity and carbon markets, stock, financial and real estate markets, as well as the labor market. Further, as Weber (2005) mentions, there are also model risks. This means, there is also the risk that the models, based on which operative and strategic decisions are assessed and ultimately taken, can be imprecise or even contain major errors and invalid assumptions.

Finally, to get the complete picture of the corporate risks for companies in the electricity sector, it is helpful to consider the electricity value chain – consisting of fuel extraction and transport, generation, trading, as well as sales and retail – as a third dimension. Note, that the transportation and distribution of electricity are not mentioned in this categorization, as these are typically not under competition but regulated. The presented taxonomy thus results in a three-dimensional structure that is illustrated in Figure 2.7. In the next section, the papers included in this thesis are allocated in this taxonomy.

2.2.3 Categorization and allocation of the thesis in the taxonomy of risks

For the reader, it might be interesting how the papers included in this thesis can be categorized in the presented taxonomy of risks. For that purpose, the following paragraphs and Figure 2.8 provide a categorization and allocate the scopes within the presented taxonomy.

For a short-term price forecasting paper, such as Paper A of this thesis, it comes quite natural that the main risk investigated is short-term market risk, and is associated with trading. The forecasting framework developed in Paper A thereby allows not only to derive a point forecast, but the different methods also allow to derive confidence intervals as well as ensemble-based distributions of the price expectation. These are valuable – if not inevitable – information for managing market risks. However, Paper A does not consider the decision-making aspect.

The main risks that are investigated in Papers B and C are the ones associated with the short-term volume and price uncertainty in the considered balancing reserve and spot market segments. These arise on the one hand from market-inherent risks, such as the bidding decisions of other market participants or load

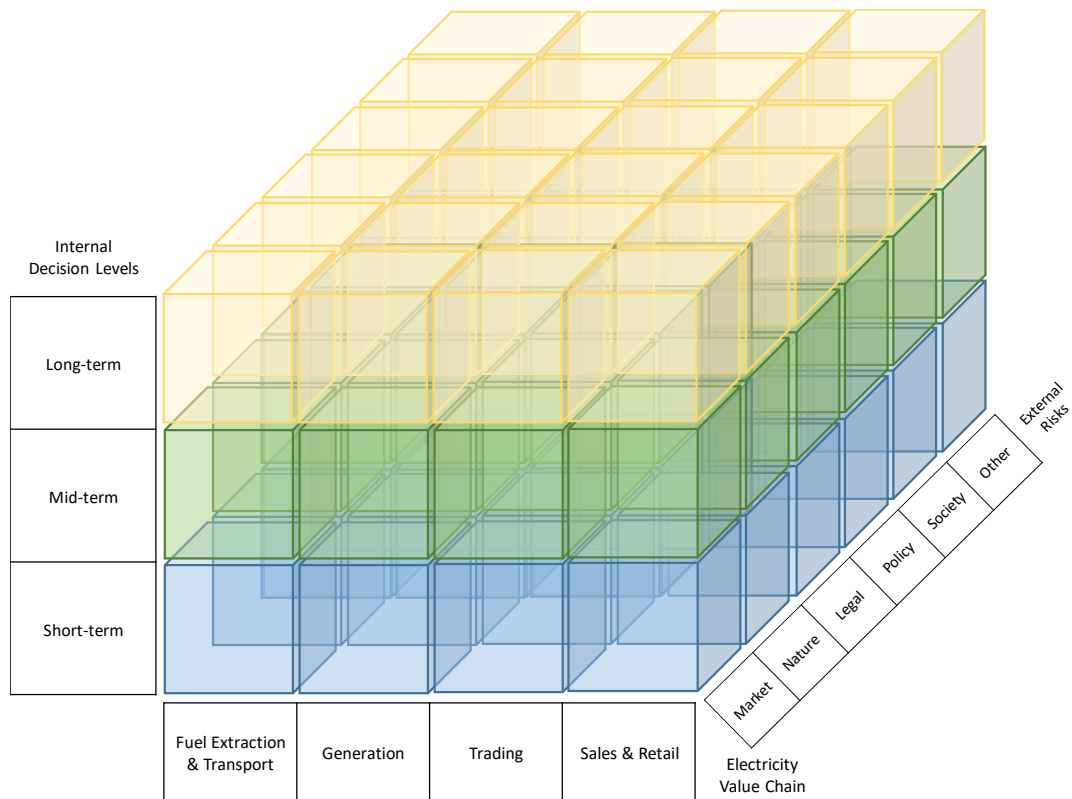


Figure 2.7: Categorization of risks in the presented taxonomy of corporate risks for companies in the electricity sector. The three dimensions “internal decision levels”, “external risks”, and “electricity value chain” allow for a precise allocation of risk topics in the complex environment of the electricity sector.

uncertainty, but on the other hand also from nature risks such as the weather that then translate into markets risks via volume and price effects. Risks linked to the weather, such as water inflows to rivers or reservoirs and the overall electricity demand, have been in the scope of research and business for a long time. However, the risks associated with the generation of solar and wind power, and particularly the proper translation into price and volume risks for market participants, is a relatively new topic for energy economics. The generation of sound scenario trees for various type days including information on prices, vRES generation volumes and the (residual) load²¹, is hence a valuable set of information for risk management by itself.

In addition, trading strategies are determined and analyzed that take the risk exposure and different risk attitudes into account. Therefore, these papers provide an important contribution to an effective management of the risks at the intersect of market and nature risks. Undoubtedly, in the light of the decarbonization of the electricity system, these risks gain more and more in importance when managing the operative internal risks of a company. In that context, it must be stressed that the market participants cannot use the traditional products of the future market to hedge against these short-term market risks.

The papers in this thesis hence have a clear focus on risks on the short-term decision level, while risks on the long-term and mid-term level are not considered in detail. Figure 2.8 summarizes the categorization and delimitation of the papers contained in this thesis in the broader taxonomy of corporate risks for companies that are active in the electricity sector.

In the following Chapter 3, the methodological background of the models developed in the papers of this thesis is provided. Section 3.1 provides an overview over times series modeling and forecasting methods, and addresses the modeling of uncertainty. Section 3.2 discusses approaches to generate scenarios from it. The subsequent use of the scenarios is such that they are used for decisions to maximize profits from market operations, while taking the risk exposure into account (Paper B and Paper C). For that purpose, Section 3.3 presents and discusses different approaches of optimization under uncertainty.

²¹The term residual load refers to the overall load minus the generation of RES and corresponds to the load that must be satisfied by conventional generation capacities.

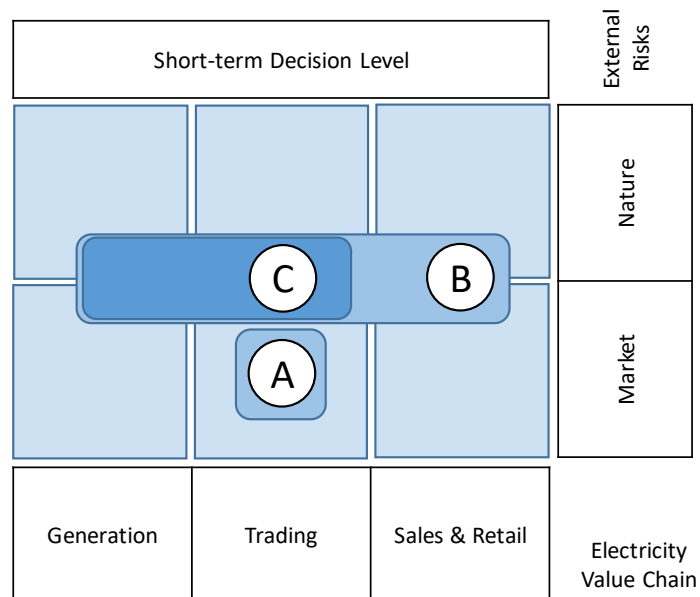


Figure 2.8: Categorization and allocation of the papers within the taxonomy of corporate risks for companies in the electricity sector (cf. Figure 2.7). The papers are allocated on the short-term (operative) decision level, at the intersect between market and nature risks, and cover the value chain across generation, trading, as well as sales and retail.

Chapter 3

Methodology

3.1 Modeling of time series and forecasting

3.1.1 Categorization of time series modeling approaches

When it comes to analyzing the energy system and electricity markets, building (stochastic) models has a long tradition in energy economics. Although one can think of many parameters to be modeled, for the sake of readability and to fit the scope of this thesis, let the parameters of interest be the balancing reserve and spot market prices. This is without loss of generality, however the prices appear to be the most relevant and challenging parameters to model. In the field of modeling electricity prices, there exists a variety of approaches that are distinguished into three categories in this thesis. Other authors (e.g., Weber, 2005; Weron, 2014; Lago et al., 2021) may present slightly different categories depending on their scope, but the general structure of the typology remains consistent with the one proposed here. The three proposed categories consist of the two classical categories (a) *fundamental models* and (b) *finance and econometric models* (as distinguished by Weber, 2005), and are complemented by the relatively new category (c) *machine learning models*.

(a) First, there are *fundamental models* that try to capture the fundamental relations in the system and derive the values for the parameter of interest from it. There exist many fundamental modeling approaches, such as cost-minimizing energy system models or agent-based electricity market simulation models. These

models vary largely in complexity and temporal as well as technical resolution. Although in other works a further distinction by optimization and simulation is undertaken, they are included in one category in this thesis, as they share the attempt to model the fundamental relations leading to the market prices. The reader is referred to a rich body of literature for further reading on fundamental models. Most relevant to this thesis, Maaz (2017) and Ortner (2017) develop fundamental models of the BRM in order to derive its prices. Further, Genoese (2010) develops a fundamental agent-based simulation model for the electricity market in order to derive its prices²².

Chiodi et al. (2015) provide a starting point to the world of cost-minimizing energy system models that will not be discussed further due to conciseness. Further, game-theoretical models (see, e.g., Ocker, 2018, for a model of the BRM) as well as system dynamics models (see, e.g., Petitet, 2016) are deployed to explain prices fundamentally. However, these model categories are also not further discussed in this thesis.

(b) Second, *finance and econometric models* mostly neglect the fundamental relations of price formation and attempt to capture the mathematical and statistical relations and properties of the time series as precisely as possible. Therefore, these are also referred to as statistical models or financial (mathematical) models. As Weron (2014) describes it perfectly concise, econometric models use “a mathematical combination of the previous prices and/or previous or current values of exogenous factors” to explain or forecast price time series.

These models are highly relevant to this thesis, as Paper A develops econometric models and Paper B as well as Paper C base their modeling of uncertainty on econometric models. However, not only econometric models are necessary to characterize uncertainty appropriately. To model the properties of price dynamics and uncertainty, such as in Paper B and C, financial models are widely used to model the stochastic residuals of econometric time series models. The next Section 3.1.2 will therefore provide an introduction to this family of finance and econometric models.

(c) Third, *machine learning models*, often also referred to as computational intelligence or artificial intelligence, attempt to model times series and have gained

²²Many works build on this model and developed it further, see also Ringler (2017); Bublitz (2019); Fraunholz (2021).

increasing interest in recent years (Lago et al., 2021). This class is hard to define precisely and undergoes a very dynamic development. However, the main approaches that are used for modeling prices time series are artificial neural networks (ANNs), models based on fuzzy logic, support vector machines and to some extent also evolutionary computation approaches (cf. Weron, 2014).

From the mentioned approaches, this thesis deploys ANNs to model reserve market prices in Paper A. Section 3.1.3 will therefore provide some background on the general idea behind ANNs and their application to forecasting of time series. The other mentioned approaches are not further discussed in the scope of this thesis.

At this point, it is important to note that none of the introduced approaches is strictly dominant over the other and therefore always preferable over all the others. Some are the most accurate in the short-term, others in the long-term, some are the most suitable in terms of explanatory power or replicating desired statistical properties, others in computational tractability, or in treating situations of data scarcity. The selection of the modeling approach is thus a challenge for itself. Further, the mentioned approaches can also be combined to generate models to explain and to forecast time series (see, e.g., Wallis, 2011, and references therein).

3.1.2 Finance and econometric time series models

Explaining and forecasting time series has been a challenge in statistics and financial mathematics for a long time. Precisely, the task is to explain the variation in the values of a dependent variable over time by its previous values and by previous or current values for exogenous variables (Weron, 2014). The forecasting task then consists in predicting the future, i.e., in going one time step further and predicting the next value(s) of the time series. The interested reader is referred to dedicated books by Box et al. (2016) and Brockwell and Davis (2006, 2016) for basics on econometric modeling of time series. Lütkepohl (2006) and Backhaus et al. (2015) provide extensions to time series models for the multivariate case that enables to model a vector time series. For the basics of mathematical finance models, the reader is referred to Pliska (2007) or similar works.

The concept that is the most important for understanding the approaches used in the papers of this thesis, is to decompose deterministic and stochastic com-

ponents of a time series. In the most simple formulation, and by neglecting any influence of exogenous variables on X_t , this can be summarized as²³:

$$X_t = X_t^{\text{deterministic}} + X_t^{\text{stochastic}}. \quad (3.1)$$

However, it must be ensured that the stochastic component follows a stationary process, that means that the (joint) probability distribution of the process, which is a random variable in the terminology of section 2.2.1 does not change over time. Therefore, inspired by Brockwell and Davis (2016) who formulate the *classical decomposition* model with a trend component, seasonal component and a stationary stochastic residual, a reformulation for Eq. 3.1 leads to a simple formulation of a time series model with trend component m_t and seasonality component s_t as follows:

$$X_t = m_t + s_t + X_t^{\text{stochastic}}. \quad (3.2)$$

The idea is then to find a suitable model for the deterministic component(s) and a suitable model for the stochastic component. Möst and Keles (2010) and Keles et al. (2012) provide a review of model alternatives for this approach to model the uncertainty of parameters in electricity markets in general and the one of electricity prices as a parameter in particular.

Based on these, Papers B and C develop stochastic price models for reserve prices for positive and negative aFRR as well as for spot market prices for the DAM and the IDM. A special characteristic of the developed models for the spot market is the joint modeling of the stochastic components for vRES feed-in, residual load, and prices. This allows to meet the stochasticity of prices in electricity markets with high vRES shares in the modeling.

When defining a stochastic model, the first step is the attempt to capture as much variation of the time series in the deterministic components as possible²⁴.

²³In these puristic finance models, the fundamentals are neglected, and the goal is to model the properties of a time series to be able to replicate them. However, when causal relationships to exogenous variables are known, one can include these to improve the explanatory power of the additive models, as done in the stochastic modeling in Paper B and Paper C. In doing so, the stochastic component is typically reduced as more of the variation is explained by the deterministic component and less remains with the stochastic component.

²⁴However, it must be noted that the issue of overfitting a model with the data is often underestimated, particularly when working with highly non-linear or machine learning models. A maximization of the share of explained variation is therefore to be understood in such way

For this purpose, the most common approaches are additive models. Typically, these make use of the previous values of the dependent variable by including an auto-regressive (AR) component, of the mean value of the previous values of the dependent variable by including a moving average (MA) component, or by including components that consider information from exogenous (X) explanatory variables. A general auto-regressive moving average (ARMA) model can thus be formulated as (Box et al., 2016):

$$X_t = \alpha_0 + \sum_{k=1}^m \alpha_k X_{t-k} + \sum_{l=1}^n \beta_l \epsilon_{t-l} + \epsilon_t, \quad (3.3)$$

where α_k capture the auto-regressive influence of previous prices X_{t-k} and β_l capture the influence of previous errors ϵ_{t-l} on the dependent variable X_t , with horizon m and l respectively. α_0 is a constant and ϵ_t captures the error term.

To treat trends, Brockwell and Davis (2016) suggest two alternatives: (a) adding a trend component to the additive model that is estimated as an exogenous variable, or (b) to eliminate the trend by differencing the time series. In the context of ARMA models, the second method is also referred to as integration, which leads to integrated ARMA (ARIMA) models. However, the formulation remains the same, but the estimation is done on the time series of the differences.

A variety of extensions and variants of the general ARMA model exists. The interested reader is referred to, e.g., Weber (2005) and Möst and Keles (2010) for descriptions of more advanced models. The most relevant configuration on an ARMA model for this thesis is a variant that is applied to forecast the differenced time series of FCR prices in Paper A. It takes into account seasonal components as well as exogenous variables. In Paper A, this is labeled SARIMAX (seasonal auto-regressive integrated moving average model with exogenous variables) and is considered as the best econometric benchmark for the ANN approach.

As discussed in Möst and Keles (2010), there exists also a variety of approaches to model the stochastic component. The simplest and most common one is to define it as a stochastic mean-reverting process, e.g., an Ornstein-Uhlenbeck process (Uhlenbeck and Ornstein, 1930). Mathematically, the process is formulated as a stochastic differential equation with the mean μ , the reversion speed κ , a Brow-

that it remains reasonable. When working with linear models or simple non-linear functions, overfitting is a minor issue.

nian motion (also referred to as Wiener process) W_t , and the diffusion factor σ . Hereby, σ can be interpreted as the volatility of the process, whereas κ determines the time the process requires to return to the mean:

$$dX_t = \kappa(\mu - X_t)dt + \sigma dW_t. \quad (3.4)$$

To be able to capture stochastic behavior that consists of alternating mean-reversion processes (e.g., to account for regimes with price peaks and regimes with regular prices), advanced stochastic processes have been developed. These contain more than one regime and are called mean-reversion jump diffusion processes or regime-switching mean-reversion processes. The transition from one regime to the other can be defined by a Markov process. The calibration of the processes within the regimes and the transition probabilities are done by the help of historical data. This approach is used to derive the price processes for the DAM and the IDM in Paper B as well as for the aFRR in Paper C of this thesis.

Another important insight, particularly with regard to providing theoretical background to the papers of this thesis, consists in the further use of the stochastic models. As described in more detail in Section 3.2, the stochastic models in their closed mathematical formulation are of no practical use for taking complex decisions under uncertainty. Therefore, they are used in Monte Carlo simulations to simulate the stochasticity, and based on this to generate time series for the stochastic component. Eventually, based on these time series, with scenario generation and reduction techniques, a set of discrete scenarios is derived. Finally, the stochastic optimization approaches presented in Section 3.3 can be applied to these scenarios.

At the end of this subsection on finance and econometric models, it is worth spending a few words on the quality of time series models. Obviously, there is a need for selection criteria to determine which lags (i.e., which previous values) and which exogenous variables to consider to obtain the model that explains the process the best. Further, there is a need to identify the model configurations that are most likely to prevail in forecasting. This discussion is briefly addressed here. For a detailed discussion, the reader is referred to James et al. (2013), Ding et al. (2018), and Hyndman and Athanasopoulos (2021).

In general, there are two approaches to compare the quality of models: (a) To compare the errors of model estimation or training, and (b) to compare the performance on a validation data set. These approaches are also referred to as in-sample validation, which compares measures for the goodness-of-fit of the models to the training data, and out-of-sample validation, which compares the predictive performance of the models with unknown data.

For (a), there are several goodness-of-fit measures and selection criteria in the literature. Besides the overall model fit, often depicted by the coefficient of determination R^2 , these measures also consider the number of used predictors to compare the expected predictive power. With the sum of squares of training residuals RSS and the total sum of squares TSS of the time series, R^2 is defined as:

$$R^2 = 1 - \frac{RSS}{TSS} \quad (3.5)$$

An R^2 of zero thereby corresponds to a model that explains no variation in the data at all, and an R^2 of one corresponds to a model for which all residuals are zero. Intuitively, the R^2 cannot become smaller, when additional predictors are added to the model. Therefore, by adding an infinite number of exogenous predictors that contain only random noise one can reach perfect model fit ($R^2 = 1$). However, this does not mean that the model can predict values outside the training data set. Being parsimonious, which means using as few predictors as possible, is therefore a quality criterion of models. With this rationale, for example the adjusted R^2 , the Bayesian information criterion (BIC), the Akaike information criterion (AIC), and the corrected AIC have been introduced to support model selection (see, e.g., Ding et al., 2018; Hyndman and Athanasopoulos, 2021, for the mathematical formulations). These penalize the number of used predictors in different ways. It must be noted, that none of these criteria is exact and superior to the others, but these are practical decision criteria.

For (b), the common approach is to compare figures like the root mean square error (RMSE), the mean absolute percentage error (MAPE), or the directional accuracy (DAC) for each of the proposed models and to rank them accordingly. However, this does not inform the exact statement of which forecasting model is better. For this statement, the goal is to compare the forecasting accuracy of competing approaches. Diebold and Mariano (1995) compare several approaches

to compare predictive accuracy and develop the so-called Diebold-Mariano test, which is a statistical hypothesis test for superiority of competing forecast models. The test compares two time series of forecasting residuals and indicates whether forecast model is significantly better than the other. The Diebold-Mariano test is applied in Paper A of this thesis. Please note that comparing the performance on a validation data set is not limited to finance and econometric models, but can equally be applied to all modeling approaches presented in this chapter.

3.1.3 Machine learning models

Machine learning models are a fast growing field and many different approaches and fields of application exist today. Even when limiting the scope to modeling and forecasting of time series, and particularly to electricity prices, several approaches remain. As the scope of this thesis is limited, this section will not go into further detail for the latter three, but focus on the most common approach to use ANNs.

Neural networks are a concept to describe the general functioning of the brain. In a neural network, an uncountable number of neurons is connected and can transmit information in a directed manner via synapses, if certain criteria are met. The information bits treated by each neuron are relatively small. However, the number and the structure of the neural network, as well as the training and adaptation to similar information patterns, allows the neural network structure to process complex and extensive input data. Eventually, it allows to determine decisions based on processed information as an output. *Artificial* neural networks are replicating this general functioning, and analogously consist of neurons that are connected to each other with edges to build a network structure.

A single neuron is build up relatively simple. As shown in Figure 3.1, input signals x are weighted with weights w and enter a transfer function Σ , typically the weighted sum, in order to provide the net input for the activation function. The activation function uses this net input and evaluates it by comparing it to a threshold value. In case the threshold is met, the neuron fires the value of the activation function to the next connected neurons, which means the neuron is activated and information is transmitted to the next neuron. The next neuron then uses this output as an input signal.

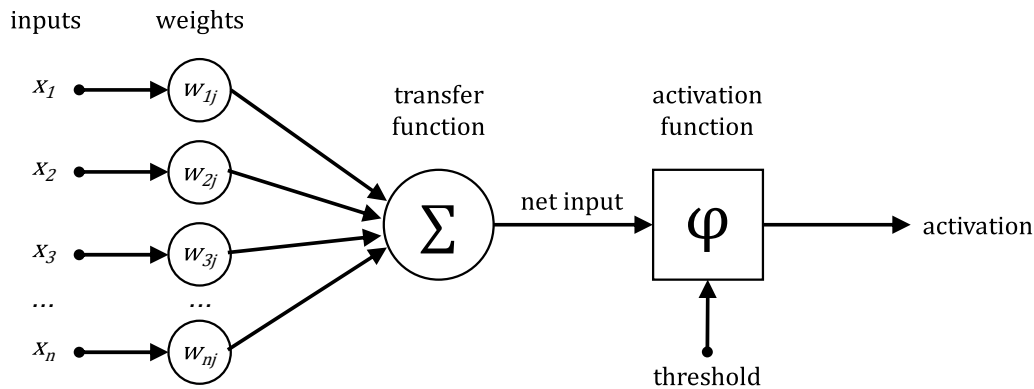


Figure 3.1: Structure and activation of a single neuron j . The inputs are weighted with weights $w_{1j} \dots w_{nj}$ to enter the transfer function Σ . The net input is then evaluated by the activation function φ , and if a threshold is met, the neuron is activated and transfers the output to the neuron it is connected to (own illustration).

With regard to neurons and neural networks, a few words should be spent on the architecture and the training. The architecture of the network is a crucial component when configuring an ANN. As shown in Figure 3.2, the general structure consists of an input layer, an output layer, and – optionally – hidden layer(s) in between. The main parameters are therefore the number of hidden layers and the number of neurons per hidden layer. This allows to capture non-linear relationships between input and output data. Intuitively, the more complex the network is, the more complex these relationships can be²⁵.

In feed-forward ANNs, this network structure is a directed graph and contains no loops. However, there are also recurrent network structures and more complex node types with inherent recurrent structure, such as gated-recurrent units (GRU) or long-short-term-memory (LSTM) units, have been developed in the machine learning community. As there are many fields of application for ANNs, the development is still ongoing and very dynamic. For this thesis, the most important insight is that the standard architecture is a feed-forward ANN. This standard architecture is available off-the-shelf, e.g., in the Python library keras (2021), and is

²⁵As noted before, there is the risk of overfitting the data. However, as the findings of Paper A show, a slight overfit sometimes can be helpful, if it is done consciously and carefully treated afterwards.

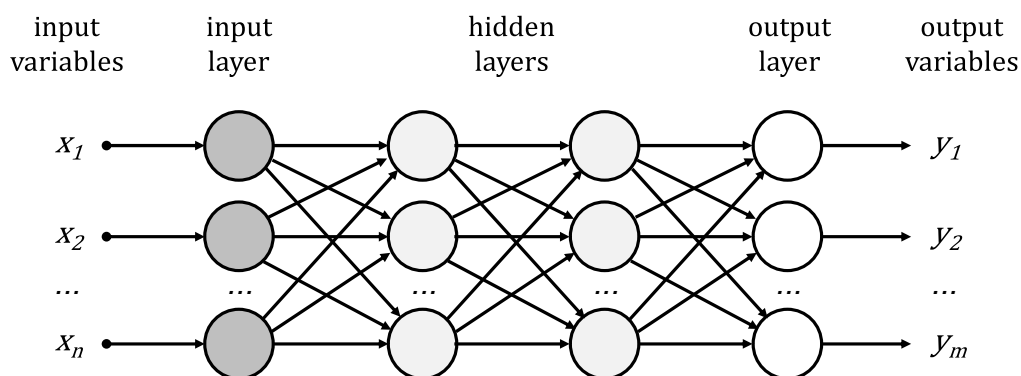


Figure 3.2: General structure of a feed-forward ANN with inputs $x_1 \dots x_n$, input layer, two hidden layers, output layer, and outputs $y_1 \dots y_m$ (own illustration).

deployed in Paper A. Due to conciseness, more advanced ANN architectures are not further discussed in this thesis.

In Paper A, different ANN configurations are developed and evaluated. For typical machine learning problems with rich databases, the architecture can be crucial to model quality. However, due to limited data availability, the case study of reserve prices cannot be considered typical in the sense of machine learning problems and requires a slightly different approach.

This approach is referred to as ensembling and pursues the idea of combining the forecasts of many (individually) wrong models to jointly yield a precise and robust forecast (cf., e.g., Hyndman and Athanasopoulos, 2021). The idea is to train an ensemble of ANNs that vary in nothing but the random starting weights of the neurons and then consider the distribution of different forecasts. Eventually, calculating the average of all members of the ensemble leads to a single forecast value²⁶. In the scope of this thesis, the information contained in the distribution of the ensemble can also be interpreted as a sample for the underlying random variable, such as the reserve price. This distribution could also be used to characterize the uncertainty of the reserve prices and would work as an information basis to derive decisions. However, since this is a practitioner approach and has no

²⁶For applications with rich databases, ensembling has hardly any impact as training many models with the same architecture will yield convergence to a single model despite random starting weights.

proper mathematical foundation, the processes in Papers B and C are estimated based on established stochastic modeling approaches instead.

Another hyperparameter in configuring an ANN is choosing the activation functions in the neurons, see Figure 3.1. Activation functions can be chosen from a set of linear and non-linear functions. The most simple one is the identity function, however more common ones are the sigmoid, the hyperbolic tangent (\tanh), the rectifier linear unit (ReLU), the exponential linear unit (ELU), or the SoftPlus activation function. The reader is referred to Sharma (2017) for the mathematical formulations. Please note that in Paper A, the ReLU was chosen as activation function.

After the architecture is set up, the ANN is ready to learn the relationships it is designed to reproduce. This learning is typically referred to as training. In the process of training, the weights of the neurons are considered as variables. Thereby, training data (i.e., a set of known input and related output variables) is fed into the ANN and by use of backpropagation, the values of the weights are fit to the data by minimizing the training errors. However, the training can be organized in various ways, as explained in more detail in Paper A. The main hyperparameters that define a training strategy are the choice of training data (i.e., which data is used for training), the number of epochs (i.e., how many training sequences are run), and the number of iterations per epoch (i.e., how many iterations of the backpropagation algorithm are run). In the case of ensembling, the ensemble size (i.e., how many separate models are trained) complements the set of hyperparameters.

With these parameters, an infinite number of training strategies can be defined. In Paper A, the focus is set on the comparison of training strategies with a slight overfit and larger ensembles with normal fit and smaller ensembles, under different architectures. In the machine learning community, there are even more hyperparameters to define more sophisticated training strategies. For example, large amounts of data can be handled more efficiently with the help of batching the training data. However, this exceeds the scope of this thesis and is moreover not needed in the case study of reserve prices and sparse data.

To conclude, in Paper A, different combinations of network architecture and the presented training strategies are implemented and benchmarked against econometric models. It must be noted that data availability is a crucial issue when

developing ANN structures, and must be taken into account when designing both deep and shallow ANNs. Despite being a standard technique when working with big data and machine learning and implementations are available off-the-shelf, the adaptation of a particular case as well as a proper experimental design requires considerable effort.

3.1.4 Limitations and extensions of forecasting

To conclude this section on time series modeling and forecasting, it is important to recall three commonplaces, which are nevertheless essential insights: (a) First, no model is perfectly able to capture reality. (b) Second, no data set is perfect. Be it a lack in sheer availability or in the quality of the data, models can never be better than the data used for training or estimation. (c) Third, and most relevant for the remainder of this thesis, uncertainty can hardly be characterized by single point forecasts as they tremendously undercomplexify the information. This third insight can easily be underlined with the example of a dice. For a single throw, a point forecast of the number of eyes of the dice is not trustworthy. For a decision maker to determine sound decisions under uncertainty, it is much more relevant to have an appropriate representation of the probability distribution for the potential outcomes than to have the best point forecast.

In electricity markets as well as in many other domains, the approach of probabilistic forecasting, i.e. forecasting intervals, density, or thresholds instead of points (cf. also Weron, 2014), has gained more and more in importance. One important representative of this approach is the so-called quantile regression. However, a main weakness of these approaches is that they are not able to properly capture complex relationships, such as conditional expectations for several uncertain parameters. Further, in forecasting applications, the error term is typically assumed to be white noise. However, as presented above, stochastic processes of single parameters tend to follow temporal patterns, too.

Therefore, to capture the uncertainty and to provide a solid information basis for decision-making, a common approach is to derive stochastic processes and to then sample from these with the help of Monte Carlo simulation. This generates a large number of possible scenarios that represent realizations of the stochastic processes, but can hardly be handled in decision making approaches. The next

section will thus briefly introduce how to derive representative discrete scenarios for decision making from the stochastic processes. In the sense of providing best available information about the future, scenario generation is therefore a logical extension of forecasting in uncertain situations.

3.2 Scenario tree generation and reduction

The previous section presented stochastic processes that enable to capture uncertainty in a closed and typically continuous formulation. However, these closed formulations cannot be used directly in the available algorithms to solve stochastic optimization problems, but discrete representations are necessary. The general idea behind scenario generation and reduction is therefore to create discrete information sets that represent real-world data or the derived stochastic processes for it as well as possible. Intuitively, there is a trade-off between information representativeness and number of scenarios. The problem was already investigated in the 1990s (e.g., Rockafellar and Wets, 1991) and early 2000s, however it is still very relevant for today's applications in stochastic modeling.

To have a common understanding of a multi-stage scenario tree, some definitions are necessary. The following standard notation is based on Gorski (2017) and slightly adapted where necessary. Let ξ be a multivariate random variable with probability distribution P . Without loss of generality, let ξ_t describe its realizations on stage $t \in \{1, 2, \dots, T\}$ for the multi-stage setting (Heitsch and Römisch, 2009). Let $\xi^t = \{\xi_1, \xi_2, \dots, \xi_t\}$ be a scenario at stage t , consisting of realizations of ξ for each stage up to stage t . Further, let $P(\xi_t|\xi^{t-1})$ be the edge probability, i.e., the probability for realization ξ_t under the condition of ξ^{t-1} . The probability of a path up to stage t is then defined as the product of the individual edge probabilities of the path, i.e., $P(\xi^t) = P(\xi_1) \prod_{i=2}^t P(\xi_i|\xi^{i-1})$. Further, let a directed graph consisting of nodes – representing the discrete realizations of ξ – and edges – containing the edge probabilities – be a multi-stage scenario tree.

The challenge of scenario generation is then to determine the tree structure and size as well as to define discrete values and associated edge probabilities, such that the uncertainty is captured in an appropriate way. To achieve this, several approaches and tree structures exist in the literature. Please note that in this regard only few attention is paid to the tree structure in this thesis. This is mainly due

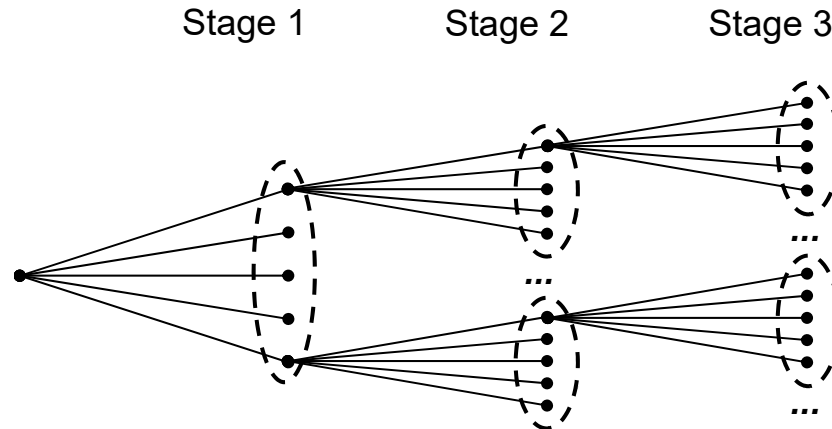


Figure 3.3: Exemplary scenario tree with three stages (own illustration).

to the fact that the developed optimization problems in this thesis consider only two-stage and three-stage trees, for which intuitive branching is possible without exploding numbers of distinct scenarios. Particularly for problems with many more stages, the so-called *curse of dimensionality* leads to hardly tractable problems, i.e., exponentially growing scenario trees when increasing the number of stages or dimensions in the state space. This curse of dimensionality has been described very early (e.g., by Bellman, 1961; Larson, 1967), and led to several algorithmic developments as will be further discussed in Section 3.3. With regard to scenario tree generation, this leads to structures that deviate from the intuitive expansion with a certain number of distinct successors for each predecessor.

Most prominently, scenario fans and scenario lattices should be mentioned. Fans only branch at certain stages of the tree, typically the first, and then consist of single scenario paths for subsequent stages (i.e., after the branching stage each predecessor has a single successor). On the other hand, scenario lattices, also referred to as recombining trees, can be thought of as a Markov process and allow to reach each possible state with some probability from each previous state. The reader is referred to, e.g., Dupacova et al. (2003) and Heitsch and Römisch (2009) for further reading on branching structures and to Löhndorf et al. (2013) for an example of scenario lattices in multi-stage stochastic optimization. For the remainder of this thesis, the tree structure of the problems is two- or three-stage and each predecessor has a certain number of successors, as shown in Figure 3.3.

After the structure of the scenario tree is determined, several approaches exist to define the discrete values and edge probabilities. The most relevant approaches can be classified into (quasi) Monte Carlo methods, methods based on probability metrics, and methods based on moment matching (Löhndorf, 2016). Further approaches are based on internal sampling and decomposition (Higle and Sen, 1996; Higle, 1998), direct sampling or bootstrapping from historical data (Kaut, 2021), and conditional sampling (Kaut and Wallace, 2007). Due to the ready availability of historical data compared to stochastic processes, the “naive” approach to sample or bootstrap from historical data is widely spread. However, it is not able to capture complex stochastic processes and it cannot be guaranteed that the sampling contains all relevant scenarios. Therefore, sophisticated methods to sample from historical data are necessary, as discussed by Kaut (2021).

Many works developing scenarios for stochastic optimization are fundamentally based on stochastic processes that are sampled based on Monte Carlo simulations and afterwards clustered. In the process of scenario generation and reduction, the first step is to simulate the stochastic process many times (e.g., 1000 times). The second step then consists of clustering to reduce the number of discrete scenarios reasonably (e.g., Keles, 2013). A commonly used clustering algorithm is k-means (MacQueen, 1967; Lloyd, 1982). After clustering typically the centroid of each cluster is selected as representative with the relative frequency as probability. This approach is applied in Paper B and Paper C of this thesis to provide the stochastic optimization with sound scenario trees. In that way, these papers provide innovative applications of the state-of-the-art in stochastic modeling and scenario generation in the electricity market context.

Another method to generate scenarios is based on moment matching. Due to conciseness, it is not discussed in depth. The idea behind this approach is to match the marginal moments and correlations of the original (multivariate) distribution. For that purpose, in an iterative procedure, random variables are generated to match the moments and then transformed to also satisfy the correlation structure. However, this transformation changes the moments of the random variable, so that it needs to be readjusted. Høyland et al. (2003) suggest an heuristic algorithm for the case of multivariate distributions. The interested reader is referred to Høyland and Wallace (2001), Kaut and Wallace (2007), Heitsch and Römisch (2009), and Löhndorf (2016) for descriptions, variants, and applications of moment matching.

Finally, approaches that generate an optimal approximation based on probability metrics shall be mentioned. The general idea behind scenario reduction with the help of probability metrics is to determine the best approximation of the original probability distribution by a discrete distribution. For this, the maximization of a predefined probability metric is used as objective criterion in a separate optimization. After the scenario tree is generated (e.g., by simulation of stochastic processes), the idea is to summarize several distinct scenarios within a single scenario without sacrificing too much of the information. This sacrifice is measured with the help of the probability metric that is maximized, and allows to reduce the total number of scenarios in a sophisticated way. For further reading and the mathematical formulation, the reader is referred to a comprehensive body of literature (Dupacova et al., 2000, 2003; Pflug, 2001; Heitsch and Römisch, 2003, 2009).

After the stochasticity is modeled and translated into a scenario tree, the essential last step is the stochastic optimization itself. The next section will therefore discuss approaches to derive optimal decisions for problems under uncertainty.

3.3 Stochastic optimization approaches

3.3.1 Optimization under uncertainty in the energy context

This section aims to give a brief overview over operations research approaches that derive optimal or optimized decisions under uncertainty. With regard to the scope of the thesis, the focus is set on such solutions techniques that are applied in energy economics when a comprehensive quantitative description of the uncertainty is available and formulated in a discrete scenario tree. In energy economics and particularly electricity markets, this is typically the case for short-term operational planning.

The scope of operational planning has been very popular ever since mathematical programming techniques evolved. With the increase of weather-dependent RES, the consideration of the stochasticity of the electricity system found its way to operational planning models. Historically, first the uncertainty of hydro power with stochastic seasonal inflows was included to determine mid-term optimal pro-

duction schedules. In recent years, vRES, such as wind and solar power, became relevant sources of uncertainty to be considered in short-term operational planning.

Stochastic optimization approaches are well-suited to cope with this kind of problems, and are the logical extension of deterministic approaches for operational planning. The operational planning is often also referred to as unit commitment, and can include many dimensions and scopes. By taking into account e.g. non-linear grid constraints, non-linear technical constraints of generation units, or complex dependencies of hydro-systems, the complexity of operational planning models can easily exceed the tractable problem classes and problem sizes. Two comprehensive recent literature review papers are available (Zheng et al., 2015; van Ackooij et al., 2018) that summarize this development from the 1960s until today. These reviews in parts build upon older reviews (such as Wallace and Fleten, 2003; Conejo et al., 2010; Römisch and Vigerske, 2010).

One kind of unit commitment problem, in accordance with Aïd et al. (2016) referred to as *trading problem* in this thesis, is of particular interest. By neglecting any grid constraints and focusing on the generation (and consumption) units in the own portfolio alone, the trader aims at maximizing the contribution margins by bidding into the available market segments. As presented in Paper B and C, with an appropriate modeling of the market segment, this leads to a complex decision problem even if the grid is neglected and technical constraints are considered in a simplified manner.

Following the idea of Rebennack (2010), the solution techniques that are relevant for the trading problem under uncertainty are distinguished into three rather general categories: (a) approaches replacing the stochastic model with deterministic models, (b) exact stochastic optimization techniques, and (c) stochastic optimization approaches that are based on sampling methods²⁷.

van Ackooij et al. (2018) also include chance-constrained and robust optimization as separate approaches for unit commitment problems under uncertainty. This also leads Weber et al. (2021) to distinguish between five major approaches to de-

²⁷Strictly speaking, the approaches in (b) and partly in (c) also replace the stochastic model with a deterministic equivalent that is then treated with decomposition techniques. Category (a) refers to approaches that replace the stochastic model with a non-equivalent deterministic model.

rive decisions under uncertainty for operational planning in energy economics²⁸. However, robust optimization approaches are mainly deployed to make solutions robust and resilient against technical failures with low probability but large impact, such as in the consideration of the grid or technical units in much detail. It will therefore not be further discussed here, but the reader is referred to van Ackooij et al. (2018) and Sun and Conejo (2021) for a detailed discussion and applications.

Furthermore, chance-constrained approaches are mainly deployed when no recourse action is available, i.e., no countermeasure to the realization of the uncertain parameter exist. The idea behind chance-constraints is to guarantee a feasible solution with a certain probability, so-called safety levels. However, this also does not apply for the trading problem²⁹, if intentional imbalances are excluded in the bidding rationale. This thesis therefore focuses on the three categories distinguished by Rebennack (2010).

3.3.2 Replacement of stochastic optimization models with deterministic models

Replacing a stochastic optimization model with deterministic models can be done in many ways³⁰. Weber et al. (2021) report replacing the uncertain parameters by their expected values and running sensitivity analyses as an approach that is still common practice in energy utilities. More sophisticated, another approach consists in solving the distinct branches of the scenario tree separately. Afterwards, a procedure must be defined how to determine a feasible solution. Progressive hedging, as introduced by Rockafellar and Wets (1991), is one variant of doing so. However, whenever the stochastic optimization model can be solved exactly or with sampling-based methods, this should be done instead of relying on deterministic

²⁸There are also heuristic solution techniques such as priority listing, guided random exploration such as nature inspired or genetic algorithms. However, as stated by both van Ackooij et al. (2018) and Weber et al. (2021), these are not competitive to mathematical approaches in operational planning problems, and are therefore not considered.

²⁹One could think of using chance-constraints for the energy balance of a BRP, i.e., ensuring that the schedule is not violated at a certain safety level. However, this would introduce an inappropriate risk to the trading strategy.

³⁰At this point, it is not intended to address the replacement of a stochastic optimization model with the deterministic equivalent, as suggested by Birge and Louveaux (2011) for two-stage models.

models. Besides the fact that convergence to an optimum can hardly be proven, the deterministic model may not consider the uncertainty contained in the scenario tree appropriately and lead to inefficient decisions.

3.3.3 Exact stochastic optimization techniques

Hence, exact stochastic optimization techniques are very popular. If the problem size is small enough, the trading problem can be solved by state-of-the-art solvers, as the representation of uncertainty with the discrete scenario trees is possible within (mixed-integer) linear programming. For two-stage or relatively small multi-stage problems, a solution with Gurobi or CPLEX as standard solvers for mixed-integer linear programs (MILPs) is still possible on server computers. However, particularly integer recourse, which refers to integer variables that affect several or all stages of the decision problem, can pose a problem to computational tractability. During modeling, much care was taken to keep the models mixed-integer linear and to keep the number of binaries tractably small. Therefore, the application of more sophisticated methods, as presented in the following, was not necessary for the preparation of the Papers B and C in this thesis.

However, when extending the scope of the models in future research, at some point decomposition methods become inevitable to solve the problems in reasonable time. The idea behind decomposition is to split the mathematical problem into several smaller problems that can be solved more easily. The preferable decomposition strategy is typically closely associated with the structure of the problem, and aims at decomposing the original problem along complicating variables or complicating constraints. Like that, units, scenarios, or decision stages are solved isolated and afterwards the solutions are merged in an iterative manner. Well-known decomposition techniques include (nested) Benders decomposition, (augmented) Lagrangian relaxation, alternating direction method of multipliers (ADMM) or Dantzig-Wolfe decomposition. Many works are dedicated to the development and application of decomposition approaches. Due to conciseness, the reader is referred to appropriate text books (e.g., Boyd, 2010; Birge and Louveaux, 2011; Pflug and Pichler, 2014) for detailed descriptions and discussions of advantages and disadvantages of the mentioned methods.

Although there are many decomposition techniques, these techniques reach their limits at a certain problem size and complexity. Particularly the nested structure of decomposition can lead to a hardly tractable number of sub-problems and/or very high computational expenses in the depth of the tree. Therefore, for larger and more complex problems, computational tractability cannot necessarily be guaranteed by decomposition alone, but must be complemented by approximate, sampling-based methods.

3.3.4 Sampling-based stochastic optimization methods

The last category includes approaches that approximate the optimal solution of a stochastic problem by sampling. In deterministic optimization, a classic approach to cope with multi-stage decision problems is dynamic programming (Bellman, 1961). By backward recursion, such problems can be solved from the last decision backwards until the first decision. The key idea is to represent the value of being in a certain state on a certain stage by a value function. For the stochastic case, e.g. Keles (2013) and Xi et al. (2014) develop stochastic dynamic programming approaches for multi-stage stochastic decision problems. Rebennack (2010) provides a thorough description and discussion of stochastic dynamic programming.

However as the major drawback, the curse of dimensionality restricts the use of stochastic dynamic programming to certain model sizes and degrees of complexity. This limits on the one hand, for example, the number of scenarios or the number of considered technical units and on the other hand, for example, the degree of technical detail or the use complicating constraints to model interdependencies between units or time steps, and makes approximate solutions necessary (Rebennack, 2010).

The standard approach for solving large-scale multi-stage stochastic problems (MSSPs) in operational planning, mainly in the hydro power context, therefore combines the ideas of Benders decomposition and dynamic programming³¹. By applying Benders decomposition, an approximation of the value function is obtained from the dual solutions of the stochastic problem at each stage. In doing

³¹Füllner and Rebennack (2021) also refer to it as “a sampling-based variant of nested Benders decomposition”.

so, the number of states to be considered is reduced. This enables to treat larger sizes of the state space and thus to overcome the curse of dimensionality.

First introduced by Pereira and Pinto (1991), it is referred to as stochastic dual dynamic programming (SDDP) until today. Rebennack (2010) and Füllner and Rebennack (2021) present SDDP and various extensions of the original approach, Shapiro (2021) dedicates a whole chapter to it. Most importantly for this thesis, the original SDDP is limited to MSSPs that are linear and where stage-wise dependent uncertain parameters do not enter the objective function. This allows to consider uncertain inflows in hydro power operational planning. However, it does not allow for stage-wise dependent uncertain prices or integer variables, which are relevant for the trading problem under uncertainty. Therefore, several extensions of SDDP exist. These include approximate dual dynamic programming (cf. Löhndorf et al., 2013; Wozabal and Rameseder, 2020; Löhndorf and Wozabal, 2021) that allows to consider uncertain prices with an approximate approach. Recently, Downward et al. (2020) introduced another variant of the SDDP with objective states, which also allows for stage-wise dependent uncertain parameters – such as prices – in the objective function. Further, a new and promising approach is SDDP that also allows for integer variables (SDDiP) (Zou et al., 2019b). However, the two have not been widely applied to energy problems up to now, with exceptions including Zou et al. (2019a) and Hjelmeland et al. (2019).

To conclude, the available stochastic optimization approaches for operational planning are rich and still developing. Within the existing literature, the approaches developed to solve the trading problem in Paper B and C are rather innovative applications than methodological breakthroughs in the field of operations research. Due to careful modeling, the developed models can be solved with standard MILP solvers and do not require sophisticated decomposition and approximation techniques. However, extensions and variants of the SDDP are considered most promising for future developments of the trading problem developed in this thesis.

Chapter 4

Case studies

The following sections contain summaries of the papers that are included in this thesis. For the detailed descriptions of methodology and results, the reader is referred to Part II.

4.1 Paper A: Modeling of frequency containment reserve prices with econometrics and artificial intelligence

4.1.1 Background information

Paper A was presented in a preliminary version at the 11th International Energy Economics Convention at TU Vienna (11. Internationale Energiewirtschaftstagung an der TU Wien) in 2019 (Kraft et al., 2019b) and got awarded the best paper award for authors under the age of 30. Afterwards, the approach was further enhanced and published in the *Journal of Forecasting* in 2020 (Kraft et al., 2020).

The author of this thesis is the lead author. The co-authors Dogan Keles and Wolf Fichtner contribute to the idea generation, the interpretation of results and to the preparation and revision of the paper.

4.1.2 Motivation and research question

The motivation behind the paper is to develop and compare state-of-the-art forecasting approaches to provide a hypothetical market participant in the German electricity market with a forecast of the FCR price for the next auction. At the time of preparation, the German reserve market for FCR is organized in weekly auctions with pay-as-bid clearing. The pay-as-bid clearing makes accurate forecasting particularly important for market participants, as submitting bids with low prices and getting accepted leads to unnecessary losses in profitability. However, on the other hand, bidding too close to the expected marginal price may be risky, if the expectation is not sound.

As the literature on forecasting techniques in general is rich, but there is a lack of literature on forecasting of reserve prices, the motivation is to develop several approaches stemming from the most relevant techniques for short-term forecasting: econometric and machine learning models. A fundamental model, the third major stream of models presented in Section 3.1, is not considered suitable. To obtain highly accurate forecasts from a fundamental model, the interactions of reserve markets with short-term electricity markets would require developing a highly detailed and accurate fundamental model of these beforehand.

The major challenge of the forecasting task is the volatility of the time series and the fact that due to market design changes, only 88 observations are available for model training (or estimation, which will be used interchangeably for better readability in the remainder of this section). Particularly for the machine learning approach, this poses difficulties, as with scarce databases the trade-off between model accuracy and overfitting is immanent. The forecasts are developed such that this trade-off is carefully addressed and that both auto-regressive characteristics of the time series and the influence of exogenous variables is appropriately accounted for.

4.1.3 Methodology

The initial time series analysis leads to the conclusion, that the original price time series is non-stationary, but the first difference of the time series is stationary. Therefore, the change of prices from one auction to the next is modeled as dependent variable. A large set of exogenous variables is considered to potentially have

explanatory power. From this set, the price range of the FCR auction, the future electricity price for the market area Germany-Austria (DE-AT), the one for France (FR), the load in DE-AT, the load in FR, the planned unavailable capacity in DE, and the planned unavailable capacity in FR are selected as set of exogenous variables³². This set is fixed for all modeling approaches in order to keep the results comparable.

To respect the information availability of market participants in the real world, an approach called rolling one-step forecasting with model re-estimation and expanding window is implemented. The idea is – after an initial training – to forecast the price of the next time step (i.e., the next auction), and then re-train the forecasting model by including the observed data point in the training set. For comparison of results, the time series of forecasted prices is created by putting the single forecasts in a row.

For the econometric model, the model selection procedure yields a SARIMAX³³ approach to be suitable, and is considered the benchmark for the machine learning models. For the machine learning approach, shallow feed-forward ANNs are found to be suitable for the scope. The ANNs are configured with one and two hidden layers with ten and 20 neurons per layer, leading to four combinations. Further configurations with recurrent structures and deeper feed-forward ANNs do not significantly improve the forecasting performance, supposedly due to the scarce data basis.

As the training data is limited, the ANNs are found to not converge to a unique point forecast when trained with different starting weights. Therefore, ensembling is done to stabilize them and to obtain a distribution of the ANN forecasts. By allowing the model training to slightly overfit the data and at the same time increasing the ensemble size to 100, an alternative to the best model fit and an ensemble size of 50 is defined. Further moving and expanding windows of training data are distinguished.

³²Obviously, there is the risk of multi-collinearity when using the same exogenous variable for neighboring market areas that also have causal relationships such as the load and the electricity price. However, there are particularities such as technology mix in electricity generation, temperature-sensitivity of the load, and dependency from certain fuel prices. These, as well as statistical analyses, justify the use of this exogenous variables set.

³³To be precise, the SARIMAX is applied to the undifferenced time series. So strictly speaking, a SARMAX model was fitted to the differenced time series.

To evaluate the different forecasting approaches, the performance indicators RMSE, MAPE, and DAC, as well as the standard deviation to account for the confidence of the forecasts, are considered. Further, Diebold-Mariano tests are run to be able to conclude about the statistical significance of the superiority of one approach over the other.

4.1.4 Results and conclusions

The results show a very good forecasting performance of the selected models, both for the econometric and the machine learning approach. Among the investigated models, ANNs with expanding training window yield the most desirable results and outperform the SARIMAX approach. Simple models trained to a slight overfit and a larger ensemble size outperform the simple models that were trained towards the best fit. The former lead to the best and most robust forecasts. However, among the best models, non is superior with statistical significance, and different performance indicators lead to different rankings. Increasing the ANN complexity, the positive effect of the slight overfit disappears. Further, it can be concluded for the investigated case of FCR prices, that the overall forecasting performance is not improved by more sophisticated models, as these suffer from overinterpreting the relationships contained in the training data.

In the broader context of this thesis, it can also be concluded that the empirical distributions and the confidence intervals of the forecast may be even more valuable than the point forecasts themselves. As they allow to capture the uncertainty, they can be useful for the development of methods to derive decisions under uncertainty.

4.2 Paper B: Short-term risk management of electricity retailers under rising shares of decentralized solar generation

4.2.1 Background information

Paper B (Russo et al., 2021) and Paper C (Kraft et al., 2021) were developed by the same group of authors. When finding that the forecasting techniques that were developed and successfully applied to FCR prices could hardly perform as accurate on aFRR and mFRR prices, a new way to approach the problem was selected. To appropriately address the opportunity of trading energy and flexibility in the short-term spot markets (i.e., the day-ahead and the intraday market), the information available to a market participant when preparing the bids for the reserve market auction must be modeled appropriately. This information is due to a large uncertainty, which is captured in scenarios that are used to derive optimal trading decisions with the help of stochastic optimization problems.

In particular, the weather dependency and volatility of vRES introduces a major uncertainty to the spot markets, with price spreads between the continuous intraday market and the day-ahead market being hardly predictable. However, the uncertainty can be characterized and captured in stochastic models. Translated into discrete scenario trees, these stochastic models provide the basis for sound decisions under uncertainty on the short-term electricity markets. Based on previous work by Keles et al. (2012), Keles (2013), and Russo and Bertsch (2020) that focuses on longer time horizons, Paper B and Paper C extend the stochastic modeling of short-term market uncertainty to inform the trading decisions of market participants on the day ahead in markets with substantial vRES uncertainty. With the scenarios obtained by the stochastic modeling, two case studies are prepared that investigate two distinct problem settings as innovative applications of stochastic optimization.

Paper B considers the case of a retailer with a customer portfolio consisting of prosumers, i.e., consumers with PV self-generation, and regular consumers. A two-stage stochastic optimization model is developed for optimal procurement and risk management on the day-ahead and intraday market. The focus is thereby set

on the stochastic modeling of the uncertainty of solar generation and its impact on prices in the different spot market segments.

As presented in Section 4.3, Paper C takes the perspective of a trader offering the generation volume and flexibility of a renewable generation portfolio in the sequence of reserve and spot markets. Therefore, in Paper C a third stage is added to the problem formulation and the scope is extended to also consider the aFRR market with stochastic prices as an opportunity. Further, the technical constraints of the generation units require the introduction of binary variables.

The manuscript of Paper B was submitted to *Energy Economics* in June 2021 and is published as a working paper (Russo et al., 2021). After receiving the reviews, the manuscript was revised and resubmitted in January 2022. Marianna Russo, who contributes the most to the stochastic modeling and writing, is the lead author. The contributions of the author of this thesis lie in the conceptualization of the problem, the development of the stochastic optimization model for the retailer, as well as in the implementation and evaluation of the case study. Further, Valentin Bertsch and Dogan Keles contribute as co-authors to the development of the research idea, to the discussions of the design of the study, and by supporting the preparation and revision process.

4.2.2 Motivation and research question

When it comes to volume risk exposure, compared to retailers in other sectors of the economy, electricity retailers are traditionally in a relatively comfortable position. On the one hand, they sell electricity to customers with existing contracts only, and these contracts typically exceed the duration of a few months. On the other hand, they are able to calculate the volumes to be procured based on the standard load profiles of customer groups multiplied with the number of customers per customer group. For the difference, i.e., consumption that is below or above the standard load profiles, the responsible distribution system operator (DSO) manages a separate balancing group (cf. Section 2.1.2) and charges the retailer a price that orientates at average historical wholesale market prices. For the DSO the risk exposure is traditionally relatively low, too, as the deviations are mainly statistical noise, and wholesale market prices are not much affected by them.

However, with an increasing share of households with PV self-generation and self-consumption, accompanied with an increasing overall share of PV generation in the energy system, the situation changes. As the procurement volumes are typically profiled³⁴ by trading on the day-ahead market, there is substantial uncertainty with regard to the eventual generation volumes of solar PV, both regarding the volumes to be supplied to the customers, and the wholesale market prices at which the supplied volumes are procured.

Even though in today's German institutional framework, this is the risk of the DSO managing the difference balancing group, from a general and scientific point of view, the risk exposure lies with the retailer. Therefore, in order to yield general and transferable results, the problem is framed to address the risk of the retailer and to assess trading strategies to manage this short-term risk by trading on the short-term electricity markets (i.e., day-ahead and intraday market)³⁵. The research question can hence be summarized to model the interrelated uncertainty stemming from vRES generation and to determine risk managing trading strategies for retailers to hedge against associated volume and price risks.

4.2.3 Methodology

The major challenge is to capture the interrelated uncertainty of vRES, and particularly PV, generation, residual load, and electricity prices on the day-ahead and intraday market. To model these uncertain parameters and their dependencies, a multi-variate stochastic differential equation is set up. This is done by firstly estimating the deterministic components of the time series, such as auto-regressive components to account for seasonal patterns.

The second step consists in modeling the stochastic residuals of the time series. For the PV generation, this is done by modeling a so-called cloud component that captures the deviation from ideal conditions for the considered season (i.e., clear

³⁴Profiling refers to breaking down financial contracts from the future markets, typically split in base and peak periods, into hourly profiles for the physical contracts on the hourly day-ahead market.

³⁵However, without loss of generality, in today's German framework, the developed methodology appropriately addresses the risk management problem of the DSO rather than the retailer. As turned out in the interview with the head of market operations of a large German DSO, this task is again sub-contracted to a trading company. So eventually, the problem is also in reality treated as a trading problem.

sky irradiation and typical temperature patterns for the season). The stochastic process is then pasted into the stochastic model for the residual load, based on which a second and interrelated stochastic residual for the residual load is identified. This second residual contains fluctuations in the overall demand as well as fluctuations in other vRES generation, such as wind power generation³⁶. Afterwards, the obtained model for the residual load enters a third interrelated equation for the day-ahead market prices. Again, the stochastic residuals of this stochastic price model are identified.

The three residuals are then jointly modeled by estimating stochastic differential equations with a multivariate mean reverting process with regime switches. To account appropriately for the stochasticity in the electricity system and market, the residuals are modeled with switching in between three regimes, a base regime as well as jumps in upward and downward direction. The regime switching probabilities are thereby determined based on historical data.

An analogous approach is developed to model the deviations from the day-ahead stage when entering the intraday trading of the respective quarter hour. In doing so, the uncertainty in terms of the three considered parameters (PV, residual load, and price), that a real-world trader would face is appropriately depicted. Please note, that the stochastic model for the “rolling” realization of intraday uncertainty is therefore path-dependent.

To obtain discrete scenarios for the considered 18 type days³⁷ from this modeling approach, the stochastic processes are simulated via Monte Carlo and afterwards clustered. This allows for each of the type days to determine a two-stage scenario tree. The first stage consists in the day-ahead scenarios, containing PV generation forecast and day-ahead market price time series, the second stage consists in the consecutive intraday scenarios, containing updated PV generation forecast and intraday market price time series based on conditional expectation.

³⁶The wind uncertainty is hence captured implicitly in this second residual, mainly because it does in opposition to PV not follow daily patterns and therefore does not support the intended study design with type days. However, for practical applications, the wind uncertainty could also be modeled explicitly, if the uncertainty for the considered day is characterized.

³⁷The three seasons summer, winter and a transition season, covering spring and fall, as well as working and weekend days are distinguished. For these six combinations, three levels of the parameter residual load are distinguished to end up with 18 type days, for which scenario trees are created and the case study is evaluated.

For the case study, scenario reduction leads to five scenarios for the day-ahead market stage (stage one), and following each of them five scenarios for the intraday stage (stage two), which leads to 25 scenario leaves with respective probabilities. This rich set of scenario trees is applied to a computationally rather lean case study of the retailer in Paper B. For Paper C, one additional stage containing the uncertainty of prices in the secondary reserve market is added to the scenario trees, leading to a computationally rather expensive three-stage stochastic optimization model. However, the uncertainty characterization and the resulting scenarios for the day-ahead and intraday market as well as the PV generation are identical in Paper B and Paper C.

The retailer's trading and risk management problem on the short-term electricity markets is modeled as a two-stage stochastic optimization model. The retailer faces uncertainty, both, via the uncertain volume to be sold to its customers with PV self-generation, and via the uncertain prices on the spot markets. The objective of the risk-neutral retailer is to maximize the expected daily contribution margins, i.e., tariff revenues minus the procurement costs. With the use of the CVaR, the expected contribution margins and the risk exposure are jointly optimized by building a linear combination as presented in Section 2.2. The decision variables are the submitted bidding curves on the day-ahead market and the intraday market for each time step. Thereby, the price levels of the bids are predetermined by the discrete price levels taken from the scenario trees, so that the submitted bidding volume on a price level is the decision to determine the bidding curve.

In this study design, the impact of different shares of customers with PV self-generation in the portfolio as well as the impact of different retail tariffs is evaluated in terms of profitability and risk exposure. This prosumer share is varied between 0% and 100%. The retail tariffs are varied to be fixed tariffs or dynamic tariffs that are indexed with the day-ahead market price. For the calibration of the retail tariffs' fixed and variable rates, real-world tariff data from the ten cheapest tariffs in 39 locations is used. For the households, no deviation from the standard load profile is assumed as reaction to dynamic tariffs. The dynamic tariff share within the customer portfolio is varied between 0% and 100%, assuming an equal distribution between regular and self-consuming customers.

4.2.4 Results and conclusions

As outlined in the previous paragraphs, the study design yields an extensive amount of results that can only briefly be summarized here. Overall, risk-hedging trading strategies and tariffs are found to have a greater impact in summer and with lower levels of system-wide residual load. This can be explained by the fact that the solar generation uncertainty affects the households demand to be served as well as the wholesale spot prices more strongly. Intuitively, the risk exposure is more pronounced with a higher share of prosumers in the portfolio.

The results unveil the potential of dynamic electricity tariffs to support a fair sharing of risks between retailers and prosumers. As a consequence, they might support to avoid a potential risk adder to be billed by the retailer to all customer groups – corresponding to a blind transfer of risks from retailer to customers and thereby also charging the regular consumers for the risk induced by the prosumers.

Further, appropriate trading strategies enable the retailer to not only increase profitability, but also to better manage the risks associated with a high penetration of RES on the short-term electricity markets. Finally, it must be noted that a high penetration of dynamic tariffs as a measure of risk hedging allows the retailer to act more risk-seeking in procurement. This leads to an increased trading activity on the riskier intraday market. However, in the type days that are evaluated for the case study, this effect remains relatively small.

4.3 Paper C: Stochastic optimization of trading strategies in sequential electricity markets

4.3.1 Background information

As mentioned in the background information of the previous section, Papers B and C use the same stochastic modeling for the PV generation, residual load, and spot market price uncertainty. An important additional contribution of Paper C is the consideration of coordination of bids for a renewable generation portfolio not only on the spot markets, but also on the balancing reserve market (BRM). Further, the consideration of technical constraints of the generation units necessitates the introduction of binary variables to the problem, making the problem a MILP. The methodology is applied to the case study of the German market setting with a day-ahead balancing reserve auction (aFRR), followed by the day-ahead electricity market, and the intraday electricity market.

The manuscript of Paper C was submitted to the *European Journal of Operational Research* in June 2021 and published as a working paper (Kraft et al., 2021). The first review round, which was completed in October 2021, stated necessary revisions to consider the manuscript for publication. At the time of writing, these revisions are prepared in order to resubmit the manuscript in short.

The author of this thesis is the lead author and developed the research idea, the study design, and the methodology. Marianna Russo as co-author is the main contributor to the characterization of uncertainty and contributes to the preparation and revision of the manuscript. Further, Dogan Keles and Valentin Bertsch contribute as co-authors to the research idea, to the interpretation of the results as well as to the writing, submission and revision process of the manuscript.

4.3.2 Motivation and research question

Since the early years of electricity market liberalization, the massive uptake in vRES generation and the changing structure of the composition of market participants led to fundamental changes in how balancing reserves and electricity is traded on the markets. A trader with a renewable generation portfolio, consisting of both, dispatchable and intermittent RES, faces a complex market structure with

several market segments competing for mostly the same goods – the energy and the flexibility of the portfolio.

Further, there are substantial sources of uncertainty that affect the trading problem: (a) The reserve market clearing prices are uncertain in advance and, due to the pay-as-bid scheme, too conservative bids can lead to large regrets. This leads to a first source of price uncertainty. (b) Further, the prices on the spot market segments depend strongly on forecasts and forecast updates of vRES generation and resulting residual demand that only unfold during the trading sequence from the day ahead towards real-time. This leads to a second source of price uncertainty. (c) Finally, the vRES generation uncertainty also induces a substantial volume uncertainty to the trading problem.

In this setting, Paper C addresses the two research questions how to characterize the uncertainty and how to optimally trade energy and flexibility in such a sequential market design setting with high shares of renewable generation. To precise the term “optimally”, these trading strategies intend not only to maximize expected contribution margins (i.e., the risk-neutral case), but also to consider the risk exposure determined by the CVaR as a coherent risk measure (i.e., the risk-averse case). Whereas many articles are available in the literature that consider parts of this scope, such an application of state-of-the-art stochastic modeling of interrelated uncertainties and the development of a mathematical program to represent the real world setting in this degree of detail is new and innovative. Further, it provides a valuable contribution not only to academia, but also to practitioners faced with the problem in reality as well as policy makers aiming for a sound design of short-term electricity markets.

4.3.3 Methodology

The approach identified to be suitable to address the research question consists of two steps. First, the uncertainty is described by stochastic processes in order to generate scenario trees based on them. In addition to what was described in the previous section (that will not be repeated for the conciseness, but is equally valid for Paper C), the stochastic modeling of BRM prices was a major challenge. Please note, that only the balancing reserve capacity prices, i.e., the result of the day ahead reserve capacity auction, are represented in the formulation of the

trading problem, as the formulation of balancing reserve energy prices is considered independent from the capacity auction. In the remainder of this section, for better readability the term *reserve price* is used for the balancing reserve capacity price. Further, the subsequent spot markets are assumed to be independent from the realization of the reserve prices, whereas the positive and the negative products of the reserve are modeled jointly.

The reserve price model contains the reserve price of the previous day, the seasonal average reserve price, as well as the expected value of the PV generation and the residual load as exogenous variables. Further, a dummy variable accounts for the distinction between working days and weekend days. Through the use of robust estimation – instead of ordinary least squares (OLS) estimation – the residuals are not assumed to be independent and identically distributed and normally distributed. The residuals are then used to estimate the stochastic process with mean-reverting processes and regime-switching behavior. By means of Monte Carlo simulation and k-means clustering for scenario generation and reduction, for each type day a set of ten scenarios with respective probabilities is generated. Each scenario thereby consists of positive and negative reserve prices for the six time steps that were explained in Section 2.1.3. Combined with the scenarios for PV generation, residual load, and spot market prices, a three-stage scenario tree with a total of 250 scenario leaves represents the uncertainty for each of the 18 type days.

The second step of the methodology consists of a multi-stage stochastic optimization of the trading decisions across the three stages (i) reserve market, (ii) day-ahead market, and (iii) intraday market. In the risk-neutral case, the objective function is to maximize the expected contribution margins of the portfolio. Further, as seen in Sections 2.2 and 4.2, by using a linear combination of the expected contribution margins and the CVaR as a coherent risk measure, the trading problem can be formulated for the case of a risk-averse trader. The decision variables contain the bidding curves for each market segment and each time step for the entire portfolio, thereby taking the price levels as pre-determined by the prices of the scenarios. A trading strategy is thus defined as a set of trading decisions for all market segments and time steps over all scenarios that leads to a technically feasible unit commitment.

One necessary simplification in modeling the problem is to collapse the intraday market to a single stage that captures for each quarter hour the information state roughly 60 minutes before real-time and represents the continuous trading as a uniform pricing auction with the ID3 price as market clearing price³⁸. Compared to the real-world setting, in which 96 quarter hour products are traded in a continuous trading, this simplification does not allow for trading profits from the continuous trading. Further, the intraday price scenarios are characterized by a persistent spread from the day-ahead market reference. However, this does not affect the overall expected value of the price and is considered an appropriate simplification to keep the problem computationally tractable. As discussed in the manuscript, other authors in literature use this simplification similarly. As long as the operation of the assets in the portfolio does not intend to profit from price fluctuations within the intraday market, which would be the case for storage assets, the trading strategies remain valid.

The generation portfolio is intended to contain vRES generation such as PV, therefore besides prices the scenario tree also contains updates on the generation forecast towards real-time. Further, the portfolio also contains biogas power plants as dispatchable units with minimum load constraints. Hence, the trading problem also has binary decision variables. These affect all decision stages and are thus so-called complicating variables. Further, the load change gradient of the dispatchable units is a crucial parameter that enters as complicating constraint. As the trading decisions in all considered market segments can lead to load changes, these must lead to market commitments remaining within the feasibility space.

Another characteristic of multi-stage stochastic optimization is the so-called non-anticipativity. This term refers to the fact, that decisions at a certain stage must be taken without knowledge about the realization of the next stage, thereby not anticipating any unveiling of uncertain information. In the mathematical formulation, this is realized by so-called non-anticipativity constraints that must hold for all decisions that are taken in one node of the tree.

A last particularity to be mentioned here is the appearance of two distinct pricing schemes. In the German market design setting which is the blueprint for the case study the BRM is cleared via pay-as-bid pricing, whereas the day-ahead

³⁸The ID3 is the weighted average price of all trades closed in the last three hours before a respective delivery period. In these three hours, the intraday trading is typically liquid.

market and – in the used simplification – the intraday market are cleared via uniform pricing. This is interesting insofar, as the pricing scheme might lead to a different optimal bidding behavior, especially in the presence of uncertainty and considering the opportunities in the given setting.

The developed trading problem is applied to an extensive case study with a renewable generation portfolio consisting of distributed PV generation and biogas plants as non-dispatchable and dispatchable units. The case study uses the German market design setting as well as generation data and prices for the considered market segments from the German market area. Analogously to the case study in Paper B, 18 type days are distinguished. Further, for each type day, ten optimal trading strategies for different risk attitudes were evaluated: the risk-neutral case as a benchmark as well as the combinations of three different confidence levels for the CVaR ($\alpha \in \{0.90, 0.95, 0.99\}$) and three different weights of the CVaR as risk measure in the objective function ($\lambda \in \{0.10, 0.25, 0.50\}$).

4.3.4 Results and conclusions

The results can be discussed on three levels of aggregation. The first level considers the overall relation between expected contribution margins and associated risk exposure for the distinguished trading strategies. This can be done graphically by plotting the two parts of the objective function for the different trading strategies (α - λ -combinations) as so-called efficient frontiers. When interpreted to be continuous, these efficient frontiers are found to have a concave shape for all considered cases. This shape suggests a moderate expense in terms of expected contribution margins for decreasing the risk exposure moderately. However, when a stark reduction of risk exposure is considered, this can be only achieved by sacrificing profitability substantially.

The second level considers the distribution of contribution margins for a single trading strategy. This is achieved by ordering the contribution margins of all leaves in the scenario tree in increasing order. With the known probabilities of the leaves, an ECDF is constructed and informs transparently about the profits and losses that can be expected. The rather risk-neutral trading strategies are thereby characterized by a large variability between profits in worst cases and best cases, whereas for strategies with stronger risk aversion the variability of the contribution

margins is significantly reduced. A similar evaluation consists in creating profit-and-loss (PnL) diagrams for single market segments that display the performance of different trading strategies for different scenarios (i.e., realizations of market prices). However, due to the coordinated bidding, these PnL diagrams need to be considered together with the diagrams for all market segments, and can only be directly compared for scenarios that are the successors of the same node.

The third level considers the submitted bidding curves in each market segment. Due to the detailed modeling of the bidding problem and the uncertainty, for each bidding strategy, each market segment³⁹, and each time step, the optimal bidding curve can be investigated separately. Obviously, such extensive results must be interpreted with care and always bearing in mind the interrelations and dependencies between the market segments and scenarios. For the reserve market bidding, the most interesting finding is a different reaction to uncertainty and the pay-as-bid pricing for the negative and the positive product.

For the case in which the spot market prices allow a profitable operation of the dispatchable unit, the opportunity to provide positive reserve is relatively high, and interchangeable with the opportunities in the later stages. The positive reserve bids in such a case are therefore typically very risky, the trader is betting on high(est) prices, being aware of the later stages as a sort of safety net for the profits. Contrary, since the plant will be running anyways, the opportunity for the negative reserve provision is relatively low. As there is no interchangeable profit opportunity on the later stages, i.e., the spot markets, the trader diversifies the bids and is also willing to accept lower and therefore less risky prices.⁴⁰

With regard to the submitted bids in the day-ahead and the intraday market, a clear pattern is observed. The intraday prices tend to be higher in expected value, but riskier. For a risk-neutral trader, this leads to more intraday trading activity, as not selling on the reserve and day-ahead markets conserves the highest chances for larger contribution margins on the last stage. In the bad or even worst cases, however, the trader is exposed to the risk to the full extent. In contrast, securing contribution margins in early stages, even if they are slightly lower in expectation, is the strategy of a risk-averse trader. Therefore, a general finding of this paper

³⁹For the bids submitted in the second and the third stage, the bidding curves are even based on the realizations of the previous stages.

⁴⁰In different constellations of the economics of dispatch, the opportunities and rationales can change. This example is presented here because it is the most intuitive for the reader.

consists in the insight that risk hedging can be effectively done by moving the trading activity to the early stages. It can be further concluded that the price spread in expected values between day-ahead and intraday market, which is also observed in reality, does not correspond to inefficient markets, but to a pricing of the risk associated with the uncertainty in the intraday stage.

Concluding, this paper develops a valuable tool for coordinated bidding on three sequential markets and associated operational planning that allows to consider uncertainties in the short-term electricity markets. An essential input to the mathematical problem is a sound modeling of the uncertainties, thereby considering apparent interdependencies between generation uncertainty and price risks in the different market segments. The investigated case study shows the inevitable need for transparent controlling of risk when trading on the short-term electricity markets. Further, stochastic optimization is a powerful mean to not only increase profits in increasingly uncertain circumstances, but also to support an effective and economically efficient risk management.

Further, the considered type days and other sensitivities can be used for asset and portfolio valuation as well as to inform strategic decisions such as investments or acquisitions. For policy makers, the tool can be used to investigate the incentive structures and its changes when considering potential market design changes in a complex and interrelated setting.

Chapter 5

Critical reflection and outlook

Models and associated case studies are used to *represent* the real world, not to *be* the real world. Therefore, it is important to be aware of the limitations of the models and to critically reflect them. The reflection in this chapter addresses both criticism on the methodological level and criticism on the content level. However, each point can also be interpreted as a promising direction, in which the developed approaches can be enhanced in future research.

Although very much effort has been put in the development of models, stark simplifications are necessary to capture the complexity of the decisions in a mathematical model. From an outsider's perspective it must appear oversimplified to approximate continuous stochastic processes by discrete scenario trees.

This is particularly valid for the scenarios and decision-making approach developed in this thesis, as the price levels on which bids are placed are taken from the scenarios. However, due to the power of state-of-the-art operations research methods, this is necessary as highly non-linear problems are hardly tractable. Further, the exponential growth in problem size, referred to as curse of dimensionality, prevents a strong increase of the number of discrete scenarios to approximate the continuous nature of the parameters. It will hence remain a challenging task to find a balance between representativeness to the real world and tractability of the problem. For the degree of modeling detail and the resulting problem sizes considered in this thesis, it appears unrealistic to deploy analytical optimization approaches on the continuous distributions of parameters that do not rely on sampling- or approximation-based solution techniques in the near future.

In this context, the number of scenarios to appropriately represent the uncertainty of a parameter under consideration may have a significant impact on the quality of the entire approach in real-world applications and may thus be chosen based on the degree of faced uncertainty case by case. However, to be able to compare the results between the considered type days and to keep the problems mathematically tractable, the selected static number of scenarios considered to represent parameter uncertainty in each stage of the type days' scenario trees seems to be an appropriate choice. However, investigating the optimal number of scenarios in each stage or for each type day as well as the impact on resulting trading strategies appears as a promising direction for further case studies.

Similarly, the number of stages limits the approaches developed in this thesis. With regard to problem structures in reality, the multi-stage setting could definitely be expanded to increase the validity of the models. This could be done by considering all reserve market segments from the primary reserve to the balancing energy auctions, or a better representation of the intraday trading structure. Particularly, a more precise representation of the continuous intraday market might help to improve the insights for the present case studies. On the one hand, the continuous nature of the intraday market is simplified by considering price indices instead of the order books and the development of stochastic price processes towards GCT. These price processes can as well be exploited commercially by trading actions, which is not included in the developed models. On the other hand, the developed intraday market price scenarios are rigid to the extent that they do not contain the possibility of a sign change of the difference between day-ahead and intraday prices throughout the day, but within one scenario intraday prices remain above, below or on the same level compared to the respective day-ahead prices.

By breaking down the representation of the intraday market to several stages, each covering smaller time intervals instead of a single stage covering the whole day, one could introduce the possibility of such a sign change with associated transition probabilities. However, as the unit commitment of the considered generation units contains hardly any temporal interdependence exceeding the start-up and load ramping behavior, this would not change the overall findings with regard to the trading decisions, but mainly make the problem more complex. Finally, the intraday stage in the first place serves as an approximation for the opportunity to be considered in the previous stages, so that this simplification is justified.

Moreover, in the context of the reserve market, only bids for the balancing capacity auctions are considered in the trading decisions, whereas balancing energy bids are not subject of the investigation. However, the technical limitations arising from possible reserve activation are considered in the problem constraints, but the activation is not explicitly modelled or simulated. In the developed approach, the balancing energy bids are considered as a trading decision that is independent from the previous trading decisions. This is reasonable in that the balancing energy bids do not constrain the other decisions and economic theory suggests bidding with marginal costs under perfect competition. Excluding the balancing energy bids from the model – and thus assuming there is no potential additional revenue from reserve activation – is therefore a reasonable simplification, but results in a conservative estimate of reserve market revenues. Further research could investigate the optimal bids for the balancing energy market and incorporate the associated revenue expectations in the trading problem. The main challenges here are to appropriately represent the interdependence between the intraday market and the reserve activation scenarios, and to determine the expected position of a bid in the merit order of activation and the corresponding activation probability.

For topical extensions such as the optimal trading strategy for battery storages in the presented multi-market setting, breaking down the intraday stage into several stages as mentioned above and including reserve activation scenarios will definitely be necessary. As the extension to storages introduces new time-coupling constraints that the presented approach could not handle appropriately, sampling-based techniques such as SDDP and variants of it appear to become inevitable.

Another aspect that is simplified is the intraday market liquidity. As the intraday market liquidity has increased significantly in the German market area and relatively small portfolios are considered, for the case studies developed in this thesis this seems to be an acceptable assumption. However, when transferring the models to other market areas or larger portfolios, adding intraday market liquidity as a parameter to the stochastic processes might become necessary.

Related to the size of the portfolio and market liquidity, another crucial simplification is the price taker assumption. As the derived bids are to be submitted to the market, a price effect – particularly for market participants with larger portfolios – is not unlikely, especially for the relatively small balancing reserve markets and the intraday market. An extension of the models to address price making appears

reasonable. Most interesting but most likely also most challenging for modelers in that context is the consideration of scenario- or even price-level-dependent price effects, in order to capture the non-linear shape of the merit order in different situations and curve segments.

Further, the scope of the developed models is limited to short-term decisions. To capture decision-making under uncertainty in electricity markets also for the mid- and the long-term decision horizon, the scope requires extension of the stochastic models and stochastic optimization approaches to also include mid- and long-term uncertainty. Particularly, the development of demand, commodity prices and relations among them can heavily influence the electricity markets and the economics of its participants. This is once more proven by the recent developments in the context of the COVID-19 pandemic such as decreasing and then steeply increasing prices for fuels and carbon emission allowances. Moreover, it shows that quantitative risk management in the real world should always be complemented by a qualitative risk management. However, the qualitative dimension is not part of this thesis.

Future research should also address how to derive strategic planning decisions, such as generation and storage expansion planning, in an increasingly uncertain economic environment. Strategic decisions typically take horizons of several years up to decades into account, for which serious predictions of economic, technological, and political parameters are essentially not available. Associated with this question, impacts of different decision rationales of agents in large-scale and long-term electricity market models can be used to study urging questions about the market design. Long-term price forecasts and stochastic processes are excluded in the papers in this thesis. However, a first attempt to address uncertainty in strategic planning is presented in Fraunholz et al. (2021), to which the author of this thesis also contributed. Albeit considering long-term uncertainty of renewable generation in that publication, the long-term price forecasts are heavily dependent on the assumed fuel and carbon emission allowance prices of the scenarios. Further, substantial policy uncertainty and technology developments are not addressed.

In order to appropriately support strategic decision-making under uncertainty, such as generation and storage expansion planning, thorough scenario-based analyses and deep dives into real option and portfolio theory would be necessary. However, this is not in the scope of this thesis and is left for further research. This

thesis provides a promising starting point in terms of methods and approaches to make better operational decisions. In next steps, these can be applied and extended to serve as a profound basis for methods to investigate short-, mid- and long-term decisions under uncertainty in electricity markets.

Chapter 6

Summary and conclusion

The aim of this thesis is to provide new methods for making better decisions under uncertainty in the short-term electricity markets. The presence of uncertainty is not new to decisions in the energy sector and is certainly prevalent in many industry sectors. Therefore, much effort has been put in supporting decisions under uncertainty in the literature. However, recent and current developments in the energy sector present new challenges that require approaches that go beyond the state of the art.

As identified in the initial chapter, the German energy sector undergoes a number of parallel developments that affect the decision-making of market participants. The phasing-out of nuclear power and simultaneous pursuit for decarbonization to achieve ambitious climate targets lead to fundamental changes in the organization of the electricity system and, consequently, the electricity markets. The selected approach to satisfy the energy demand in the future is based on a high share of renewable energy sources such as photovoltaics and wind energy. Their main characteristic is the fact that their generation capacity cannot be dispatched on demand but is highly dependent on weather conditions. Hence, a large share of renewable generation introduces uncertainty and volatility to the system. As a consequence, market participants rely on forecasts, not only with regard to the demand to be satisfied, but also with regard to the available supply. This ultimately leads to more uncertainty and more volatility in market prices.

In the electricity market, these fundamental changes have been accompanied by the introduction of new market segments that are cleared sequentially until

close to real time and determine prices of energy, flexibility, and related services. For market participants, these can be viewed as different revenue opportunities with different profit and risk characteristics.

Thus, the overarching research question investigated in this thesis is how to optimally operate and trade assets in the short-term electricity markets in the presence of uncertainty. This question is subdivided into (a) how to appropriately model the uncertainty and (b) how to make optimal trading decisions under uncertainty in the sequence of short-term electricity markets.

Against this background, this thesis presents the institutional framework of the electricity market with a focus on Germany and Europe. Then, necessary definitions of uncertainty and risk are introduced and a taxonomy of corporate risks in energy sector is developed. Subsequently, the thesis presents and develops several methods that are essential to address the formulated research questions. First, approaches for modeling and forecasting time series are presented and transferred to the stochastic context. Second, the extension of these approaches to stochastic modeling is discussed and approaches for scenario generation and reduction are introduced. Third, mathematical methods for determining optimal decisions under uncertainty are introduced. Based on these approaches and the related findings, three case studies are developed to answer the research questions.

Price forecasts make predictions about the future and are essential to derive trading decisions under imperfect information. In Paper A, several time series models are developed and applied to reserve price forecasting. Methods from econometrics and machine learning are compared, all of which are found to be suitable. Among the models that perform well, artificial neural network ensembles are found to be the most accurate forecast models.

In some cases, however, price forecasts are not sufficient to capture the uncertainty faced by market participants. In such cases, having an adequate representation of the uncertainty and possible scenarios is more valuable for deriving optimal decisions than having a point forecast. Paper B provides such a modeling approach to capture the uncertainty introduced by volatile renewable energy sources in the short-term electricity market context. Using historical data, interrelated stochastic processes are modeled and estimated for solar generation, residual load, and the prices on the considered markets. Two-stage scenario trees containing the uncertain parameters relevant for the day-ahead and the intraday market are generated

for different type days and applied to the case study of a retailer. The retailer faces not only the uncertainty of market prices, but also the uncertainty of the quantity to be supplied to its prosumers. By means of trading strategies – derived by stochastic optimization – and different tariff schemes, options for appropriate risk management under different risk attitudes are derived. It can be concluded that an increasing share of prosumers in the portfolio increases the risk exposure of the retailer and that dynamic tariffs are an efficient mean for a fair sharing of risks between prosumers and the retailer.

For generation portfolios that provide balancing reserve and sell energy in the spot markets, the sequence of trading decisions and associated uncertainties becomes even more complex. Paper C addresses this scope by including the secondary reserve market as a third market segment besides the day-ahead and the intraday market into the trading problem under uncertainty. For a portfolio consisting of dispatchable and intermittent renewable generation units, optimal trading decisions are derived using a three-stage stochastic mixed-integer linear problem, and the trade-off between profits and risk exposure is balanced efficiently. Different levels of risk aversion are distinguished to derive a set of optimal trading strategies for decision support. With regard to the market segments, it can be concluded that risk-neutral decision-making tends to focus on the intraday market, and thereby exposes the profits to a large risk. A reduction of risk exposure – at the price of a moderate reduction of expected profits – can be achieved through trading in the day-ahead market and the reserve market. The developed case studies provide a rich set of insights regarding the particularities and the interplay of reserve and spot markets from a market participant’s perspective. However, as highlighted in the outlook, several promising extensions to the developed methodology and case studies, as well as their application to new technologies, are ready to pave the way for future research.

Overall, the thesis highlights the importance of adequately accounting for uncertainty when deriving trading decisions in short-term electricity markets. The new challenges for market participants associated with the ongoing changes in the energy sector require sophisticated methods and solutions. Optimal trading and risk management on an operative level is essential for the success of the energy transition, as it enables not only an optimal allocation of goods and assets, but also of risks. Moreover, it enables new technologies to enter the electricity mar-

kets based on sound business models and transparent profit and risk estimates. In electricity systems organized by liberalized power markets, these aspects are fundamental building blocks of the decarbonization projects of Germany and the world.

References

- 50Hertz, Amprion, TenneT, TransnetBW, 2020a. Anbieterworkshop der deutschen Übertragungsnetzbetreiber zum Regelarbeitsmarkt: 28.01.2020, Frankfurt. URL: <https://www.regelleistung.net/ext/tender/remark/download/128315996>.
- 50Hertz, Amprion, TenneT, TransnetBW, 2020b. Berechnung des regelzonenübergreifenden einheitlichen Bilanzgleichsenergiepreises (reBAP): Modellbeschreibung. URL: <https://www.transnetbw.de/files/pdf/strommarkt/Ermittlung-reBAP-und-Umgang-mit-Korrekturen-gueltig-ab-01-07-2020.pdf>.
- 50Hertz, Amprion, TenneT, TransnetBW, 2020c. Prequalification Process for Balancing Service Providers (FCR, aFRR, mFRR) in Germany (PQ conditions). URL: https://www.regelleistung.net/ext/download/PQ_Bedingungen_FCR_aFRR_mFRR_en.
- 50Hertz, Amprion, TenneT, TransnetBW, 2021. Abschaltbare Lasten. URL: <https://www.regelleistung.net/ext/static/abla>.
- 50Hertz, Amprion, TenneT, TransnetBW, 2022. Präqualifizierte Leistung in Deutschland (01.01.2022). URL: https://www.regelleistung.net/ext/download/pq_capacity.
- ACER, CEER, 2021. Annual Report on the Results of Monitoring the Internal Electricity and Natural Gas Markets in 2020. URL: https://extranet.acer.europa.eu/Official_documents/Acts_of_the_Agency/Publication/ACER%20Market%20Monitoring%20Report%202020%20E2%80%93%20Electricity%20Wholesale%20Market%20Volume.pdf.

- Agora Energiewende, 2017. Flexibility in thermal power plants - With a focus on existing coal-fired power plants. URL: https://www.agora-energiewende.de/fileadmin/Projekte/2017/Flexibility_in_thermal_plants/115_flexibility-report-WEB.pdf.
- Aïd, R., Gruet, P., Pham, H., 2016. An optimal trading problem in intraday electricity markets. *Mathematics and Financial Economics* 10, 49–85. doi:10.1007/s11579-015-0150-8.
- Albert, K., 1996. Elektrischer Eigenbedarf: Energietechnik in Kraftwerken und Industrie. 2., korrigierte aufl. ed., VDE-Verl., Berlin and Offenbach.
- Artzner, P., Delbaen, F., Eber, J.M., Heath, D., 1999. Coherent Measures of Risk. *Mathematical Finance* 9, 203–228. doi:10.1111/1467-9965.00068.
- Backhaus, K., Erichson, B., Weiber, R., 2015. Fortgeschrittene Multivariate Analysemethoden. Springer Berlin Heidelberg, Berlin, Heidelberg. doi:10.1007/978-3-662-46087-0.
- Bellman, R.E., 1961. Adaptive Control Processes. Princeton University Press. doi:10.1515/9781400874668.
- Bergschneider, C., Karasz, M., Schumacher, R., 2001. Risikomanagement im Energiehandel: Grundlagen, Techniken und Absicherungsstrategien für den Einsatz von Derivaten. Schäffer-Poeschel, Stuttgart.
- Birge, J.R., Louveaux, F., 2011. Introduction to stochastic programming. Springer series in operations research and financial engineering. 2. ed. ed., Springer, New York, NY. URL: http://sub-hh.ciando.com/book/?bok_id=320411, doi:10.1007/978-1-4614-0237-4.
- Boomsma, T.K., Juul, N., Fleten, S.E., 2014. Bidding in sequential electricity markets: The Nordic case. *European Journal of Operational Research* 238, 797–809. doi:10.1016/j.ejor.2014.04.027.
- Box, G.E.P., Jenkins, G.M., Reinsel, G.C., Ljung, G.M., 2016. Time series analysis: Forecasting and control. Wiley series in probability and statistics. fifth edition ed., Wiley and EBSCO Industries, Hoboken, New Jersey and Ipswich,

- Massachusetts. URL: <https://search.ebscohost.com/login.aspx?direct=true&scope=site&db=nlebk&db=nlabk&AN=1061322>.
- Boyd, S., 2010. Distributed Optimization and Statistical Learning via the Alternating Direction Method of Multipliers. *Foundations and Trends in Machine Learning* 3, 1–122. doi:10.1561/22000000016.
- Bradley, S., 2019. Imprecise Probabilities. URL: <https://plato.stanford.edu/entries/imprecise-probabilities/>.
- Brockwell, P.J., Davis, R.A., 2006. Time series: Theory and methods. Springer series in statistics. 2nd ed., corrected. ed., Springer, New York , Heidelberg. URL: <http://swbplus.bsz-bw.de/bsz250382792cov.htm>.
- Brockwell, P.J., Davis, R.A., 2016. Introduction to time series and forecasting. Springer Texts in Statistics. third edition ed., Springer, Switzerland. URL: <https://link.springer.com/book/10.1007/978-3-319-29854-2>, doi:10.1007/978-3-319-29854-2.
- Bublitz, A., 2019. Capacity remuneration mechanisms for electricity markets in transition. Dissertation. Karlsruhe Institute of Technology (KIT). Karlsruhe. doi:10.5445/IR/1000096476.
- Bublitz, A., Keles, D., Zimmermann, F., Fraunholz, C., Fichtner, W., 2019. A survey on electricity market design: Insights from theory and real-world implementations of capacity remuneration mechanisms. *Energy Economics* 80, 1059–1078. doi:10.1016/j.eneco.2019.01.030.
- Bundesnetzagentur, 2021. Monitoringbericht 2020: Monitoringbericht gemäß § 63 Abs. 3 i. V. m. § 35 EnWG und § 48 Abs. 3 i. V. m. § 53 Abs. 3 GWB. URL: https://www.bundesnetzagentur.de/SharedDocs/Mediathek/Berichte/2020/Monitoringbericht_Energie2020.pdf?__blob=publicationFile&v=8.
- Chiodi, A., Giannakidis, G., Labriet, M., Ó Gallachóir, B., Tosato, G., 2015. Introduction: Energy Systems Modelling for Decision-Making, in: Giannakidis, G., Labriet, M., Ó Gallachóir, B., Tosato, G. (Eds.), *Informing Energy and*

- Climate Policies Using Energy Systems Models. Springer International Publishing, Cham. volume 30 of *Lecture Notes in Energy*, pp. 1–12. doi:10.1007/978-3-319-16540-0-1.
- Chung, K.L., 2001. A course in probability theory. 3rd ed. ed., Academic Press, San Diego. URL: <https://ebookcentral.proquest.com/lib/kxp/detail.action?docID=298257>.
- Conejo, A.J., Carrión, M., Morales, J.M., 2010. Decision making under uncertainty in electricity markets. volume 153 of *International series in operations research and management science*. Springer, New York, NY.
- Consentec, 2012. Weiterentwicklung des Ausgleichsenergie- Preissystems im Rahmen des Verfahrens BK6-12-024 der Bundesnetzagentur: Gutachten im Auftrag der Bundesnetzagentur für Elektrizität, Gas, Telekommunikation, Post und Eisenbahnen. URL: https://www.bundesnetzagentur.de/DE/Beschlusskammern/1_GZ/BK6-GZ/2012/BK6-12-024/BK6-12-024_consentec_Gutachten_2012_10_10.pdf?__blob=publicationFile&v=4.
- Consentec, 2020. Beschreibung von Konzepten des Systemausgleichs und der Regelreservemärkte in Deutschland: Erläuterungsdokument im Auftrag der deutschen regelzonenverantwortlichen Übertragungsnetzbetreiber. URL: <https://www.regelleistung.net/ext/tender/remark/download/128323412>.
- Cramton, P., Ockenfels, A., 2012. Economics and Design of Capacity Markets for the Power Sector. *Zeitschrift für Energiewirtschaft* 36, 113–134. doi:10.1007/s12398-012-0084-2.
- Cramton, P., Ockenfels, A., Stoff, S., 2013. Capacity Market Fundamentals. *Economics of Energy & Environmental Policy* 2. doi:10.5547/2160-5890.2.2.2.
- dena, 2016. Momentanreserve 2030: Bedarf und Erbringung von Momentanreserve 2030. Analyse der dena-Plattform Systemdienstleistungen. URL: https://www.dena.de/fileadmin/dena/Dokumente/Pdf/9142_Studie_Momentanreserve_2030.pdf.
- dena, 2020. Systemsicherheit 2050: Systemdienstleistungen und Aspekte der Stabilität im zukünftigen Stromsystem. URL: <https://www.dena.de/fileadmin/>

- dena/Publikationen/PDFs/2020/dena_Systemsicherheit_2050_LANG_WEB.pdf.
- Diebold, F.X., Mariano, R.S., 1995. Comparing Predictive Accuracy. *Journal of Business & Economic Statistics* 13, 253–263. doi:10.1080/07350015.1995.10524599.
- Ding, J., Tarokh, V., Yang, Y., 2018. Model Selection Techniques: An Overview. *IEEE Signal Processing Magazine* 35, 16–34. doi:10.1109/MSP.2018.2867638.
- Downward, A., Dowson, O., Baucke, R., 2020. Stochastic dual dynamic programming with stagewise-dependent objective uncertainty. *Operations Research Letters* 48, 33–39. doi:10.1016/j.orl.2019.11.002.
- Dupacova, J., Consigli, G., Wallace, S.W., 2000. Scenarios for Multistage Stochastic Programs. *Annals of Operations Research* 100, 25–53. doi:10.1023/A:1019206915174.
- Dupacova, J., Gröwe-Kuska, N., Römisch, W., 2003. Scenario reduction in stochastic programming. *Mathematical Programming* 95, 493–511. doi:10.1007/s10107-002-0331-0.
- Ehrhart, K.M., Ocker, F., 2021. Design and regulation of balancing power auctions: an integrated market model approach. *Journal of Regulatory Economics* 60, 55–73. doi:10.1007/s11149-021-09430-7.
- Ehrhart, K.M., Ocker, F., Ott, M., 2021. Analyse des neu eingeführten Regelarbeitsmarktes. *Energiewirtschaftliche Tagesfragen* 71, 48–50.
- Ellsberg, D., 1961. Risk, Ambiguity, and the Savage Axioms. *The Quarterly Journal of Economics* 75, 643. doi:10.2307/1884324.
- ENTSO-E, 2021a. Imbalance Netting. URL: https://www.entsoe.eu/network_codes/eb/imbalance-netting/.
- ENTSO-E, 2021b. Single Intraday Coupling (SIDC). URL: https://www.entsoe.eu/network_codes/cacm/implementation/sidc/.

- ENTSO-E, 2021c. Transparency Platform. URL: <https://transparency.entsoe.eu/>.
- EPEX Spot, 2021. Trading at EPEX Spot 2021. URL: https://www.epexspot.com/sites/default/files/2021-05/21-03-15_Trading%20Brochure.pdf.
- European Commission, 2017. Commission Regulation (EU) 2017/2195 of 23 November 2017 establishing a guideline on electricity balancing: 2017/2195.
- European Commission, 2021. Quarterly Report on European Electricity Markets: Volume 13, issue 4, fourth quarter of 2020. URL: https://ec.europa.eu/energy/sites/default/files/quarterly_report_on_european_electricity_markets_2020.zip.
- Felling, T., Felten, B., Osinski, P., Weber, C., 2019. Flow-Based Market Coupling Revised - Part II: Assessing Improved Price Zones in Central Western Europe. SSRN Electronic Journal doi:10.2139/ssrn.3404046.
- Fraunhofer ISE, 2021. Nettostromerzeugung in Deutschland 2020: Erneuerbare Energien erstmals über 50 Prozent: Öffentliche Nettostromerzeugung in Deutschland in 2020. URL: <https://www.ise.fraunhofer.de/de/presse-und-medien/news/2020/nettostromerzeugung-in-deutschland-2021-erneuerbare-energien-erstmals-ueber-50-prozent.html>.
- Fraunholz, C., 2021. Market Design for the Transition to Renewable Electricity Systems. doi:10.5445/IR/1000133282.
- Fraunholz, C., Miskiw, K.K., Kraft, E., Fichtner, W., Weber, C., 2021. On the Role of Risk Aversion and Market Design in Capacity Expansion Planning, in: KIT Working Paper in Production and Energy No. 62, Karlsruhe Institute of Technology (KIT), Karlsruhe. URL: www.iip.kit.edu, doi:10.5445/IR/1000140411.
- Füllner, C., Rebennack, S., 2021. Stochastic dual dynamic programming and its variants. URL: http://www.optimization-online.org/DB_FILE/2021/01/8217.pdf.

- Genoese, M., 2010. Energiewirtschaftliche Analysen des deutschen Strommarkts mit agentenbasierter Simulation. Nomos Verlagsgesellschaft mbH & Co. KG, Baden-Baden. URL: <http://nbn-resolving.org/urn:nbn:de:bsz:31-epflicht-1198047>.
- Gorski, V., 2017. Scenario Trees Models vs. Lattice Models in Stochastic Optimization. Master Thesis. TU Munich.
- Handelsblatt, 2019. Gericht kippt umstrittenes Mischpreisverfahren für den Strommarkt (23.07.2019). URL: <https://www.handelsblatt.com/unternehmen/energie/bundesnetzagentur-gericht-kippt-umstrittenes-mischpreisverfahren-fuer-den-strommarkt/24691294.html>.
- Heitsch, H., Römisch, W., 2003. Scenario Reduction Algorithms in Stochastic Programming. *Computational Optimization and Applications* 24, 187–206. doi:10.1023/A:1021805924152.
- Heitsch, H., Römisch, W., 2009. Scenario tree modeling for multistage stochastic programs. *Mathematical Programming* 118, 371–406. doi:10.1007/s10107-007-0197-2.
- Higle, J.L., 1998. Variance Reduction and Objective Function Evaluation in Stochastic Linear Programs. *INFORMS Journal on Computing* 10, 236–247. doi:10.1287/ijoc.10.2.236.
- Higle, J.L., Sen, S., 1996. Stochastic decomposition: A statistical method for large scale stochastic linear programming. volume 8 of *Nonconvex optimization and its applications*. Kluwer Academic Publishers, Dordrecht. URL: <http://swbplus.bsz-bw.de/bsz055497772cov.htm>.
- Hjelmeland, M.N., Zou, J., Helseth, A., Ahmed, S., 2019. Nonconvex Medium-Term Hydropower Scheduling by Stochastic Dual Dynamic Integer Programming. *IEEE Transactions on Sustainable Energy* 10, 481–490. doi:10.1109/TSTE.2018.2805164.

- Høyland, K., Kaut, M., Wallace, S.W., 2003. A Heuristic for Moment-Matching Scenario Generation. *Computational Optimization and Applications* 24, 169–185. doi:10.1023/A:1021853807313.
- Høyland, K., Wallace, S.W., 2001. Generating Scenario Trees for Multistage Decision Problems. *Management Science* 47, 295–307. doi:10.1287/mnsc.47.2.295.9834.
- Hyndman, R.J., Athanasopoulos, G., 2021. *Forecasting: principles and practice*: 3rd edition. OTexts: Melbourne, Australia. URL: [OTexts.com/fpp3](https://otexts.com/fpp3).
- James, G., Witten, D., Hastie, T., Tibshirani, R., 2013. *An Introduction to Statistical Learning*. volume 103. Springer New York, New York, NY. doi:10.1007/978-1-4614-7138-7.
- Just, S., Weber, C., 2008. Pricing of reserves: Valuing system reserve capacity against spot prices in electricity markets. *Energy Economics* 30, 3198–3221. doi:10.1016/j.eneco.2008.05.004.
- Just, S., Weber, C., 2015. Strategic behavior in the German balancing energy mechanism: Incentives, evidence, costs and solutions. *Journal of Regulatory Economics* 48, 218–243. doi:10.1007/s11149-015-9270-6.
- Kaut, M., 2021. Scenario generation by selection from historical data. *Computational Management Science* 19, 6. doi:10.1007/s10287-021-00399-4.
- Kaut, M., Wallace, S.W., 2007. Evaluation of Scenario-Generation Methods for Stochastic Programming. *Pacific Journal of Optimization* , 257–271.
- Keles, D., 2013. *Uncertainties in energy markets and their consideration in energy storage evaluation*. Dissertation. Karlsruhe Institute of Technology (KIT). Karlsruhe. doi:10.5445/KSP/1000035365.
- Keles, D., Genoese, M., Möst, D., Fichtner, W., 2012. Comparison of extended mean-reversion and time series models for electricity spot price simulation considering negative prices. *Energy Economics* 34, 1012–1032. doi:10.1016/j.eneco.2011.08.012.
- keras, 2021. Keras API reference. URL: <https://keras.io/api/>.

- Kitzing, L., Mitchell, C., Morthorst, P.E., 2012. Renewable energy policies in Europe: Converging or diverging? *Energy Policy* 51, 192–201. doi:10.1016/j.enpol.2012.08.064.
- Kraft, E., Keles, D., Fichtner, W., 2018. Analysis of Bidding Strategies in the German Control Reserve Market, in: 2018 15th International Conference on the European Energy Market (EEM), IEEE. doi:10.1109/EEM.2018.8469903.
- Kraft, E., Keles, D., Fichtner, W., 2020. Modeling of frequency containment reserve prices with econometrics and artificial intelligence. *Journal of Forecasting* 39, 1179–1197. doi:10.1002/for.2693.
- Kraft, E., Ocker, F., Keles, D., Fichtner, W., 2019a. On the Impact of Voluntary Bids in Balancing Reserve Markets, in: 2019 16th International Conference on the European Energy Market (EEM), IEEE. doi:10.1109/EEM.2019.8916455.
- Kraft, E., Rominger, J., Mohiuddin, V., Keles, D., 2019b. Forecasting of Frequency Containment Reserve Prices Using Econometric and Artificial Intelligence Approaches, in: 11. Internationale Energiewirtschaftstagung an der TU Wien (IEWT), Vienna, Austria, 13. - 15. Februar 2019. doi:10.5445/IR/1000091736/pub.
- Kraft, E., Russo, M., Keles, D., Bertsch, V., 2021. Stochastic Optimization of Trading Strategies in Sequential Electricity Markets, in: KIT Working Paper in Production and Energy No. 58, Karlsruhe Institute of Technology (KIT), Karlsruhe. URL: www.iip.kit.edu, doi:10.5445/IR/1000134346.
- Lago, J., Marcjasz, G., de Schutter, B., Weron, R., 2021. Forecasting day-ahead electricity prices: A review of state-of-the-art algorithms, best practices and an open-access benchmark. *Applied Energy* 293, 116983. doi:10.1016/j.apenergy.2021.116983.
- Larson, R., 1967. A survey of dynamic programming computational procedures. *IEEE Transactions on Automatic Control* 12, 767–774. doi:10.1109/TAC.1967.1098755.

- Laur, A., Nieto-Martin, J., Bunn, D.W., Vicente-Pastor, A., 2018. Optimal procurement of flexibility services within electricity distribution networks. *European Journal of Operational Research* doi:10.1016/j.ejor.2018.11.031.
- Lloyd, S., 1982. Least squares quantization in PCM. *IEEE Transactions on Information Theory* 28, 129–137. doi:10.1109/TIT.1982.1056489.
- Löhndorf, N., 2016. An empirical analysis of scenario generation methods for stochastic optimization. *European Journal of Operational Research* 255, 121–132. doi:10.1016/j.ejor.2016.05.021.
- Löhndorf, N., Wozabal, D., 2021. The Value of Coordination in Multimarket Bidding of Grid Energy Storage. *Operations Research* (under review) tbd.
- Löhndorf, N., Wozabal, D., Minner, S., 2013. Optimizing Trading Decisions for Hydro Storage Systems Using Approximate Dual Dynamic Programming. *Operations Research* 61, 810–823. doi:10.1287/opre.2013.1182.
- Lütkepohl, H., 2006. New introduction to multiple time series analysis. Springer, Berlin. URL: <http://www.loc.gov/catdir/enhancements/fy0663/2005927322-d.html>.
- Maaz, A., 2017. Auswirkungen von strategischem Bietverhalten auf die Marktpreise am deutschen Day-Ahead-Spotmarkt und den Regelleistungsauktionen. Dissertation. RWTH Aachen. Aachen.
- Mack, I., 2014. Energy trading and risk management: A practical approach to hedging, trading and portfolio diversification. Wiley finance series, John Wiley & Sons Singapore, Hoboken, NJ. URL: <https://learning.oreilly.com/library/view/-/9781118339343/?ar>.
- MacQueen, J., 1967. Some methods for classification and analysis of multivariate observations, in: *Proceedings of the fifth Berkeley symposium on mathematical statistics and probability*, pp. 281–297.
- Markowitz, H.M., 1968. *Portfolio selection*. Yale university press.

- Morales, J.M., Conejo, A.J., Perez-Ruiz, J., 2010. Short-Term Trading for a Wind Power Producer. *IEEE Transactions on Power Systems* 25, 554–564. doi:10.1109/TPWRS.2009.2036810.
- Möst, D., Keles, D., 2010. A survey of stochastic modelling approaches for liberalised electricity markets. *European Journal of Operational Research* 207, 543–556. doi:10.1016/j.ejor.2009.11.007.
- Newbery, D., 2016. Missing money and missing markets: Reliability, capacity auctions and interconnectors. *Energy Policy* 94, 401–410. doi:10.1016/j.enpol.2015.10.028.
- Newbery, D., Pollitt, M.G., Ritz, R.A., Strielkowski, W., 2018. Market design for a high-renewables European electricity system. *Renewable and Sustainable Energy Reviews* 91, 695–707. doi:10.1016/j.rser.2018.04.025.
- Ocker, F., 2018. Balancing Power Auctions: Theoretical and Empirical Analyses. Dissertation. Karlsruhe Institute of Technology (KIT). Karlsruhe. doi:10.5445/IR/1000084832.
- Ocker, F., Ehrhart, K.M., Belica, M., 2018. Harmonization of the European balancing power auction: A game-theoretical and empirical investigation. *Energy Economics* 73, 194–211. doi:10.1016/j.eneco.2018.05.003.
- Ocker, F., Jaenisch, V., 2020. The way towards European electricity intraday auctions – Status quo and future developments. *Energy Policy* 145, 111731. doi:10.1016/j.enpol.2020.111731.
- Ortner, A., 2017. Electricity Balancing Markets in Europe: Fundamental modeling approaches and case studies assuming perfect competition. Dissertation. TU Vienna. Vienna.
- Oxford Learner's Dictionary of Academic English, 2021. Entries to "Uncertainty" and "Risk". URL: <https://www.oxfordlearnersdictionaries.com/definition/academic>.
- Pereira, M.V.F., Pinto, L.M.V.G., 1991. Multi-stage stochastic optimization applied to energy planning. *Mathematical Programming* 52, 359–375. doi:10.1007/BF01582895.

- Petitot, M., 2016. Ph.D. thesis. Paris.
- Pflug, G., 2001. Scenario tree generation for multiperiod financial optimization by optimal discretization. *Mathematical Programming* 89, 251–271. doi:10.1007/PL00011398.
- Pflug, G.C., Pichler, A., 2014. *Multistage Stochastic Optimization*. Springer International Publishing, Cham. doi:10.1007/978-3-319-08843-3.
- Pilipović, D., 2007. *Energy risk: Valuing and managing energy derivatives*. 2nd ed. ed., McGraw-Hill, New York. URL: <http://www.loc.gov/catdir/enhancements/fy0739/2007004861-b.html>.
- Plazas, M.A., Conejo, A.J., Prieto, F.J., 2005. Multimarket Optimal Bidding for a Power Producer. *IEEE Transactions on Power Systems* 20, 2041–2050. doi:10.1109/TPWRS.2005.856987.
- Pliska, S.R., 2007. *Introduction to mathematical finance: Discrete time models*. Blackwell, Malden, Massachusetts.
- Rebennack, S., 2010. *A Unified State-Space and Scenario Tree Framework for Multi-Stage Stochastic Optimization: An Application to Emission-Constrained Hydro-Thermal Scheduling*. PhD Thesis. University of Florida.
- Ringler, P., 2017. *Erzeugungssicherheit und Wohlfahrt in gekoppelten Elektrizitätsmärkten*. Dissertation. Karlsruhe Institute of Technology (KIT). Karlsruhe. doi:10.5445/IR/1000064573.
- Rockafellar, R.T., Wets, R.J.B., 1991. Scenarios and policy aggregation in optimization under uncertainty. *Mathematics of operations research* 16, 119–147.
- Römisch, W., Vigerske, S., 2010. Recent Progress in Two-stage Mixed-integer Stochastic Programming with Applications to Power Production Planning, in: Pardalos, P.M., Rebennack, S., Pereira, M.V.F., Iliadis, N.A. (Eds.), *Handbook of Power Systems I*. Springer Berlin Heidelberg, Berlin, Heidelberg. volume 100 of *Energy Systems*, pp. 177–208. doi:10.1007/978-3-642-02493-1-8.

- Rumsfeld, D.H., 2002. DoD News Briefing - Secretary Rumsfeld and Gen. Myers (February 12, 2002 11:30 AM EDT). URL: <https://archive.ph/20180320091111/http://archive.defense.gov/Transcripts/Transcript.aspx?TranscriptID=2636>.
- Russo, M., Bertsch, V., 2020. A looming revolution: Implications of self-generation for the risk exposure of retailers. *Energy Economics* 92, 104970. doi:10.1016/j.eneco.2020.104970.
- Russo, M., Kraft, E., Bertsch, V., Keles, D., 2021. Short-term Risk Management for Electricity Retailers Under Rising Shares of Decentralized Solar Generation, in: KIT Working Paper in Production and Energy No. 57, Karlsruhe Institute of Technology (KIT), Karlsruhe. URL: www.iip.kit.edu, doi:10.5445/IR/1000134345.
- Schröder, A., Kunz, F., Meiss, J., Mendelevitch, R., von Hirschhausen, C., 2013. Current and Prospective Costs of Electricity Generation until 2050: DIW Data Documentation. URL: https://www.diw.de/documents/publikationen/73/diw_01.c.424566.de/diw_datadoc_2013-068.pdf.
- Shapiro, A., 2021. Chapter 8: Computational Methods, in: Shapiro, A., Dentcheva, D., Ruszczyński, A. (Eds.), *Lectures on Stochastic Programming: Modeling and Theory*, Third Edition. Society for Industrial and Applied Mathematics, Philadelphia, PA, pp. 361–401. doi:10.1137/1.9781611976595.ch8.
- Sharma, S., 2017. Activation Functions in Neural Networks. URL: <https://towardsdatascience.com/activation-functions-neural-networks-1cbd9f8d91d6>.
- Siemonsmeier, M., Baumanns, P., van Bracht, N., Schönefeld, M., Schönbauer, A., Moser, A., Dahlhaug, O., Heidenreich, S., 2018. Hydropower Providing Flexibility for a Renewable Energy System: Three European Energy Scenarios: A HydroFlex report. URL: https://www.h2020hydroflex.eu/wp-content/uploads/2019/01/HydroFlex-Report_Three-European-Energy-Scenarios.pdf.
- S&P Global Platts, 2015. World electric power plants database. URL: <http://www.platts.com/products/world-electric-power-plants-database>.

- Stoft, S., 1997. Transmission pricing zones: simple or complex? *The Electricity Journal* 10, 24–31. doi:10.1016/S1040-6190(97)80294-1.
- Sun, X.A., Conejo, A.J., 2021. *Robust Optimization in Electric Energy Systems*. volume 313. Springer International Publishing, Cham. doi:10.1007/978-3-030-85128-6.
- Swider, D.J., 2006. *Handel an Regelernergie- und Spotmärkten: Methoden zur Entscheidungsunterstützung für Netz- und Kraftwerksbetreiber*. Dissertation. Universität Stuttgart. Stuttgart.
- Swider, D.J., Weber, C., 2007. Bidding under price uncertainty in multi-unit pay-as-bid procurement auctions for power systems reserve. *European Journal of Operational Research* 181, 1297–1308. doi:10.1016/j.ejor.2005.11.046.
- TransnetBW, 2021. Abschaltbare Lasten. URL: <https://www.transnetbw.de/de/strommarkt/systemdienstleistungen/abschaltbare-lasten>.
- Uhlenbeck, G.E., Ornstein, L.S., 1930. On the Theory of the Brownian Motion. *Physical Review* 36, 823–841. doi:10.1103/PhysRev.36.823.
- van Ackooij, W., Danti Lopez, I., Frangioni, A., Lacalandra, F., Tahanan, M., 2018. Large-scale unit commitment under uncertainty: an updated literature survey. *Annals of Operations Research* 271, 11–85. doi:10.1007/s10479-018-3003-z.
- van den Bergh, K., Boury, J., Delarue, E., 2016. The Flow-Based Market Coupling in Central Western Europe: Concepts and definitions. *The Electricity Journal* 29, 24–29. doi:10.1016/j.tej.2015.12.004.
- Wallace, S.W., Fleten, S.E., 2003. Stochastic Programming Models in Energy: Chapter 10, in: Ruszczyński, A.P., Shapiro, A. (Eds.), *Stochastic programming*. Elsevier, Amsterdam and Boston. *Handbooks in operations research and management science*.
- Wallis, K.F., 2011. Combining forecasts – forty years later. *Applied Financial Economics* 21, 33–41. doi:10.1080/09603107.2011.523179.

- Weber, C., 2005. Uncertainty in the Electric Power Industry: Methods and Models for Decision Support. volume 77 of *International Series in Operations Research & Management Science*. Springer Science+Business Media Inc, New York, NY. URL: <http://dx.doi.org/10.1007/b100484>, doi:10.1007/b100484.
- Weber, C., Heidari, S., Bucksteeg, M., 2021. Coping with Uncertainties in the Electricity Sector - Methods for Decisions of Different Scope. *Economics of Energy & Environmental Policy* 10. doi:10.5547/2160-5890.10.1.cweb.
- Weron, R., 2014. Electricity price forecasting: A review of the state-of-the-art with a look into the future. *International Journal of Forecasting* 30, 1030–1081. doi:10.1016/j.ijforecast.2014.08.008.
- Wolke, T., 2015. Risikomanagement. De Gruyter. doi:10.1515/9783110353877.
- Wozabal, D., Rameseder, G., 2020. Optimal bidding of a virtual power plant on the Spanish day-ahead and intraday market for electricity. *European Journal of Operational Research* 280, 639–655. doi:10.1016/j.ejor.2019.07.022.
- Xi, X., Sioshansi, R., Marano, V., 2014. A stochastic dynamic programming model for co-optimization of distributed energy storage. *Energy Systems* 5, 475–505. doi:10.1007/s12667-013-0100-6.
- Zheng, Q.P., Wang, J., Liu, A.L., 2015. Stochastic Optimization for Unit Commitment—A Review. *IEEE Transactions on Power Systems* 30, 1913–1924. doi:10.1109/TPWRS.2014.2355204.
- Zou, J., Ahmed, S., Sun, X.A., 2019a. Multistage Stochastic Unit Commitment Using Stochastic Dual Dynamic Integer Programming. *IEEE Transactions on Power Systems* 34, 1814–1823. doi:10.1109/TPWRS.2018.2880996.
- Zou, J., Ahmed, S., Sun, X.A., 2019b. Stochastic dual dynamic integer programming. *Mathematical Programming* 175, 461–502. doi:10.1007/s10107-018-1249-5.

List of abbreviations

aFRR automatic Frequency Restoration Reserve. 20–26, 31, 48, 50, 71, 72, 77

AIC Akaike information criterion. 51

ANN artificial neural network. 47, 49, 52–56, 69, 70

ARMA auto-regressive moving average. 49

BIC Bayesian information criterion. 51

BRM balancing reserve market. 11, 12, 19, 21–25, 29, 30, 46, 77, 78, 80

BRP balancing responsible party. 19, 21, 26, 62

CCGT combined cycle gas turbine. 28

CDF cumulative distribution function. 34, 36

CRM capacity remuneration mechanism. 11, 13

CVaR conditional value-at-risk. 38, 75, 78, 79, 81

DAC directional accuracy. 51, 70

DAM day-ahead market. 25, 48, 50

DSM demand side management. 31

DSO distribution system operator. 72, 73

EBGL Electricity Balancing Guideline. 21, 24

- ECDF** empirical cumulative distribution function. 34, 36, 81
- EEG** Germany's Renewable Energy Act *Erneuerbare-Energien-Gesetz*. 9, 10
- ENTSO-E** European Network of Transmission System Operators for Electricity. 22
- EPEX Spot** European Power Exchange. 15, 16, 23
- FCR** Frequency Containment Reserve. 20–26, 31, 49, 68–71
- GCT** gate closure time. 13, 19, 24, 26, 86
- IDM** intraday market. 25, 48, 50
- IGCC** International Grid Control Cooperation. 20
- MAPE** mean absolute percentage error. 51, 70
- mFRR** manual Frequency Restoration Reserve. 20–26, 31, 71
- MILP** mixed-integer linear program. 63, 65, 77
- MOL** merit order list. 21
- MSSP** multi-stage stochastic problem. 64, 65
- NEMO** nominated electricity market operator. 15
- NRV** *Netzregelverbund*. 21, 22
- OCGT** open cycle gas turbine. 28
- OLS** ordinary least squares. 79
- OTC** over-the-counter. 15
- PPA** power purchase agreement. 15
- PV** photovoltaic. 4, 10, 11, 15, 71, 73–75, 77, 79–81

-
- reBAP** *regelzonenübergreifender einheitlicher Ausgleichsenergiepreis*. 25
- RES** renewable energy sources. 4, 10, 43, 60, 76, 77
- RMSE** root mean square error. 51, 70
- SDDP** stochastic dual dynamic programming. 65, 87
- TSO** transmission system operator. 19–23, 25, 26, 29, 31, 32
- VaR** value-at-risk. 37, 38
- vRES** volatile renewable energy sources. 4, 10, 11, 15, 16, 18, 29, 32, 40, 43, 48, 61, 71, 73, 74, 77, 78, 80

Part II

Research papers

Paper A

Modeling of frequency containment reserve prices with econometrics and artificial intelligence

Emil Kraft ^a, Dogan Keles ^a, Wolf Fichtner ^a

^a *Karlsruhe Institute of Technology (KIT), Chair of Energy Economics, Karlsruhe, Germany*

Published in *Journal of Forecasting*, suggested citation:

Kraft, E.; Keles, D.; Fichtner, W. (2020): Modeling of frequency containment reserve prices with econometrics and artificial intelligence. In: *Journal of Forecasting*, 39 (8), S. 1179–1197. <http://dx.doi.org/10.1002/for.2693>.



Received: 31 July 2019 | Revised: 17 March 2020 | Accepted: 9 April 2020

DOI: 10.1002/for.2693

SPECIAL ISSUE ARTICLE

WILEY

Modeling of frequency containment reserve prices with econometrics and artificial intelligence

Emil Kraft | Dogan Keles | Wolf Fichtner

Institute for Industrial Production (IIP),
Chair of Energy Economics, Karlsruhe
Institute of Technology (KIT), Karlsruhe,
Germany

Correspondence

Emil Kraft, Chair of Energy Economics,
Karlsruhe Institute of Technology (KIT),
Institute for Industrial Production (IIP),
Hertzstraße 16, 76187 Karlsruhe,
Germany.
Email: emil.kraft@kit.edu

Funding information

Bundesministerium für Wirtschaft und
Energie, Grant/Award Number: 03SIN120

Abstract

The forecasting of prices for electricity balancing reserve power can essentially improve the trading positions of market participants in competitive auctions. Having identified a lack of literature related to forecasting balancing reserve prices, we deploy approaches originating from econometrics and artificial intelligence and set up a forecasting framework based on autoregressive and exogenous factors. We use SARIMAX models as well as neural networks with different structures and forecast based on a rolling one-step forecast with reestimation of the models. It turns out that the naive forecast performs reasonably well but is outperformed by the more advanced models. In addition, neural network approaches outperform the econometric approach in terms of forecast quality, whereas for the further use of the generated models the econometric approach has advantages in terms of explaining price drivers. For the present application, more advanced configurations of the neural networks are not able to further improve the forecasting performance.

KEYWORDS

artificial neural network, balancing reserve, econometrics, electricity price, time series forecasting

1 | INTRODUCTION AND MOTIVATION

Transmission system operators (TSOs) have responsibility for a secure electricity system operation, which includes ensuring a stable grid frequency of 50 hertz within their designated control areas. This is achieved by continuously balancing power feed-in and withdrawal.

To balance frequency perturbations, balancing reserve capacity is deployed by the TSOs. Balancing reserve capacity is characterized by a short reaction time and the ability to increase or decrease the power feed-in quickly upon request. Depending on the response and the activation time, three different qualities are

distinguished in continental Europe. The different quality requirements lead to market segments for primary (frequency containment reserve, FCR), secondary (automatic frequency restoration reserve, aFRR), and tertiary (manual frequency restoration reserve, mFRR) balancing reserve power, in which FCR has, at 30 seconds, the shortest activation time. In the past, mainly conventional generation such as nuclear, coal and gas power plants, but also hydropower, were the only providing technologies of balancing reserve power. In recent years, new technologies entered the market and, by today, renewable energies such as biomass, photovoltaics and wind power, but also battery storage, are technically capable of providing balancing reserve. Because market

This is an open access article under the terms of the Creative Commons Attribution-NonCommercial License, which permits use, distribution and reproduction in any medium, provided the original work is properly cited and is not used for commercial purposes.

© 2020 The Authors. Journal of Forecasting published by John Wiley & Sons Ltd

liberalization TSOs are not allowed to own generation capacity, they procure positive and negative reserve capacities meeting different quality requirements through public tenders. These markets for balancing reserve coexist alongside derivative and spot markets for electricity, enabling additional return opportunities for generators by meeting the respective requirements.

The auctions for FCR take place on a weekly basis each Tuesday at 3 p.m. and are dedicated to the provision of FCR in both a positive and negative direction for the following week. Market participants place a capacity price bid and are compensated according to pay-as-bid pricing.

This paper focuses on forecasting the prices of the largest European FCR market, in which the TSOs of the control zones of Austria, Belgium, France, Germany, the Netherlands, and Switzerland jointly¹ procure roughly 1.4 gigawatts of FCR capacity for the upcoming week in an auction. Providers of FCR are compensated for capacity reservation based on the reserve power price, whereas delivered energy itself is not a matter of compensation.² Therefore, market players require appropriate forecasts of the week-ahead FCR power prices to be successful in the related auctions.

An individual supplier faces the tradeoff between the profit from selling FCR and the opportunity costs of the alternative use of flexible capacity, like bidding on the day ahead or the intraday market. Additionally, if the supplier decides to provide FCR, the technical unit has to be online for the entire week of provision. In the case of a power plant with minimum load requirements, the provider risks costs induced by negative contribution margins. Therefore, in order to prepare an adequate offer for the FCR tender and the other market segments, high-quality price forecasts are inevitable.

However, forecasting of FCR power prices has hardly been addressed in the forecasting literature (see Section 2). For this reason, we develop and introduce adequate forecasting models based on seasonal integrated autoregressive moving average (ARMA) models with exogenous regressors (SARIMAX) as explanatory variables and compare their results with methods from a second model family, the neural-network-based models. From the latter, we set up an experiment design to develop high-performing neural networks. The goal of this study is to find not only well-performing forecast

methods but also their appropriate configuration in terms of hyperparameters and training strategies.

We find that both neural networks and SARIMAX models are capable of forecasting FCR prices reasonably well. For the neural networks, the simple network structures outperform the more sophisticated ones. The applied overfitting and ensembling techniques lead to significantly better forecast results and provide a solution to the problem of training data scarcity.

The main contributions and novelty of this paper are as follows:

- 1 Application and comparison of statistical and neural network models to price forecasting in reserve power markets that increasingly gain more importance in the energy transition era.
- 2 Description and discussion of training strategies for forecasting reserve power prices with neural networks on a scarce data basis.
- 3 Definition and discussion of appropriate target variable in the case of FCR prices in a market that is designed as a pay-as-bid auction.
- 4 Discussion on suitability and performance of simple and more sophisticated network structures for the mentioned market prices.

In this context, the paper is structured as follows. In Section 2, we review different approaches to forecast short-term electricity market prices in the literature. In Section 3, we deploy forecasting approaches considering autoregressive processes and exogenous drivers: precisely, a SARIMAX approach and artificial neural network models (ANN). Hereby, we consider feedforward units and set up an experiment design which deploys different model structures and training strategies. Finally, in Section 4, we apply the approaches to the stated forecasting problem and compare the performances. In Section 5, we conclude the findings and provide an outlook on future developments.

2 | RELATED LITERATURE

Among the first looking into the issue of reserve pricing and costs from a market perspective are Kirsch and Singh (1995). They provide an overview over the cost components of reserve power: opportunity costs of foregone sales, costs of uneconomic operation, potential startup and shutdown costs, costs resulting from frequent load changes and costs caused by efficiency losses. In addition, as applies for pricing electricity in the wholesale market, on the one hand the short-term marginal costs have to be considered. These are mainly determined by

¹Note that France joined the procurement union in 2017 and subsequently provides more than a third of the required FCR. However, the market entry of France is considered in the model building, as the structural change may have introduced correlations and dynamics, which data from before 2017 do not contain.

²This is due to the fact that activation is hardly predictable and the delivered energy amount has an expected value of zero.

fuel and operation costs and can be increased due to partial load operation and decreased efficiency. On the other hand, the capital costs and other fixed costs need to be recovered by contribution margins generated in the market in the long term.

Weron (2014) finds that the actual modeling and forecasting of prices from balancing reserve and ancillary services markets has been comparatively rare in the literature. Exceptions include Olsson and Söder (2008), who model real-time balancing reserve power market prices in the Nordic market by using combined SARIMA and discrete Markov process models. They conclude that the developed model combination is suitable to use for the generation of real-time balancing power price scenarios. Klæboe, Eriksrud, and Fleten (2013) benchmark time-series-based forecasting models, and Dimoulkas, Amelin, and Hesamzadeh (2016) apply a hidden Markov model to forecast balancing reserve market prices for the Nordic market. They argue that activation of the balancing reserve occurs randomly and an activation-based price is therefore hardly predictable. Unfortunately, unlike the tenders considered in the present paper, the considered market design in the Nordic market is based on payments for reserve activation and not for the provision of reserve power.

Just and Weber (2008) consider an equilibrium model with two alternative competitive markets: the secondary balancing reserve power and an hourly electricity spot market. They value the provision of balancing reserve by quantifying the opportunity to spot market sales and deduce a development of capacity prices for secondary balancing reserve power for the German case. However, they do not apply the equilibrium model to forecast prices and do not include FCR in their investigations.

Finally, Wang, Zareipour, and Rosehart (2014) investigate the application of established stochastic approaches for modeling the behavior of operating reserve and regulation prices in the North American electricity markets, which, like the Nordics, are based on activation rather than provision of balancing reserve power. The investigated models are descriptive and not designed for generating short-term forecasts. The authors point out that reserve and regulation prices are characterized by higher volatility, lower mean, more frequent price spikes, and a more skewed distribution compared to electric energy prices. Thus modeling reserve power prices is potentially more challenging.

In contrast to forecasting reserve market prices, forecasting of electricity spot market prices is a field that has been pervasively studied (Weron, 2014). For example, Kiesel and Paraschiv (2017) and Bublitz, Keles, and Fichtner (2017) mention fundamental price drivers such

as load, fuel prices, unavailable generation capacity, and renewable energies' feed-in as suitable exogenous regressors to forecast electricity prices.

ANN forecasting of hourly day-ahead electricity prices and a comparison to econometric benchmarks was first applied by Catalão, Mariano, Mendes, and Ferreira (2007), who find a good forecasting performance of ANN on the Spanish and the Californian market. Lago, Ridder, and Schutter (2018) study the Belgian day-ahead electricity market and consider a large set of possible forecasting models, concluding a significant dominance of machine learning over the statistical models in terms of forecasting accuracy. Ugurlu, Oksuz, and Tas (2018) and Oksuz and Ugurlu (2019) forecast the Turkish day-ahead and intraday market electricity prices with different neural networks configurations, including feedforward, gated recurrent unit (GRU) and long short-term-memory (LSTM) model designs. The authors conclude a significant dominance of GRU model designs and state an improvement with increasingly sophisticated network structures. Giovanelli, Sierla, Ichise, and Vyatkin (2018) forecast the hourly day-ahead balancing prices of the Finnish market and compare neural networks in various parameter configurations with support vector regression and autoregressive integrated moving average (ARIMA) models. They find that the amount of training data is a key impact on the forecasting performance of the models, whereas different training strategies, algorithms, and activation functions performed similarly well.

The methodological approach of comparing models originating from econometrics with machine learning models has been applied to several scopes in the literature. Chatfield (1996) and Adya and Collopy (1998) provide a theoretical foundation for the need to consider both econometric models and machine learning approaches such as neural networks in forecasting. They conclude that the model setup requires a careful choice of external regressors with regard to out-of-sample-fit in order to respect model uncertainty (Chatfield, 1996) and that well-designed ANN models have the potential to outperform econometric approaches in forecasting applications (Adya & Collopy, 1998). Early studies deploying both econometric and ANN models include applications in forecasting electricity demand (Liu et al., 1991), consumer expenditure (Church & Curram, 1996), retail sales (Alon, Qi, & Sadowski, 2001), foreign exchange rates (Qi & Zhang, 2001; Yao & Tan, 2000), gross domestic product (GDP) growth (Tkacz, 2001), stock returns (Olson & Mossman, 2003; Qi & Zhang, 2001), and inflation rates (Binner, Bissoondeal, Elger, Gazely, & Mullineux, 2005). The studies confirm the conclusion regarding the forecasting potential of well-designed

neural networks drawn by Adya and Collopy and suggest the adaption of the study design to FCR price forecasting.

However, for all mentioned studies the data basis for training the model is comprehensive. In particular, the studies on electricity prices rest on hourly data of several years and the neural networks thus have plenty of observations to learn from. Further, spot market prices are typically well explainable by fundamental factors (see, e.g., Bublitz et al., 2017; Kiesel & Paraschiv, 2017; Weron, 2014). Conversely, a challenge in forecasting balancing reserve market prices lies in the fact that they are hardly explainable by fundamental drivers (Kraft, Keles, & Fichtner, 2018; Ocker, Ehrhart, & Belica, 2018). However, Ocker and Ehrhart (2017) find evidence for collusion among market participants and serial correlation in the auction results of the secondary reserve market. Another key challenge in this paper is based on a relatively sparse database, consisting of weekly data from the years 2017 and 2018. To cope with the data scarcity, we deploy ensembling and overfitting strategies (see Section 3) that, to the best knowledge of the authors, have not been deployed in electricity price forecasting before.

We are well aware that commercial providers offer forecasts for the considered FCR market. Unfortunately, however, these commercial providers publish neither their methodologies in detail nor historic forecast time series as a benchmark. In the next section, we will therefore follow Weron (2014), who classifies short-term price forecasting models into time series analysis approaches and artificial intelligence or machine learning approaches. We will set up and deploy forecasting models for the FCR price based on both time series analysis (SARIMAX) and ANN.

3 | METHODOLOGY

The literature review in the previous section displayed a lack of scientific publications in the field of FCR price forecasting and suggested the application of, on the one hand, approaches coming from time series analysis, and, on the other hand, approaches coming from machine learning. To obtain a benchmark that is neither time series based nor machine learning based, a naive forecast³ is taken as a benchmark. Preliminary analyses showed that for FCR prices the naive forecast outperforms linear regression and can well compete with a SARIMA approach (Kraft, Rominger, Mohiuddin, & Keles, 2019). In Section 3.1, owing to the pay-as-bid auction design, first the dependent variable is defined and its

time series is analyzed briefly. In Section 3.2, the exogenous variables required for the forecasting approaches are introduced and their preprocessing is explained. Sections 3.3 finally presents the setup and training of the SARIMAX and ANN models.

3.1 | Definition of dependent variable and time series analysis

As FCR tenders are pay-as-bid auctions, there is no uniform settlement price but each market participant receives its price bid as remuneration. Prior to setting up a highly sophisticated forecasting model, it is necessary to define a suitable dependent variable. Analysis of the FCR market results from 2014 to 2018:Q3 (Figure 1) shows the range of accepted bids as well as the capacity-weighted average price in each auction. From the relatively low gap between the capacity-weighted average price and the respective marginal price (except for single spikes), we conclude that the capacity-weighted average is a suitable target variable for the forecast. The main errors induced by using the capacity-weighted average instead of the maximum price, for example, arise in periods with price spikes. However, considering that a risk-neutral trader would not speculate on the height of price spikes, the capacity-weighted average remains the favorable forecast target.

The time series contains seasonality, mainly induced by a strong price increase over the Christmas holidays and a moderate price increase in early summer of each year. In general, the time series shows a decreasing trend. To check the time series for stationarity, it was tested with Kwiatkowski–Phillips–Schmidt–Shin (KPSS) unit root tests (Kwiatkowski, Phillips, Schmidt, & Shin, 1992). The nondifferenced time series rejects the stationarity null hypothesis at 1% significance; the series of first differences (shown in Figure 2) does not reject the stationarity null hypothesis. The econometric models will therefore be estimated with a SARIMAX approach with

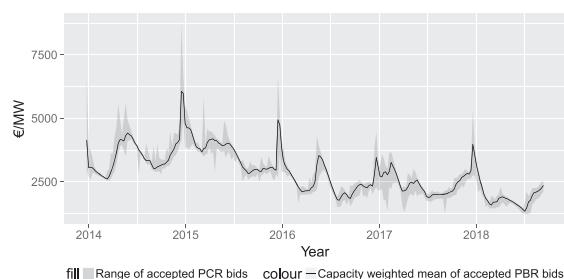


FIGURE 1 FCR price development from 2014 to 2018:Q3 (own illustration based on data from regelleistung.net, 2019)

³The naive forecast equals the expectation of having the same price as in the last auction.

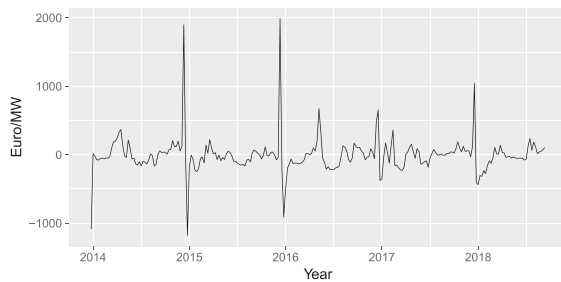


FIGURE 2 First differences of capacity-weighted average of accepted FCR bids from 2014 to 2018:Q3 (own illustration based on data from regelleistung.net, 2019)

the undifferentiated time series of capacity-weighted averages as dependent variable y . The SARIMAX approach allows us to endogenously model the first differences Δy of the time series in order to derive forecasts regarding the forecast target. The autocorrelation function (ACF) of the differenced time series indicates a significant correlation with lag 1, lag 2, lag 50, and lag 52 (see Figure 3). Thus, for model training and prediction, Δy_{t-1} , Δy_{t-2} , Δy_{t-50} , and Δy_{t-52} are supplied as the respective lags.

For the ANN models, the dependent variable is defined as the first difference Δy of the capacity-weighted price time series, corresponding to the difference between the price of the current and the price of the previous auction. In order to return to the desired FCR price prediction, the predicted difference is added to the FCR price of the previous auction. This procedure complies intuitively with the SARIMAX model, which likewise intends to estimate the first differences instead of the actual forecast target, and is therefore considered a suitable comparative approach.

Table 1 summarizes the statistical properties of mean, median, standard deviation, skewness, and kurtosis for the times series of the differences of FCR prices in the period of investigation 2017⁴ to 2018:Q3 with a total number of 88 observations.

3.2 | Identification and pre-processing of exogenous variables

As there is no explicit literature on exogenous regressors with regard to balancing reserve prices, several regressors that are commonly used in models for other electricity prices (see, e.g., Bublitz et al., 2017; Kiesel &

⁴As France joined the joint auction at the start of 2017, data from before that date may not include all interdependencies and lead to a wrong model fitting.

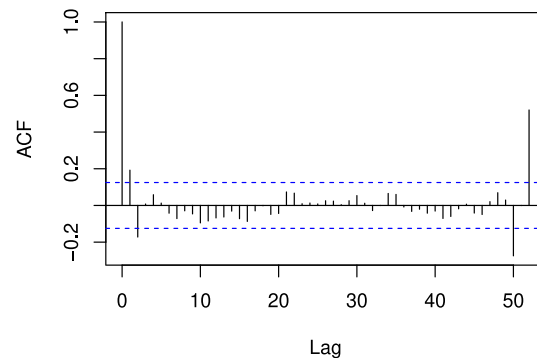


FIGURE 3 Autocorrelation function (ACF) of differenced time series (own illustration based on data from regelleistung.net, 2019) [Colour figure can be viewed at wileyonlinelibrary.com]

Paraschiv, 2017) are considered as exogenous regressors in this study. Representing, among others, opportunity costs for reserve provision and a scarcity in the market, the following possible predictors are identified:

- price range and skewness of FCR bids in previous auction (regelleistung.net, 2019);
- average electricity price of week-ahead future German–Austrian (DE-AT)⁵ and French (FR) market area (EEX, 2019);
- average day-ahead electricity spot market price in DE-AT and FR (EEX, 2019);
- average load forecast and realized load for DE-AT and FR (ENTSO-E, 2019);
- number of German public holidays in a week (ENTSO-E, 2019);
- planned unavailable capacity in DE-AT and FR (ENTSO-E, 2019).

Note that exogenous factors like wind and photovoltaic power feed-in are not considered, as the auction for FCR procurement takes place 1 week ahead and the volatile renewable feed-in is hardly predictable at these time-scales. However, the future price includes the effect of the expected wind and photovoltaic power feed-in in the respective week due to the merit-order effect. We thus implicitly consider for volatile renewable energy sources to some extent.

For the selection of predictors from the list above, the *corrected* Akaike information criterion (AIC; Hyndman &

⁵As the DE-AT future product was split up into DE and AT future products, the volume-weighted average of DE-AT and DE futures is taken for 2018.

TABLE 1 Descriptive statistics of the differences of FCR prices

Variable	<i>n</i>	Mean	Median	SD	Skewness	Kurtosis
Differences, FCR price	88	-8.13	9.62	178.58	1.91	15.38

Athanasopoulos, 2013) of a linear regression model⁶ applied to 2017 data is used. Other popular information criteria for model selection contain the regular AIC and the Bayesian information criterion (BIC). By penalizing the number of parameters, the corrected AIC accounts for and adjusts the tendency of the AIC to prefer models with too many parameters when sample sizes are relatively low. Due to the relatively low sample size, the AIC was not considered in predictor selection. By penalizing the number of parameters, the corrected AIC accounts for and adjusts the tendency of the AIC to prefer models with too many parameters when sample sizes are relatively low. Among all predictor combinations, the set of exogenous predictors containing the *FCR price range*, the *future price DE-AT*, the *future price FR*, the *load in DE-AT*, the *load in FR* and the *planned unavailable capacity in DE* achieved the lowest corrected AIC, corresponding to the best fit in the linear regression on the 2017 data. A selection based on the BIC leads to a similar parameter set as the ranks of the models sorted by BIC are comparable to the ranks sorted by the corrected AIC. For example, the best model in terms of BIC chooses the *load forecast in FR* instead of the *realized load in FR* and drops the *future price of FR*. For the scope of the paper to configure and compare the SARIMAX and ANN forecasts, we consider the choice of regressors according to the corrected AIC to be suitable. As French nuclear power plants contribute a significant share to the FCR provision, the *planned unavailable capacity in FR* is added to the predictor set chosen by the corrected AIC. Although the chosen predictor set x may not be the best for all models, all forecasting approaches are deployed in the following with the same selected set for reasons of consistency and comparability.⁷

⁶Linear regression models the differences of the FCR price time series (dependent variable = Δy) with the different sets of exogenous variables. The regression was chosen over a simple correlation analysis as the latter might not respect interdependencies between the independent variables. In particular, load and electricity prices are highly correlated and should thus not be handled independently.

⁷The predictor set containing the *planned unavailable capacity in France* instead of the *planned unavailable capacity in Germany* was the eighth best (of 16,383) behind variations of the highly correlated *load and load forecast in Germany* and *in France*. The corrected AIC penalizes adding a predictor to the set; thus the predictor set finally used was not among the favorites of corrected AIC. Nevertheless, as mentioned above, we consider the *unavailable capacity in France* a relevant predictor variable and included it in the investigation.

The preprocessing consists of a validity check of the raw data, the calculation of descriptives to be used in the modeling (e.g. weighted average, range or skewness), and finally a normalization. Normalization has been discussed at many points in the context of time series forecasting and neural networks (see, e.g., Kaastra & Boyd, 1996; Keles, Scelle, Paraschiv, & Fichtner, 2016). For ANN, it is particularly important to choose the normalization range according to the intended activation function of the neurons. As having a common value range of all target and predictor variables leads to a more stable functioning of the related fitting algorithms and does not change the results, we normalize the data between zero and one by subtracting the minimum value and dividing by the range of values.

3.3 | Setup and training of models

For training and forecasting with the SARIMAX and ANN models, a cross-validation approach called *rolling one-step forecast with model reestimation* is set up (see, e.g., Arlot & Celisse, 2010). In this approach, models are fitted with training data in order to predict the value of the single next step. In the reference training strategy the training data set is extended by one step for each forecast step, which is also referred to as an expanding window. In our case, the initial training data set consists of the 52 observations from 2017. As can be seen in Figure 4, the training data set for week 1 of 2018 consists of all 2017 data, the training data set for week 2 of 2018 consists of the 2017 data plus week 1 of 2018, and so on. In this way, the best information available to the trader at the forecasting time is used in the forecast. As a consequence, there is no single model but as many models as forecasting steps for each approach presented in the following paragraphs.

As the analysis of the price time series in Section 3.1 revealed different price characteristics over time, in addition to the expanding window, a rolling window of size 10 is considered in the experimental design for training the ANN. The rationale behind having a rolling window is to make the networks more adaptive to changing dependencies over time and to focus on the recent observations, not distorting the network learning from nonrelevant information from the past. However, the rolling window obviously bears the risk of further enhancing the data scarcity problem and leading to worse prediction

configured. The choice of the number of *neurons per hidden layer* is important in the setup of a network. Generally, there is no optimal model configuration algorithm, but there are many rules-of-thumb. One of them suggests a number below the half of input nodes and approximately two thirds of the sum of input and output nodes. Although this is only a rule-of-thumb and the choice is problem specific, we conclude 10 to be a reasonable number of neurons per hidden layer for the reference model. To gain insight into the sensitivity of the number of neurons per layer, in the experimental design the design variable is varied with levels 10 and 20.

The second hyperparameter choice in the model configuration is the *number of hidden layers*. For the reference model, one hidden layer is chosen. Originating from the structure, deeper networks are more adaptive to the training data and thus able to learn more complex relationships. A drawback of deep networks, especially those that are trained with relatively few data, is the risk of overfitting. To investigate the dependency of the prediction on the amount of layers, a second configuration with two hidden layers is deployed.

As important as the configuration of the model structure is the definition of the training strategy. In this paper, the term *training strategy* comprises the selection of *training data* to be available and the way these are processed in the training process, defined by the *training hyperparameters*. To provide the networks with the same input data as the SARIMAX approach, for each prediction a lookback of two steps into the data is implemented, containing the values of the dependent variable and their lags of 50 and 52 as well as seven exogenous variables, leading to 22 input nodes.

The last stage before training and evaluating the networks is the definition of the *training hyperparameters*. As applies for the network configuration, the training is subject to the tradeoff between utilizing all information that is contained in the training data and overfitting the model to the training data. Training the models requires the setting of the hyperparameters *number of batches*, *number of epochs*, and *iterations per epoch*, defining the way the training data set is split into training batches and how the training in terms of weight optimization is executed. As our models face relatively small data sets, batching the training data is not necessary (*number of batches* = 1).

For the other hyperparameters, *number of epochs* = 30 (representing the number of training sequences), and *iterations per epoch* = 20 (representing the number of iterations optimizing the tensor weights per sequence) lead to favorable training results for the reference model configuration with the expanding window training data outlined above. As shown in Figure 5, the choice of

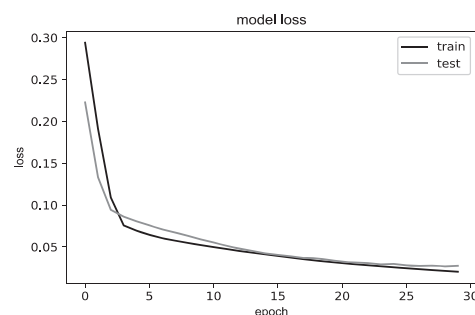


FIGURE 5 Exemplary training history of the reference feedforward network with training hyperparameter set “fit” (number of batches = 1, number of epochs = 30, iterations per epoch = 20). The black line depicts the loss of model training, and the gray line depicts the loss of a random 10% validation split extracted from the training data

hyperparameters yields a desirable training fit and avoids overfitting. Hereby, due to the rolling one-step forecast with model reestimation setup, we consider it suitable to take a 10% validation split randomly selected from the training data and do not apply a hold-out-sample validation. The validation split is only conducted for the hyperparameter selection. After the hyperparameters are selected, owing to data scarcity the validation split is dropped for model training. The training of the ANN is thus conducted with the entire training data set to account for all relevant information.

Since the model training starts with random weights and is therefore indeterministic, an ensemble of networks is deployed for each configuration. Ensembling is a common technique similarly proposed by Hyndman and Athanasopoulos (2013). For applications with rich databases (see Section 2 for examples) for model training and validation, ensembling is not very important as model training mostly converges to a single model. However, in our case with a scarce training data basis, ensembling allows us to obtain robust forecasts from numerous indeterministic models. For the reference training hyperparameters, we run the fitting process 50 times to obtain 50 independent ANN of each model structure for each forecasting step. The prediction values of these are then averaged to obtain a single representative prediction value for the respective forecast step. As a measure of robustness, the standard deviation of the different forecasts within the ensemble is reported in Section 4. Although different hyperparameters could yield better training results, they also bear the risk of overfitting the data.

An alternative training strategy consists of intentionally overfitting the training data to some extent and compensating the overfit by increasing the *ensemble size*. To

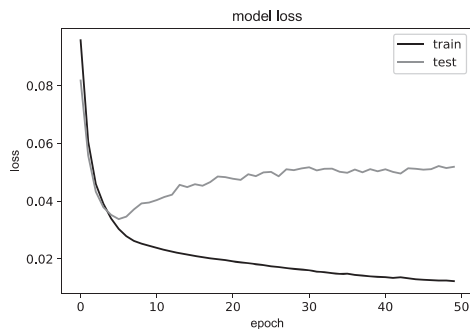


FIGURE 6 Exemplary training history of the reference feedforward network with training hyperparameter set “overfit” (number of batches = 1, number of epochs = 50, iterations per epoch = 30). The black line depicts the loss of model training, and the gray line depicts the loss of a random 10% validation split extracted from the training data

examine the performance of this strategy compared to the reference “fit” hyperparameter set, a second set of training hyperparameters “overfit” is implemented. Increasing the number of epochs to 50 and the iterations per epoch to 30 leads to a slight overfit for the reference model configuration. As the exemplary training history in Figure 6 shows, the performance of the model on the validation data becomes worse as the model fit increases with advancing training. However, equipped with an ensemble size of 100, these intentionally overfit models might, on average, perform better than the fit models as the overfitting residuals balance each other out.

In the end, the presented experiment design with four factors and two levels each leads to 16 different model configurations. Table 2 summarizes the factors and their levels in the network configuration and training process. In the following, the abbreviation for a combination of a network configuration and a training strategy is built by combing the entries of Table 2—for example, “FF1_10_E_F” for the reference with one hidden layer, 10 neurons per hidden layer, an expanding training window, and the training hyperparameters “fit.”

The training and evaluation of the ANN models are implemented in keras,¹⁰ a common machine learning library available for Python and R. On a machine with a 2.50 GHz 64-bit processor (central processing unit, CPU) and 16 GB RAM, depending on the model configuration and training strategy, the training and evaluation of one setup takes between 2 and 6 hours for the 37 forecasting steps. However, the training time could be significantly reduced by the use of parallelization and a graphics processing unit (GPU) for the computations.

¹⁰For more information on keras see <https://keras.io/>.

4 | RESULTS

The results consist of the out-of-sample performance of the presented model framework. The forecasted time series for a selection of approaches in comparison to the real time series of FCR prices of the testing period (01/2018–09/2018) are presented in Figure 7. The selection consists of the naive forecast, the SARIMAX approach, as well as ANN approaches “FF1_10_E_F,” “FF1_20_E_F,” “FF1_10_E_Ov,” “FF1_20_E_Ov,” “FF2_10_E_F,” and “FF2_10_E_Ov.” Due to conciseness, the plots for the complete set of examined configurations of the ANN experiment design have been moved to Figure A in the Appendix.

A first graphical comparison of the developed forecasts (Figure 7) indicates that both the econometric and ANN approaches are able to forecast the level of the FCR price quite well. For the SARIMAX approach, both the point forecast and the 95% confidence intervals are provided. The latter indicate the robustness of the estimated model for each forecast step. It can be observed that for all time steps the prediction target (dashed line) lies within the confidence interval, complying with a desirable robustness. As there is no mathematical equivalent for confidence intervals in the ANN approaches, the robustness of the models is determined with the standard deviation of the point forecasts obtained from ensembling for each forecast step (provided by Table 3). An artefact confidence interval for the ANN approaches could be constructed from the residuals’ distribution of sufficiently large ensembles (e.g. 1,000 networks instead of 50). The residuals would then represent an empirical distribution, whose 2.5% and 97.5% quantiles could be interpreted as the confidence interval. However, computational limitations do not allow us to generate ensembles of size 1,000 for each forecasting step and all model designs. We cannot build a reliable distribution for the residuals based on an ensemble of size 50. Without a reliable distribution, no confidence interval in a mathematical sense can be derived and the construction of confidence intervals for ANN is excluded.

The good fit also counts for the naive approach, so that the benefit of the more sophisticated models does not become clear at the first inspection of the results. A second view reveals that the deviation between the forecasted values and the real test data is especially smaller when the overall price level and in particular the price variations decrease. For the high price levels (first parts of the price curve), it is observable that the ANN approaches perform better and almost approach the real price curve. These differences become more visible if the residuals—that is, the single forecast errors—are directly analyzed. Figure 8 shows that, compared to the naive and

TABLE 2 Experimental design for neural networks

Factor	Level reference	Level variation
<i>Network configuration</i>		
Number of hidden layers	FF1 (1 hidden layer)	FF2 (2 hidden layers)
Number of neurons per hidden layer	10	20
<i>Training strategy</i>		
Training data	E (expanding window)	R (rolling window)
Training hyperparameters	F (fit): number of batches = 1, number epochs = 30, iterations per epoch = 20, ensemble size = 50	Ov (overfit): number of batches = 1, number epochs = 50, iterations per epoch = 30, ensemble size = 100

Note. A design consists of a combination of the hyperparameters' number of hidden layers, number of neurons per hidden layer and the training strategy defined by the training data and the training hyperparameters

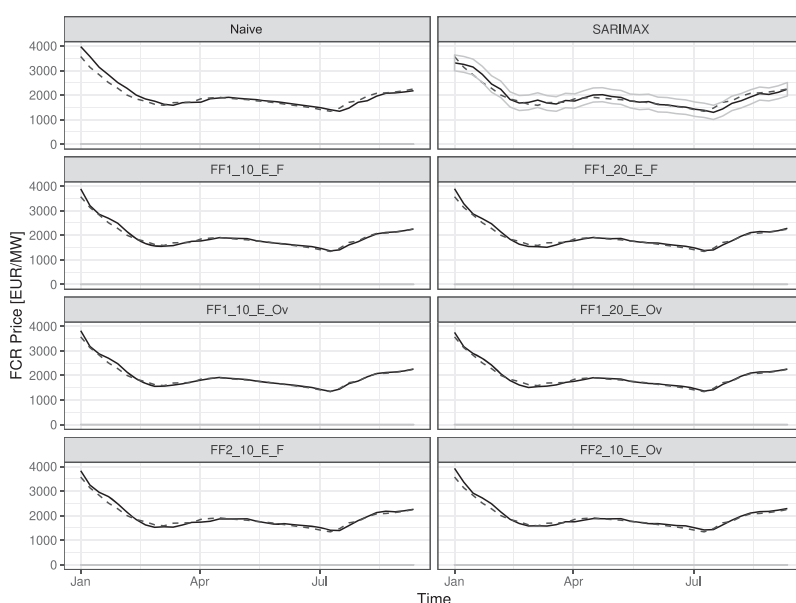


FIGURE 7 Selection of FCR price forecasts in test period 2018:Q1–Q3 (original FCR price data from regelleistung.net, 2019). Solid lines are the forecasted FCR prices, and dashed lines represent the realized FCR price. All forecasting approaches show a relatively good fit

the SARIMAX approach, the errors of the ANN approaches are particularly lower for the first part of the test period (until April), when real FCR prices have a strong decline and are exposed to more fluctuations. The residuals indicate a serial correlation that was also reported in more detail in the preliminary works of Kraft et al. (2019). Generally, the residuals of well-fitted SARIMAX models should be independent and identically distributed. In the rolling one-step forecast with model reestimation setup deployed in this paper, each forecasting step reestimates the model, which leads to distinct SARIMAX models for each forecasting step.

Further investigations address the structure of the SARIMAX residuals to check for conditional

heteroskedasticity. Figure 8 therefore exemplarily provides the residuals of the SARIMAX model estimated for the last forecasting step. It can be observed that the residuals are not perfectly homoskedastic. Although no substantial autocorrelation is observable, the volatility of the time series appears to be heterogeneous over time. The residuals in 2017 are larger compared to those in 2018 and, in particular, the year change from 2017 to 2018 produces two data points with a larger volatility compared to the rest of the time series. To address the suspected heteroskedasticity of the SARIMAX residuals, a SARIMAX-generalized autoregressive conditional heteroskedasticity (GARCH) approach was tested. However, the limited data basis

TABLE 3 Root mean square error (RMSE), mean absolute percentage error (MAPE), directional accuracy (DAC), and mean standard deviation (σ) of the model forecasts

Design	RMSE	MAPE	DAC	σ
Naive	158.16	5.24%	91.70%	n/a
SARIMAX	136.82	5.18%	75.00%	140.03
FF1_10_E_F	86.38	2.78%	100.00%	127.81
FF1_20_E_F	94.13	3.27%	91.70%	125.75
FF1_10_E_Ov	72.16	1.97%	97.20%	108.05
FF1_20_E_Ov	72.71	2.89%	97.20%	120.78
FF1_10_R_F	185.71	6.32%	66.70%	183.35
FF1_20_R_F	190.94	6.52%	75.00%	175.02
FF1_10_R_Ov	194.97	6.43%	72.20%	178.68
FF1_20_R_Ov	194.05	6.80%	72.20%	167.71
FF2_10_E_F	101.42	3.94%	80.60%	147.43
FF2_20_E_F	119.77	4.75%	77.80%	134.81
FF2_10_E_Ov	104.07	3.45%	86.10%	147.30
FF2_20_E_Ov	114.96	4.79%	80.60%	128.12
FF2_10_R_F	181.49	6.22%	69.40%	158.77
FF2_20_R_F	189.05	6.23%	72.20%	131.80
FF2_10_R_Ov	192.37	5.74%	80.60%	142.14
FF2_20_R_Ov	184.20	6.02%	77.80%	120.63

Note. For ANN the reported σ is calculated as the empirical standard deviation of residuals, whereas for SARIMAX σ is the mean theoretical σ of the 37 forecast models. The simplest design FF1_10_E_F reaches 100% of DAC, but is dominated by FF1_10_E_Ov and FF1_20_E_Ov in terms of RMSE. The best design by RMSE and MAPE is FF1_10_E_Ov. These three designs are indicated in bold font. The more sophisticated designs and the designs with a rolling training window have a similar performance to the SARIMAX and naive forecast. All designs involving ensembling show a moderate standard deviation, indicating robust model training and the need for ensembling

(residuals contain only 52–88 observations for the different forecasting steps) impedes the deployment of GARCH models, as the estimation does not converge. Related literature suggests sample sizes of at least 500 (respectively 700) are required to obtain good results for GARCH volatility estimation (Hwang & Valls Pereira, 2006; Ng & Lam, 2006). Unfortunately, in our case the data basis is too scarce to apply GARCH and we are restricted to the chosen SARIMAX approach as econometric comparative to the ANN.

The naive approach is performing similarly well (respectively even better) in periods when prices remain more or less constant over time. However, this is quite obvious, as this approach applies the last week's real value to the current week's forecast. In periods with

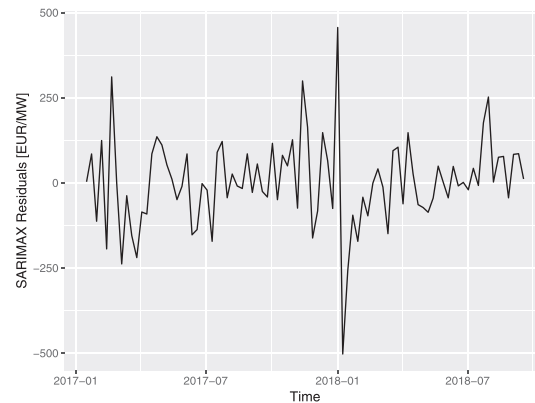


FIGURE 8 Exemplary residuals time series of the SARIMAX model for the last forecasting step. It can be observed that the residuals do not contain substantial autocorrelation and that the volatility of the residuals is increased at the year change from 2017 to 2018

hardly any changes, the approach will therefore produce desirable results.

However, we are more interested in approaches that can also capture periods when prices undergo price changes, as future FCR prices might change much more frequently and in a more pronounced way. The market is more and more opened for new players and technologies, such as battery storage, that will bring much more dynamics into the market. In this respect, the ANN approaches are able to capture price dynamics, which obviously cannot be covered by the naive approach. Moreover, in the case of FCR prices, ANN approaches cover the dynamics in volatile periods significantly better than the applied SARIMAX approach.

Interestingly, Figure 8 demonstrates that SARIMAX errors are more frequently fluctuating around 0 EUR/MW, while those of the ANN forecasts remain in the positive or negative scale longer. As Figure B in the Appendix indicates, the fluctuations around 0 EUR/MW also apply to the ANN configurations with a rolling training window, and for some forecasting steps a rolling window training strategy can yield a better forecast than an expanding window approach. This indicates that, by including seasonal factors or limiting the training data to a rolling window, the performance of the ANN approaches can be improved for some time periods. However, determining such factors based on the short period, for which weekly FCR prices are available, leads to overfitting for other periods, and therefore does not improve the overall forecasting performance itself. The concerns regarding the impeded exploitation of strengths of the ANN approach that are discussed in Section 3.3 prove

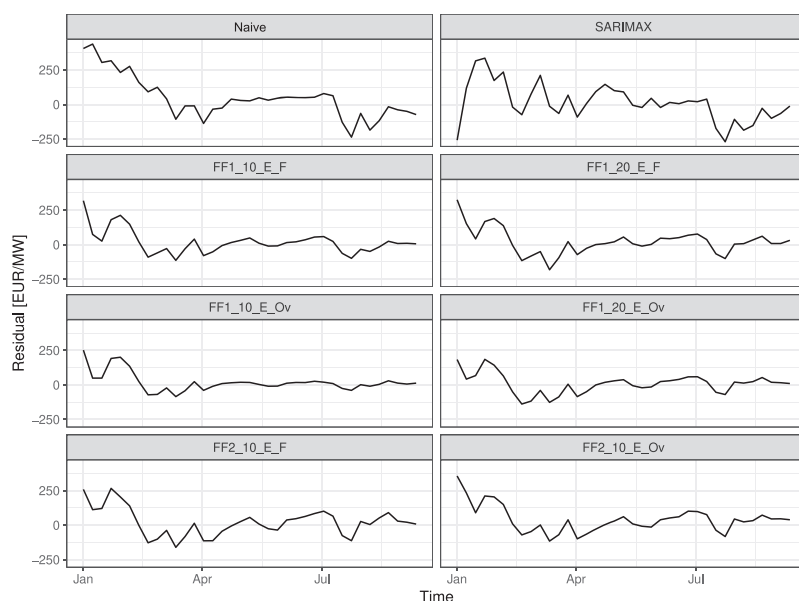


FIGURE 9 Residuals of FCR price forecasts in test period 2018:Q1–Q3 (original FCR price data from regelleistung.net, 2019). Due to the larger ensemble size, the ANN approaches with overfit (Ov) produce smoother residuals compared to those with fit (F)

right. As the rolling window training strategies cannot exploit the entirety of training data provided to the expanding window training, the overall forecasting performance decreases. Training with an expanding window is therefore preferable to the rolling window approach. In particular, if the network structures become more sophisticated, the model requires as many training data points as possible to be performant.

The residuals of the ANN approaches are distributed relatively symmetrical around zero, as can be seen in the illustration of error histograms in Figure C in the Appendix. However, to derive further insights regarding the distribution of the residuals, the number of forecasting steps is too small.

Whereas Figures 7 and 9 enable a qualitative discussion, Table 3 presents the quantitative performance and robustness measures. The performance measures again indicate that having a mean absolute prediction error (MAPE) below 7% all proposed models perform reasonably well. With regard to the root mean square errors (RMSE) and the MAPE, the feedforward ANN with an expanding training window all outperform the naive forecast and the SARIMAX models. The directional accuracy (DAC) confirms these observations. Whereas the best model in terms of RMSE and MAPE fails to predict the direction of change once (97.2% accuracy), the model design FF1_10_E_F reaches 100% accuracy in the considered forecasting steps.

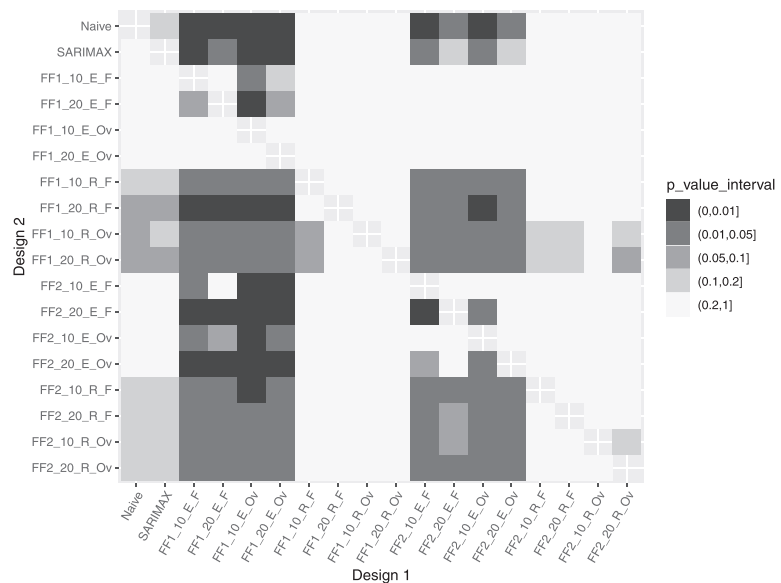
Surprisingly, adding a second layer to the networks does not improve the forecasting. The dominating designs for the prediction task are the ANN with one

hidden layer and an expanding training window. With an RMSE of 72.16 and a MAPE of 1.97%, the configuration with 10 neurons per layer and the “overfit” training (FF1_10_E_Ov) yields the best results. Increasing the number of neurons to 20 (FF1_20_E_Ov) or changing the training strategy to “fit” (FF1_10_E_F) leads to slightly worse results. Interestingly, the FF1_20_E_Ov design dominates the FF1_10_E_F design in terms of RMSE but is outperformed in terms of MAPE, meaning the residuals are on average larger but have smaller large residuals, which is penalized more strongly in the RMSE measure.

The design variable *neurons per layer* reveals an interesting, yet intuitive, pattern. Apart from the best-performing design with one hidden layer, expanding window and overfit training, the forecasts of the networks with 20 neurons per layer are more robust than the comparable networks with only 10 neurons. However, except for two cases with rolling window, the performance in terms of RMSE and MAPE is better for the configurations with only 10 neurons per hidden layer. The increased number of neurons leads to more convergence in the weight optimization and thus to more stable results, yet the convergence may be prone to overtraining of the relationships in the training data compared to the simpler configurations with only 10 neurons.

The last variable in the experimental design are the training hyperparameters, for which the two sets “fit” and “overfit” are distinguished. For the simple networks (one hidden layer, 10 or 20 neurons), the strategy to overfit and build a larger ensemble yields a massive

FIGURE 10 Results of Diebold–Mariano testing whether the forecasts obtained from design 1 are significantly better than the forecast obtained from design 2. It can be observed that the designs with expanding training window dominate those with rolling training window. Only the best three models (FF_10_E_F, FF_10_E_Ov, FF_20_E_Ov) are better than the SARIMAX approach at the 1% significance level and six ANN models perform better at the 5% significance level



improvement in forecasting performance. Regarding robustness, there is a slight increase (decrease in mean standard deviation of model forecasts) in the overfit training configurations.¹¹ Increasing the ensemble size from 50 to 100 has a smoothing effect on the ANN forecasts and results in an increased forecasting performance. This observation goes hand in hand with the residuals illustrated in Figure 9, where the overfit designs produce smoother residuals compared to their respective fit design. The observation holds for the more sophisticated networks in terms of robustness, whereas both fit and overfit designs provide sufficiently robust forecasts. As was observed for the number of neurons per hidden layer, the models in the overfit configurations tend to converge more strongly as more weight optimizations are conducted in the training process, which turns out to be slightly more robust. However, the overfit does not

necessarily yield a better performance. The RMSE and MAPE show no clear tendency towards the “fit” or “overfit” training as both perform similarly well.¹² Generally, the standard deviation of the forecasts within the ensembles indicates the necessity to build ensembles as the training results in different networks. Conversely, for the SARIMAX approach, only one model is calculated for each forecasting step. The average standard deviation of all SARIMAX models is 140.03. However, this robustness measure is hardly comparable to the standard deviation of the ANN described above. While for the ANN we report an empirical standard deviation of residuals, the σ of SARIMAX is the mean theoretical standard deviation of the 37 forecast models.

To verify the statistical significance of the results, Figure 10 presents the results of a one-sided Diebold–Mariano test. The test compares two time series of residuals and indicates whether one is significantly lower than the other—that is, whether one forecast model is significantly better than the other (Diebold & Mariano, 1995). We find that the results reported in Table 3 mostly prove significant. The designs with expanding training window are significantly better than those trained with rolling training window on at least 5% significance level. The best three models in terms of MAPE and RMSE (FF_10_E_F, FF_10_E_Ov, FF_20_E_Ov) are better than the SARIMAX approach at the 1% significance level.

¹¹The standard deviation amongst the 50 predictions of each model for each type is calculated for each step and then averaged over all prediction steps. In the presentation of results, it was considered that the ensemble size of the “overfit” designs is twice that of the “fit” designs. However, repeatedly sampling 50 observations from the overfit ensembles shows that the ensemble size is not decisive for the robustness measure. However, the forecasting performance decreases with reduction of the ensemble size in the overfit training strategy, particularly strong in configurations with rolling training windows.

¹²As mentioned earlier, a further sophistication of model configurations with recurrent structures and gated-recurrent units did not yield improvements compared to the networks presented in this paper. This is in line with the results for the configurations with two hidden layers compared to the one with one hidden layer and the tendency to

overtraining for the more sophisticated configurations in the results presented. For more details, see the Annex.

However, the SARIMAX and naive approach compete well with the forecast performance of the ANN with rolling training window. The best ANN design in terms of MAPE and RMSE (FF_10_E_Ov) dominates all but the second-best design in terms of RMSE (FF_20_E_Ov) at 5% significance level.

To conclude, the variety of models examined in this paper offers another approach to forecasting. A solution to ally the strengths of the model classes and configurations and to balance out the shortfalls can consist of combining the different approaches. However, to build the best combination of approaches for each forecasting step, one must be aware of the strengths and weaknesses of the approaches and build a subjective market expectation. For this task, human experience is inevitable.

Finally, it is worth mentioning that the goal of this paper is to investigate approaches and configure a suitable model framework to forecast FCR prices. The presentation of the results focuses rather on the comparison of the different approaches than on the detailed discussion of single models and their coefficients' interpretation, as our goal was not to uncover the influence of the explaining variables, but to determine the performing modeling approaches and model configurations for FCR price forecasting. However, to gain more insights regarding the interdependencies and predictive power of the single exogenous variables, a detailed investigation of exemplary models from the considered approaches is an interesting direction for future research.

5 | CONCLUSION AND OUTLOOK

In this paper, we investigated approaches to forecast the price of FCR, the fastest balancing reserve that is jointly procured in weekly auctions by TSOs in Austria, Belgium, France, Germany, the Netherlands, and Switzerland. As this research scope was not formerly discussed in literature, several approaches were deployed, considering autoregressive and exogenous variables. Such a model framework has, to our knowledge, not been formerly set up or discussed.

The exogenous factors with most explanatory power are identified as the *price range* of the previous auction, the *future prices* of the German–Austrian and the French market area, the *load* in the German–Austrian and the French market area and the *planned unavailable* capacity in Germany and France. The models based on autoregressive and exogenous factors are suitable to forecast prices. Within the developed models, ANN with expanding training window yield desirable results and clearly outperform the naive forecast and the SARIMAX approach. Simple models equipped with a slight overfit

and a larger ensemble size outperform the simple models that were trained aspiring to the best fit and lead to the best and most robust forecast results in the case of forecasting FCR prices. With an increase in model complexity, the positive effect of the slight overfitting strategy vanishes. Furthermore, the overall forecasting performance is not improved by more sophisticated models, as these might overtrain the relationships in the training data.

In the interpretation of these results, one must always bear in mind that econometrics and artificial intelligence approaches are only capable of drawing conclusions from data of the past. Thus changed bidding behavior by market participants or technological changes in FCR market are hardly predictable by these kinds of forecasting models. Based on assumptions (e.g., market diffusion of battery storages, market exit of conventional power plants) we could consider forecasts for the long-term FCR price development. However, this is not in the scope of this paper and needs to be addressed by future research. The main contributions of this paper are the application and comparison of statistical and neural network models to FCR price forecasting. This comprises the definition of an appropriate target variable as well as the discussion of modeling techniques and training strategies for forecasting on a scarce data basis. Finally, a discussion on the suitability and performance of simple and more sophisticated network structures for FCR price forecasting completes the contributions.

In the ongoing research, the models will be used as a basis for the formulation and optimization of bidding strategies in the European balancing reserve market. In this context, the application of SARIMAX models has the advantage that the models are open to an interpretation of the estimated coefficients, whereas the ANN approaches tend to be black boxes that yield the best results, especially in times of increased FCR price volatility, but lack interpretability. The reestimation and number of models complicate a fundamental model interpretation, as model lags, parameters and coefficients vary between the models. However, the goal in this paper is to make the forecast as accurate as possible, and reestimation increases the quality of the forecast.

Finally, the market design for FCR is in an ongoing process of change. On the one hand, the involved TSOs changed the product duration from 1 week to 1 day beginning July 2019 and intend to move to 4-hour products in the near future. This makes the consideration of forecast-based exogenous factors like wind and solar generation possible and necessary in price formation and therefore needs to be included in future studies of FCR prices. In the course of these changes, the pricing rule changed from pay-as-bid to uniform

pricing. However, the approaches developed in this study are well suited and extendable to cope with these changes and to produce reliable forecasts of FCR prices in a modified market design.

ACKNOWLEDGMENTS

This paper is a part of the work within the SINTEG project C/sells, funded by the German Federal Ministry for Economic Affairs and Energy (grant number 03SIN120).

DATA AVAILABILITY STATEMENT

Data are available on request from the authors. The data that support the findings of this study are available from the corresponding author upon reasonable request.

ORCID

Emil Kraft  <https://orcid.org/0000-0001-9237-4488>

REFERENCES

- Adya, M., & Collopy, F. (1998). How effective are neural networks at forecasting and prediction? A review and evaluation. *Journal of Forecasting*, 17(5–6), 481–495.
- Alon, I., Qi, M., & Sadowski, R. J. (2001). Forecasting aggregate retail sales. *Journal of Retailing and Consumer Services*, 8(3), 147–156. [https://doi.org/10.1016/S0969-6989\(00\)00011-4](https://doi.org/10.1016/S0969-6989(00)00011-4)
- Arlot, S., & Celisse, A. (2010). A survey of cross-validation procedures for model selection. *Statistics Surveys*, 4, 40–79. <https://doi.org/10.1214/09-SS054>
- Binner, J., Bissoondeal, R., Elger, T., Gazely, A., & Mullineux, A. (2005). A comparison of linear forecasting models and neural networks: An application to Euro inflation and Euro Divisia. *Applied Economics*, 37(6), 665–680. <https://doi.org/10.1080/0003684052000343679>
- Brockwell, P. J., & Davis, R. A. (2016). *Introduction to time series and forecasting*. Cham, Switzerland: Springer. <https://doi.org/10.1007/978-3-319-29854-2>
- Bublitz, A., Keles, D., & Fichtner, W. (2017). An analysis of the decline of electricity spot prices in Europe: Who is to blame? *Energy Policy*, 107, 323–336. <https://doi.org/10.1016/j.enpol.2017.04.034>
- Catalão, J. P. S., Mariano, S. J. P. S., Mendes, V. M. F., & Ferreira, L. A. F. M. (2007). Short-term electricity prices forecasting in a competitive market: A neural network approach. *Electric Power Systems Research*, 77(10), 1297–1304. <https://doi.org/10.1016/j.epsr.2006.09.022>
- Chatfield, C. (1996). Model uncertainty and forecast accuracy. *Journal of Forecasting*, 15(7), 495–508.
- Church, K. B., & Curram, S. P. (1996). Forecasting consumers' expenditure: A comparison between econometric and neural network models. *International Journal of Forecasting*, 12(2), 255–267. [https://doi.org/10.1016/0169-2070\(95\)00631-1](https://doi.org/10.1016/0169-2070(95)00631-1)
- Diebold, F. X., & Mariano, R. S. (1995). Comparing predictive accuracy. *Journal of Business & Economic Statistics*, 13(3), 253–263.
- Dimoukias, I., Amelin, M., Hesamzadeh, M. (2016). Forecasting balancing market prices using hidden Markov models. In 2016 13th International Conference on European Energy Market (EEM), 6–9 June 2016, Porto, Portugal.
- EEX. (2019). EEX market data. Retrieved from <http://www.eex.com>
- ENTSO-E. (2019). Transparency platform of European Network of Transmission System Operators for Electricity (ENTSO-E) Retrieved from <https://transparency.entsoe.eu>
- Giovanelli, C., Sierla, S., Ichise, R., & Vyatkin, V. (2018). Exploiting artificial neural networks for the prediction of ancillary energy market prices. *Energies*, 11(7), 1906–1928. <https://doi.org/10.3390/en11071906>
- Glorot, X., Bordes, A., Bengio, Y. (2011). Deep sparse rectifier neural networks. In 14th International Conference on Artificial Intelligence and Statistics (AISTATS) 2011, Fort Lauderdale, FL.
- Hwang, S., & Valls Pereira, P. L. (2006). Small sample properties of GARCH estimates and persistence. *European Journal of Finance*, 12(6–7), 473–494. <https://doi.org/10.1080/13518470500039436>
- Hyndman, R., & Athanasopoulos, G. (2013). *Forecasting: Principles and practice* (Print ed.). Melbourne, Australia: OTexts.
- Hyndman, R., & Khandakar, Y. (2008). Automatic time series forecasting: The forecast Package for R. *Journal of Statistical Software*, 27(3), 1–22. <https://doi.org/10.18637/jss.v027.i03>
- Just, S., & Weber, C. (2008). Pricing of reserves: Valuing system reserve capacity against spot prices in electricity markets. *Energy Economics*, 30(6), 3198–3221. <https://doi.org/10.1016/j.eneco.2008.05.004>
- Kaasra, I., & Boyd, M. (1996). Designing a neural network for forecasting financial and economic time series. *Neurocomputing*, 10(3), 215–236. [https://doi.org/10.1016/0925-2312\(95\)00039-9](https://doi.org/10.1016/0925-2312(95)00039-9)
- Keles, D., Scelle, J., Paraschiv, F., & Fichtner, W. (2016). Extended forecast methods for day-ahead electricity spot prices applying artificial neural networks. *Applied Energy*, 162, 218–230. <https://doi.org/10.1016/j.apenergy.2015.09.087>
- Kiesel, R., & Paraschiv, F. (2017). Econometric analysis of 15-minute intraday electricity prices. *Energy Economics*, 64, 77–90. <https://doi.org/10.1016/j.eneco.2017.03.002>
- Kirsch, L. D., & Singh, H. (1995). Pricing ancillary electric power services. *Electricity Journal*, 8(8), 28–36. [https://doi.org/10.1016/1040-6190\(95\)90014-4](https://doi.org/10.1016/1040-6190(95)90014-4)
- Klæboe, G., Eriksrud, A., Fleten, S. (2013). Benchmarking time series based forecasting models for electricity balancing market prices (Working paper). Washington, DC: George Washington University, Center of Economic Research.
- Kraft, E., Keles, D., Fichtner, W. (2018). Analysis of bidding strategies in the German control reserve market. In 15th EEM, Lodz, Poland, 27–29 June 2018.
- Kraft, E., Rominger, J., Mohiuddin, V., & Keles, D. (2019). Forecasting of frequency containment reserve prices using econometric and artificial intelligence approaches. In 11th International Symposium on Energy Economics, TU Vienna (IEWT), Vienna, Austria, 13–15 February 2019.
- Kwiatkowski, D., Phillips, P., Schmidt, P., & Shin, Y. (1992). Testing the null hypothesis of stationarity against the alternative of a unit root. *Journal of Econometrics*, 54(1–3), 159–178. [https://doi.org/10.1016/0304-4076\(92\)90104-Y](https://doi.org/10.1016/0304-4076(92)90104-Y)
- Lago, J., Ridder, F., & Schutter, B. (2018). Forecasting spot electricity prices: Deep learning approaches and empirical comparison

- of traditional algorithms. *Applied Energy*, 221, 386–405. <https://doi.org/10.1016/j.apenergy.2018.02.069>
- LeCun, Y., Bengio, Y., & Hinton, G. (2015). Deep learning. *Nature*, 521(7553), 436–444. <https://doi.org/10.1038/nature14539>
- Liu, X. Q., Ang, B. W. & Goh, T. N. (1991): Forecasting of electricity consumption: a comparison between an econometric model and a neural network model. In: 1991 IEEE International Joint Conference on Neural Networks. Singapore: IEEE, 1254-1259 Vol. 2.
- Ng, H., & Lam, K. P. (2006). How does sample size affect GARCH Models? In *9th Joint Conference on Information Sciences (JCIS)*, Taiwan, ROC, 08–11 October 2006. Paris, France: Atlantis Press.
- Ocker, F., Ehrhart, K.-M., & Belica, M. (2018). Harmonization of the European balancing power auction: A game-theoretical and empirical investigation. *Energy Economics*, 73C, 194–211.
- Ocker, F.; Ehrhart, K.-M. (2017). The “German Paradox” in the balancing power markets. In: *Renewable and Sustainable Energy Reviews*, 67, S. 892–898. <https://doi.org/10.1016/j.rser.2016.09.040>
- Oksuz, I., & Ugurlu, U. (2019). Neural network based model comparison for intraday electricity price forecasting. *Energies*, 12 (23), 4557–4571. <https://doi.org/10.3390/en12234557>
- Olson, D., & Mossman, C. (2003). Neural network forecasts of Canadian stock returns using accounting ratios. *International Journal of Forecasting*, 19(3), 453–465. [https://doi.org/10.1016/S0169-2070\(02\)00058-4](https://doi.org/10.1016/S0169-2070(02)00058-4)
- Olsson, M., & Söder, L. (2008). Modeling real-time balancing power market prices using combined SARIMA and Markov processes. *IEEE Transactions on Power Apparatus and Systems*, 23(2), 443–450. <https://doi.org/10.1109/TPWRS.2008.920046>
- Qi, M., & Zhang, G. P. (2001). An investigation of model selection criteria for neural network time series forecasting. *European Journal of Operational Research*, 132(3), 666–680. [https://doi.org/10.1016/S0377-2217\(00\)00171-5](https://doi.org/10.1016/S0377-2217(00)00171-5)
- Ramachandran, P., Barret, Z., & Quoc, L. V. (2017). Searching for activation functions. arXiv: 1710.05941, <https://arxiv.org/pdf/1710.05941v2>.
- regelleistung.net. (2019). Internetplattform zur Vergabe von Regelleistung [Internet platform for balancing power procurement]. Retrieved from <https://www.regelleistung.net>
- Tkacz, G. (2001). Neural network forecasting of Canadian GDP growth. *International Journal of Forecasting*, 17(1), 57–69. <https://doi.org/10.1016/S0169-2070%2800%2900063-7>
- Ugurlu, U., Oksuz, I., & Tas, O. (2018). Electricity price forecasting using recurrent neural networks. *Energies*, 11(5), 1255–1276. <https://doi.org/10.3390/en11051255>
- Wang, P., Zareipour, H., & Rosehart, W. (2014). Descriptive models for reserve and regulation prices in competitive electricity markets. *IEEE Transactions on Smart Grid*, 5(1), 471–479. <https://doi.org/10.1109/TSG.2013.2279890>
- Weron, R. (2014). Electricity price forecasting. A review of the state-of-the-art with a look into the future. *International Journal of Forecasting*, 30(4), 1030–1081. <https://doi.org/10.1016/j.ijforecast.2014.08.008>
- Yao, J., & Tan, C. L. (2000). A case study on using neural networks to perform technical forecasting of forex. *Neurocomputing*, 34 (1–4), 79–98. [https://doi.org/10.1016/S0925-2312\(00\)00300-3](https://doi.org/10.1016/S0925-2312(00)00300-3)

AUTHOR BIOGRAPHIES

Emil Kraft studied at École polytechnique fédérale de Lausanne (EPFL) and Karlsruhe Institute of Technology (KIT) and graduated as Industrial Engineer in 2017. Currently, he is research associate and PhD candidate in the research group “Energy Markets and Energy System Analysis” at the Chair of Energy Economics at the Institute for Industrial Production. His research focuses on the analysis and modelling of balancing energy markets and decision taking under uncertainty in the electricity markets context.

Dr. Dogan Keles graduated as Industrial Engineer from Karlsruhe Institute of Technology (KIT) in 2006 and received his PhD (Dr. rer. pol.) in 2013. During his work at the KIT he analysed uncertainties in energy markets and developed methods to evaluate energy investments. During his Senior Research Fellowship at Durham University in 2019, he carried out research on the effect of RES on electricity markets and designing systems with large shares of renewables. Currently, Dogan Keles is head of the research group “Energy Markets and Energy System Analysis” at the Chair of Energy Economics.

Prof. Dr. Wolf Fichtner studied Industrial Engineering and Management at the University of Karlsruhe (TH) from 1988 on. In 1998 he received his PhD (Dr. rer. pol.). After his habilitation in 2004, he initially worked as a university lecturer at the Institute for Industrial Production before joining EnBW Energie Baden-Württemberg AG as a project manager. In 2005, he accepted a call to the Brandenburg University of Technology in Cottbus, where he was head of the Department of Energy Economics until 2008. Since the end of 2008, he has been head of the Chair of Energy Economics at the Institute for Industrial Production at Karlsruhe Institute of Technology and head of the French-German Institute for Environmental Research (DFIU). Since 2012, he has been Director at the Karlsruhe Service Research Institute.

How to cite this article: Kraft E, Keles D, Fichtner W. Modeling of frequency containment reserve prices with econometrics and artificial intelligence. *Journal of Forecasting*. 2020;39: 1179–1197. <https://doi.org/10.1002/for.2693>

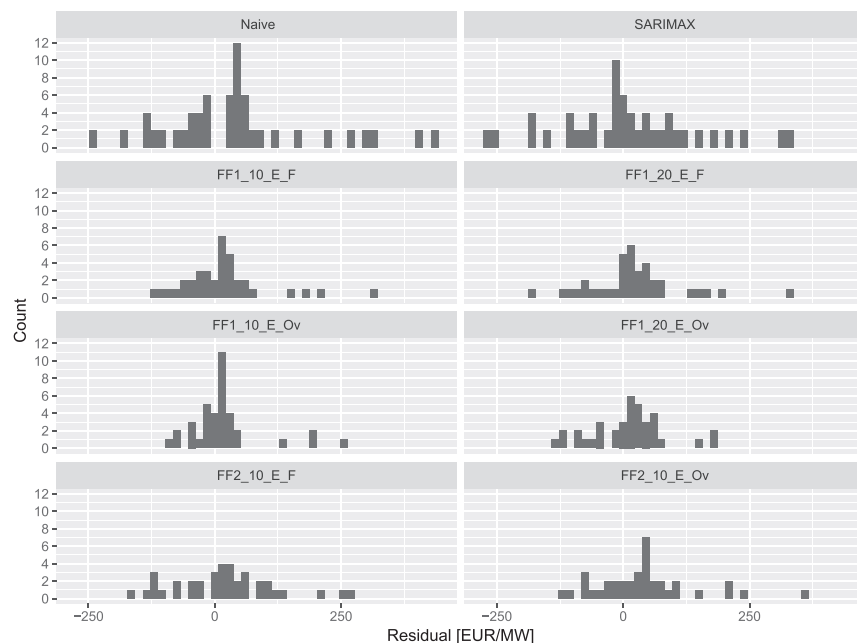
APPENDIX A

Here, supplementary illustrations of the results are presented as well as the hyperparameters, training strategies, and results of the network structures with GRU that were mentioned but not reported in Sections 3 and 4.

Figure A shows the histograms of residuals of FCR price forecasts in the test period. Figures B and C show the FCR price forecasts and residuals in the test period that were not shown in Figures 7 and 9 but reported in Table 3.

Tables A and B show the experimental design deployed for the GRU neural networks and the forecasting results. Hereby, one design consists of the combination of the hyperparameters *number of hidden layers*, *number of neurons* per hidden layer, and the *training strategy* defined by the training data and the training hyperparameters that are provided in Table A. Table B provides, analogously to Table 3, the performance indicators RMSE, MAPE, and DAC, and the robustness measure σ of the model forecasts for the GRU networks. Regarding forecasting performance, no improvement to the feedforward networks can be observed. However, regarding robustness, the standard deviations are generally smaller, which indicates model training is converging more strongly compared to the feedforward networks. To conclude, in our case the models with GRU lead to more robust forecasts around less accurate estimates.

FIGURE A Histograms of residuals of FCR price forecasts in test period 2018:Q1–Q3. It can be observed that the ANN residuals follow a relatively symmetric distribution around zero. The better models have a higher count in the bins closer to zero. To derive more insights regarding the residuals' distribution, more observations would be required



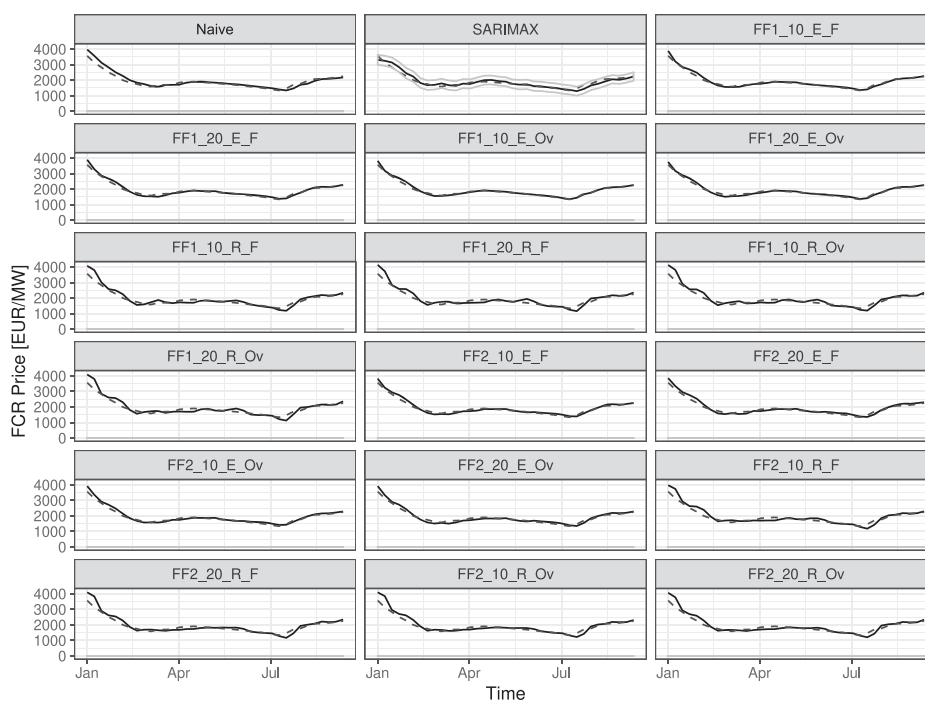


FIGURE B FCR price forecasts in test period 2018:Q1–Q3 (original FCR price data from regelleistung.net, 2019). Solid lines are the forecasted FCR prices, and dashed lines represent the realized FCR price. In addition to the choice of models presented in Section 4, for completeness all deployed model designs reported in the results are shown, indicating a suitable fit for all designs

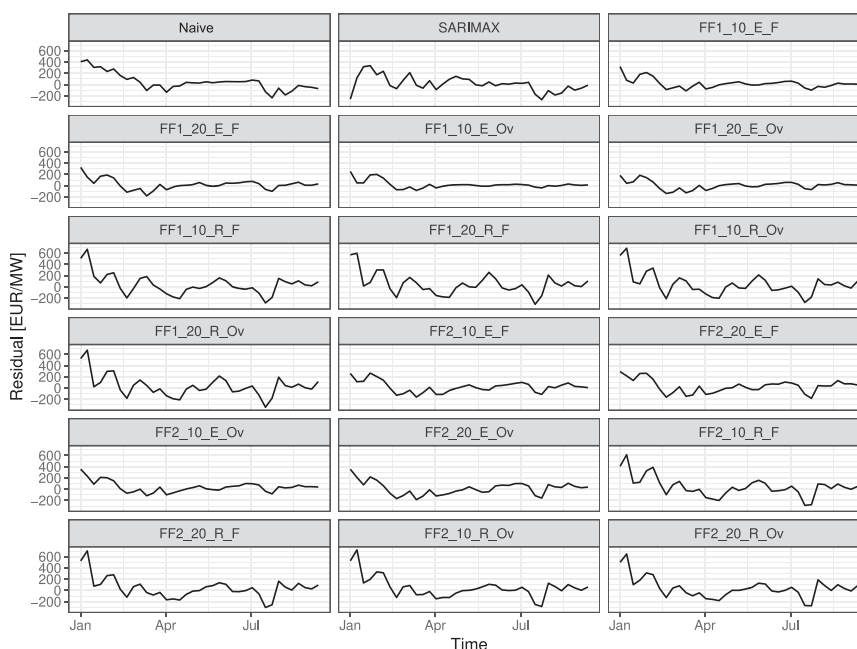


FIGURE C Residuals of FCR price forecasts in test period 2018:Q1–Q3 (original FCR price data from regelleistung.net, 2019). For completeness and supplementary to the choice of models presented in Section 4, all deployed model designs reported in the results are shown. The residuals of similar model configurations show similar residual shapes

TABLE A Experimental design for GRU neural networks

Factor	Level reference	Level variation
<i>Network configuration</i>		
Number of hidden layers	GRU1 (1 hidden layer)	GRU2 (2 hidden layers)
Number of neurons per hidden layer	10	20
<i>Training strategy</i>		
Training data	E (expanding window)	R (rolling window)
Training hyperparameters	F (fit): number of batches = 1, number of epochs = 30, iterations per epoch = 20, ensemble size = 50	Ov (Overfit): number of batches = 1, number epochs = 50, iterations per epoch = 30, ensemble size = 100

TABLE B Root mean square error (RMSE), mean absolute percentage error (MAPE), directional accuracy (DAC), and mean standard deviation (σ) of the model forecasts with GRU networks

Design	RMSE	MAPE	DAC	σ
GRU1_10_E_F	124.47	4.65%	91.70%	50.58
GRU1_20_E_F	190.71	5.49%	86.10%	170.09
GRU1_10_E_Ov	142.55	4.81%	88.90%	68.92
GRU1_20_E_Ov	174.25	6.03%	83.30%	69.37
GRU1_10_R_F	166.00	7.99%	86.10%	62.56
GRU1_20_R_F	205.11	10.24%	77.80%	57.60
GRU1_10_R_Ov	197.59	9.35%	80.60%	74.79
GRU1_20_R_Ov	220.20	10.57%	77.80%	99.65
GRU2_10_E_F	151.74	5.10%	88.90%	44.48
GRU2_20_E_F	174.61	5.66%	86.10%	70.13
GRU2_10_E_Ov	216.30	9.52%	80.60%	80.16
GRU2_20_E_Ov	205.19	6.71%	77.80%	195.88
GRU2_10_R_F	196.78	8.52%	80.60%	55.06
GRU2_20_R_F	224.23	10.05%	77.80%	55.64
GRU2_10_R_Ov	217.63	9.68%	77.80%	79.12
GRU2_20_R_Ov	224.86	10.12%	77.80%	83.73

Note. No improvement compared to the feedforward networks is achieved. The standard deviations are generally smaller, which indicates a more robust model training, but RMSE, MAPE, and DAC indicated no better forecasting performance.

Paper B

Short-term risk management of electricity retailers under rising shares of decentralized solar generation

Marianna Russo ^{a,b}, Emil Kraft ^c, Valentin Bertsch ^d, Dogan Keles ^e

^a *NEOMA Business School, Department of Finance, Mont-Saint-Aignan, France*

^b *Norwegian University of Science and Technology (NTNU), NTNU Business School, Trondheim, Norway*

^c *Karlsruhe Institute of Technology (KIT), Chair of Energy Economics, Karlsruhe, Germany*

^d *Ruhr University Bochum, Chair of Energy Systems and Energy Economics, Bochum, Germany*

^e *Technical University of Denmark (DTU), Department of Technology, Management and Economics, Lyngby, Denmark*

Submitted to *Energy Economics*, published as working paper in the KIT working paper series in production and energy.

Suggested citation:

Russo, M.; Kraft, E.; Bertsch, V.; Keles, D. (2021): Short-term Risk Management for Electricity Retailers Under Rising Shares of Decentralized Solar Generation. In: KIT Working Paper in Production and Energy No. 57, Karlsruhe Institute of Technology (KIT), Karlsruhe. <http://dx.doi.org/10.5445/IR/1000134345>.

Short-term Risk Management of Electricity Retailers Under Rising Shares of Decentralized Solar Generation

Marianna Russo^{*,a}, Emil Kraft^b, Valentin Bertsch^c, and Dogan Keles^d

^a*NTNU Business School, Norwegian University of Science and Technology, 7491, Trondheim, Norway*

^b*Chair of Energy Economics, Karlsruhe Institute of Technology (KIT), Institute for Industrial Production (IIP), Karlsruhe, Germany*

^c*Chair of Energy Systems and Energy Economics, Ruhr University Bochum, Germany*

^d*Technical University of Denmark (DTU), Department of Technology, Management and Economics, Lyngby, Denmark*

Abstract

Electricity retailers face increasing uncertainty due to the ongoing expansion of unpredictable, distributed generation in the residential sector. We analyze how increasing levels of households' solar PV self-generation affect the short-term decision-making and associated risk exposure of electricity retailers in day-ahead and intraday markets. First, we develop a stochastic model accounting for correlations between solar load, residual load and price in sequentially nested wholesale spot markets across seasons and type of day. Second, we develop a computationally tractable two-stage stochastic mixed-integer optimization model to investigate the trading portfolio and risk optimization problem faced by retailers. Through conditional value-at-risk we assess retailers' profitability and risk exposure to different levels of PV self-generation by assuming different retail tariff schemes. We find risk-hedging trading strategies and tariffs to have greater impact in Summer and with low levels of residual load in the system, i.e. when the solar generation uncertainty affect more the households demand to be served and the wholesale spot prices. The study is innovative in unveiling the potential of dynamic electricity tariffs, which are indexed to spot prices, to sustain a high penetration of renewable energy source while promoting risk sharing between customer and retailer. Our findings have implications for electricity retailers facing load and revenue risks in wholesale spot markets, likewise for regulators and policy-makers interested in electricity market design.

*Corresponding author. E-mail: marianna.russo@ntnu.no.

Acknowledgments. We thank GET AG for kindly providing us with the retail tariff data for Germany used in this study. We thank Dr. Kai Sander (Netze BW GmbH) for the fruitful discussions and practical insights on uncertainties and associated risk exposure. This work has emanated from Marianna Russo's research time at the Economic and Social Research Institute, Dublin. Marianna Russo acknowledges funding from the ESRI's Energy Policy Research Center and the SFI Energy Systems Integration Partnership Programme (ESIPP) number SFI/15/SPP/E3125. Marianna Russo also acknowledges research support by COST Action "Fintech and Artificial Intelligence in Finance - Towards a transparent financial industry" (FinAI) CA19130. The authors acknowledge the financial support of the German Federal Ministry of Education and Research under grant number 03SFK1F0-2 (ENSURE – Neue Energienetzstrukturen für die Energiewende). The opinions, findings and conclusions or recommendations expressed in this material are those of the authors and do not necessarily reflect the views of the Energy Policy Research Center and Science Foundation Ireland. All errors remain our own.

Keywords: Electricity markets, Stochastic model, Stochastic programming, Retailer uncertainty modeling, Risk management

JEL classification: C10, C50, G10, Q42, Q48

1 Introduction

Increasing levels of distributed and large-scale variable renewable generation have different effects on short-term wholesale power markets. The uncertainty and intermittency introduced by weather-dependent generation translate into both volume and price risks, which affect the profitability and decision-making of retailers and generators. With large-scale renewable generation, day-ahead predictions on high levels of renewable energy increase the risk-related hedging pressure of generators. Furthermore, with distributed renewable generation, growing renewable power production raises the hedging needs of retailers (Koolen et al., 2021), particularly when considering rooftop solar PV installations (Russo and Bertsch, 2020). The deployment of rooftop solar PV systems has significantly expanded in recent years, mostly by virtue of supporting policies, such as net metering and fiscal incentives. In some markets, incentive schemes for households lead to an economic preference for solar PV self-consumption compared to buying electricity from the grid (IRENA, 2019). The competitiveness of distributed solar PV systems is apparent from their deployment in large markets, such as Brazil, China, Germany and Mexico. At a global level, around 40% of total solar PV capacity in 2050 would be distributed (rooftop), with the remaining 60% utility scale (IRENA, 2019). Yet, as far as rising solar PV self-generation increases the need of retailers for forecast adjustments, large adjustment volumes influence subsequent spot (day-ahead and intraday) prices and the retailers' risk exposure in short-term wholesale power markets, thus exacerbating the already-existing optimization issues faced by the electricity retailer to manage uncertainty in power markets. In the light of market efficiency considerations, increasing attention is to be paid thus on the short-term risk of electricity retailers, following a surge in the decentralized variable renewable generation and consumers' engagement as prosumers.

In this paper we have chosen to investigate the risk optimization problem faced by the electricity

retailer acting in the day-ahead and intraday markets, while considering volume risk induced by the households' solar PV self-generation. The retailer's decision-making problem with intermittent renewables has been explored in the literature (e.g. Conejo et al., 2010; Yang et al., 2017). Whereas the potential for risk transfer through derivative products can rise significantly for wind power, hedging solar risk is likely to remain difficult (Hain et al., 2018), mainly for retailers increasingly exposed to the volume risk driven by growing levels of solar PV self-generation on the demand side (Russo and Bertsch, 2020; Koolen et al., 2021). The variability of the electricity demand, its short-term inelasticity, and the supply rigidity expose retailers to a real-time volume risk, which is more complex to hedge within the day-ahead market, since high differences can emerge between predictions in the day-ahead and intraday market. Engaging in risk management strategies in the intraday market, which is closer to the actual realization, has proved to offer higher efficiency compared to the day-ahead and therefore weekly, monthly and yearly forward market (Boroumand et al., 2015, 2019). Nonetheless, pre-positioning in the day-ahead market and adjusting in the intraday market can result in a complex task for the retailer, mainly when risk management strategies fail to transfer the real-time unpredictability of self-generation to the consumer. The role of the intraday adjustment trading, and the extent to which this trading may foster risk sharing between electricity retailers and prosumers have been less explored in literature and are the focus of this paper. In addressing the short-term risk optimization problem faced by electricity retailers with households' self-generation, this study engages with practitioners and policy makers interested in the power market dynamics following increasing penetration of distributed renewable energy sources, and in the adequacy of price signals for investments and market design.

The contribution of this paper is threefold: First, we explicitly model the stochastic process of prices and solar generation in the day-ahead and intraday market, likewise inter-dependencies within and between the two markets. Simulations are thus carried to account for uncertainty in the ensuing stochastic optimization problem. We consider the German market since it is at the forefront of decentralized solar PV installations worldwide. Furthermore Germany shares a similar intraday continuous trading design with other electricity markets, such as in France and the Scandinavian

countries. Therefore, lessons learned from the German case should provide others with valuable insights concerning managing renewable energy risk in modern liberalized electricity markets. Second, we model the multistage trading problem faced by the retailer in the day-ahead and intraday market. We assume a computationally tractable two-stage stochastic optimization problem where day-ahead trading decisions for one single day are modeled in the first-stage, and the intraday balancing decisions under uncertainty are modeled in the second stage. Since we explicitly assume that the retailer faces the uncertainty of fluctuating rooftop solar PV generation until delivery, this approach aims to accurately model the underlying information flow between day-ahead and intraday market, thus reducing biases and often over-optimistic decisions (Wozabal and Rameseder, 2020). Third, we explore different retail pricing schemes with progressive levels of indexation to the wholesale spot prices. Since the retailer faces the risks caused by volatile customer demand and spot market prices, we investigate the potential for spot-indexed retail tariffs to represent a risk-sharing tool for retailers exposed to rising shares of decentralized solar PV self-generation.

The rest of the paper is organized as follows. In Section 2 we review related work on the retailer short-term decision-making process and the pertaining uncertainties requiring the solution of a complex optimization problem involving several uncertain quantities. The input variables are describe in Section 3. In Section 4, we describe our methodological approach. We present the stochastic model developed to jointly capture load and price uncertainties in the day-ahead and intraday markets, and elaborate on a set of simulations to represent the retailer's uncertainty in wholesale spot markets. Therefore, we define the retailer trading optimization problem under uncertainty, and extend it to the short-term risk management problem, subject to increasing levels of solar PV self-generation. In Section 5, we present our results in relation to the retailer's optimization problem and their short-term risk management. Results and implications are discussed in Section 6, while Section 7 offers concluding remarks and directions for future research.

2 Literature on The Retailer’s Short-Term Decision-Making Process

Electricity markets are organized as a sequence of nested forward energy markets, allowing participants to trade different contracts (from yearly to quarter-hourly) at different points in time (Ela et al., 2018; Cretì and Fontini, 2019). This market design is thought to provide participants with the opportunity to adjust their positions up to a few minutes before the delivery, thus accommodating the inherent uncertainties of electricity markets. Since electricity for the same delivery period is traded in multiple markets, the retailer trading problem on these nested markets is interdependent. As intermediaries in competitive electricity markets, retailers need to procure the electricity required by their customers (i.e. load) in wholesale markets through different sources, like futures and bilateral contracts, or on the spot markets. While in wholesale markets the load uncertainty is adjusted in the spot markets through spot prices, in retail markets prices are based on tariffs, generally fixed for a longer period (Boroumand and Zachmann, 2012; Battle, 2013). Therefore, serving the electricity demand of the residential sector at pre-specified tariffs and partially for pre-specified volumes is an obligation posed to the retailers (Newbery et al., 2018).

By procuring electricity for resale to final consumers, retailers are exposed to the volume risk, mostly over short-term horizons, i.e. from a few days or hours to real-time. While intraday markets allow for a finer adjustment of the day-ahead positions up to 15-minute resolution, the electricity generated by the renewable energy facilities has to be traded day-ahead to be adjusted intra-daily (Kiesel and Paraschiv, 2017). Furthermore, significant differences can emerge between day-ahead and intraday prices depending upon substitution effects between thermal and renewable energy generation (i.e. merit order effect), with intraday prices decreasing relatively to the day-ahead prices for increasing levels of renewable generation, or vice versa (Karanfil and Li, 2017; Kiesel and Paraschiv, 2017). Due to the surge in the distributed variable renewable generation, and the resulting greater requirement for close to real-time adjustments (e.g. Di Cosmo and Malaguzzi Valeri, 2018; Goodarzi et al., 2019), increasing attention is to be paid on the retailer’s short-term re-

balancing in the intraday market and implications for market efficiency. The empirically observed positive correlation between price and load in wholesale electricity markets (e.g. Deng and Oren, 2006; Weron, 2007; Gelabert et al., 2011) implies an increasing short-term risk exposure for the retailers, depending on the difference between spot and retail prices (Willems and Morbee, 2010; Aid et al., 2011; Dagoumas et al., 2017; Russo and Bertsch, 2020). With increasing penetration of rooftop solar PV systems and greater intraday uncertainties, imbalance costs are expected to raise for retailers, thus leading to potential financial distress for retailers who fail to hedge properly.

The importance of assessing the short-term effects of variable renewable energy generation on electricity markets is highlighted by the growing interest in the impact of wind and solar power forecast errors on intraday electricity prices (e.g. Garnier and Madlener, 2015; Bunn et al., 2018; Kath and Ziel, 2018; Kulakov and Ziel, 2019; Maciejowska et al., 2019; Uniejewski et al., 2019; Gianfreda et al., 2020; Kremer et al., 2020; Messner et al., 2020; Narajewski and Ziel, 2020a,b; Li and Paraschiv, 2021). Specularly to generators (Garnier and Madlener, 2015; Bunn et al., 2018; Maciejowska et al., 2019), retailers are confronted with the optimal decision of where to buy the electricity required to satisfy the customers' demand. This decision-making process depends upon the load uncertainty and the relation between prices in the day-ahead and intraday markets. Some previous research addresses the short-term trading problem faced by the electricity retailer in spot markets (Nojavan et al., 2019; Dadashi et al., 2020; Deng et al., 2020, and references therein). Yet, there is a paucity of studies addressing the optimal trading problem faced by electricity retailers in wholesale spot markets following increasing levels of solar PV self-generation, and consequently greater load uncertainty in the residential sector.

Various methods have been explored in the literature to model the optimal procurement problem in electricity markets. These methods include stochastic approaches (Ruszczyński and Shapiro, 2003; Wallace and Fleten, 2003) and robust optimization (Ben-Tal et al., 2009; Bertsimas et al., 2011). By considering a finite batch of possible realizations, stochastic approaches are adopted by practitioners and researchers due to their suitability in capturing uncertainty (e.g. Van Der Weijde and Hobbs, 2012; Morales et al., 2014; Mohan et al., 2015; Abbaspourtorbati et al., 2016; Boffino

et al., 2019; Dadashi et al., 2020; Deng et al., 2020; Laur et al., 2020). In contrast, in robust optimization models uncertainty is represented through uncertainty sets, often derived from the historical data, thus resulting in flexible and computationally tractable models (Parisio et al., 2012; Zugno and Conejo, 2015; Nojavan et al., 2017; Nazari-Heris and Mohammadi-Ivatloo, 2018; Nojavan et al., 2019). Nonetheless, as argued by Wozabal and Rameseder (2020), research involving trading strategies in electricity markets often models price or renewable generation as stochastic but fails to model the multi-settlement structure of the power markets. Similarly, in optimization problems some research often treats all the variables as deterministic.

In dealing with the optimal trading problem of the electricity retailer, who faces load and price uncertainties in wholesale spot markets while maximizing their revenue stream, we follow the approach in Conejo et al. (2010) and Wozabal and Rameseder (2020). We propose a two-stage stochastic optimization model for the German short-term electricity market where the first stage models the retailer's decision-making process on the day-ahead market; the second stage models their decision-making process in the intraday market. Uncertainty enters the problem via stochastic solar PV generation and short-term electricity prices. Yet, compared to previous research, in our optimization problem, we consider the impact of such stochasticity on prices through econometric modeling the inter-dependencies between load and prices in wholesale spot markets. With the increasing penetration of distributed renewable energy sources in worldwide power markets still only a recent phenomenon, to the best of our knowledge the research in this paper is the first to combine all the mentioned uncertainties via joint stochastic modeling, portfolio optimization and empirical validation to analyze the implications of distributed renewable technologies, such as rooftop solar PV systems on the short-term risk management problem of the retailer in wholesale spot power markets.

3 Input Variables: Definition and Data Sources

The German electricity market has been subject to a high renewable energy sources (RES) penetration, in particular rooftop solar PV systems in the residential sector, making this market a suitable case study to investigate retailers' risk exposure to increasing self-generation. The period under investigation runs from the 1st July 2019 to the 29th February 2020. This sample period is chosen to account for some major changes in the German market design, occurred during 2018 until July 2019, including the split of the Austrian market from the German market in October 2018. As the market split changed both the demand and the supply structure, price formation on both the day-ahead and the intraday market was affected. We use data until February 2020 to overcome the implications of COVID-19 and consequent lockdown on electricity markets starting from March 2020. Therefore, the period July 2019- February 2020 results as the most recent period where no structural market changes and economic downturns happen, which may have affected both the demand and supply of electricity in the German market. To study this risk exposure we consider three different seasons: a Transition season (September-November), Summer (July-August) and Winter (December-February). For each season, we consider a typical (i.e. average) working day and a typical weekend day.

In this study, both the day-ahead and the intraday market are considered. The day-ahead market is operated through a sealed-bid auction which takes place once a day, all year round. All hours of the following day are traded in this auction. The buy and sell volume-price bids are submitted by the market participants before the closure of the gate, at 12 pm. Aggregated demand and supply curves are thus recovered based on respectively the buy-bids and sell-bids for each hour of the following day. The hourly uniform market clearing price, namely the day-ahead price, lies at the intersection of both curves. Therefore, to recover the structure of the day-ahead market, data on the day-ahead forecast of the total, solar and wind loads at quarter-hourly frequency were collected from the ENTSO-E Transparency Platform (in MW)¹. The German hourly day-ahead auction price

¹<https://transparency.entsoe.eu/>

(DE-LU, EUR/MWh) was retrieved through the EPEX-Spot².

The intraday set of information consists of a further forecast update of the wind and solar load (and consequently for the total load) at 8:00 am of the actual delivery day, wherein however forecast is conditional on the day-ahead forecasts³. Consequently, intraday forecast and actual (realized) total, solar and wind loads were also recovered from the ENTSO-E platform at quarter-hourly frequency. Finally, the actual, day-ahead and intraday residual load were computed by subtracting the wind and solar loads from the corresponding total load, likewise a thermal generation must-run requirement of 23 GW⁴.

On the continuous intraday market, trade is executed as soon as a buy- and sell-order match and electricity can be traded up to five minutes before delivery. The ID3 price index for the continuous intraday market is the volume-weighted average of the price of all trades taking place in the time window starting from three hours before the delivery and up to thirty minutes before the delivery. So, for example the ID3-price for the delivery in the quarter from 12 pm to 12:15 pm is the volume-weighted average of all transactions with time stamp between 9 am and 11:30 am. Hence, market participants use the intraday market to make last minute adjustments and to balance their positions closer to real-time. Similarly to the day-ahead auction price, the continuous intraday ID3 price index was obtained from EPEX-Spot⁵.

To fit the electricity demand of the residential sector the households' standard load profile (SLP) is used. This profile is based on historical data for households with an annual consumption of 3,500 kWh at quarter-hourly resolution (BDEW, 2021). While the load profile of individual households can deviate from the SLP, the SLP is a suitable indicator for the electricity demand of larger groups of households (Hayn et al., 2018), thus representing a standard tool for retailers. Table 1 provides an overview of the variables used in the empirical analysis, along with their frequencies and sources.

²<http://www.epexspot.com/en/market-data/dayaheadauction>

³ENTSO-E also admits current forecast, where wind and solar forecast is the last update of the current forecast, which shall be regularly updated and published during intraday trading. The forecast published at 8 am of the delivery day is published twice, as "current forecast" and "intraday forecast at 8.00".

⁴The must-run capacity also includes technical restrictions and market commitments. Source: Bundesnetzagentur (2019)

⁵ibid.

Table 1: Overview of the variables used in the empirical analysis

Variable (unit)	Frequency	Description	Data source
Solar PV load (MW), DA	Quarter-hourly	Day-ahead forecast solar PV load	European Network of Transmission System Operators (ENTSO-E) https://transparency.entsoe.eu/
Solar PV load (MW), ID	Quarter-hourly	Intraday forecast solar PV load	ibid.
Solar PV load (MW), Actual (MW)	Quarter-hourly	Realized solar PV load	ibid.
Wind load (MW), DA	Quarter-hourly	Day-ahead forecast wind load	ibid.
Wind load (MW), ID	Quarter-hourly	Intraday forecast wind load	ibid.
Wind load (MW), Actual	Quarter-hourly	Realized wind load	ibid.
Total load (MW), DA	Quarter-hourly	Day-ahead forecast total electricity demand	ibid.
Total load (MW), Actual	Quarter-hourly	Realized total electricity demand	ibid.
Household standard load profile (MW)	Quarter-hourly	Standardized electricity demand in the residential sector	German Association of Energy and Water Industries (BDEW) https://www.bdew.de/
Price (EUR/MWh), DA	Hourly	Market clearing price in the day-ahead auctions (DE-LU)	European Power Exchange (EPEX) https://www.epexspot.com/en
ID3 price (EUR/MWh), ID	Quarter-hourly	Intraday electricity prices in the continuous trading	European Energy Exchange Transparency Platform http://www.eex-transparency.com/de

4 Overview of the Methodological Approach

To model uncertainties in day-ahead and intraday markets, while preserving the sequential market setting, and the key characteristics of each market, we develop a two-step procedure. In the first step, we jointly model and simulate load and price uncertainties in the day-ahead market at hourly resolution, while accounting for season and type of day specificities as detailed in Section 4.1. Based on these simulated series, different scenarios are generated. In the second step, uncertainties in the intraday market are jointly modelled at quarter-hourly resolution. For each day-ahead scenario, coherent intraday realizations are generated, thus resulting in distinct scenario trees that capture the retailer's uncertainties in the day-ahead and intraday markets, as outlined in Section 4.2. In a third stage, the scenario trees are used to evaluate the retailer's trading decisions under uncertainty. More detailed, we consider the trading portfolio optimization of the electricity retailer via a two-stage stochastic mixed-integer linear program, as described in Section 4.3. The scenarios and stochastic programming approach are used to investigate the decision-making problem of the retailer wishing to optimize their contribution margins and the associated risk exposure in the day-ahead and intraday markets with increasing levels of solar PV self-generation in the residential sector, as described in Section 4.4. An overview of the whole methodological approach is given in Fig.1.

4.1 Modeling uncertainty in the day-ahead market

In modeling uncertainty in the day-ahead market, the dynamic relationships between solar infeed, residual load and prices are considered in a stepwise procedure. First, we account for negative values and outliers in the residual load and price time series. The time series of the day-ahead and intraday residual load are shifted up so to reach the smallest recorded positive value over the full sample period and the two markets, which however does not occur in the sample. This permits a correct recoding of the series in the simulation process (Keles et al., 2012). Hence, the series are logarithmized to reach variance stabilization. A similar procedure is applied to the day-ahead

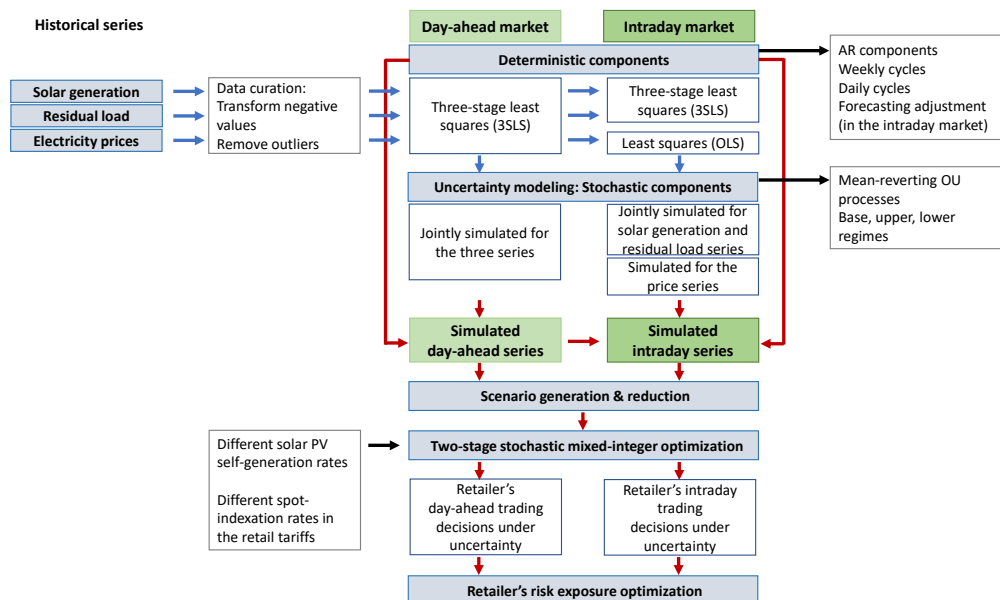


Figure 1: Overview of the whole methodological approach

and intraday price series. Outliers, i.e. observations above and below the upper and lower 2.5% percentiles of the empirical distribution in the season and in the market are also removed and replaced with the corresponding percentile (e.g. Janczura et al., 2013).

4.1.1 Solar PV generation

In this study, we assume that the rooftop solar PV generation of the retailer's households is perfectly correlated with the system-wide solar generation published by the TSOs. This complies with an evenly distributed customer portfolio. Therefore, we model the system-wide solar PV profile, likewise the seasonal and daily features of the deviations of the solar PV generation from its theoretical profile. As in Lingohr and Müller (2019), the solar PV generation process is described by a continuous-time process $S_t, t \geq 0$:

$$S_t = IC_t \times \Lambda_t \times V_t, \quad (1)$$

where $S_t \geq 0$; $IC_t \geq S_t \geq 0$ is the installed capacity; $\Lambda_t \geq 0$ is a deterministic function describing seasonal variations; and $V_t \geq 0$ denotes any irregular influence. Λ_t can be regarded as the normalized theoretically possible maximum solar PV generation profile and represents the 'clear sky' solar radiation (Bacher et al., 2009). As in Russo and Bertsch (2020), it is computed as the average of the clear sky solar radiation of thirty-nine locations in Germany, weighted for the installed solar PV capacity in the area around selected locations. Therefore, $IC_t \times \Lambda_t$ represents the normalized theoretically possible maximum solar PV generation profile, while V_t assumes the physical interpretation of cloud component. This component causes deviations of the actual solar generation from its theoretically possible maximum profile and is explicitly modelled to account for its impact on the residual load and prices.

After logarithmizing the data in Eq.1, the discretized hourly cloud component v_t is assumed to be characterized by an autoregressive component, as in Benth and Ibrahim (2017), and by an hourly seasonal component, as in Keles et al. (2013) for the wind capacity utilization. To account for this hourly seasonal component of the cloudiness, the average value \bar{v}_h^{DA} of the cloud component v_t^{DA} is determined for each hour $h=0, \dots, 23$, of the day throughout each season over the sample period (Summer, Transition season, Winter). Therefore, the following dynamic for the cloud component is assumed:

$$v_t^{DA} = \sum_{p=1}^P v_{t-p}^{DA} + \sum_{h=0}^{23} \bar{v}_h^{DA} * 1(h|h = t \bmod 24) + X_t^{DA}, \quad (2)$$

where the resulting residual component X_t^{DA} contains neither seasonal or intraday regularities and is thus suitable for stochastic simulations.

4.1.2 Residual load

The hourly residual load l_t^{DA} is assumed to be a function of the cloud component v_t^{DA} and defined in an additive way:

$$l_t^{DA} = f(v_t^{DA}) + \sum_{h=0}^{23} \bar{l}_h^{DA} * 1(h|h = t \bmod 24) + Weekends + Y_t^{DA}, \quad (3)$$

where $f(v_t^{DA})$ is a deterministic function of v_t^{DA} , capturing the relationship between cloudiness and residual load; \bar{l}_h^{DA} is a hourly cycle, which similar to the cloud component is defined as the hourly average of the residual load in the season. Public holiday effects and weekend effects (*Weekends*) are also considered, which account for differences in the load of a typical business day with respect to a weekend/holiday. The residual component Y_t^{DA} represents thus the deseasonalized and stochastic component of the residual load. A polynomial function is used to approximate the deterministic function $f(v_t^{DA})$ of the cloud component in Eq.2, as implied by Fig.2.

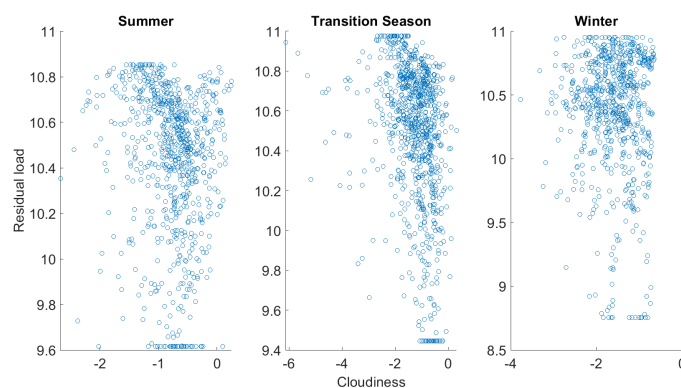


Figure 2: Relationship between the log residual load and cloudiness in the day-ahead market

4.1.3 Day-ahead prices

Following Burger et al. (2004), Schermeyer et al. (2018), and Benth and Ibrahim (2017) the hourly day-ahead price p_t^{DA} is modeled as a function of the residual load and an autoregressive component as follows:

$$p_t^{DA} = \sum_{k=1}^K l_{t-k}^{DA} + \sum_{q=1}^Q p_{t-q}^{DA} + \sum_{h=0}^{23} \bar{p}_h^{DA} * 1(h|h = t \bmod 24) + Weekends + Z_t^{DA}, \quad (4)$$

where \bar{p}_h^{DA} is an hourly cycle, defined as the residual load and cloudiness cycles while (*Weekends*) account for public holiday and weekend effects. Finally, Z_t^{DA} represents the residual and stochastic component of the day-ahead prices. Following the visual inspection of the scatter plot in Fig.3, the

relationship between residual load and price in the day-ahead market is assumed to be linear. Eq.2 -

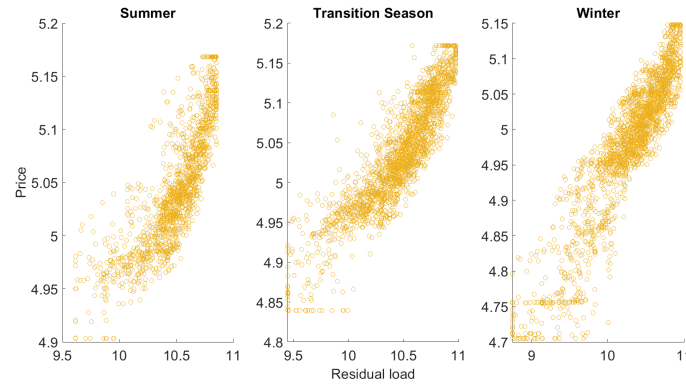


Figure 3: Relationship between log prices and residual load in the day-ahead market

Eq.4 result in a system of three equations, which for each season is jointly estimated through three-stage least squares (3SLS) (Zellner and Theil, 1992) to reflect the daily blind auction mechanism of the German market described above. The 3SLS estimation method is adopted since it allows to obtain efficient estimates in the presence of contemporaneously correlated residuals, which would be expected since the day-ahead forecast of solar PV generation, residual load and price are jointly determined.

4.1.4 Modeling and simulating the stochasticity of the solar PV generation, residual load, and day-ahead price processes

Similar to Keles et al. (2012) and Coulon et al. (2013), the remaining stochastic components of the day-ahead solar PV generation, residual load and price variables, i.e. X_t^{DA} , Y_t^{DA} , Z_t^{DA} respectively, are assumed to be mean-zero Ornstein–Uhlenbeck (OU) processes, since their mean levels are incorporated in the deterministic/seasonal functions in Eq.2 - Eq.4. Because logarithms of the variables are modeled, a multivariate OU process can be formulated for their changes through stochastic differential equations (SDEs) via Itô's lemma. Yet the relationship between the three variables can be dimmed by the consequences of outages, transmission problems and other constraints. Consequently, jumps in the series can occur, even at periods of low or average demand

(Christensen et al., 2009; de Lagarde and Lantz, 2018). Furthermore, similarly to wind, the volatility of solar generation has been observed to increase the electricity price volatility, due to the high day-to-day variability of the solar generation (Ballester and Furió, 2015; Rintamäki et al., 2017). Therefore, as in Keles et al. (2012) and Coulon et al. (2013), jump processes are added to the OU process to mimic this additional stochastic variability.

To accommodate the features above, and in the spirit of Keles et al. (2012), solar generation, residual load and prices are assumed to mainly remain at a base level, defined “base regime” and then to simultaneously jump into a higher (or lower) “jump regime”, where they are assumed to remain for some hours according to their mean reverting dynamics, before jumping back to their base regime. Higher and lower jump regimes are defined as values that are above and below 3σ , respectively (after assuming a mean-zero OU process, as mentioned above). Base, higher jump and lower jump regimes are separately computed for the summer, transition and winter seasons. Consequently, the base regime corresponds to values in the interval $[-3\sigma; +3\sigma]$.

A regime-switching approach, with a different model for the base, higher jump, and lower jump regime is thus introduced. The base regime is modeled through a system of SDE as follows:

$$d\mathbf{U}_t^{DA,Base} = -\boldsymbol{\beta}^{DA,Base} \mathbf{U}_t^{DA,Base} dt + \boldsymbol{\Sigma}^{DA,Base} d\mathbf{W}_t^{DA,Base}, \quad (5)$$

where $\mathbf{U}_t^{DA,Base}$ is the 3×1 vector of the stochastic processes $X_t^{DA}, Y_t^{DA}, Z_t^{DA}$ in the base regime; $\boldsymbol{\beta}^{DA,Base}$ is the 3×3 drift matrix, which determines the “reversion speed” of the stochastic components towards their long-term mean zero. The stochastic component $\boldsymbol{\Sigma}^{DA,Base} d\mathbf{W}_t^{DA,Base}$ corresponds to a multivariate Brownian motion: $\boldsymbol{\Sigma}^{DA,Base}$ is the 3×3 covariance matrix, and $\mathbf{W}_t^{DA,Base}$ is a 3-dimensional vector of independent Wiener processes. Hence, $d\mathbf{W}_t^{DA,Base} = \boldsymbol{\varepsilon}_t dt^{1/2}$ follows a multivariate normal distribution where each Wiener process has mean zero and variance dt . By applying the Itô’s lemma and following Meucci (2009), the solution to the system of SDE in Eq.5 is:

$$\mathbf{U}_{t+\delta} = e^{-\boldsymbol{\beta}\delta} \mathbf{U}_t + \mathbf{v}_{t+\delta}, \quad (6)$$

where $\mathbf{v}_{t+\delta} \equiv \int_t^{t+\delta} e^{\beta(s-t)} \Sigma d\mathbf{W}_s \sim \mathcal{N}(0, \Omega)$. (Note that in Eq.6 we dropped the superscripts $DA, Base$ to ease the notation.) δ is the time difference of the day-ahead series between t and $t+1$, i.e. one hour. The solution in Eq.6 is a vector autoregressive process of order one, i.e. VAR(1), which reads $\mathbf{U}_{t+1} = A\mathbf{U}_t + \mathbf{v}_{t+1}$ where A is a suitable 3×3 matrix, such that $A = e^{-\beta\delta}$ while $\Omega \equiv \Sigma\Sigma'$ (Meucci, 2009). The Maximum Likelihood (ML) estimator is used to recover the parameter matrices A and Ω from the historical stochastic components $X_t^{DA}, Y_t^{DA}, Z_t^{DA}$. The substitution of A and Ω delivers the original parameter matrices $-\beta$ and Σ of the exact solution in Eq.6, which are used to generate the simulated paths of the three stochastic components in the base regime.

The jump regimes are defined as extended versions of the base regime. Upward and downward jumps in the stochastic components of the day-ahead solar generation, residual load and prices are replaced by their mean values in the estimation of the mean reversion parameters in Eq.5, so to preserve the sample length. The added or subtracted ‘‘jump height’’ to the base regime process corresponds to the deviation of the jump value from the mean. A multivariate normal distribution is thus used to model the jump heights of the three stochastic processes $X_t^{DA}, Y_t^{DA}, Z_t^{DA}$. The distribution is based on the means and covariance matrix estimated from the historical deviations of the jump values from their corresponding mean. Accordingly, the upper and lower regimes are defined as:

$$\begin{aligned} \mathbf{U}_t^{DA,uJ} &= \mathbf{U}_t^{DA,Base} + \boldsymbol{\epsilon}_t^{DA,uJ}, & \boldsymbol{\epsilon}_t^{DA,uJ} &\sim \mathcal{N}(\boldsymbol{\mu}^{DA,uJ}, \boldsymbol{\Sigma}^{DA,uJ}), \\ \mathbf{U}_t^{DA,lJ} &= \mathbf{U}_t^{DA,Base} - \boldsymbol{\epsilon}_t^{DA,lJ}, & \boldsymbol{\epsilon}_t^{DA,lJ} &\sim \mathcal{N}(\boldsymbol{\mu}^{DA,lJ}, \boldsymbol{\Sigma}^{DA,lJ}), \end{aligned} \quad (7)$$

where $\boldsymbol{\epsilon}_t^{DA,uJ}$ ($\boldsymbol{\epsilon}_t^{DA,lJ}$) represents the upward (downward) jump height; $\boldsymbol{\mu}_t^{DA,uJ}$ ($\boldsymbol{\mu}_t^{DA,lJ}$) is the 3-dimensional mean vector of the upward (downward) jump heights; and $\boldsymbol{\Sigma}^{DA,uJ}$ ($\boldsymbol{\Sigma}^{DA,lJ}$) is the 3×3 covariance matrix of the upward (downward) heights. It is noteworthy that this approach is separately applied for the summer, transition and winter season series. Transition probabilities for the upward and downward jumps of the three stochastic components $X_t^{DA}, Y_t^{DA}, Z_t^{DA}$ are thus separately computed for the three seasons. The probabilities of switching from the base regime to

the upper regime and backwards are defined by:

$$\begin{aligned}
P_{BB} &= \frac{\text{card} \{U_t \in [\mu - 3\sigma, \mu + 3\sigma] \wedge U_{t+1} \in [\mu - 3\sigma, \mu + 3\sigma]\}}{\text{card} \{U_t \in [\mu - 3\sigma, \mu + 3\sigma]\}}, \\
P_{BU} &= \frac{\text{card} \{U_t \in [\mu - 3\sigma, \mu + 3\sigma] \wedge U_{t+1} \in [\mu + 3\sigma, \max(U)]\}}{\text{card} \{U_t \in [\mu - 3\sigma, \mu + 3\sigma]\}}, \\
P_{UB} &= \frac{\text{card} \{U_t \in [\mu + 3\sigma, \max(U)] \wedge U_{t+1} \in [\mu - 3\sigma, \mu + 3\sigma]\}}{\text{card} \{U_t \in [\mu + 3\sigma, \max(U)]\}}, \\
P_{UU} &= \frac{\text{card} \{U_t \in [\mu + 3\sigma, \max(U)] \wedge U_{t+1} \in [\mu + 3\sigma, \max(U)]\}}{\text{card} \{U_t \in [\mu + 3\sigma, \max(U)]\}}.
\end{aligned} \tag{8}$$

where the superscript DA is dropped to ease notation. P_{BB} is the probability of remaining in the base regime; P_{UU} is the probability of remaining in the upper jump regime; P_{BU} and P_{UB} are the probabilities to move from the base to the upper jump regime, and vice versa respectively. The probabilities of switching from the base to the lower jump regime and backwards (P_{BL} , P_{LB} , P_{LL}) are computed analogue to Eq.8, whereas the corresponding interval for downward jumps is defined as $[\min(U), \mu - 3\sigma]$. These probabilities are thus combined to define the transition probabilities matrix T_t :

$$T = \begin{bmatrix} P_{BB} & P_{BU} & P_{BL} \\ P_{UB} & P_{UU} & P_{UL} \\ P_{LB} & P_{LU} & P_{LL} \end{bmatrix}, \tag{9}$$

where $P_{UL} = P_{LU}=0$, i.e. no transition from the upper jump to the lower jump regime, and vice versa, as suggested by empirical evidence. Based on their computed transition matrices, the hourly regime switching of three stochastic processes X_t^{DA} , Y_t^{DA} , Z_t^{DA} are simulated for each season following the approach in Keles et al. (2013). A state parameter δ is used to identify the regime. For $\delta=0$, a base regime is identified and thus used in the simulation process. If $\delta=1$ ($\delta=-1$), an upper (lower) jump regime is instead identified and a upper (lower) jump is thus added (subtracted) from

the simulated, i.e.:

$$U_{t,s}^{DA,Sim} = \begin{cases} U_{t,s}^{DA,Base} + \epsilon_{t,s}^{DA,uJ}, & \epsilon_{t,s}^{DA,uJ} \sim \mathcal{N}(\mu^{DA,uJ}, \Sigma^{DA,uJ}) & \text{if } \delta = 1 \\ U_{t,s}^{DA,Base} & & \text{if } \delta = 0 \\ U_{t,s}^{DA,Base} - \epsilon_{t,s}^{DA,lJ}, & \epsilon_{t,s}^{DA,lJ} \sim \mathcal{N}(\mu^{DA,lJ}, \Sigma^{DA,lJ}) & \text{if } \delta = -1 \end{cases} \quad (10)$$

For $s = 1, 2, \dots, S$, $U_{t,s}^{DA,Base}$, $\epsilon_{t,s}^{DA,uJ}$, and $\epsilon_{t,s}^{DA,lJ}$ represent the s^{th} simulated processes obtained from Monte Carlo simulations of the multivariate processes in Eq.5 and Eq.7.

To capture and describe the uncertainty in the day-ahead market, Monte Carlo simulations are conducted for each season by considering $S=1,000$ trials. After assuming for each trial a burn-in period of 28 days or 672 hours, 24 hours from 12 am to 11 pm are extracted from each simulated series. These series correspond to 1,000 simulations of the stochastic components of the day-ahead cloudiness, residual load and price for one day. Therefore, the deterministic components in Eq.2 - Eq.4 are added to the simulated stochastic components. These log series are thus transformed to retrieve their levels, while the residual load and price series are also shifted down to recover their original levels. This procedure allows to obtain 1,000 hourly cloudiness, residual load and price series of one typical working day (Monday-Friday) and 1,000 hourly cloudiness, residual load and price series of one typical weekend day (Saturday-Sunday) for each of the three seasons. Therefore, distinct and seasonal paths are recovered for working and weekend (and holidays) days, which account for the historically observed differences in the load and price values between working days and weekends/holidays across the seasons. In contrast, while cloudiness paths are differentiated across seasons, they are assumed to be the same in working and weekend days. The 1,000 series resulting from the Monte Carlo simulation are "reduced" to a recombining stochastic tree. This scenario generation-and-reduction is carried out by implementing the k-means clustering algorithm (MacQueen et al., 1967). This algorithm aims to partition a set of simulations s_1, \dots, s_n into m clusters C_1, \dots, C_m such that an intra-cluster distance is minimized. The k-means algorithm used in this study employs the city block distance. Therefore, for each cluster, the absolute distance is computed with respect to the median of the points in that cluster. The number of clusters is identified by us-

ing silhouette plots and values to analyze the results of different k-means clustering solutions. The k-means algorithm is a mainstay clustering approach in many application domains, e.g. biology, market segmentation, internet search, digital imaging, power network allocation (Likas et al., 2003; Jain, 2010). It has been extensively used in the literature on energy systems for trading off computing time and precision (Green et al., 2014; Osório et al., 2015; Zhang et al., 2021, and references therein). A similar scenario generation-and-reduction approach is adopted by Gröwe-Kuska et al. (2000) and Heitsch and Römis (2009). Fleten and Kristoffersen (2007) apply the approach in a similar way to stochastic programming of trading strategies for hydro-power in electricity markets. For scenario reduction, the authors use Lagrangian relaxation of a optimization problem instead of k-means clustering, as used in this study. Nonetheless, both the Lagrangian relaxation and k-means clustering follow the same goal of preserving the variety and uncertainty of the simulations and reducing the number of scenarios to be considered.

By following the k-means clustering approach above, three clusters are identified for each typical day (working day and weekend) and season (Summer, Winter, Transition season), which correspond to a high, medium, and low scenario of the solar PV generation. For each scenario, numerous consistent nodes can be derived by symmetrically defining deviation ranges. We use the following approach. For each scenario, simulations in the cluster are grouped and averaged in five nodes, based on their distance from a reference point, assumed to be the mean of the simulated residual load series in the cluster, as computed at 12 pm. Starting from this first node, four nodes are identified by averaging simulations in the range up to one standard deviation above and below the mean of the cluster, and simulations above and below one standard deviation from the mean of the cluster. Therefore, the three nodes in the range up to one standard deviation from the mean are assumed to be equally probable, with a probability of 25%. Equal probability is also assumed for the nodes above and below one standard deviation from the mean (12.5%). In all, these probabilities resemble probabilities drawn from a normal distribution. Finally, a spline interpolation method is used to obtain cloudiness and residual load series at quarter-hourly resolution. The quarter-hourly day-ahead price series are obtained by assuming the hourly day-ahead price constant in the quarter-of-hour

segments of the specific hour. The resulting fifteen nodes of the three series, i.e. five nodes for each of the three scenarios (high, medium and low) are used to design the intraday realizations and scenario trees, as described below.

4.2 Modeling uncertainty in the intraday market

In the intraday market, series at quarter-hourly resolution are taken. The updated forecast of the load and solar generation is used to model the uncertainty towards real-time. Since intraday solar and residual load forecasts follow their respective day-ahead forecasts, we use the same econometric approach adopted for the day-ahead market. Yet, since the ID3 price index is determined in the continuous market and up to thirty minutes before the delivery, the stochastic process of the intraday prices is modeled separately from the solar and residual load stochastic processes.

4.2.1 Solar PV generation

Similar to the day-ahead market, we model the intraday cloud component, that is the deviation of the intraday solar PV generation from its theoretical (seasonal and intraday) profile, and from the day-ahead profile, i.e.:

$$v_{\tau}^{ID} = v_{\tau}^{DA} + \sum_{p=1}^P v_{\tau-p}^{ID} + \sum_{q=0}^{95} \bar{v}_q^{ID} * 1(q|q = \tau \bmod 96) + X_{\tau}^{ID}, \quad (11)$$

where the intraday cloud component v_{τ}^{ID} is assumed to be a function of the day-ahead cloud component, likewise of an autoregressive component and a seasonal component. Similar to the day-ahead process, the seasonal component is obtained as the average value \bar{v}_q^{ID} of the cloud component v_{τ}^{ID} for each quarter-of-hour in the day ($q=0, \dots, 95$) and for each season in the sample period (Summer, Transition season, Winter). The resulting residual component X_{τ}^{ID} is thus used for stochastic simulations.

4.2.2 Residual load

Following updates in the intraday forecasts of the solar PV and wind generation, forecasts of the residual load l_τ^{ID} are also updated at quarter-hourly resolution, and assumed to be a linear function of the day-ahead forecasts and of the intraday cloud component. An autoregressive component is also considered in the process:

$$l_\tau^{ID} = l_\tau^{DA} + v_\tau^{ID} + \sum_{p=1}^P l_{\tau-p}^{ID} + \sum_{q=0}^{95} \bar{l}_q^{ID} * 1(q|q = \tau \text{ mod } 96) + Weekends + Y_\tau^{ID}, \quad (12)$$

where \bar{l}_q^{ID} is a quarter-of-hour cycle is defined as the quarterly hour average of the intraday residual load in the season. Public holiday effects and weekend effects (*Weekends*) are also considered. The residual component Y_τ^{ID} represents thus the deseasonalized and stochastic component of the residual load factor in the intraday market. Parameter estimates in Eq.11-12 are obtained through the 3SLS estimation method to account for contemporaneous correlations between the jointly determined intraday solar PV generation and residual load forecasts.

4.2.3 Intraday prices

Following Kiesel and Paraschiv (2017), the intraday ID3 price process is described in terms of its distance from the day-ahead price, i.e. $p_\tau^{ID} - p_\tau^{DA} = \Delta p_\tau$. The day-ahead price p_τ^{DA} , at quarter-hourly resolution, is obtained from the hourly series p_t^{DA} via spline interpolation (Lahmiri, 2015; Steinert and Ziel, 2019). The model specification reads as follows:

$$\begin{aligned} \Delta p_\tau = & \sum_{j=1}^J \Delta p_{\tau-j} + p_{\tau-1}^{DA} + \Delta p_{\tau-1}^{ID} + \sum_{k=3}^K \Delta l_{\tau-k} + \sum_{r=3}^R \Delta v_{\tau-r} + \sum_{q=0}^{95} \bar{\Delta} p_\tau * 1(q|q = \tau \text{ mod } 96) + \\ & + Weekends + Z_\tau^{ID}, \end{aligned} \quad (13)$$

where $p_{\tau-1}^{DA}$ is the first-order lag of the day-ahead price at quarter-hourly resolution; $\Delta p_{\tau-1}^{ID}$ represents increments in the intraday price series. As in Kiesel and Paraschiv (2017), these increments account for the price formation process in the intraday market, which is based on continuous trades

of several quarter-hourly products. Therefore, the increment captures the change in the price of a certain quarter of an hour when new information on solar forecasts becomes available. Δl_τ is the distance of the actual (realized) residual load from its intraday forecast l_τ^{ID} ; likewise Δv_τ is the distance of the actual solar generation from its intraday forecast v_τ^{ID} , thus representing the solar forecast error. Here the actual residual load and solar generation are assumed to be exogenous and corresponding to the 15-minute average of the historical actual observations for the season in the sample period. Parameters in Eq.13 are estimated through least-square error.

4.2.4 Modeling and simulating the stochasticity of the solar PV, residual load and intraday price processes

Similar to the day-ahead market, the remaining stochastic components of the intraday solar PV generation and residual load, i.e. X_τ^{ID} and Y_τ^{ID} respectively, are assumed to follow a multivariate mean-zero OU process. Jump processes are thus added to account for the uncertainty. Base, higher and lower jump regimes are identified following the approach described in Section 4.1 and by taking as upwards and downwards the values of X_τ^{ID} and Y_τ^{ID} that are above and below 3σ their corresponding mean values in the season. The base regime is thus modeled through SDE as follows:

$$d\mathbf{U}_\tau^{ID,Base} = -\boldsymbol{\beta}^{ID,Base} \mathbf{U}_\tau^{ID,Base} d\tau + \boldsymbol{\Sigma}^{ID,Base} d\mathbf{W}_\tau^{ID,Base}, \quad (14)$$

where $\mathbf{U}_\tau^{DA,Base}$ is the 2×1 vector of the stochastic processes X_τ^{ID}, Y_τ^{ID} in the base regime; $\boldsymbol{\beta}^{ID,Base}$ is the 2×2 positive definite symmetric drift matrix; $\boldsymbol{\Sigma}^{ID,Base}$ is the 2×2 constant diffusion matrix and $\mathbf{W}_\tau^{ID,Base}$ is a 2-dimensional Wiener process. The jump regimes are thus defined as extended versions of the base regime like for the day-ahead market:

$$\begin{aligned} \mathbf{U}_\tau^{ID,uJ} &= \mathbf{U}_\tau^{ID,Base} + \boldsymbol{\epsilon}_\tau^{ID,uJ}, & \boldsymbol{\epsilon}_\tau^{ID,uJ} &\sim \mathcal{N}(\boldsymbol{\mu}^{ID,uJ}, \boldsymbol{\Sigma}^{ID,uJ}), \\ \mathbf{U}_\tau^{ID,lJ} &= \mathbf{U}_\tau^{ID,Base} - \boldsymbol{\epsilon}_\tau^{ID,lJ}, & \boldsymbol{\epsilon}_\tau^{ID,lJ} &\sim \mathcal{N}(\boldsymbol{\mu}^{ID,lJ}, \boldsymbol{\Sigma}^{ID,lJ}), \end{aligned} \quad (15)$$

where $\epsilon_{\tau}^{ID,uJ}$ ($\epsilon_{\tau}^{ID,lJ}$) represents the upward (downward) jump height; $\mu_{\tau}^{ID,uJ}$ ($\mu_{\tau}^{ID,lJ}$) is the 2-dimensional mean vector of the upward (downward) jump heights; and $\Sigma^{ID,uJ}$ ($\Sigma^{ID,lJ}$) is the 2×2 variance-covariance matrix of the upward (downward) heights. Finally, the probabilities for X_{τ}^{ID} and Y_{τ}^{ID} to switch from the base regime to the upper regime and backwards are computed as in Eq.8 and used to define the transition probabilities matrix as in Eq.9.

Similarly to the day-ahead series, the stochastic component of the intraday ID3 price Z_{τ}^{ID} is assumed to follow an univariate mean-reverting OU process with a base, upper jump and lower jump regimes, i.e.:

$$\begin{aligned} dZ_{\tau}^{ID,Base} &= -\beta^{ID,Base} Z_{\tau}^{ID,Base} d\tau + \sigma^{ID,Base} dW_{\tau}^{ID,Base}, \\ Z_{\tau}^{ID,uJ} &= Z_{\tau}^{ID,Base} + \epsilon_{\tau}^{ID,uJ}, \quad \epsilon_{\tau}^{ID,uJ} \sim \mathcal{N}(\mu^{ID,uJ}, \sigma^{ID,uJ}), \\ Z_{\tau}^{ID,lJ} &= Z_{\tau}^{ID,Base} - \epsilon_{\tau}^{ID,lJ}, \quad \epsilon_{\tau}^{ID,lJ} \sim \mathcal{N}(\mu^{ID,lJ}, \sigma^{ID,lJ}). \end{aligned} \quad (16)$$

The parameter estimates in Eq.11-Eq.13 and the simulated day-ahead scenarios are thus used to obtain intraday scenarios. For each of the five nodes of the high, medium and low day-ahead scenarios, the corresponding intraday node is retrieved for the cloudiness, residual load and ID3 price index, thus generating high, medium and low intraday scenarios coherent with the day-ahead scenarios. Yet still the intraday nodes represent the deterministic and predictable component of the intraday series, to which a stochastic component is added as obtained from Monte Carlo simulations of the processes in Eq.14-Eq.16 with 1,000 trials. Similar to the day-ahead market, for each scenario, numerous consistent nodes can be derived by symmetrically defining deviation ranges. We assume the average of the simulated processes as the representative node for the intraday cloudiness, residual load and price. Therefore, for each of these nodes, we assume a range of possible realizations, which are obtained by adding (subtracting) to the node one and two standard deviations of the historical differences between intraday and day-ahead series, as computed for each quarter-of-hour in the season. For each day-ahead node, five possible realizations are assumed in the intraday market, resulting in 5×5 nodes. Intraday nodes in the range up to one standard deviation from the mean are assumed to be equally probable, with probability of 25%. Equal probability is also assumed

for the nodes above and below one standard deviation from the mean (12.5%), thus resembling probabilities drawn from a normal distribution.

In all, for a typical working/weekend day, we obtain a scenario tree of $3 \times 5 \times 5$ possible states. It follows that to obtain the ID3 price index realizations, the corresponding realizations for the intraday cloudiness and residual load series are used. The resulting scenario tree, which is depicted in Fig.4, permits to characterize the uncertainty surrounding the forecasting process in liberalized electricity wholesale spot markets through a discrete representation of its realizations in a probability space.

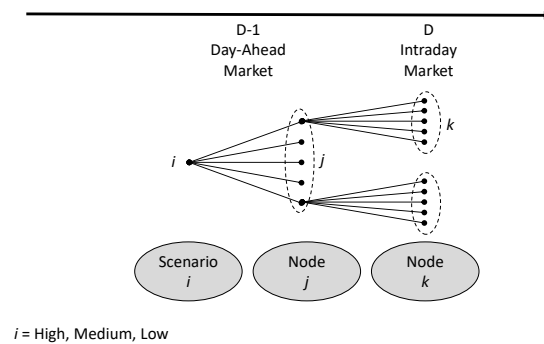


Figure 4: Scenario tree with different nodes in the day-ahead and intraday markets

4.3 Retailers' trading portfolio optimization problem

When an electricity retailer faces volume and price risks in purchasing load to be served from the wholesale market, conventional risk management optimization methods are observed to be quite inefficient due to the difficulty of formulating a multi-period optimization that incorporates correlated price and demand risks (Kettunen et al., 2010). In this context, we develop a two-stage stochastic optimization approach, which accounts for correlated uncertainties of both electricity prices and loads, and which permits the consideration of the conditional value-at-risk (CVaR) as

risk metric to optimize risk hedging across intermediate stages in the planning horizons. Hereby, the retailer procures electricity on the spot markets (day-ahead spot market and continuous intraday trading) in order to resell it via predefined tariff schemes to household customers according to their residual demand, i.e. according to the standard load profile net of the solar PV generation in case the household has a solar installation. It is worth noting that we do not consider the potential impact of battery storage systems on temporal shifts in residual demand, or smart metering and intelligent electric devices for demand side management. Therefore, in this study, the hypothesis that the retailer can participate in short-term demand response programs to adjust the uncertainty brought by the self-sufficiency is not considered⁶.

We consider input data for the German market area and a hypothetical retailer with 100,000 household customers, that are spatially distributed such that the German PV generation is representative for the portfolio PV generation. For customers without PV generation, the load to be served by the retailer in a typical working/weekend day of the season corresponds to the standard load profile q_{qh} , where qh represents the quarter-of-hour of the day. For customers with PV generation, the residual demand q_{qh}^{RD} to be served by the retailer is calculated as q_{qh} minus the solar PV self-generation. This self-generation is determined under uncertainty in the intraday cloudiness v_{qh}^{ID} , as described in Section 4.2. For each scenario j of the day-ahead market, and corresponding realization k in the intraday market, the residual demand to be served after accounting for the PV self-generation is defined as follows:

$$q_{j,k,qh}^{\text{RD}} = \max \{ q_{qh} - (1 - v_{j,k,qh}^{\text{ID}}) \cdot P^{\text{inst.}}, 0 \}, \quad (17)$$

where $P^{\text{inst.}}$ represents the rooftop solar PV installed capacity. Therefore, in the absence of cloudiness, i.e. $v_{j,k,qh}^{\text{ID}}=0$, the solar PV self-generation reaches its theoretical maximum, given a certain amount of installed capacity. Following the approach in Ruppert et al. (2016) and Russo and Bertsch (2020), rooftop solar PV systems with capacity up to 12 kW are considered, i.e. in-

⁶We refer to Fett et al. (2021) who investigate potential impacts of household PV battery storage systems on day-ahead electricity markets on a system level.

stallations for residential buildings up to 80 m², and with a median size of 7 kW⁷. Therefore, in our empirical analysis, P^{inst} in Eq.17 is assumed to be 7 kW.

According to the last published statistics, the number of residential buildings in Germany amounted to 19.2 million at the end of 2019⁸, while almost 2 million rooftop solar PV systems were installed in Germany, thus representing an installation rate ϕ of PV systems in the residential sector of 10%⁹. Due to the lack of granular data on generation from solar PV systems, the solar system load and capacity factor is used indeed to infer the profile of self-generation at quarter-hourly basis. On average, a solar PV capacity factor of 10% was observed in Germany during the sample period, as recovered from the historical data. This factor is used to compute the total amount of solar PV self-generation. For each season, the quarter-hourly self-generation profile in a typical day is obtained by assuming the same quarter-hourly profile of the system solar load on an average day of the season in the sample¹⁰.

We frame the retailer's trading strategy problem and risk investigation by assuming metering of deviations from the standard load profile on a quarter-hourly basis, as supposed after completion of the smart meter roll-out program¹¹. In this case, the participation of the retailer in the wholesale spot markets to balance all the potential profit and loss is mandatory. We also rule out the hypothesis that the retailer has self-consumption, or storage and generation facilities to cope with deviations of the actual load from the standard load profile, as led by solar PV self-generation. Consequently, the amount of self-generation exceeding households' demand is not accounted for, since this excess

⁷Source: Core Energy Market Data Register Ordinance, MaStRV. https://www.bundesnetzagentur.de/EN/Areas/Energy/Companies/CoreEnergyMarketDataRegister/CoreDataReg_node.html.

⁸Source: Statista Research Department. <https://de.statista.com/statistik/daten/studie/70094/umfrage/wohngebaeude-bestand-in-deutschland-seit-1994/>. Access on 31.05.2021.

⁹Source: Strom-Report: Photovoltaik in Deutschland. <https://strom-report.de/photovoltaik/>. Access on 31.05.2021.

¹⁰While this approach represents a simplification, it is reasonable for retailers with a national customer portfolio, as assumed in this study, the aggregated PV load profile of which largely follows the same pattern of the system solar PV load profile.

¹¹Currently, the majority of households are metered on a semi-annual or annual basis. This metering system makes it hard for the retailer to identify and account for deviations from the standard load profile in the short term. In Germany, dedicated distribution system operators actively manage so-called difference balancing groups on the spot markets to balance expected deviations from the standard load profile. The costs of these deviations are thus rolled over to the involved retailers via an excess/shortage price, determined on a monthly basis. Accordingly, the developed methodology can be easily applied to manage different balancing groups in the current German market design.

is fed into the grid either based on a remuneration scheme or sold by the household itself. We finally assume that the household electricity demand is inelastic to wholesale spot prices due to the prevalence of fix components (i.e. taxes, grid fees and renewables support levy) in the retail tariffs, which represent a distortion to the price signals coming from the market.

A risk-neutral retailer maximizes the expected value of contribution margins $\mathbb{E}_{(j,k) \in \Omega}(\pi_{j,k})$ over all scenarios (j, k) in the discrete probability space Ω , which contains the tariff revenues from the customers $\mathbb{E}_{(j,k) \in \Omega}(\rho_{j,k}^{\text{tariff}})$, the procurement costs on the day-ahead and intraday markets, i.e. $\mathbb{E}_{(j,k) \in \Omega}(\kappa_{j,k}^{\text{DA}})$ and $\mathbb{E}_{(j,k) \in \Omega}(\kappa_{j,k}^{\text{ID}})$, and the potential imbalance costs $\mathbb{E}_{(j,k) \in \Omega}(\kappa_{j,k}^{\text{Imb}})$ ¹², that is:

$$\mathbb{E}_{(j,k) \in \Omega}(\pi_{j,k}) = \mathbb{E}_{(j,k) \in \Omega}(\rho_{j,k}^{\text{tariff}}) - \mathbb{E}_{(j,k) \in \Omega}(\kappa_{j,k}^{\text{DA}}) - \mathbb{E}_{(j,k) \in \Omega}(\kappa_{j,k}^{\text{ID}}) - \mathbb{E}_{(j,k) \in \Omega}(\kappa_{j,k}^{\text{Imb}}). \quad (18)$$

The tariff revenues are determined by fixed and dynamic base rates, namely $\tau^{\text{base,fix}}$ and $\tau^{\text{base,dyn}}$, which represent the fix components of the retail prices. The tariff revenues are also determined by fixed and dynamic energy rates, i.e. $\tau^{\text{energy,fix}}$ and $\tau^{j,qh,\text{energy,dyn}}$, which are energy-based and thus proportional to the served load. As mentioned above, we distinguish between retailer's customers with and without PV self-generation ($q_{j,k,qh}^{\text{RD}}$ and q_{qh} in Eq.17, respectively). By assuming n to be the number of households, $\phi \in [0, 1]$ the share of customers with rooftop solar PV systems, and $\delta \in [0, 1]$ the share of customers with dynamic tariffs. Hence, the tariff revenues from the costumers are given by:

$$\mathbb{E}_{(j,k) \in \Omega}(\rho_{j,k}^{\text{tariff}}) = \sum_{j=1}^J pr_j \sum_{k=1}^K pr_k \left((1 - \delta) \cdot (\tau^{\text{base,fix}} + ((1 - \phi) \cdot q_{qh} + \phi \cdot q_{j,k,qh}^{\text{RD}}) \cdot \tau^{\text{energy,fix}}) + \right. \\ \left. (\delta \cdot (\tau^{\text{base,dyn}} + ((1 - \phi) \cdot q_{qh} + \phi \cdot q_{j,k,qh}^{\text{RD}}) \cdot \tau_{qh}^{\text{energy,dyn}})) \right) \cdot n. \quad (19)$$

Procurement costs on day-ahead market and intraday market are based on the day-ahead sce-

¹²The contract of German balancing responsible parties explicitly forbids intentional imbalances while forcing to close positions with market operations. To cope with this rule, in this study we assume an imbalance price sufficiently high and equal to 10,000 EUR/MWh to ensure imbalance volumes and costs to be zero.

narios j and corresponding intraday realizations k , as described Sections 4.1 and 4.2. The scenario-based prices lda and lid represent the price levels at which the retailer can place volumes as selling and buying bids, i.e. $x_{lda,j,h}^{\text{DA,bid,buy/sell}}$ and $x_{lid,j,k,qh}^{\text{ID,bid,buy/sell}}$ in the day-ahead market and in intraday market, respectively. Price-volume bids lead to demand and supply curves, which are submitted on at hourly time step h in the day-ahead market, and at quarter-hourly time step qh in the intraday market.

By using binary acceptance parameters $\beta_{lda,j,h}^{\text{DA}}$ and $\beta_{lid,j,k,qh}^{\text{ID}}$, trades are determined from the submitted bids, thus allowing for modeling the retailer's non-anticipative trading strategies and scenario-based contribution margins¹³. As bids are possible in both buying and selling direction, the retailer might intentionally take either a short or a long position to profit from potential price spreads between the day-ahead and intraday market. Procurement costs on the intraday market are defined as:

$$\mathbb{E}_{(j,k) \in \Omega}(\kappa_{j,k}^{\text{ID}}) = \sum_{j=1}^J pr_j \sum_{k=1}^K pr_k \left(\sum_{qh}^{QH} \sum_{lid}^{LID} ((1 - \beta_{lid,j,k,qh}^{\text{ID}}) \cdot x_{lid,j,k,qh}^{\text{ID,bid,buy}} \cdot p_{j,k,qh}^{\text{ID}} + \beta_{lid,j,k,qh}^{\text{ID}} \cdot x_{lid,j,k,qh}^{\text{ID,bid,sell}} \cdot (-p_{j,k,qh}^{\text{ID}})) \cdot \Delta t \right), \quad (20)$$

where the term Δt adapts for the 15 minutes resolution of the intraday market (i.e., $\Delta t = 0.25$). Following Ottesen et al. (2018) and Laur et al. (2018), and using the approach in Kraft et al. (2021), we model the continuous intraday market as one hypothetical auction, with the intraday ID3 index price p_{τ}^{ID3} in Section 4.2.3 as the price for each quarter hour qh . In doing so, we consider the hypothetical auction as a uniform pricing auction, thus limiting the potentially greater price volatility and risk exposure due to the arrival process towards gate closure time in the continuous intraday. It is worth noting that if the retailer is short in one market segment, the term of the costs can potentially become negative indicating revenues. Procurement costs in the day-ahead market

¹³In Kraft et al. (2021), a bidding framework is developed that allows for both selling and buying bids. To remain consistent, β denotes the acceptance of selling bids. To evaluate the buying bids predominant in this study, the opposite of the binary parameter, i.e. $(1 - \beta)$, is applied.

are defined analogously to Eq. 20.

Based on the current contract for balancing responsible parties in Germany, the volume of a short or long position on the spot markets is limited to a certain percentage $q^{\max, \text{short/long}}$ of the maximum schedule volume of the day¹⁴. As the retailer does not trade any generation, storage, or demand apart from the load to be served, the maximum short position on the day-ahead market is defined as follows:¹⁵

$$-\max_{qh \in QH} \left((1 - \phi) \cdot q_{qh} + \phi \cdot \max_{k \in K} q_{j,k,qh}^{\text{RD}} \right) \cdot n \cdot q^{\max, \text{short}} \leq x_{j,h}^{\text{DA,trade}} \quad \forall j \in J, h \in H. \quad (21)$$

(The short position constraints for the intraday market are defined analogously.)

Since the market design requires closed positions, any imbalances $x_{j,k,qh}^{\text{imb}}$ in the day-ahead and intraday positions ($x_{j,h}^{\text{DA,trade}}$ and $x_{j,k,qh}^{\text{ID,trade}}$, respectively) need to be balanced by the TSO, i.e.:

$$x_{j,h}^{\text{DA,trade}} + x_{j,k,qh}^{\text{ID,trade}} + x_{j,k,qh}^{\text{imb}} = x_{j,h}^{\text{DA,trade}} + x_{i,j,k,qh}^{\text{ID,trade}} \quad \forall (j, k) \in \Omega, h \in H, qh(h) \in QH(H), \quad (22)$$

where $x_{j,h}^{\text{DA,trade}}$ and $x_{i,j,k,qh}^{\text{ID,trade}}$ represent all trades in the day-ahead and the intraday markets, respectively. The notation $qh(h)$ indicates a mapping of quarter hours to the respective hour, that is $qh1$, $qh2$, $qh3$, and $qh4$ represent the four quarters of hour $h1$ of the day, and so on. To ensure the non-anticipativity of the trading strategy, the retailer submits the same bids under the same set of information. For the bids submitted to the day-ahead market, this constraint translates into:

$$x_{lda,j,h}^{\text{DA,bid}} = x_{lda,j+1,h}^{\text{DA,bid}} \quad \forall lda \in LDA, \{j \in J \mid \text{Ord}(j) < |J|\}, h \in H, \quad (23)$$

with $\text{Ord}(j)$ representing the ordinal number of the scenario j in the set J and $|J|$ the cardinality of set J . The intraday market constraints on the realizations k are defined in analogous way.

One major shortfall of determining trading strategies in a risk-neutral way and with the associ-

¹⁴In the current contract, a strategic position of 10% is allowed, which is thus used in this study.

¹⁵Note, that considering the maximum scenario value $\max_{k \in K} q_{j,k,qh}^{\text{RD}}$ of residual load over all k in Eq. 21 is a rather relaxed interpretation of the strategic position constraints. However, the peak demand of the standard load profile is observed in the evening. At that time, the uncertainty in solar generation is low and the scenarios differ only slightly.

ated uncertainty is that the probability distribution of potential scenario outcomes is reduced to one single figure, i.e. the expected value. Yet, the expected value is affected by abnormal values in the distribution, thus driven by a few scenario leaves with extreme values but low probabilities. Furthermore, the risk-neutral determination of trading strategies does not take into account outcome uncertainty, which is of particular relevance for a retailer under competitive pressure. Therefore, the hypothesis of risk-neutrality may lead to trading strategies overestimating the retailer's risk exposure in terms of low contribution margins and thus profitability. With increasing volumes of variable renewable generation in the energy system, and consequent impact on electricity prices, it becomes paramount for the retailer to assess the distribution of contribution margins by including risk considerations within the probability space Ω .

We use the approach of Conejo et al. (2010) as reformulated by Kraft et al. (2021), and include into the retailer's trading problem the conditional value-at-risk (CVaR) risk metric with a level $\alpha=95\%$ (see e.g. Alexander, 2008; Conejo et al., 2010, for the mathematical definition)¹⁶. By including the expected value and the CVaR, the target function is extended to a multi-objective optimization where $\lambda \in [0, 1]$ denotes the weight allocated to the risk metric: $\lambda=0\%$ is equivalent to the risk-neutral problem above; increasing values of λ correspond to a growing risk-aversion. We also include into the target function two additional constraints: the first, η , represents the value-at-risk, i.e. the quantile value at $(1-\alpha\%)$; the second, s , represents the (positive) difference between η and the contribution margin π in a single scenario. Hence, the retailer's decision-making problem under uncertainty is reformulated as follows (see Conejo et al., 2010; Kraft et al., 2021, for further details):

$$\max \quad (1 - \lambda) \cdot \mathbb{E}_{(j,k) \in \Omega}(\pi_{j,k}) + \lambda \cdot \left(\eta - \frac{1}{1 - \alpha} \sum_{j=1}^J pr_j \sum_{k=1}^K pr_k \cdot s_{j,k} \right) \quad (24)$$

¹⁶As a coherent risk metric, the CVaR has the properties of monotonicity, sub-additivity, homogeneity, and translational invariance. With regard to portfolio problems, the sub-additivity is a particularly desirable property as it allows to scale or combine portfolios, and thereby ensures the validity of the decision calculus in terms of risk exposure. The level of α denotes the quantile of the loss distribution assumed to assess the risk exposure. In this study, we consider $\alpha = 95\%$ as suitable level in the determination of bids, thereby capturing the expected value of the 5% greatest losses for the retailer.

$$\eta - \pi_{j,k} \leq s_{j,k} \quad \forall (j, k) \in \Omega \quad (25)$$

$$s_{j,k} \geq 0 \quad \forall (j, k) \in \Omega \quad (26)$$

In the next section, the developed approach is used to solve the retailer's trading optimization problem and investigate the retailer's risk exposure and trading adjustment to increasing levels of PV self-sufficiency.

4.4 Retailer's risk-management problem with increasing solar PV self-generation: A case study with fixed and dynamic energy tariffs

The retailer's risk-management problem, and their risk exposure to increasing levels of solar PV self-generation are investigated by assuming different installation rates of PV systems in the residential sector, i.e. different shares of residential houses with installed rooftop solar PV systems. An installation rate $\phi=10\%$ is assumed, which is the *status quo* in Germany (Section 4.3). We also assume installation rates $\phi=30\%$ and $\phi=50\%$, which are in line with the solar photovoltaic expansion targets in Germany (from 54 to 150 GW by 2030, and 25% of electricity needs powered with solar energy by 2050 (Bundesministerium für Wirtschaft und Energie, 2021)). By maintaining the solar PV capacity factor constant at 10%, the levels of PV self-generation corresponding to the different penetration rates are computed for a typical day in the season, as described in Section 4.3. Hence, the computed self-generation levels are subtracted from the standard load profile to obtain the residual demand of the residential sector, as in Eq.17.

We notice that a lower demand from customers with PV systems implies lower revenues for the retailer, as generated by the energy rates (Eq.19). To evaluate the impact that more dynamic retail tariffs may have on the risk exposure and management of the retailer, we consider two different retail tariff schemes. In the first scheme, we assume a fixed retail tariff, i.e. the most common and currently applied tariff structure in Germany. This tariff is composed of a fixed base rate and

a fixed energy rate. The fixed base rate is valued in EUR per time interval (e.g. EUR/a), while the fixed energy rate is valued in EUR per unit of energy demanded (e.g. EUR-ct/kWh). We collect from GET AG¹⁷ the ten most competitive retail tariffs from the 39 locations considered in the stochastic modeling of solar generation and subtract the fixed rate (i.e. taxes, grid fees and renewables support levies) to isolate energy rate used to evaluate the retailer's net revenues. Fig. 5 depicts the collected fixed base rates and fixed energy rates. For the purpose of our study, we use the median value as representative of the sample in the empirical analysis. The median fixed base rate is 6.87 EUR/month or 0.23 EUR/day; after removing levies, taxes and grid fees as provided by GET AG, the median fixed energy rate is 0.058 EUR/kWh (i.e. 58.24 EUR/MWh). In the

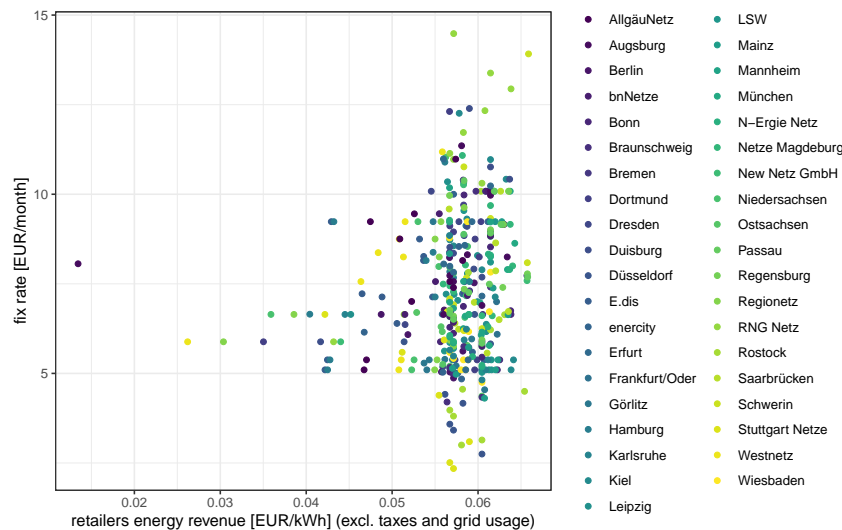


Figure 5: Fixed base rates and energy rates in Germany for 39 different locations, net (Source: GET AG)

second tariff scheme, we consider a dynamic tariff with a fixed base rate and a time-varying energy rate. The time-varying energy rate is assumed to be indexed to day-ahead electricity prices. In this second scheme, the fixed base rate is calibrated so as to obtain the same contribution margin of the fixed tariff scheme in the sample. This guarantees the reliability of our analysis on the impact of increasing self-sufficiency and dynamic tariffs on the retailer's net revenues and risk exposure.

¹⁷<https://www.get-ag.com/>

For the second tariff scheme, a fixed base rate of 0.453 EUR/day is computed. We maintain the assumption of price-inelasticity of electricity demand, likewise the assumption of no electricity storage allowing for adjustments to the PV feed-in and self-generation patterns in the retailer's portfolio.

We investigate the retailer's trading optimization problem with increasing levels of solar PV self-generation by assuming an increasing number of costumers with PV generation in the retailer portfolio, as defined in Eq.17, and consistent with installation rates $\phi=30\%$ and $\phi=50\%$. We assume a hypothetical retailer with 100,000 household customers as in Section 4.3, and consider the implications of increasing self-sufficiency under the two tariff schemes described above by assuming that customers with and without PV self-generation and costumers with fixed and dynamic tariffs are equally distributed in the retailer portfolio¹⁸. ϕ denotes the share of customers with PV installations, i.e. the PV installation rate, while the share of customers with a dynamic tariff is denoted by δ . In our case study, we consider $\delta=0\%$, i.e. the *status quo* of the market with no indexation to the day-ahead prices in the energy rate, and $\delta=50\%$ and $\delta=100\%$. This case study is of particular interest to assess the extent to which tariff schemes can affect risk sharing in electricity markets with increasing levels of distributed variable renewable generation. Results from the stochastic modeling and retailer's trading optimization are presented in the following section.

5 Results

Table 2 shows descriptive statistics of the time series for dependent variables used in the empirical analysis. We distinguish between Summer, Transition season and Winter, and observe that in Summer and Winter, the intraday solar PV generation and ID3 price are on average above their day-ahead values for the corresponding delivery period. The opposite holds during the Transition season. Not surprisingly, differences between the intraday and day-ahead solar PV are larger and

¹⁸Although a bias introduced by the self-selection of certain customers' group towards certain tariffs is possible, we consider this assumption to be legitimate as there is no technical flexibility to be exploited economically. However, extending the approach to customers with PV battery storage systems would require a investigation of individual economic incentives.

more volatile in Winter. Differences between intraday and day-ahead price are larger, in absolute value, during the Transition season but more volatile in Winter, is response to the greater uncertainty of the solar PV generation, and consequently of the residual load. Overall, skewness and kurtosis imply a departure from the assumption of a Gaussian distribution, as also suggested by the Jarque-Bera statistics and their p-values (JB and JB p-value in columns nine and ten of the table). The Augmented Dickey-Fuller tests reject the null hypothesis of non-stationarity.

5.1 Day-ahead and intraday stochastic modeling

Parameter estimates of deterministic components of the day-ahead and intraday series, as described in Eq.2-Eq.4 and Eq.11-Eq.13 are presented in Appendix A.1 and A.2, respectively. The OU parameter estimates for the day-ahead stochastic components X_t, Y_t, Z_t in the base regime are shown in Tab.3. The mean-reverting parameters in the diagonal of the matrix $\beta^{DA,Base}$ point to a higher persistence of the residual load when compared to the cloudiness and price series across the system. In contrast, the prices series show the lowest persistence. Higher volatility is observed in the residual load and price series during the Transition season and in Winter, as indicates by the parameters in the diagonal of the matrix $\Sigma^{DA,Base}$. The opposite holds for the cloudiness component, which is more volatile in Summer. Overall, the out-of-diagonal parameters of the matrix validate the positive correlation linking cloudiness, residual load and price. Lower jump regime produce more spiked series compare to the upper jump regime, as implied by the parameters μ in Tab.4. In all, the lower regime is also more volatile than the upper regime, as indicated by the estimated covariance matrices Σ . Series in the lower regime are also more volatile than in the base regime, thus in line with findings in Coulon et al. (2013).

Parameter estimates of the stochastic component of the intraday cloudiness and residual load series (Tab. 5) are in line with the results observed in day-ahead market, thus suggesting the highest persistence of the cloudiness across seasons with respect to the residual load. Yet, residual load is found to be more volatile than cloudiness in the intraday market across the seasons. Furthermore, in contrast to the day-ahead market, more spiked series are observed in the upper rather than in

Table 2: Descriptive statistics

Summer	Mean	Median	Min	Max	St.Dev.	Skew	Kurt	JB	JB p-value	ADF	ADF p-value	Obs.
Solar PV load (MW), DA	11105	10914	1	29409	8296	0.197	1.797	263.5	0.001	-16.21	0.001	5952
Solar PV load (MW), ID	11146	10851	1	29622	8317	0.202	1.812	258.4	0.001	-16.44	0.001	5952
Residual load (MW), DA	14188	14758	-20414	33539	9567	-0.575	3.292	349.6	0.001	-9.870	0.001	5952
Residual load (MW), ID	14284	14778	-18415	33834	9413	-0.539	3.173	295.5	0.001	-10.05	0.001	5952
Price (EUR/MWh), DA	38.27	37.69	-49.62	80.01	11.11	-1.082	11.71	4993	0.001	-5.120	0.001	1488
ID3 Price (EUR/MWh), ID	38.45	37.45	-116.2	174.53	15.61	-0.316	19.59	68329	0.001	-13.31	0.001	5952
Delta price (EUR/MWh), (ID-DA)	0.179	-0.225	-100.8	115.17	10.97	0.863	16.20	43893	0.001	-14.40	0.001	5952
Transition season	Mean	Median	Min	Max	St.Dev.	Skew	Kurt	JB	JB p-value	ADF	ADF p-value	Obs.
Solar PV load (MW), DA	7226	5936	1	26943	6115	0.845	3.049	490.4	0.001	-9.77	0.001	8736
Solar PV load (MW), ID	7200	5788	1	27216	6189	0.874	3.094	526.3	0.001	-9.56	0.001	8736
Residual load (MW), DA	14566	15015	-19315	44328	11707	-0.172	2.690	78.13	0.001	-10.76	0.001	8736
Residual load (MW), ID	14489	14819	-21842	44681	11879	-0.170	2.654	85.7	0.001	-10.82	0.001	8736
Price (EUR/MWh), DA	38.38	38.05	-37.29	87.12	12.20	-0.599	6.179	692.7	0.001	-6.351	0.001	2184
ID3 Price (EUR/MWh), ID	36.69	37.51	-94.3	200.3	18.78	-1.368	13.13	40060	0.001	-13.80	0.001	8736
Delta price (EUR/MWh), (ID-DA)	-1.227	-0.825	-98.5	140.2	12.58	-1.109	16.31	66183	0.001	-15.84	0.001	8736
Winter	Mean	Median	Min	Max	St.Dev.	Skew	Kurt	JB	JB p-value	ADF	ADF p-value	Obs.
Solar PV load (MW), DA	4190	3404	1	15705	3597	0.911	3.206	482.2	0.001	-9.194	0.001	8736
Solar PV load (MW), ID	4362	3488	1	16790	3777	0.889	3.105	455.2	0.001	-9.85	0.001	8736
Residual load (MW), DA	10189	10512	-22072	42688	13470	-0.068	2.343	164.0	0.001	-9.963	0.001	8736
Residual load (MW), ID	10230	10611.5	-20394	42696	13328	-0.042	2.318	171.8	0.001	-9.97	0.001	8736
Price (EUR/MWh), DA	29.85	32.25	-50.43	76.47	15.93	-1.040	5.155	815.3	0.001	-7.978	0.001	2184
ID3 Price (EUR/MWh), ID	30.79	33.46	-80.6	438.8	20.66	0.678	29.25	25152	0.001	-12.21	0.001	8736
Delta price (EUR/MWh), (ID-DA)	0.982	0.96	-90.4	397.4	14.81	3.082	78.41	20831	0.001	-16.24	0.001	8736

Table 3: Parameter estimates of the stochastic components in base regime: Day-ahead series

Summer	$\beta^{DA,Base}$			$\Sigma^{DA,Base}$		
	X	Y	Z	X	Y	Z
X	0.3286	-0.0311	-0.1836	0.00614	0.00014	0.00006
Y	-0.0016	0.2415	0.2695	0.00014	0.00207	0.00011
Z	-0.0055	0.0022	1.9412	0.00006	0.00011	0.00056
Transition season	$\beta^{DA,Base}$			$\Sigma^{DA,Base}$		
	X	Y	Z	X	Y	Z
X	0.612	-0.143	0.462	0.00432	0.00039	0.00014
Y	-0.004	0.343	1.473	0.00039	0.00476	0.00017
Z	-0.003	0.030	2.198	0.00014	0.00017	0.00078
Winter	$\beta^{DA,Base}$			$\Sigma^{DA,Base}$		
	X	Y	Z	X	Y	Z
X	0.641	-0.019	0.022	0.00036	-0.00002	0.00002
Y	0.050	0.437	0.930	-0.00002	0.01019	0.00041
Z	0.037	0.019	2.270	0.00002	0.00041	0.00116

Table 4: Parameter estimates of the stochastic components in the upper jump and lower jump regimes: Day-ahead series

Summer	$\epsilon^{DA,uJ}$				$\epsilon^{DA,lJ}$			
	μ	Σ			μ	Σ		
X	0.018	0.008527	0.000028	0.000021	0.0310	0.0150021	0.0001185	0.0000143
Y	0.001	0.000028	0.000262	0.000001	0.0001	0.0001185	0.0000287	0.0000001
Z	0.001	0.000021	0.000001	0.000032	0.0005	0.0000143	0.0000001	0.0000226
Transition season	$\epsilon^{DA,uJ}$				$\epsilon^{DA,lJ}$			
	μ	Σ			μ	Σ		
X	0.050	0.031659	0.000078	0.000003	0.0631	0.040807	0.014639	0.000040
Y	0.001	0.000078	0.000290	-0.000001	0.0168	0.014639	0.022301	0.000011
Z	0.001	0.000003	-0.000001	0.000044	0.0006	0.000040	0.000011	0.000032
Winter	$\epsilon^{DA,uJ}$				$\epsilon^{DA,lJ}$			
	μ	Σ			μ	Σ		
X	0.058	0.02063	0.00019	-0.00004	0.0623	0.039472	0.004743	-0.000031
Y	0.004	0.00019	0.00168	0.00004	0.0101	0.004743	0.004888	0.000021
Z	0.001	-0.00004	0.00004	0.00010	0.0014	-0.000031	0.000021	0.000108

the lower regimes (Tab.6), thus implying more frequent upward adjustments in the cloudiness and residual load intraday forecasting process. High persistence and volatility are also observed in the intraday ID3 prices when compared to the day-ahead price series (Tab.7). Similar to the cloudiness and residual load series, ID3 prices are in all more spiked and volatile in the higher regime. Parameter estimates of these stochastic components are thus used to generate 1,000 path over one typical working and weekend day for each of the three seasons. The resulting scenario trees are presented in the next section.

Table 5: Parameter estimates of the stochastic components in the base regime: Intraday cloudiness and residual load series

Summer	$\beta^{ID,Base}$		$\Sigma^{ID,Base}$	
	X	Y	X	Y
X	0.1665	-0.0065	0.000022	0.000002
Y	0.0883	1.2913	0.000002	0.000167
Transition season	β^{ID}		$\Sigma^{ID,Base}$	
	X	Y	X	Y
X	0.3221	0.0097	0.000002	0.000001
Y	-0.4380	1.2956	0.000001	0.000171
Winter	$\beta^{ID,Base}$		$\Sigma^{ID,Base}$	
	X	Y	X	Y
X	0.7539	-0.0061	0.000007	0.000002
Y	-0.3567	1.0473	0.000002	0.000417

Table 6: Parameter estimates of the stochastic components in the upper jump and lower jump regimes: Intraday cloudiness and residual load series

Summer	$\epsilon^{ID,uJ}$			$\epsilon^{ID,lJ}$		
	μ	Σ		μ	Σ	
X	0.0052	0.000292	0.000002	0.0060	0.000530	0.000002
Y	0.0006	0.000002	0.000023	0.0004	0.000002	0.000018
Transition season	$\epsilon^{ID,uJ}$			$\epsilon^{ID,lJ}$		
	μ	Σ		μ	Σ	
X	0.0096	0.000830	0.000009	0.0085	0.000858	0.000003
Y	0.0010	0.000009	0.000047	0.0007	0.000003	0.000038
Winter	$\epsilon^{ID,uJ}$			$\epsilon^{ID,lJ}$		
	μ	Σ		μ	Σ	
X	0.0126	0.001144	-0.00002	0.0097	0.001139	0.000005
Y	0.0018	-0.000018	0.00016	0.0018	0.000005	0.000162

Table 7: Parameter estimates of the stochastic component in base regime of the intraday ID3 price

	$\beta^{ID3,Base}$	$\sigma^{ID3,Base}$
Summer	1.744	0.0029
Transition season	2.064	0.0087
Winter	1.437	0.0047

Table 8: Parameter estimates of the stochastic component in the upper jump and lower jump regimes of the intraday ID3 prices

	$\epsilon^{ID3,uJ}$		$\epsilon^{ID3,lJ}$	
	μ	σ	μ	σ
Summer	0.0010	0.0107	0.0007	0.0087
Transition season	0.0030	0.0245	0.0025	0.0218
Winter	0.0027	0.0212	0.0036	0.0255

5.2 Scenario trees

In all, the scenario generation-and-reduction procedure described in Section 4.1.4 and Section 5 results in totally 540 nodes, and 90 scenario trees across the three seasons (Summer, Transition

season, Winter) and the two typical days (working and weekend day), as depicted in Fig.4. For illustration purposes, we plot the scenario trees for the low, medium and high scenario obtained for one typical working day in Summer. These scenarios correspond to high, medium and low levels of solar PV generation respectively, i.e. low, medium and high levels of cloudiness, residual load and prices in the scenario generation-reduction, as filtered through the clustering algorithm. The choice of driving attention on a working day in Summer is motivated by the intuition that solar PV generation and self-generation should have a greater impact on the retailer's trading decisions and risk-exposure in Summer and during a business day, i.e. when the levels of solar generation and total load are expected to be higher.

Fig.6 shows the obtained nodes for the day-ahead solar PV generation, residual load and prices in the low (left charts), medium (mid) and high (right) scenarios. Solid black line show the historical values, i.e. the average working day in the sample season as computed from the hourly averages; solid blue lines represent the expected day-ahead profile j_1 obtained from the scenario-reduction procedure. Dashed lines represent day-ahead profiles j_2 and j_3 , which are above and below one standard deviation from the expected profile. These nodes have 25% probability of realization; dotted lines correspond to more extreme day-ahead profiles j_4 and j_5 , which are above and below one standard deviation from the expected profile and have 12.5% probability of realization. Despite the limited randomness of the solar PV generation (top charts), the simulated paths well capture the iconic *duck-curve* effect of the solar PV generation on the residual load, and the load-to-price relationship, while the three scenarios remain consistent with the historical values¹⁹. Fig. 7 provides distributional information of the historical and simulated day-ahead series through boxplots. On each blue box, the central red mark indicates the median, the bottom and top edges of the box indicate the 25th and 75th percentiles, respectively. The whiskers extend to the most extreme data points, which are not considered outliers. The simulated five nodes in the medium scenario (mid plots) well reproduce the distribution of the historical series, being this scenario obtained

¹⁹As solar PV generation increases during the day, it reduces the residual load. The residual load drops in the middle of the day (like a belly) and then raises as the solar generation reduces (like a neck), thus leading to the definition of a *duck-curve*

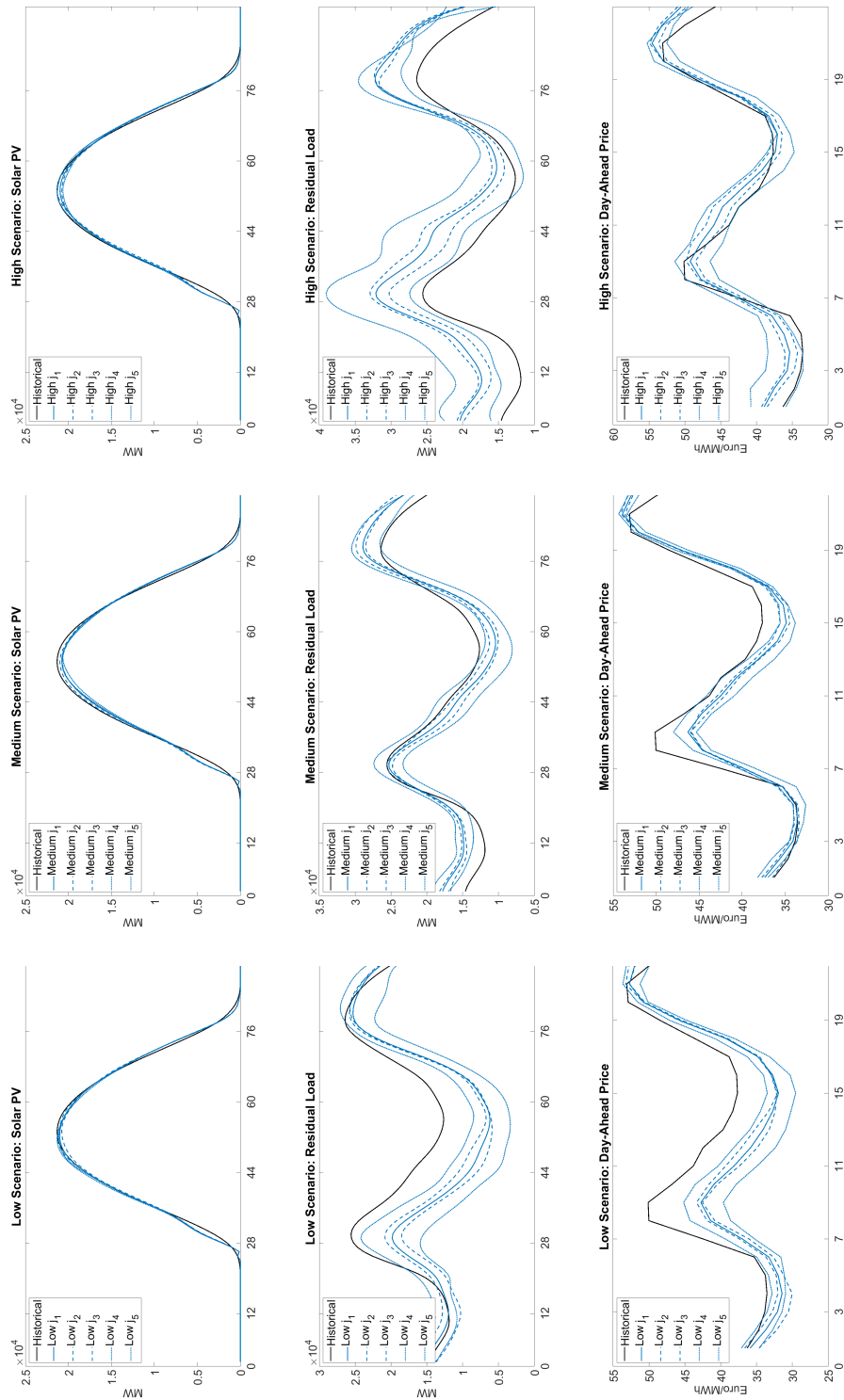


Figure 6: Historical and simulated day-ahead series: Summer working day

from the partition of simulated paths that are in the variance cluster closest to the median of all the simulated paths. Nodes in the high and low scenarios (left and right plots, respectively) represent the partitions of simulated paths in highest and lowest variance clusters respectively, and such that their median point is above and below the all-point median of the corresponding nodes in the medium scenario. Therefore, consistent with the identified three scenarios, boxplots indicate that the correlation structure between solar PV generation, residual load and price in the day-ahead market is well reproduced across nodes in the three scenarios. Results for the simulated series in transition and Winter seasons are reported in the Appendix. The scenario trees depicted in Fig.8 show the possible intraday realizations k of the day-ahead node j_1 in the low, medium and high scenario in Fig.6. These scenario trees reflect the adjustment process occurring between day-ahead and intraday market, following the arrive of new information and consequent update of the solar forecasting error. The intraday realizations k_1 represent expected intraday profiles minimizing the forecasting error, thus leading to intraday realizations close to the expected day-ahead profiles (blue solid lines in the plots). For growing forecasting errors, greater deviations are observed in the intraday residual load and price profiles, which are consistent with the duck-curve effect and the positive correlation between residual load and price, as also unveiled by the historical values (black solid lines). Furthermore, the intraday realizations well capture the empirically observed jagged pattern of the intraday prices, as noticed by comparing the historical observations (black solid lines) with the simulated values. This pattern is of particular interest when investigating trading strategies in the intraday market, and thus the retailer's trading and risk optimization problem with increasing levels of solar PV self-generation. Results from this analysis are presented below.

5.3 Retailer's trading optimization in the day-ahead and intraday market

In this section, the results of the retailer's trading optimization problem are presented. For illustration purposes and in line with the scenario trees presented in Section 5.2, the results for the day-ahead node j_1 and all its possible intraday realizations k in the typical summer working day are shown, and for the low and high scenarios, i.e. for high (low) and low (high) levels of solar PV

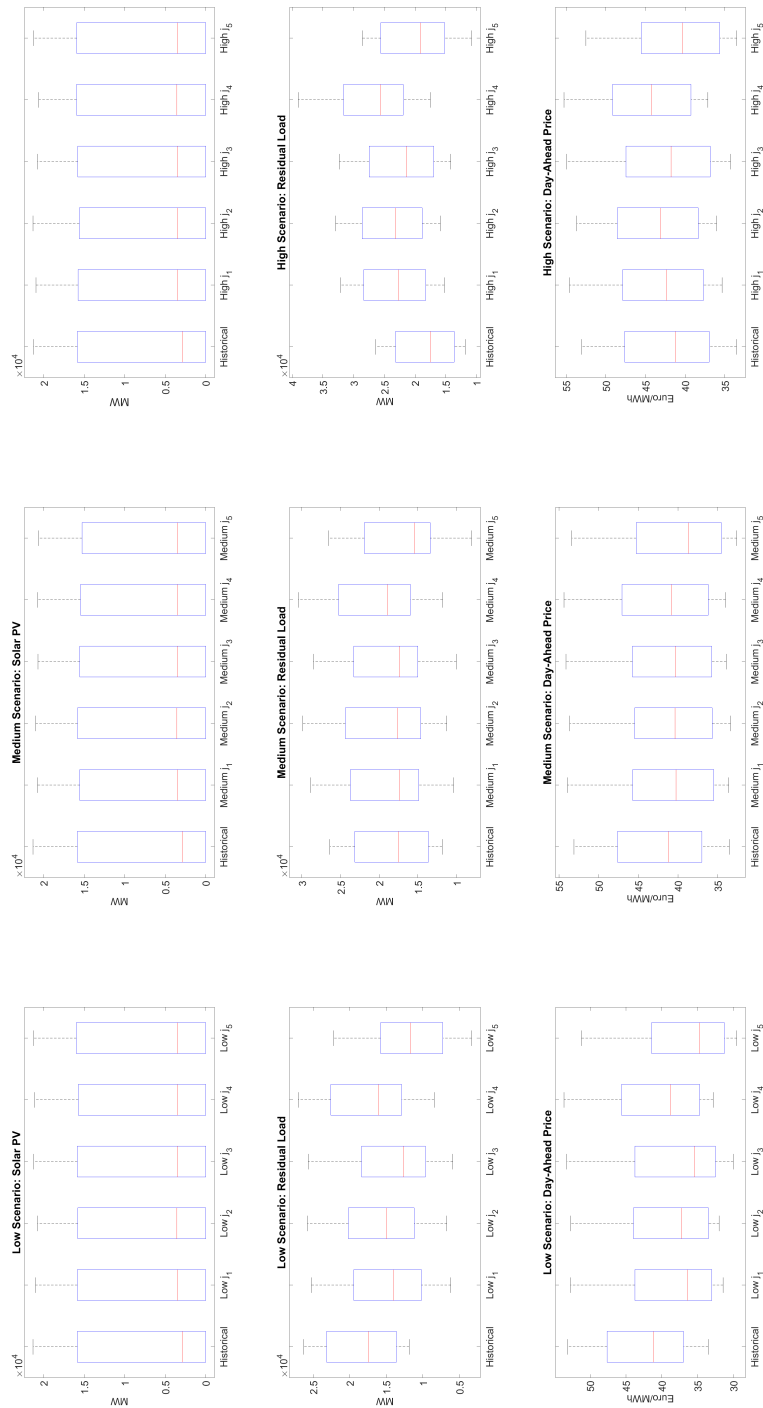


Figure 7: Distribution of the historical and simulated day-ahead series: Summer working day

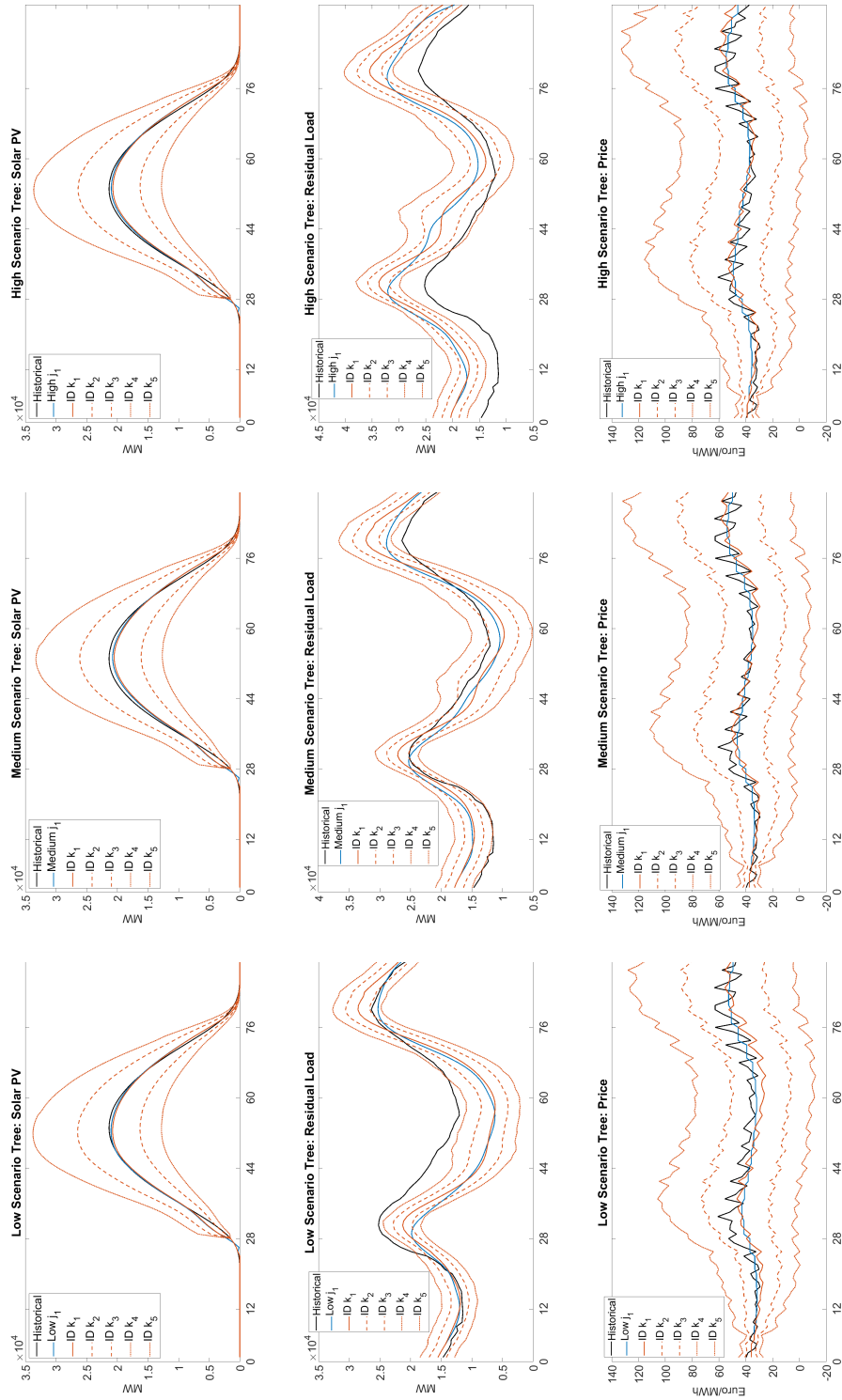


Figure 8: Scenario trees for the representative day-ahead node j_1 and its intraday realizations k : Summer working day

generation (residual load) since these scenarios can be expected to better represent the implications of high levels of self-sufficiency for a retailer serving customers with decentralized self-generation. Results concerning the retailer's trading strategies in the medium scenario, and for the transition and Winter seasons are reported in the Appendix.

Fig.9 and Fig.10 summarize the retailer's optimal trading strategies in the day-ahead and intraday markets in the low scenario. These figures show the buying and selling bids of the retailer in the two markets for different levels of their risk aversion, as indicated by the parameter λ , with increasing levels of solar PV generation (corresponding to installation rates of 10% and 50%) and under the two different retail tariff schemes, i.e. for 0% and 100% indexation of the dynamic energy rate to the day-ahead price²⁰. Buying/selling positions are denoted by the direction of the marker in the plots; the acceptance probability of the bids is denoted by the colour gradation while bidding volumes are indicated by the size of the marker. It should be noted that bids submitted on the day-ahead market do not anticipate realizations in the intraday market, and are thus consistent over the represented scenario tree.

In the low scenario, a risk-neutral retailer ($\lambda=0\%$) takes buying positions in the day-ahead market during the solar generation peak between 11 am and 3 pm (left column of Fig.9). This trading strategy is consistent across different levels of self-generation and tariff schemes, and implies the preference of a risk-neutral retailer to buy electricity in the day-ahead market for the solar-peak hours against the expectation of potentially higher prices in the intraday market, as driven by lower than expected levels of solar generation (Fig.10). Yet, in all the risk-neutral retailer is more prone to take buying positions in the intraday market, in particular in the evening, i.e. when the expected price benefit of the solar generation and the impact of self-generation are less evident.

Differently from a risk-neutral retailer, a more risk-averse retailer ($\lambda=10\%$) prefers to take buying positions in the day-ahead market, in particular for the hours starting from 7 pm onward

²⁰The increasing solar PV penetration level is not considered to take place on a system level in the stochastic price model. For the results to remain comparable, we rather compare larger shares of households with rooftop solar PV systems in the retailer's portfolio by assuming unchanged market circumstances and solar system load. However, this assumption is likely to underestimate the importance of risk hedging under higher penetration of distributed renewable generation, since price volatility is likely to increase with increasing shares of variable generation.

and for low levels of self-generation. This trading behavior is more evident in the tariff scheme without indexation to the day-ahead price, thus in line with a strategy focused on reducing the risk exposure to the solar self-generation in the intraday market. This reasoning is supported by the observed selling positions in the intraday market for the morning and evening hours, i.e. when the impact of the solar generation (and self-generation) uncertainty on residual load and price is higher (Fig.8). The trading positions of a moderately risk-averse retailer are mixed and imply a propensity to take selling positions in the day-ahead market, mostly at the sunrise and sunset, and in the case of tariff with 0% indexation to the day-ahead prices. The mirroring buying positions in the intraday market suggest some trading adjustment to benefit of lower than expected intraday prices. Yet, the exposure of this retailer in the intraday market reduces for high levels of self-generation, when buying positions in the day-ahead market increase, mostly in the night hours and despite the presence of a more dynamic tariff (100% day-ahead price-indexation). In the high scenario, i.e. with lower levels of solar generation and high levels of residual load (Fig.11 and Fig.12), the risk-neutral retailer takes buying positions on the day-ahead market during the solar-peak hours and in the evening. This is more evident at 10% of self-sufficiency, regardless of the tariff scheme. Exposure in the intraday market increases for increasing levels of self-sufficiency thus under the expectation of potentially lower prices in the intraday market. Thus similar to the low scenario, a risk-neutral retailer in the high scenario is probably willing to take buying positions in the intraday market. The day-ahead buying positions of risk-averse retailers visibly increase in the high scenario, in response to lower levels of solar generation. Interestingly, buying positions in the day-ahead market are greater with the first retail tariff scheme, with 0% indexation to the day-ahead price. In contrast, the selling positions of a risk-averse retailer increase in the intraday market, mainly for high levels of self-generation and for the evening hours, i.e. after the sunset, thus implying some trading adjustment with respect to the day-ahead buying positions. Implications for the retailer's risk exposure of these trading strategies are discussed in the next section.

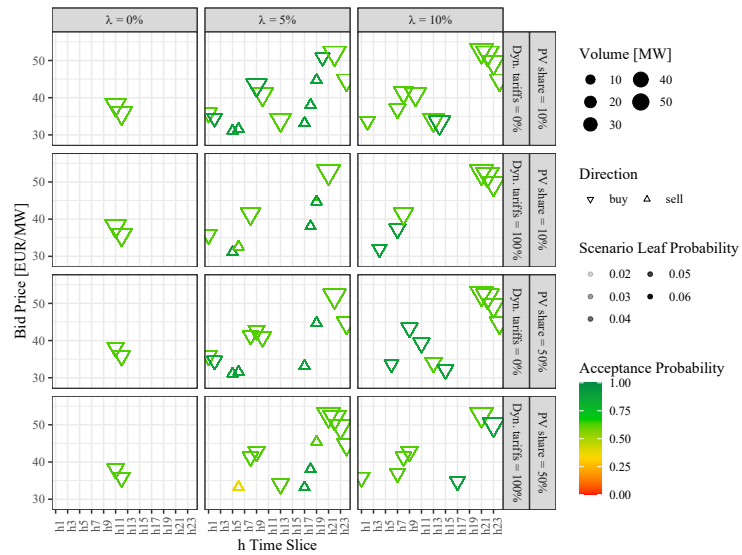


Figure 9: Retailer's day-ahead trading strategy in the summer working day: Low scenario

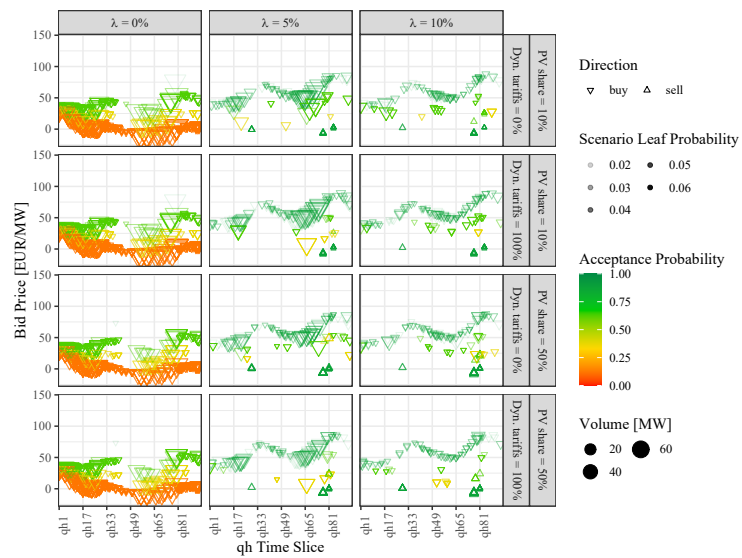


Figure 10: Retailer's intraday trading strategy in the summer working day: Low scenario

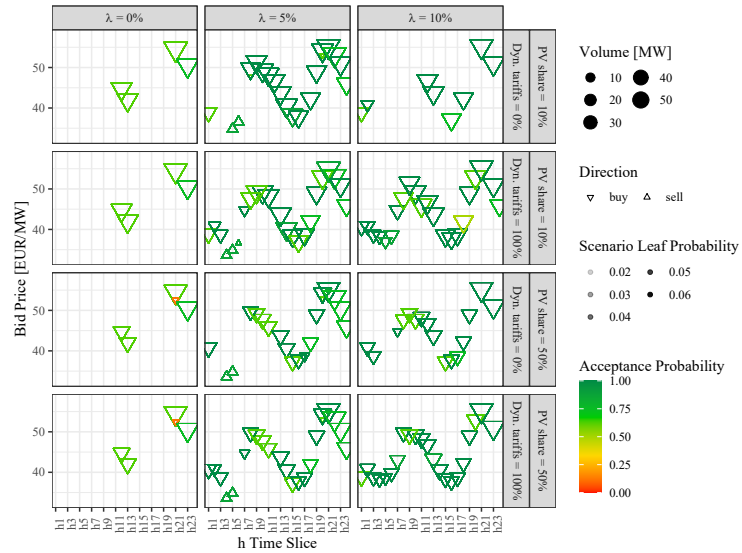


Figure 11: Retailer's day-ahead trading strategy in the summer working day: High scenario

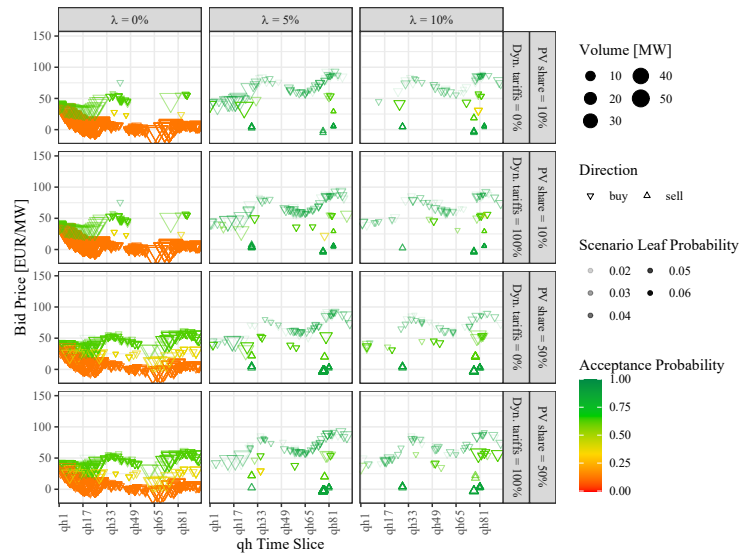


Figure 12: Retailer's intraday trading strategy in the summer working day: High scenario

5.4 Retailer's portfolio risk management with increasing solar PV self-generation

In this section, we present evidence of the retailer's risk exposure and management in the low and high scenarios presented in the previous section. Fig. 13 and Fig.14 show the empirical cumulative distribution functions (ECDFs) of the contribution margin of the retailer at 10% and 50% of solar PV self-generation and under the two retail tariff schemes (0% and 100% day-ahead price indexation of the retail energy tariff). The ECDFs are depicted for values of the risk preference λ in the target function in Eq.24: 0% (risk neutral, red line in the figures), 5% (low risk aversion, in yellow), and 10% (high risk aversion, green) and for a CVaR level at confidence level $\alpha = 95\%$. The horizontal lines in the plots represent the expected contribution margins at each level of λ .

In all, these figures point to a reduction of the retailer's expected contribution margin for increasing levels of self-generation without any indexation to the day-ahead price in the retail tariff. This reduction is higher in the low scenario, i.e. with higher solar PV generation (from around 40,000 EUR/day to 35,000 EUR/day, Fig.13) compared to the high scenario (from around 37,500 EUR/day to 32,000 EUR/day, Fig.14). Yet, under a highly dynamic tariff scheme with complete indexation to the day-ahead price ($\delta = 100\%$), the expected contribution margin of the retailer remains almost unchanged for increasing levels of self-sufficiency and across scenarios (45,000 EUR/day). Interestingly, the ECDFs imply greater but more uncertain and dispersed contribution margins at lower levels of self-sufficiency for different risk preferences. For instance, in the low scenario (Fig.13), 10% of self-sufficiency implies a contribution margin for a risk-neutral retailer (red line) ranging from 17,000 EUR/day to 60,000 EUR/day with a 0%-indexed tariff, and from 24,000 EUR/day to 65,000 EUR/day with a 100%-indexed tariff. At 50% of self-sufficiency, these margins range from 20,000 EUR/day to 49,000 EUR/day with the 0%-indexed tariff, and from 30,000 EUR/day to 60,000 EUR/day with the 100%-indexed tariff. Same dynamics are observed in ECDFs under the high scenario (Fig.14), where however lower dispersion in the contribution margin is observed. Further evidence concerning the variability of the risk exposure of the retailer is provided in the bar plots in Fig.15 and Fig.16, which depict the contribution margin of the retailer

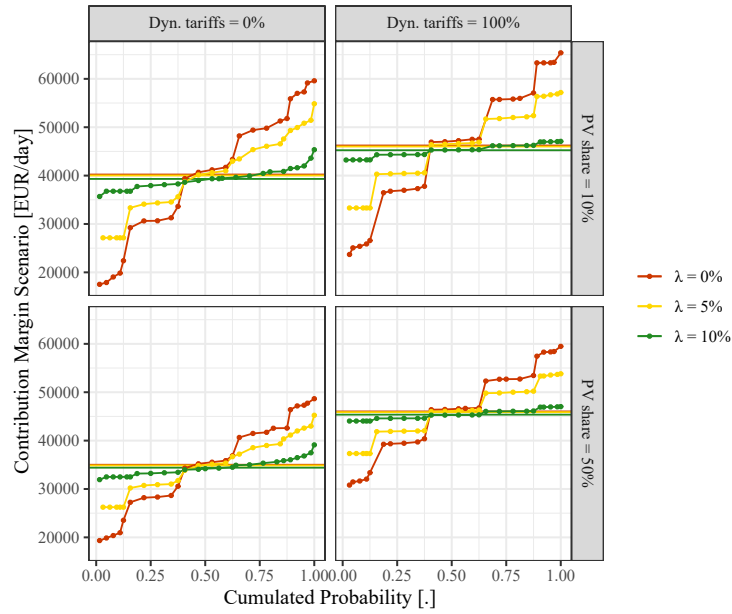


Figure 13: Empirical cumulative distribution functions of contribution margins for the summer working day: Low scenario

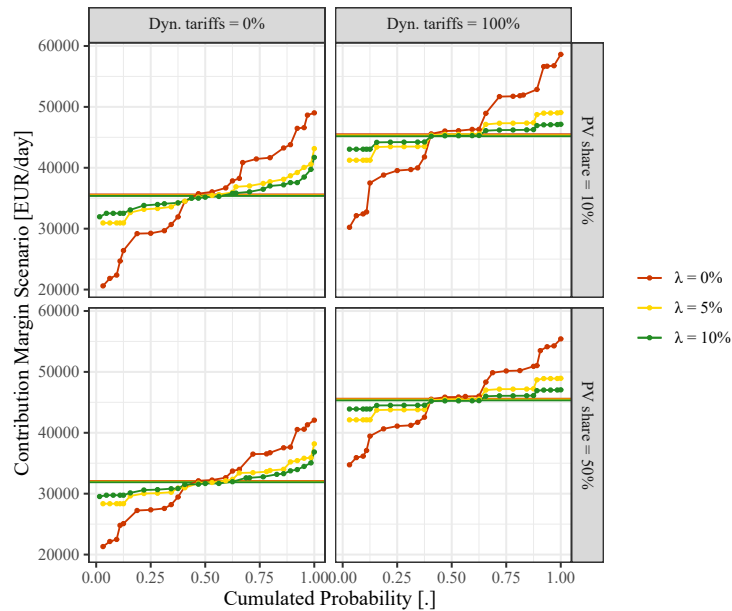


Figure 14: Empirical cumulative distribution functions of contribution margins for the summer working day: High scenario

across the five possible intraday realizations of the day-ahead node j_1 in the low and high scenarios, respectively. As mentioned above, the j_1 node represent the typical, i.e. expected summer working day in the low and high scenario. The charts point to a lower contribution margins across scenarios for 50% of solar PV self-generation when compared to 10% levels. Yet, variability across intraday realizations for a risk-neutral retailer ($\lambda = 0\%$) and with a 10% self-generation. This variability is clearly reduced for risk-averse retailers ($\lambda = 5\%$ and $\lambda = 10\%$, respectively). Contribution margins in the intraday market are higher and more dispersed in the low scenario with high solar PV generation, and with fixed tariffs (0% indexation). In contrast, dynamic tariffs (100% indexation) contribute towards higher and less volatile margins, particularly at 50% of self-generation ²¹. In all, these findings imply higher risk exposure in the intraday market for a risk-neutral retailer with static tariffs and increasing levels of solar PV generation and self-generation. Fig.17 depicts the retailer's efficient frontiers in the low (top charts) and high (bottom charts) scenarios for different levels of self-generation (10% and 50%) and with fixed (0% day-ahead price indexation) rather than highly dynamic (100% day-ahead price indexation) retail tariffs. These frontiers depict the highest expected contribution margin at each given level of risk (indicated by the corresponding CVaR), and risk preference λ . From the perspective of the risk-neutral retailer, in the leftmost end of the curves, greater risk exposure is observed for increasing levels of self-generation. In the low scenario and with a static retail tariff (i.e. Dyn. tariff=0%), for comparable CVaR values (18,500-19,000 EUR/day) the retailer's expected contribution margin diminishes from around 40,000 EUR/day at 10% of self-generation to around 35,000 EUR/day at 50% of self-generation. In the high scenario, the expected lost contribution margin amount to around 11,000 EUR/day, i.e. from around 35,000 EUR/day at 10% of self-generation to roughly 26,000 EUR/day at 50% for CVaR values of approximately 19,000 EUR/day and 21,000 EUR/day. Yet, when considering more dynamic retail tariff, i.e. Dyn.Tariff=100%, the risk exposure of the risk-neutral appears to increase.

²¹It should be noted that due to lower levels of (residual) load, wholesale spot prices are typically below the yearly average in Summer. The dynamic indexation captures this seasonal variation. The fixed tariff scheme however is constant throughout the year, which implies higher specific contribution margins (EUR per served MWh) in Summer compared to Transition season and Winter. We refer to the Appendix for results on the transition and Winter season with higher wholesale spot prices.

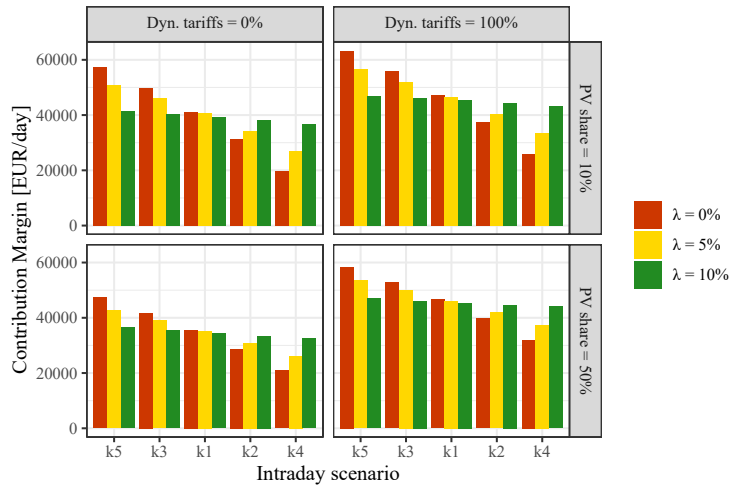


Figure 15: Retailer's contribution margin variability in the intraday market: Low scenario

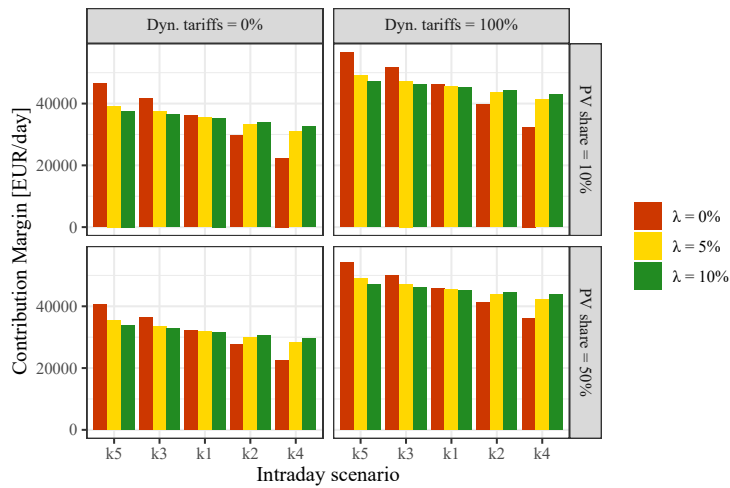


Figure 16: Retailer's contribution margin variability in the intraday market: High scenario

This finding is intuitive as the price uncertainty has an influence on both the tariff revenues and the procurement costs. In the low scenario, the expected contribution margin remains almost constant to roughly 46,500 EUR/day for increasing levels of self-generation against CVaR values increasing from 24,000 EUR/day at 10% to 31,000 EUR/day at 50% of PV self-generation. A comparable effect is observed in the high scenario.

From the perspective of the most risk-averse retailer ($\lambda=10\%$ in the rightmost end of the curves), an increase in the risk exposure is also noticeable when considering a static retail tariff in the low scenario, the retailer's expected contribution margin reduces from around 39,5000 EUR/day at 10% of self-generation to around 35,500 EUR/day at 50% of self-generation for CVaR values of approximately 36,500 and 37,500 EUR/day. In contrast, in the high scenario, thus for lower levels of solar PV generation, the expected contribution margin increases of around 2,500 EUR/day, i.e. from around 35,000 EUR/day at 10% of self-generation to roughly 37,500 EUR/day at 50%, against a decrease in the CVaR of approximately 3,000 EUR/day (from 32,000 EUR/day at 10% of self-sufficiency to 29,000 EUR/day at 50%). When considering more dynamic retail tariff, i.e. Dyn.Tariff=100%, an expected contribution margin of approximately 45,500 EUR/day is observed in the low scenario against a CVaR value of 43,500 EUR/day at both 10% and 50% of self-generation. Similar values are observed in the high scenario. Therefore, with highly dynamic retail tariff assuming 100%-indexation of the energy rate to the day-ahead price, the risk exposure of the risk-averse retailer remains unchanged for increasing levels of self-generation, and this is consistent across different scenarios of solar PV generation. The implications of the results presented in this section are discussed in the next section.

6 Discussion

The comprehensive investigation above provides interesting insights to evaluate the risk optimization problem faced by the retailer with increasing levels of solar PV self-generation in the residential sector. While a higher volume-risk has been observed in previous research with greater

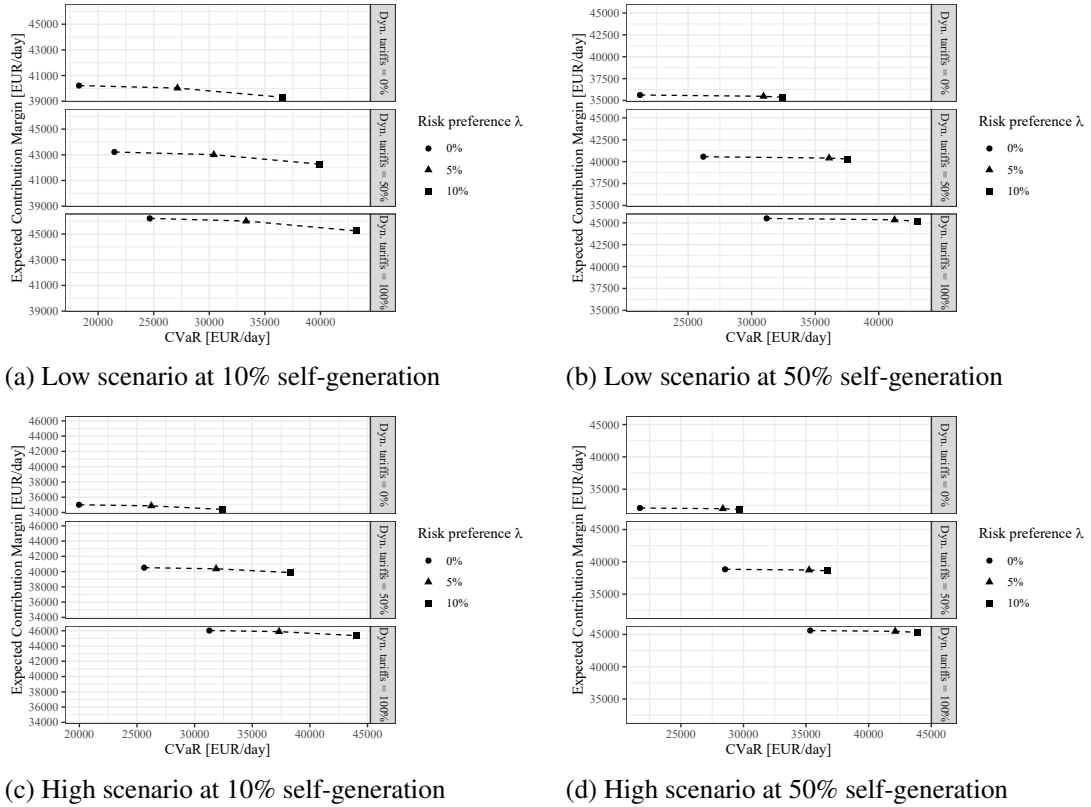


Figure 17: Efficient frontier of trading decisions for different risk preferences of the retailer

self-generation (Russo and Bertsch, 2020; Koolen et al., 2021), results in this study offer a broader understanding of the trading decision and risk optimization problem faced by the retailer in the day-ahead and intraday markets to adjust to this increasing short-term risk.

Results on the retailer's optimal trading strategy in Fig.9-Fig.12 imply that increasing PV self-generation, while affecting a risk-neutral retailer only marginally, has a significantly larger impact on a risk-averse retailer. The risk-neutral retailer remains exposed to the higher load uncertainty of the intraday market by preferring to take buying positions in the day-ahead market only for the solar-peak hours, i.e. when solar load uncertainty is greater and, in the high scenario, at the sunset, i.e. when the expected solar generation is lower and its expected uncertainty is also higher. This trading strategy remains unchanged despite changes in the retail tariff scheme and is consistent

with a risk-neutral retailer preferring to adjust the position on the intraday market, where prices are expected to be lower with high solar self-generation. Interestingly, we do not find evidence of selling positions in the day-ahead and intraday market, thus suggesting the preference of a risk-neutral retailer for adjusting the positions in the intraday market by buying at prices above the expected level rather than by selling at prices below the expected level. In contrast, we observe that the risk-averse retailer is more likely to increase the exposure in the day-ahead market to cope with the higher load uncertainty driven by the self-generation. In all, our results are in line with Kettunen et al. (2010) and Kraft et al. (2021). Yet, findings in this study also imply an increase in the day-ahead buying positions likewise in the intraday selling positions of the risk-averse retailer for higher levels of solar PV self-generation. We can therefore infer that a risk-averse retailer is more likely to accept buying in the day-ahead market and lower selling prices in the intraday market to reduce their load-risk exposure. We also highlight that trading strategies in the day-ahead and intraday markets are found to be driven by the retailer's risk preferences and by the levels of self-generation, which directly affect the retailer's load-risk exposure. Trading strategies are instead unaffected by the considered retail tariff schemes, and the presence or not of indexation to the day-ahead prices. However, such indexation is relevant when investigating the retailer revenue-risk exposure and their risk-management problem.

While the ECDFs in Fig.13 and Fig.14 unveil the adverse impact of increasing self-generation on the contribution margin of the retailer, they also point to the role of differently designed retail tariff schemes as hedging instrument for retailers exposed to increasing revenue-risk. While self-generation significantly reduces the expected contribution margin of the retailer, dynamic retail tariffs, with energy rates partially or fully indexed to the spot (day-ahead in this study) prices, may offset this reduction and potentially increase the expected margin of the retailer. The efficient frontiers in Fig.17, which are defined by the highest (i.e. non-dominated) expected contribution margins for 95%-CVaR for different risk attitudes, open the possibility for dynamic tariffs to allow a transfer of the load-risk from the retailer to the consumers thus preserving the expected contribution margin of the retailer. This is mostly evident for a risk-averse retailer by noticing that both

their expected contribution margin and 95%-CVaR remain unchanged for increasing levels of self-generation with a dynamic tariff fully indexed to the day-ahead price, while in the case a risk-neutral retailer this tariff contributes to maintain the expected contribution margin unchanged against an increase of the 95%-CVaR. With a 0%-indexed tariff and for increasing levels of self-generation, we observe both an increase in the 95%-CVaR and a reduction of the expected contribution margin of the risk-neutral retailer, thus implying a significant increase of their revenue-risk exposure with self-generation compared to a risk-averse retailer.

7 Conclusions and Outlook

This paper investigates the risk management problem faced by electricity retailers in day-ahead and intraday markets following the uncertainty driven by increasing levels of solar PV self-generation in the residential sector. Compared to previous studies, we jointly model the solar generation, load and price stochasticities in the nested day-ahead and intraday markets, thus capturing the inherently correlated price and quantity uncertainties. We consider these uncertainties to assess the retailers' trading problem in a two-stage stochastic optimization model, which thus accounts for the risks rising from both uncertain prices and quantities. We mark a contribution in considering the retailers' multi-stage trading optimization and decision-making in the day-ahead and intraday market while explicitly incorporating solar generation, load and price risks. These move stochastically in path-dependent and correlated processes, such that the risk optimization is effectively carried out along the considered short-term trading horizon. Therefore, the approach in this study allows to draw valuable insights on the risk exposure and optimization of retailers procurement strategy with increasing levels of solar PV self-generation.

In all, the results of the risk optimization unveil greater load-risk exposure for retailers in the day-ahead market with higher levels of self-generation, as implied by an increase of the buying positions in this market. The results also indicate a growth of the price-risk exposure in the intraday market, where an increase of selling positions is observed for lower and more volatile intraday

prices. These dynamics become even more evident when considering a risk-averse rather than a risk-neutral retailer, thus highlighting the importance of risk preferences when evaluating retailers' optimal trading strategies. Our findings imply a reduction of the retailer's expected contribution margin of 10% on a typical summer working day when assuming an increase of self-generation in the residential sector from 10% to 50%. Yet, findings also imply that this reduction can be offset when assuming more dynamic and spot-indexed retail tariffs, which allow a risk-averse retailer to transfer load and price risks to the consumers. While this outcome may rely on the assumed inelasticity of the households' electricity demand to wholesale spot prices, thus representing a limitation of this study, nonetheless our findings are of particular interest for practitioners, policymakers and regulators. First, they highlight the role of intraday trading to cope with the increasing short-term uncertainty driven by the penetration of distributed (variable) generation and consumers' engagement. Therefore, our findings contribute towards a better understanding of the importance of well-functioning and liquid intraday markets for the profitability and risk-mitigation costs of retailers. Second, in emphasizing the importance of intraday trading adjustment for retailers, findings in this study also point to the need for different hedging approaches to mitigate the greater risk-exposure implicit in more prosumer-oriented electricity markets. In particular, our results unveil the potential for electricity tariffs, which are indexed to the spot price, to induce retailer-consumer/prosumer risk sharing. Whereas this outcome relies on the German market considered in this study, and does not account for price (in)elasticities in retail markets and/or for the efficiency and costs of such spot-indexed tariffs, it represents a contribution in a still under-researched question concerning the optimal design of the retailer-prosumer relationship. This question is relevant for practitioners, policymakers and regulators and further research is needed for considerations of risk exposure and sharing in evolving electricity markets.

References

- Abbaspourtorbati, F., Conejo, A. J., Wang, J., and Cherkaoui, R. (2016). Three-or two-stage stochastic market-clearing algorithm? *IEEE Transactions on Power Systems*, 32(4):3099–3110.
- Aïd, R., Chemla, G., Porchet, A., and Touzi, N. (2011). Hedging and vertical integration in electricity markets. *Management Science*, 57(8): 1438–1452.
- Alexander, C. (2008). *Value-at-risk models*. John Wiley & Sons.
- Bacher, P., Madsen, H., and Nielsen, H. A. (2009). Online short-term solar power forecasting. *Solar energy*, 83(10):1772–1783.
- Ballester, C. and Furió, D. (2015). Effects of renewables on the stylized facts of electricity prices. *Renewable and Sustainable Energy Reviews*, 52:1596–1609.
- Battle, C. (2013). *Electricity Retailing*. In: I. J. Pérez-Arriaga (ed.), Regulation of the Power Sector, Power Systems, Springer-Verlag London 2013, p. 443-499.
- BDEW (2021). Standardlastprofile strom (standard load profile electricity).
- Ben-Tal, A., El Ghaoui, L., and Nemirovski, A. (2009). *Robust optimization*. Princeton university press.
- Benth, F. E. and Ibrahim, N. A. (2017). Stochastic modeling of photovoltaic power generation and electricity prices. *Journal of Energy Markets*, 10(3): 1–33.
- Bertsimas, D., Brown, D. B., and Caramanis, C. (2011). Theory and applications of robust optimization. *SIAM review*, 53(3):464–501.
- Boffino, L., Conejo, A. J., Sioshansi, R., and Oggioni, G. (2019). A two-stage stochastic optimization planning framework to decarbonize deeply electric power systems. *Energy Economics*, 84:104457.

-
- Boroumand, R.-H., Goutte, S., Guesmi, K., and Porcher, T. (2019). Potential benefits of optimal intra-day electricity hedging for the environment: The perspective of electricity retailers. *Energy Policy*, 132:1120–1129.
- Boroumand, R. H., Goutte, S., Porcher, S., and Porcher, T. (2015). Hedging strategies in energy markets: The case of electricity retailers. *Energy Economics*, 51: 503–509.
- Boroumand, R. H. and Zachmann, G. (2012). Retailers' risk management and vertical arrangements in electricity markets. *Energy Policy*, 40: 465–472.
- Bundesministerium für Wirtschaft und Energie (2021). Gesetz für den ausbau erneuerbarer energien. http://www.bgbl.de/xaver/bgbl/start.xav?startbk=Bundesanzeiger_BGB1&jumpTo=bgbl120s3138.pdf.
- Bunn, D. W., Gianfreda, A., and Kermer, S. (2018). A trading-based evaluation of density forecasts in a real-time electricity market. *Energies*, 11(10):2658.
- Burger, M., Klar, B., Müller, A., and Schindlmayr, G. (2004). A spot market model for pricing derivatives in electricity markets. *Quantitative Finance*, 4(1): 109–122.
- Christensen, T., Hurn, S., and Lindsay, K. (2009). It never rains but it pours: modeling the persistence of spikes in electricity prices. *The Energy Journal*, 30(1).
- Conejo, A. J., Carrión, M., Morales, J. M., et al. (2010). *Decision making under uncertainty in electricity markets*, volume 1. Springer.
- Coulon, M., Powell, W. B., and Sircar, R. (2013). A model for hedging load and price risk in the Texas electricity market. *Energy Economics*, 40: 976–988.
- Cretì, A. and Fontini, F. (2019). *Economics of electricity: Markets, competition and rules*. Cambridge University Press.

- Dadashi, M., Haghifam, S., Zare, K., Haghifam, M.-R., and Abapour, M. (2020). Short-term scheduling of electricity retailers in the presence of demand response aggregators: A two-stage stochastic bi-level programming approach. *Energy*, 205:117926.
- Dagoumas, A. S., Koltsaklis, N. E., and Panapakidis, I. P. (2017). An integrated model for risk management in electricity trade. *Energy*, 124: 350–363.
- de Lagarde, C. M. and Lantz, F. (2018). How renewable production depresses electricity prices: Evidence from the german market. *Energy Policy*, 117:263–277.
- Deng, S.-J. and Oren, S. S. (2006). Electricity derivatives and risk management. *Energy*, 31(6-7): 940–953.
- Deng, T., Yan, W., Nojavan, S., and Jermisittiparsert, K. (2020). Risk evaluation and retail electricity pricing using downside risk constraints method. *Energy*, 192:116672.
- Di Cosmo, V. and Malaguzzi Valeri, L. (2018). Wind, storage, interconnection and the cost of electricity generation. *Energy Economics*, 69: 1–18.
- Ela, E., Milligan, M., Bloom, A., Cochran, J., Botterud, A., Townsend, A., and Levin, T. (2018). Overview of wholesale electricity markets. In *Electricity Markets with Increasing Levels of Renewable Generation: Structure, Operation, Agent-based Simulation, and Emerging Designs*, pages 3–21. Springer.
- Fett, D., Fraunholz, C., and Keles, D. (2021). Diffusion and system impact of residential battery storage under different regulatory settings.
- Fleten, S.-E. and Kristoffersen, T. K. (2007). Stochastic programming for optimizing bidding strategies of a nordic hydropower producer. *European Journal of Operational Research*, 181(2):916–928.
- Garnier, E. and Madlener, R. (2015). Balancing forecast errors in continuous-trade intraday markets. *Energy Systems*, 6(3):361–388.

-
- Gelabert, L., Labandeira, X., and Linares, P. (2011). An ex-post analysis of the effect of renewables and cogeneration on Spanish electricity prices. *Energy Economics*, 33: S59–S65.
- Gianfreda, A., Ravazzolo, F., and Rossini, L. (2020). Comparing the forecasting performances of linear models for electricity prices with high res penetration. *International Journal of Forecasting*, 36(3):974–986.
- Goodarzi, S., Perera, H. N., and Bunn, D. (2019). The impact of renewable energy forecast errors on imbalance volumes and electricity spot prices. *Energy Policy*, 134:110827.
- Green, R., Staffell, I., and Vasilakos, N. (2014). Divide and conquer? k -means clustering of demand data allows rapid and accurate simulations of the british electricity system. *IEEE Transactions on Engineering Management*, 61(2):251–260.
- Gröwe-Kuska, N., Kiwiel, K., Nowak, M., Römisch, W., and Wegner, I. (2000). Power management under uncertainty by lagrangian relaxation. In *Proceedings of the 6th International Conference Probabilistic Methods Applied to Power Systems PMAPS*, volume 2.
- Hain, M., Schermeyer, H., Uhrig-Homburg, M., and Fichtner, W. (2018). Managing renewable energy production risk. *Journal of banking & finance*, 97:1–19.
- Hayn, M., Zander, A., Fichtner, W., Nickel, S., and Bertsch, V. (2018). The impact of electricity tariffs on residential demand side flexibility: results of bottom-up load profile modeling. *Energy Systems*, 9(3):759–792.
- Heitsch, H. and Römisch, W. (2009). Scenario tree modeling for multistage stochastic programs. *Mathematical Programming*, 118(2):371–406.
- IRENA (2019). Future of Solar Photovoltaic. International Renewable Energy Agency. November 2019.
- Jain, A. K. (2010). Data clustering: 50 years beyond k -means. *Pattern recognition letters*, 31(8):651–666.

- Janczura, J., Trück, S., Weron, R., and Wolff, R. (2013). Identifying spikes and seasonal components in electricity spot price data: A guide to robust modeling. *Energy Economics*, 38:96–110.
- Karanfil, F. and Li, Y. (2017). The role of continuous intraday electricity markets: The integration of large-share wind power generation in Denmark. *The Energy Journal*, 38(2): 107–130.
- Kath, C. and Ziel, F. (2018). The value of forecasts: Quantifying the economic gains of accurate quarter-hourly electricity price forecasts. *Energy Economics*, 76:411–423.
- Keles, D., Genoese, M., Möst, D., and Fichtner, W. (2012). Comparison of extended mean-reversion and time series models for electricity spot price simulation considering negative prices. *Energy Economics*, 34(4): 1012–1032.
- Keles, D., Genoese, M., Möst, D., Ortlieb, S., and Fichtner, W. (2013). A combined modeling approach for wind power feed-in and electricity spot prices. *Energy Policy*, 59: 213–225.
- Kettunen, J., Salo, A., and Bunn, D. W. (2010). Optimization of electricity retailer’s contract portfolio subject to risk preferences. *IEEE Transactions on Power Systems*, 25(1): 117–128.
- Kiesel, R. and Paraschiv, F. (2017). Econometric analysis of 15-minute intraday electricity prices. *Energy Economics*, 64: 77–90.
- Koolen, D., Bunn, D., and Ketter, W. (2021). Renewable energy technologies and electricity forward market risks. *The Energy Journal*, 42(4).
- Kraft, E., Russo, M., Keles, D., and Bertsch, V. (2021). Stochastic optimization of trading strategies in sequential electricity markets.
- Kremer, M., Kiesel, R., and Paraschiv, F. (2020). An econometric model for intraday electricity trading. *Philosophical Transactions of the Royal Society A*, Forthcoming, page Available at <https://doi.org/10.2139/ssrn.3489214>.
- Kulakov, S. and Ziel, F. (2019). The impact of renewable energy forecasts on intraday electricity prices. Available at <https://arxiv.org/pdf/1903.09641.pdf>.

-
- Lahmiri, S. (2015). Comparing variational and empirical mode decomposition in forecasting day-ahead energy prices. *IEEE Systems Journal*, 11(3):1907–1910.
- Laur, A., Nieto-Martin, J., Bunn, D. W., and Vicente-Pastor, A. (2018). Optimal procurement of flexibility services within electricity distribution networks. *European Journal of Operational Research*.
- Laur, A., Nieto-Martin, J., Bunn, D. W., and Vicente-Pastor, A. (2020). Optimal procurement of flexibility services within electricity distribution networks. *European Journal of Operational Research*, 285(1):34–47.
- Li, W. and Paraschiv, F. (2021). Modelling the evolution of wind and solar power infeed forecasts. *Journal of Commodity Markets*, page 100189.
- Likas, A., Vlassis, N., and Verbeek, J. J. (2003). The global k-means clustering algorithm. *Pattern recognition*, 36(2):451–461.
- Lingohr, D. and Müller, G. (2019). Stochastic modeling of intraday photovoltaic power generation. *Energy Economics*, 81: 175–186.
- Maciejowska, K., Nitka, W., and Weron, T. (2019). Day-ahead vs. intraday—forecasting the price spread to maximize economic benefits. *Energies*, 12(4):631.
- MacQueen, J. et al. (1967). Some methods for classification and analysis of multivariate observations. In *Proceedings of the fifth Berkeley symposium on mathematical statistics and probability*, volume 1, pages 281–297. Oakland, CA, USA.
- Messner, J. W., Pinson, P., Browell, J., Bjerregård, M. B., and Schicker, I. (2020). Evaluation of wind power forecasts—an up-to-date view. *Wind Energy*, 23(6):1461–1481.
- Meucci, A. (2009). Review of statistical arbitrage, cointegration, and multivariate ornstein-uhlenbeck. *Cointegration, and Multivariate Ornstein-Uhlenbeck (May 14, 2009)*.

- Mohan, V., Singh, J. G., and Ongsakul, W. (2015). An efficient two stage stochastic optimal energy and reserve management in a microgrid. *Applied energy*, 160:28–38.
- Morales, J. M., Zugno, M., Pineda, S., and Pinson, P. (2014). Electricity market clearing with improved scheduling of stochastic production. *European Journal of Operational Research*, 235(3):765–774.
- Narajewski, M. and Ziel, F. (2020a). Econometric modelling and forecasting of intraday electricity prices. *Journal of Commodity Markets*, 19:100107.
- Narajewski, M. and Ziel, F. (2020b). Ensemble forecasting for intraday electricity prices: Simulating trajectories. *Applied Energy*, 279:115801.
- Nazari-Heris, M. and Mohammadi-Ivatloo, B. (2018). Application of robust optimization method to power system problems. *Classical and recent aspects of power system optimization*, pages 19–32.
- Newbery, D., Pollitt, M., Ritz, R., and Strielkowski, W. (2018). Market design for a high-renewables European electricity system. *Renewable and Sustainable Energy Reviews*, 91: 695–707.
- Nojavan, S., Nourollahi, R., Pashaei-Didani, H., and Zare, K. (2019). Uncertainty-based electricity procurement by retailer using robust optimization approach in the presence of demand response exchange. *International Journal of Electrical Power & Energy Systems*, 105:237–248.
- Nojavan, S., Zare, K., and Mohammadi-Ivatloo, B. (2017). Robust bidding and offering strategies of electricity retailer under multi-tariff pricing. *Energy Economics*, 68:359–372.
- Osório, G., Lujano-Rojas, J., Matias, J., and Catalão, J. (2015). A new scenario generation-based method to solve the unit commitment problem with high penetration of renewable energies. *International Journal of Electrical Power & Energy Systems*, 64:1063–1072.

- Ottesen, S. Ø., Tomasgard, A., and Fleten, S.-E. (2018). Multi market bidding strategies for demand side flexibility aggregators in electricity markets. *Energy*, 149:120–134.
- Parisio, A., Del Vecchio, C., and Vaccaro, A. (2012). A robust optimization approach to energy hub management. *International Journal of Electrical Power & Energy Systems*, 42(1):98–104.
- Rintamäki, T., Siddiqui, A. S., and Salo, A. (2017). Does renewable energy generation decrease the volatility of electricity prices? an analysis of denmark and germany. *Energy Economics*, 62:270–282.
- Ruppert, M., Hayn, M., Bertsch, V., and Fichtner, W. (2016). Impact of residential electricity tariffs with variable energy prices on low voltage grids with photovoltaic generation. *International Journal of Electrical Power & Energy Systems*, 79: 161–171.
- Russo, M. and Bertsch, V. (2020). A looming revolution: Implications of self-generation for the risk exposure of retailers. *Energy Economics*, 92:104970.
- Ruszczynski, A. and Shapiro, A. (2003). Stochastic programming models. *Handbooks in operations research and management science*, 10:1–64.
- Schermeyer, H., Vergara, C., and Fichtner, W. (2018). Renewable energy curtailment: A case study on today's and tomorrow's congestion management. *Energy Policy*, 112: 427–436.
- Steinert, R. and Ziel, F. (2019). Short-to mid-term day-ahead electricity price forecasting using futures. *The Energy Journal*, 40(1).
- Uniejewski, B., Marcjasz, G., and Weron, R. (2019). Understanding intraday electricity markets: Variable selection and very short-term price forecasting using lasso. *International Journal of Forecasting*, 35(4):1533–1547.
- Van Der Weijde, A. H. and Hobbs, B. F. (2012). The economics of planning electricity transmission to accommodate renewables: Using two-stage optimisation to evaluate flexibility and the cost of disregarding uncertainty. *Energy Economics*, 34(6):2089–2101.

- Wallace, S. W. and Fleten, S.-E. (2003). Stochastic programming models in energy. *Handbooks in operations research and management science*, 10:637–677.
- Weron, R. (2007). *Modeling and forecasting electricity loads and prices: A statistical approach*. Wiley Finance Series, John Wiley & Sons Ltd.
- Willems, B. and Morbee, J. (2010). Market completeness: How options affect hedging and investments in the electricity sector. *Energy Economics*, 32(4): 786–795.
- Wozabal, D. and Rameseder, G. (2020). Optimal bidding of a virtual power plant on the spanish day-ahead and intraday market for electricity. *European Journal of Operational Research*, 280(2):639–655.
- Yang, J., Zhao, J., Luo, F., Wen, F., and Dong, Z. Y. (2017). Decision-making for electricity retailers: A brief survey. *IEEE Transactions on Smart Grid*, 9(5):4140–4153.
- Zellner, A. and Theil, H. (1992). Three-stage least squares: simultaneous estimation of simultaneous equations. In *Henri Theil's Contributions to Economics and Econometrics*, pages 147–178. Springer.
- Zhang, H., Hu, X., Cheng, H., Zhang, S., Hong, S., and Gu, Q. (2021). Coordinated scheduling of generators and tie lines in multi-area power systems under wind energy uncertainty. *Energy*, 222:119929.
- Zugno, M. and Conejo, A. J. (2015). A robust optimization approach to energy and reserve dispatch in electricity markets. *European Journal of Operational Research*, 247(2):659–671.

A Appendixes

A.1 Parameter estimates for the deterministic component of the day-ahead series

Table 9: Summer season

Summer	Cloudiness ^{DA}		Residual load ^{DA}		Price ^{DA}	
	Coeff.	Std.err.	Coeff.	Std.err.	Coeff.	Std.err.
Intercept			-0.623***	0.178		
Cloudiness _{t-1} ^{DA}	0.160***	0.013				
Cloudiness _{t-24} ^{DA}	0.601***	0.020				
Cloudiness _t ^{DA}			0.107***	0.027		
(Cloudiness _t ^{DA}) ²			0.114***	0.037		
(Cloudiness _t ^{DA}) ³			0.021*	0.012		
Residual load _t ^{DA}					0.161***	0.007
Residual load _{t-1} ^{DA}			0.882***	0.009	-0.138***	0.008
Price _{t-1} ^{DA}					1.009***	0.023
Price _{t-2} ^{DA}					-0.189***	0.019
Daily cycle ^{DA}	0.255***	0.024	0.179***	0.018	0.132***	0.010
Weekends					-0.002*	0.001
Daily cycle ^{DA} × Weekends			-0.005***	0.001		
Adjusted R-squared	0.873		0.945		0.942	
S.E. of regression	0.184		0.067		0.014	
Durbin-Watson stat	0.877		0.407		1.774	
Mean dependent var	-0.405		10.47		5.041	
S.D. dependent var	0.517		0.288		0.059	
Sum squared resid	49.52		6.628		0.292	

Table 10: Transition season

Transition season	Cloudiness ^{DA}		Residual load ^{DA}		Price ^{DA}	
	Coeff.	Std.err.	Coeff.	Std.err.	Coeff.	Std.err.
Intercept					0.354***	0.049
Cloudiness _{t-1} ^{DA}	0.147***	0.009				
Cloudiness _{t-24} ^{DA}	0.778***	0.013				
Cloudiness _t ^{DA}			0.218***	0.019		
(Cloudiness _t ^{DA}) ²			0.125***	0.009		
(Cloudiness _t ^{DA}) ³						
Residual load _t ^{DA}					0.197***	0.007
Residual load _{t-1} ^{DA}			0.935***	0.013	-0.154***	0.008
Price _{t-1} ^{DA}					0.874***	0.019
Price _{t-2} ^{DA}					-0.149***	0.019
Daily cycle ^{DA}	0.085***	0.014	0.013***	0.013	0.115***	0.010
Weekends					-0.003**	0.001
Daily cycle ^{DA} × Weekends			-0.002*	0.001		
Adjusted R-squared	0.871		0.760		0.952	
S.E. of regression	0.288		0.175		0.016	
Durbin-Watson stat	1.036		1.623		1.982	
Mean dependent var	-0.514		10.46		5.037	
S.D. dependent var	0.800		0.357		0.073	
Sum squared resid	178.4		65.76		0.559	

Table 11: Winter season

Winter	Cloudiness ^{DA}		Residual load ^{DA}		Price ^{DA}	
	Coeff.	Std.err.	Coeff.	Std.err.	Coeff.	Std.err.
Intercept			-0.580***	0.131	0.399205***	0.058
Cloudiness _{t-1} ^{DA}	0.100***	0.010				
Cloudiness _{t-24} ^{DA}	0.759***	0.014				
Cloudiness _t ^{DA}			0.268***	0.027		
(Cloudiness _t ^{DA}) ²			0.1501***	0.015		
(Cloudiness _t ^{DA}) ³						
Residual load _t ^{DA}					0.176***	0.007
Residual load _{t-1} ^{DA}			0.938***	0.007	-0.144***	0.007
Price _{t-1} ^{DA}					0.875***	0.021
Price _{t-2} ^{DA}					-0.071***	0.020
Daily cycle ^{DA}	0.147***	0.017	0.118***	0.014	0.049***	0.010
Weekends						
Daily cycle ^{DA} × Weekends			-0.005***	0.001	-0.001***	0.000
Adjusted R-squared	0.899		0.932		0.958	
S.E. of regression	0.261		0.135		0.022	
Durbin-Watson stat	0.807		0.739		1.993	
Mean dependent var	-0.538		10.27		4.979	
S.D. dependent var	0.819		0.520		0.106	
Sum squared resid	146.4		39.49		1.017	

A.2 Parameter estimates for the deterministic component of the intraday Series

Table 12: Cloudiness and residual load: Summer season

Summer	Cloudiness ^{ID}		Residual load ^{ID}	
	Coeff.	Std.error	Coeff.	Std.error
Intercept				
Cloudiness _t ^{DA}	0.987***	0.002		
Cloudiness _{t-1} ^{ID}	0.021***	0.002		
Cloudiness _t ^{ID}			0.002***	0.0003
Residual load _t ^{DA}			0.181***	0.005
Residual load _{t-1} ^{ID}			1.188***	0.014
Residual load _{t-2} ^{ID}			-0.096***	0.020
Residual load _{t-3} ^{ID}			-0.194***	0.020
Residual load _{t-4} ^{ID}			-0.089***	0.012
Daily cycle ^{ID}	-0.001*	0.001	0.010***	0.001
Weekends			0.172***	0.022
Daily cycle ^{ID} × Weekends			-0.017***	0.002
Adjusted R-squared	0.997		0.999	
S.E. of regression	0.031		0.010	
Durbin-Watson stat	0.166		1.690	
Mean dependent var	-0.398		10.47	
S.D. dependent var	0.521		0.284	
Sum squared resid	5.644		0.635	

Table 13: Cloudiness and residual load: Transition season

Transition season	Cloudiness ^{ID}		Residual load ^{ID}	
	Coeff.	Std.error	Coeff.	Std.error
Intercept				
Cloudiness _t ^{DA}	0.996***	0.001		
Cloudiness _{t-1} ^{ID}	0.021***	0.001		
Cloudiness _t ^{ID}			0.001***	0.0002
Residual load _t ^{DA}			0.132***	0.004
Residual load _{t-1} ^{ID}			1.333***	0.011
Residual load _{t-2} ^{ID}			-0.236***	0.018
Residual load _{t-3} ^{ID}			-0.133***	0.018
Residual load _{t-4} ^{ID}			-0.095***	0.010
Daily cycle ^{ID}	-0.001*	0.0004	-0.001**	0.0005
Weekends			0.110***	0.018
Daily cycle ^{ID} × Weekends			-0.011***	0.002
Adjusted R-squared	0.997		0.999	
S.E. of regression	0.043		0.012	
Durbin-Watson stat	0.605		1.799	
Mean dependent var	-0.524		10.45	
S.D. dependent var	0.857		0.365	
Sum squared resid	16.20		1.336	

Table 14: Cloudiness and residual load: Winter season

Winter	Cloudiness ^{ID}		Residual load ^{ID}	
	Coeff.	Std.error	Coeff.	Std.error
Intercept				
Cloudiness ^{DA} _t	0.984***	0.001		
Cloudiness ^{ID} _{t-1}	0.010***	0.002		
Cloudiness ^{ID} _t				
Residual load ^{DA} _t			0.148***	0.004
Residual load ^{ID} _{t-1}			1.059***	0.006
Residual load ^{ID} _{t-2}				
Residual load ^{ID} _{t-3}			-0.134***	0.013
Residual load ^{ID} _{t-4}			-0.084***	0.010
Daily cycle ^{ID}	-0.005***	0.001	0.010***	0.001
Weekends			0.120***	0.020
Daily cycle ^{ID} × Weekends			-0.012***	0.002
Adjusted R-squared	0.996		0.998	
S.E. of regression	0.050		0.023	
Durbin-Watson stat	0.240		1.578	
Mean dependent var	-0.538		10.28	
S.D. dependent var	0.837		0.504	
Sum squared resid	22.18		4.586	

Table 15: Δ price (ID3-DA)

	Summer		Transition season		Winter	
	Coeff.	Std.error	Coeff.	Std.error	Coeff.	Std.error
Intercept	-0.793***	0.060	0.518***	0.089	-0.692***	0.091
Δ Price _{t-1}	-0.700***	0.039	0.551***	0.017	0.495***	0.039
Δ Price _{t-2}	0.0223**	0.010	0.037***	0.012		
Δ Price _{t-3}	0.030***	0.010	0.020*	0.012		
Δ Price _{t-4}	0.371***	0.011	0.285***	0.016	0.450***	0.035
Price ^{DA} _t	-1.22***	0.042				
Price ^{ID3} _{t-1}	1.063***	0.043	-0.102***	0.014	-0.306***	0.041
Δ Residual load _{t-3} (Act. - ID)	0.037***	0.009	-0.205***	0.054	0.128***	0.030
Δ Cloudiness _{t-3} (Act. - ID)	0.002**	0.001	0.002**	0.001		
Daily cycle	0.317***	0.014	-0.09***	0.018	0.259***	0.018
Weekends	0.222**	0.111	-0.230*	0.152	0.421***	0.155
Daily cycle x weekends	-0.046**	0.022	0.045*	0.030	-0.085***	0.031
Adjusted R-squared	0.603		0.745		0.584	
S.E. of regression	0.032		0.057		0.052	
Durbin-Watson stat	1.639		1.831		1.643	
Mean dependent var	-0.001		-0.009		0.003	
S.D. dependent var	0.051		0.112		0.081	
Sum squared resid	6.075		27.87		23.96	

A.3 Scenario trees

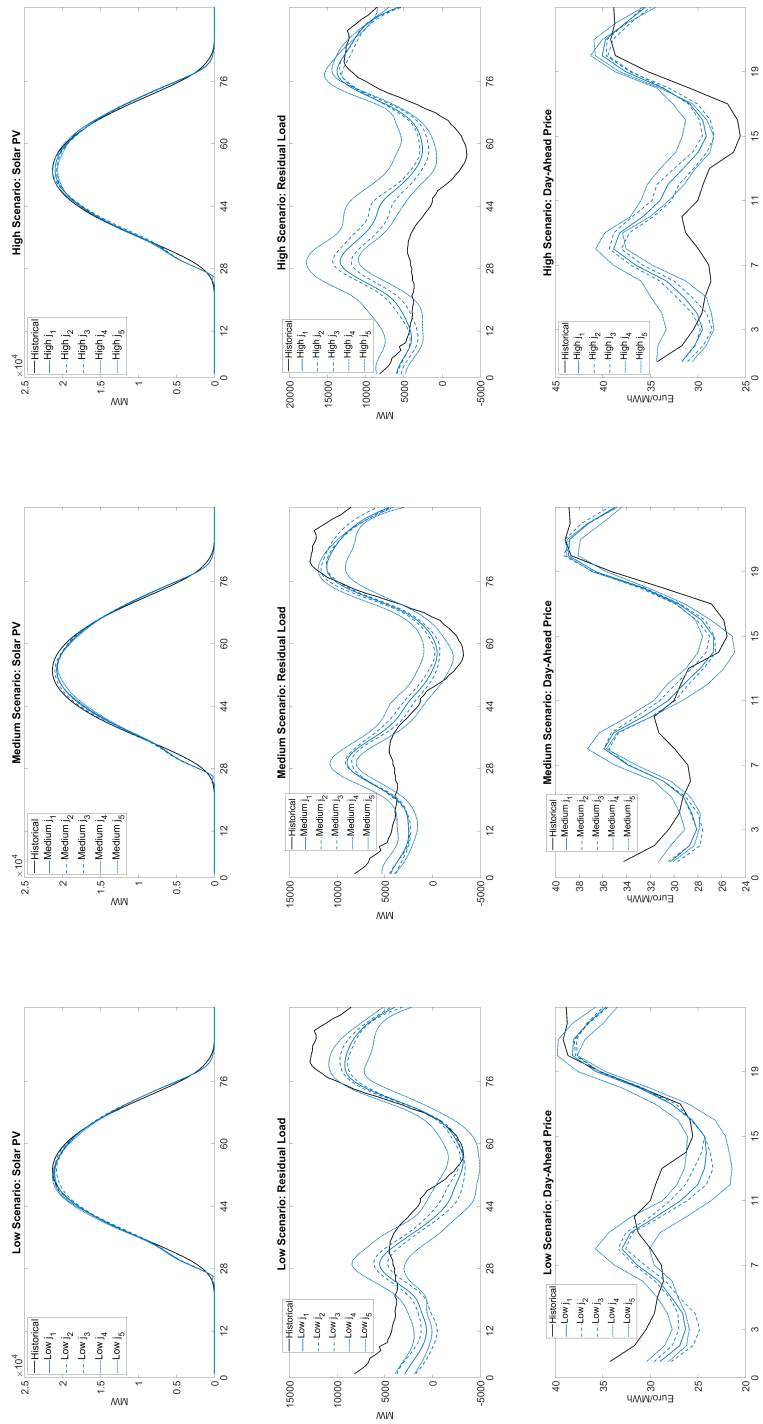


Figure 18: Historical and simulated day-ahead series: Summer weekend day

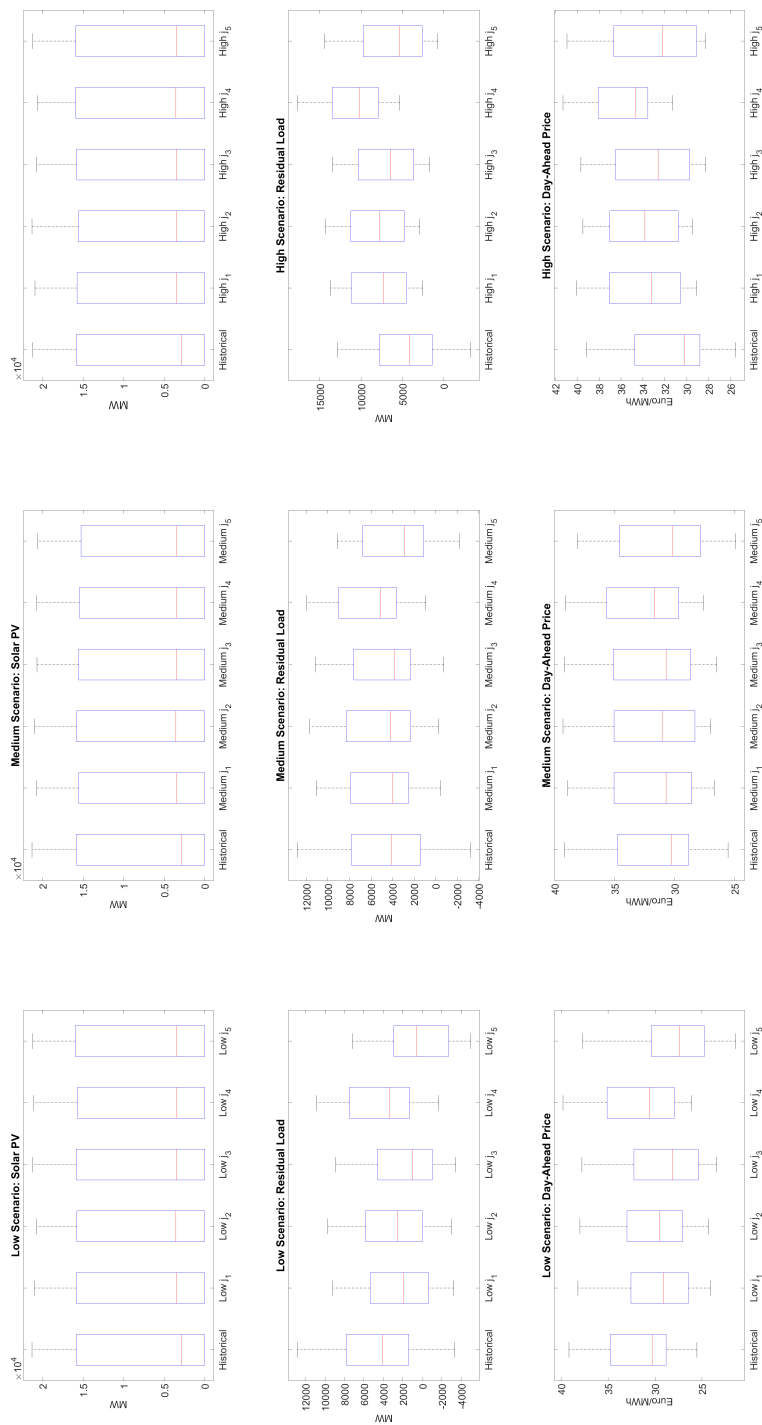


Figure 19: Distribution of the historical and simulated day-ahead series: Summer weekend day

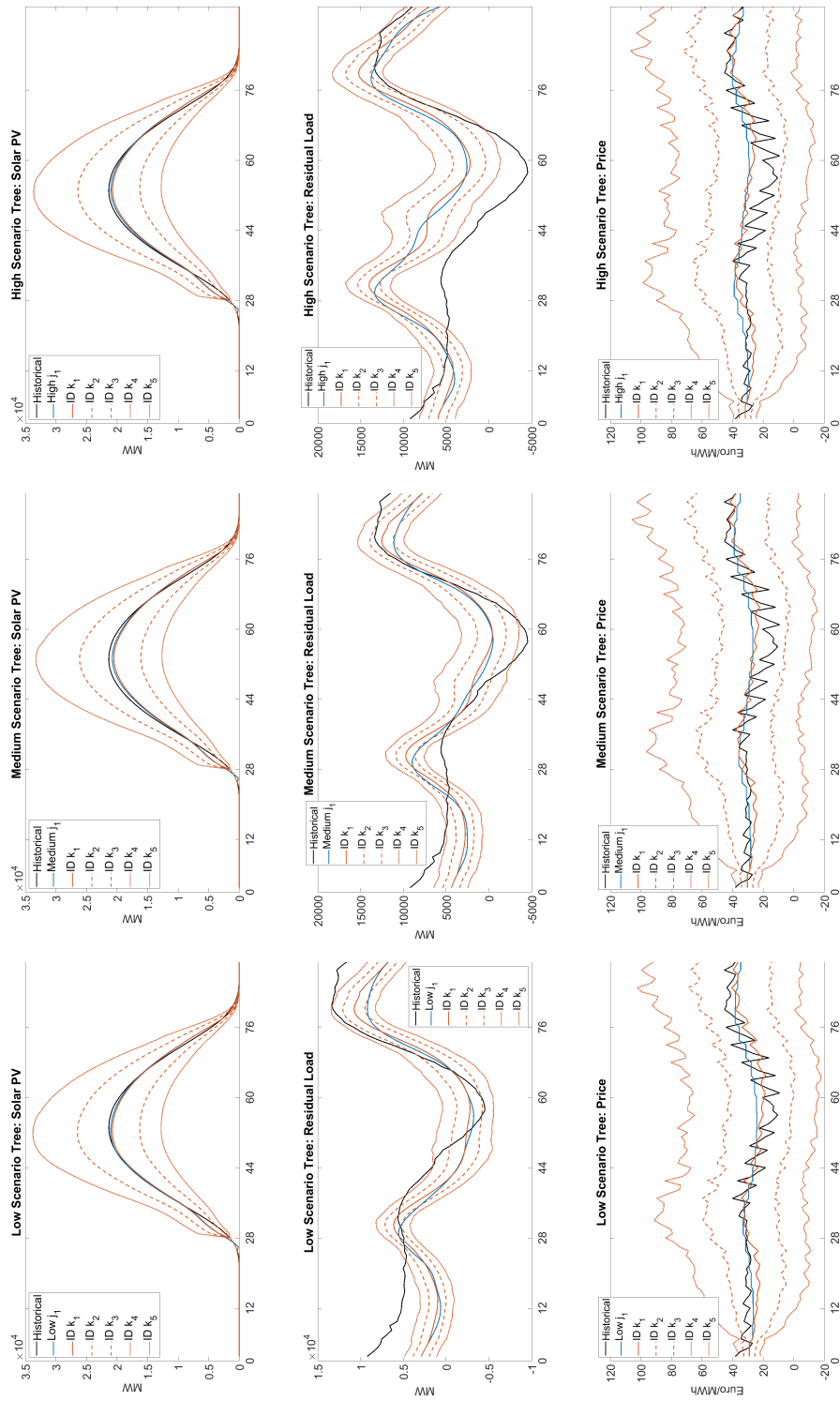


Figure 20: Scenario trees for the representative day-ahead node j_1 and its intraday realizations k : Summer weekend day

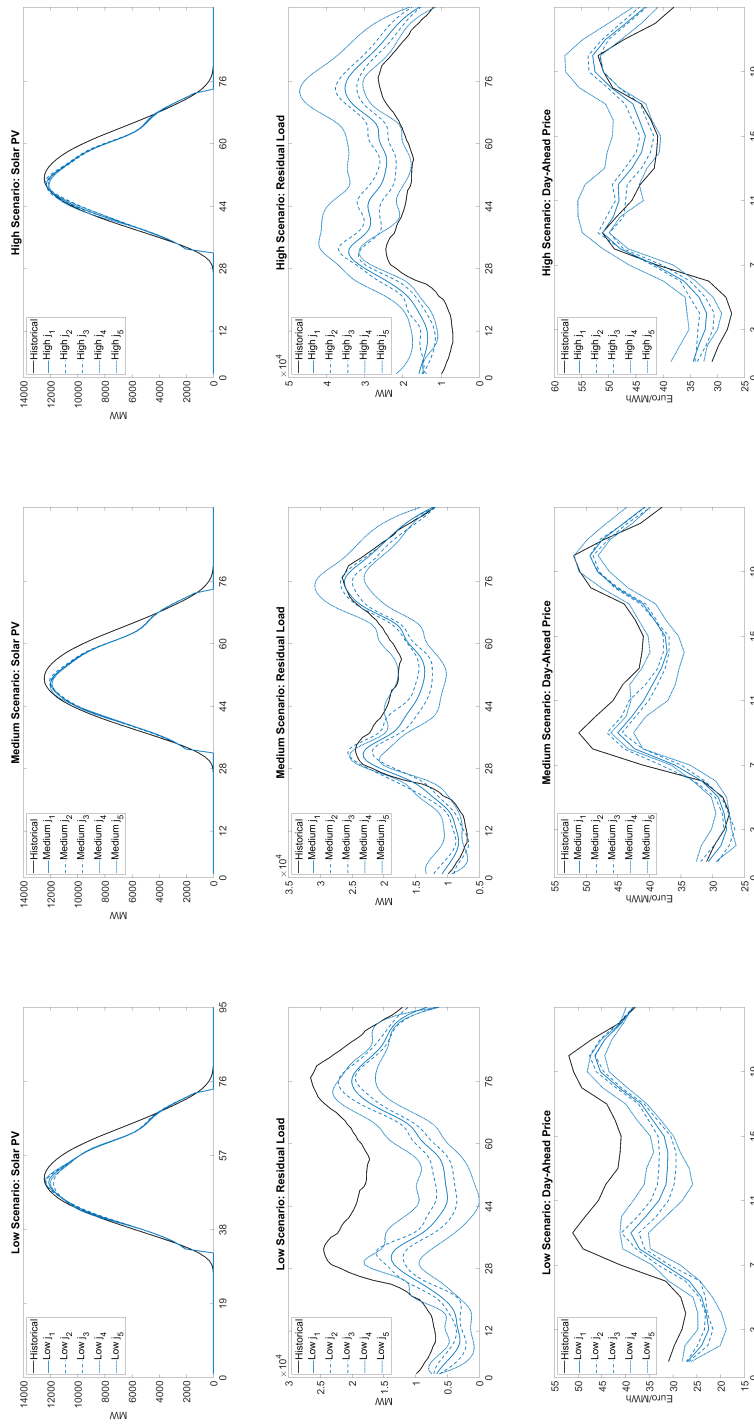


Figure 21: Historical and simulated day-ahead series: Transition season working day

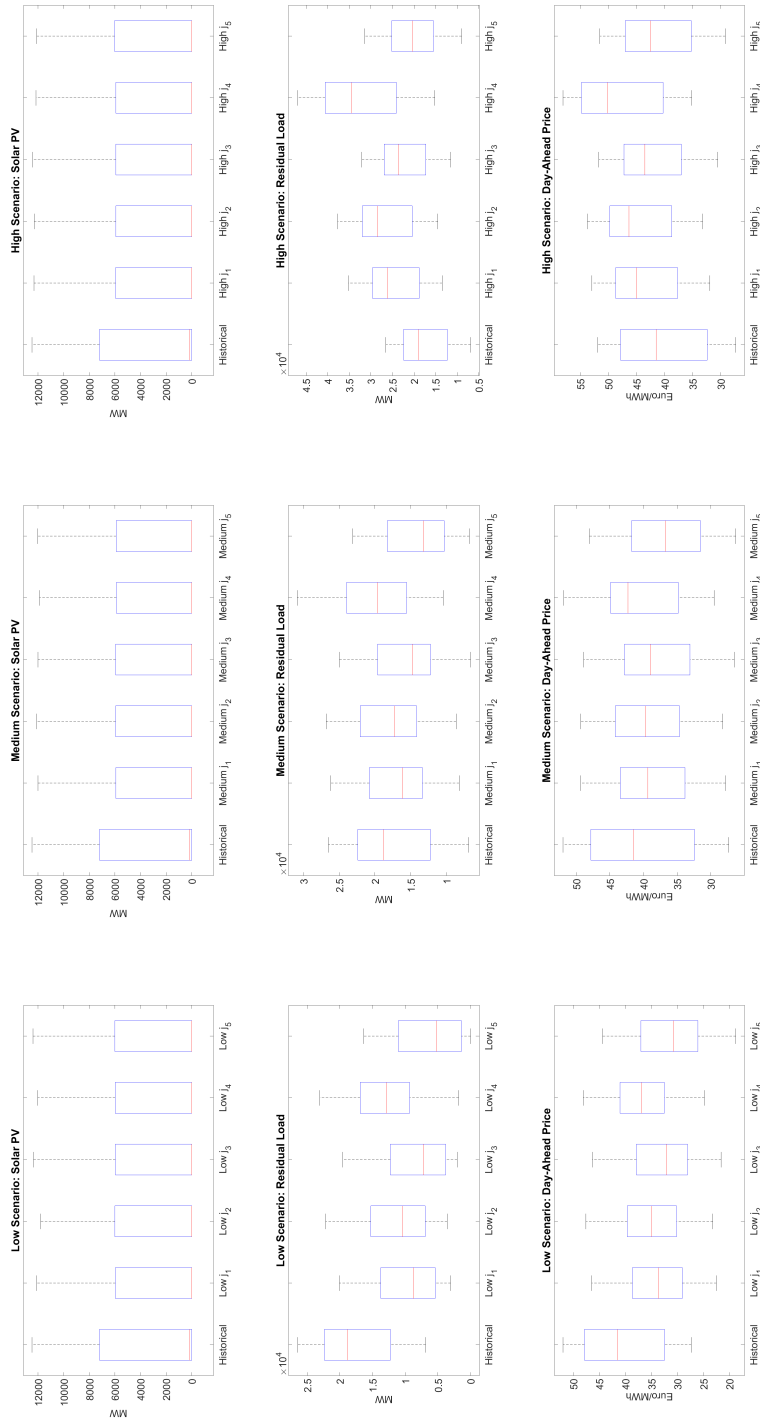


Figure 22: Distribution of the historical and simulated day-ahead series: Transition season working day

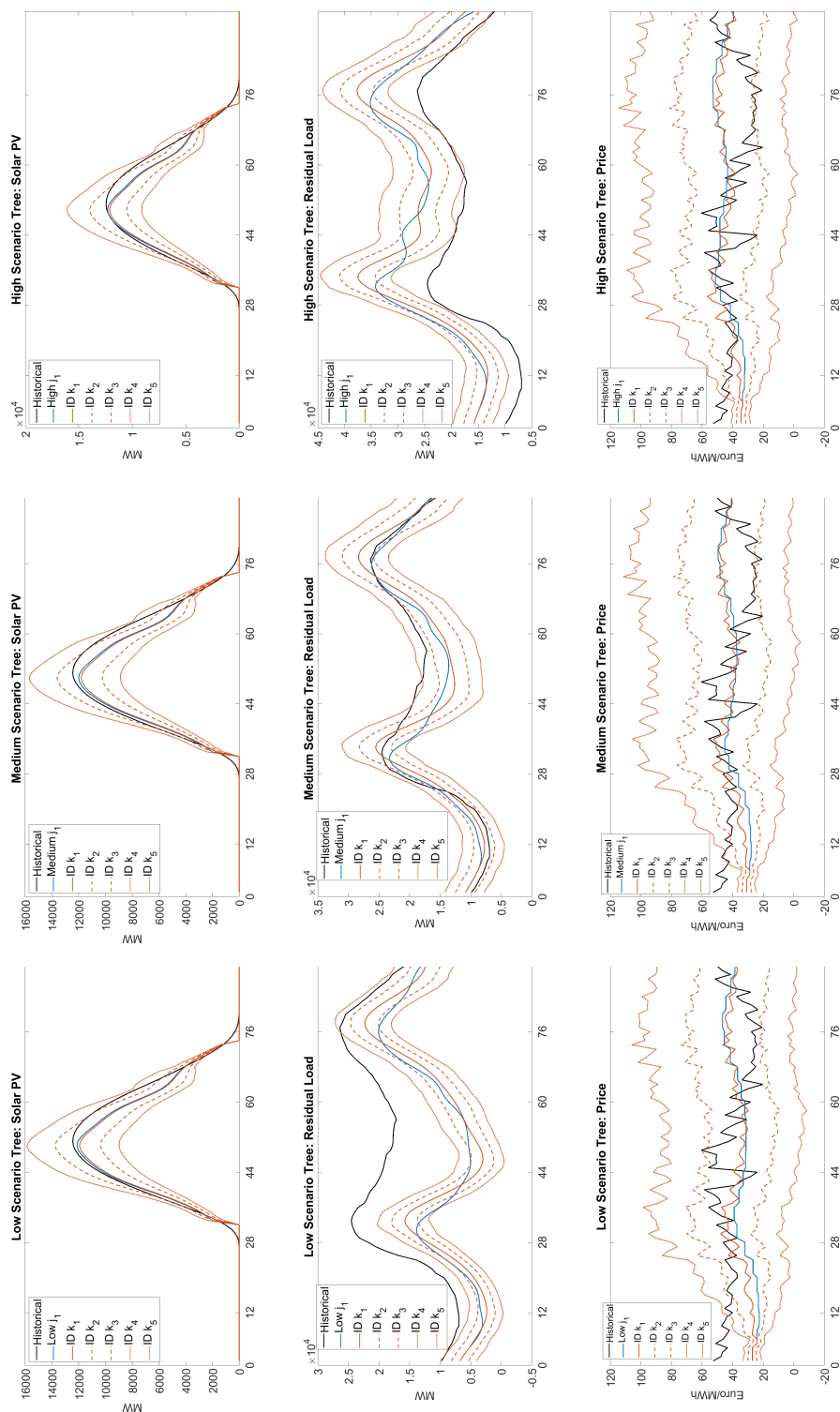


Figure 23: Scenario trees for the representative day-ahead node j_1 and its intraday realizations k : Transition season working day

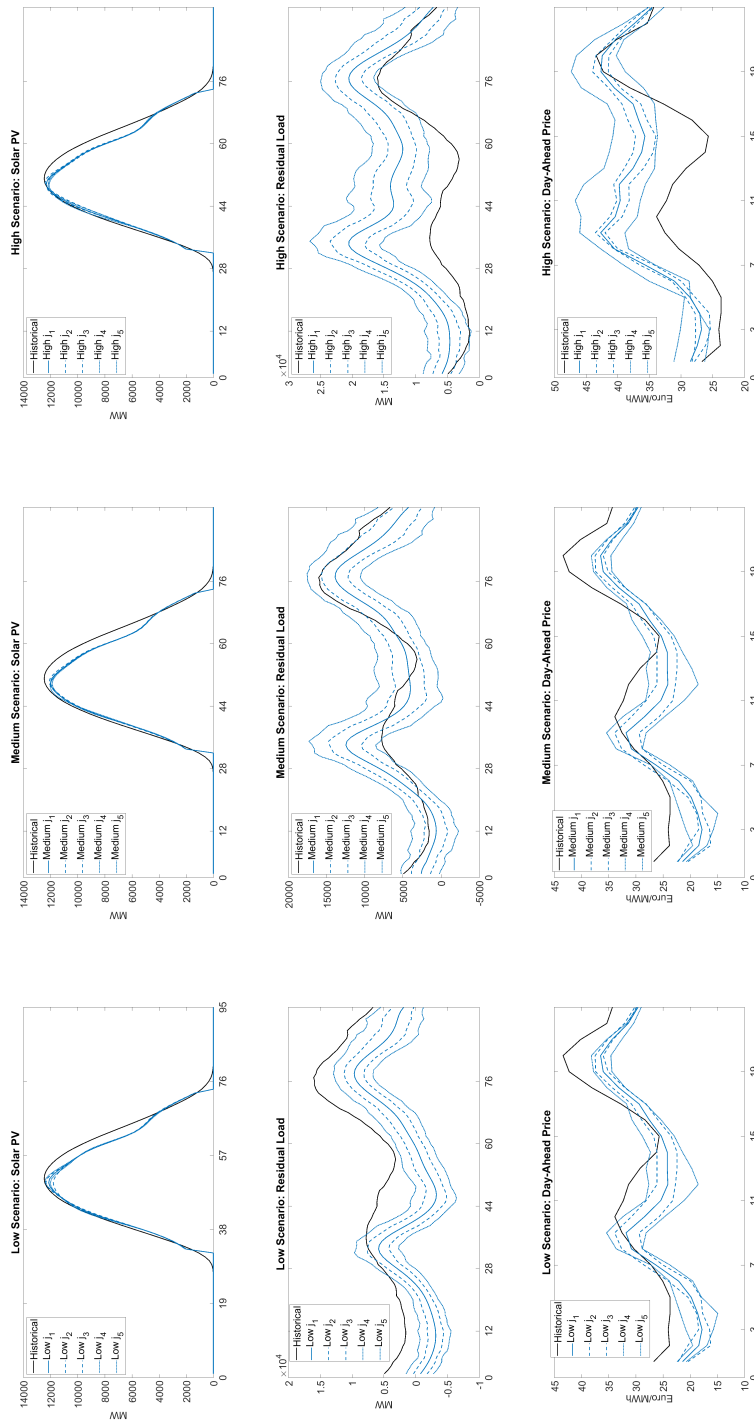


Figure 24: Historical and simulated day-ahead series: Transition season weekend day



Figure 25: Distribution of the historical and simulated day-ahead series: Transition season weekend day

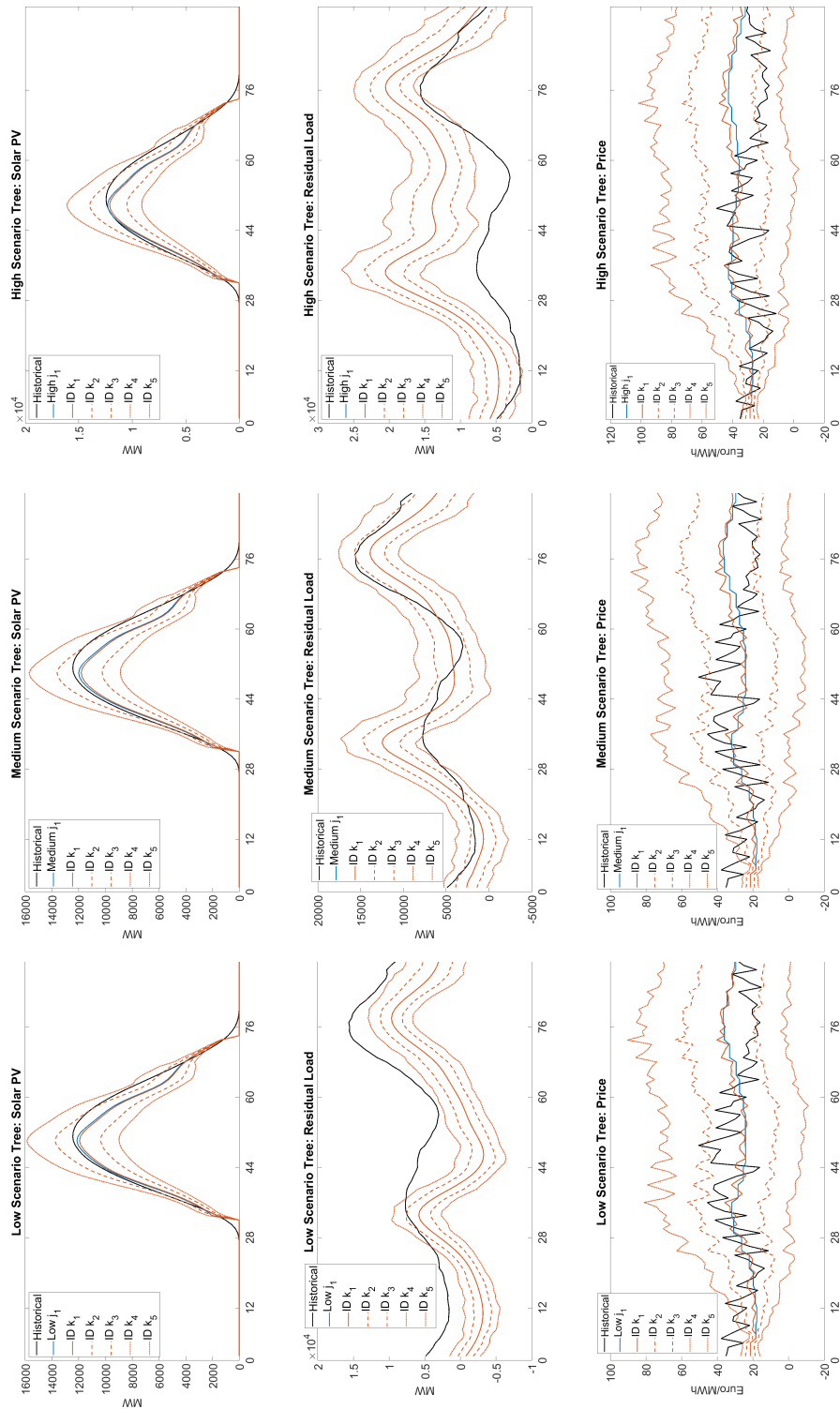


Figure 26: Scenario trees for the representative day-ahead node j_1 and its intraday realizations k : Transition season weekend day

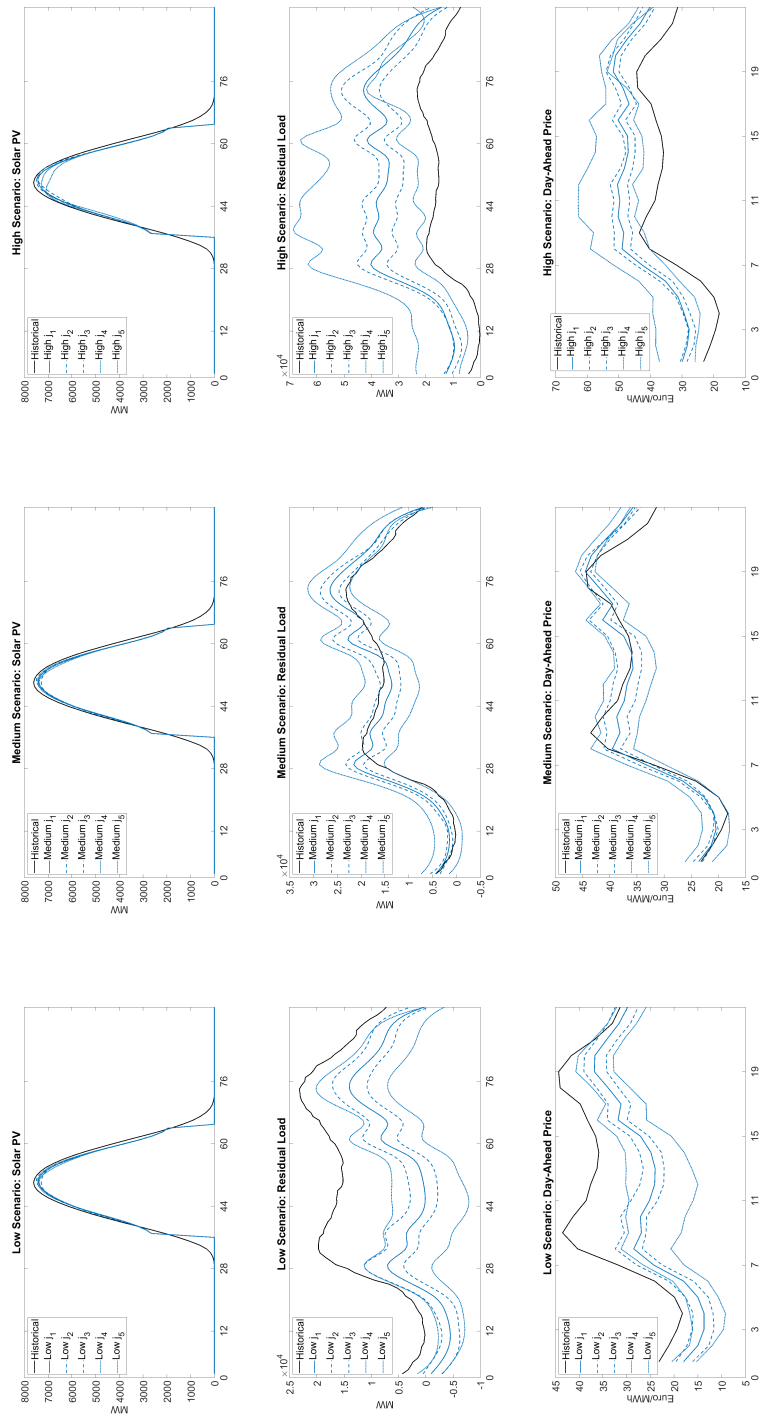


Figure 27: Historical and simulated day-ahead series: Winter working day

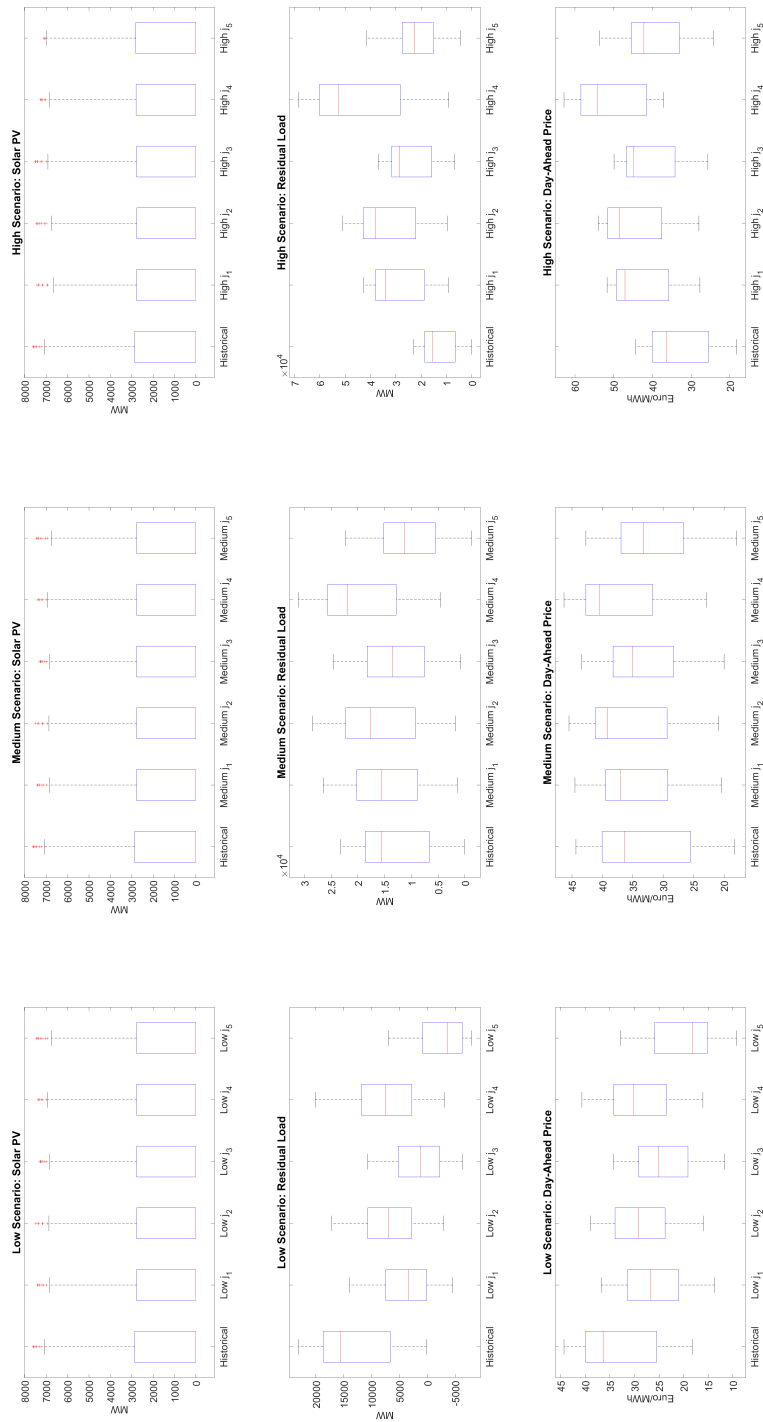


Figure 28: Distribution of the historical and simulated day-ahead series: Winter working day

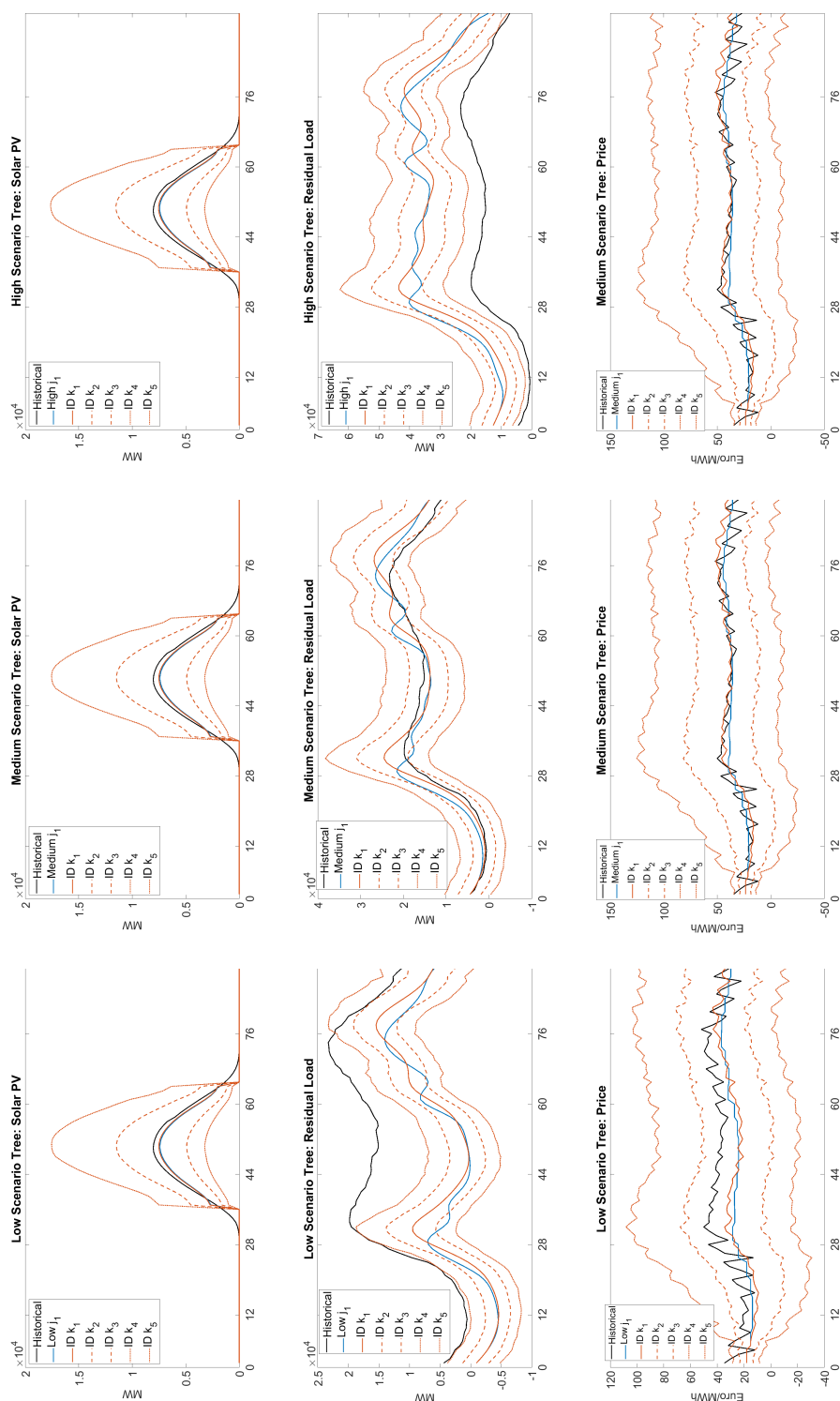


Figure 29: Scenario trees for the representative day-ahead node j_1 and its intraday realizations k : Winter working day

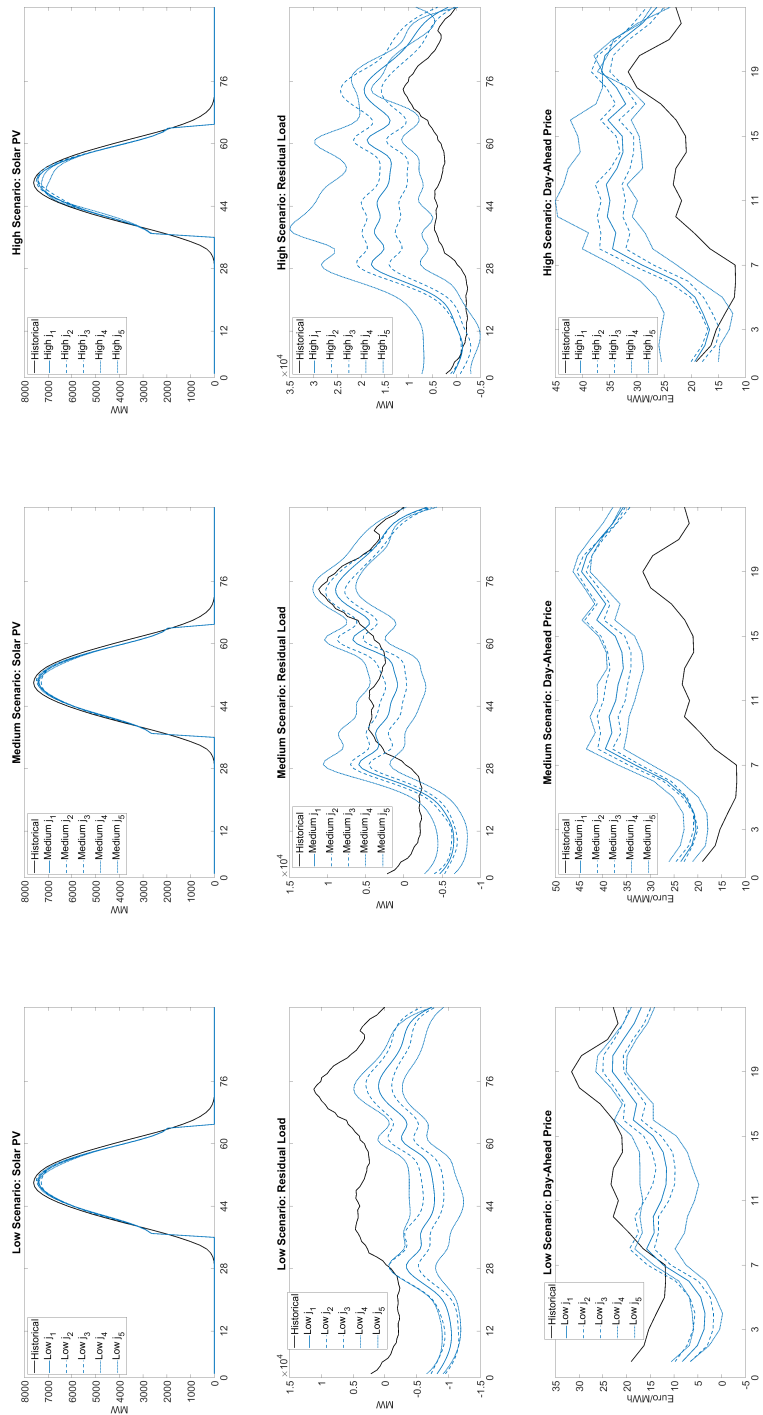


Figure 30: Historical and simulated day-ahead series: Winter weekend day

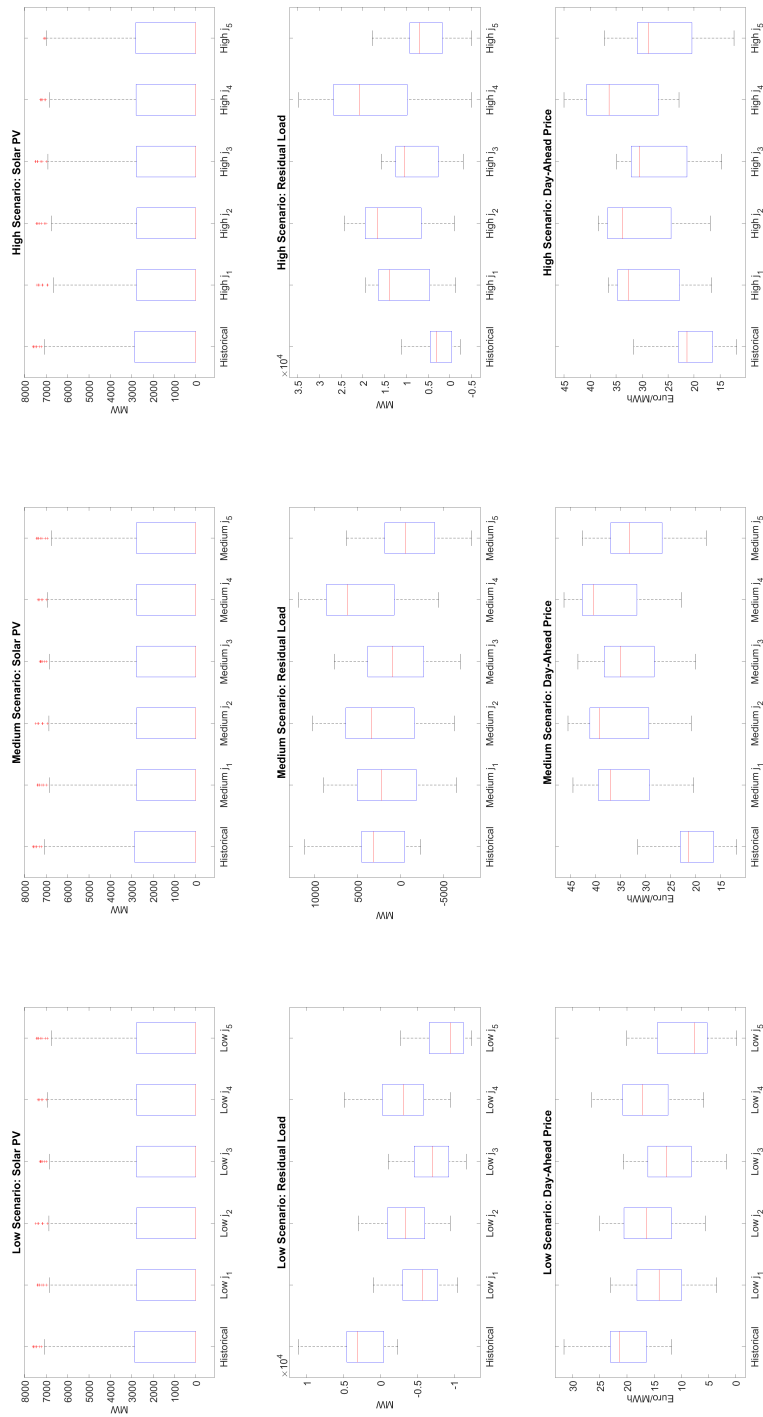


Figure 31: Distribution of the historical and simulated day-ahead series: Winter weekend day

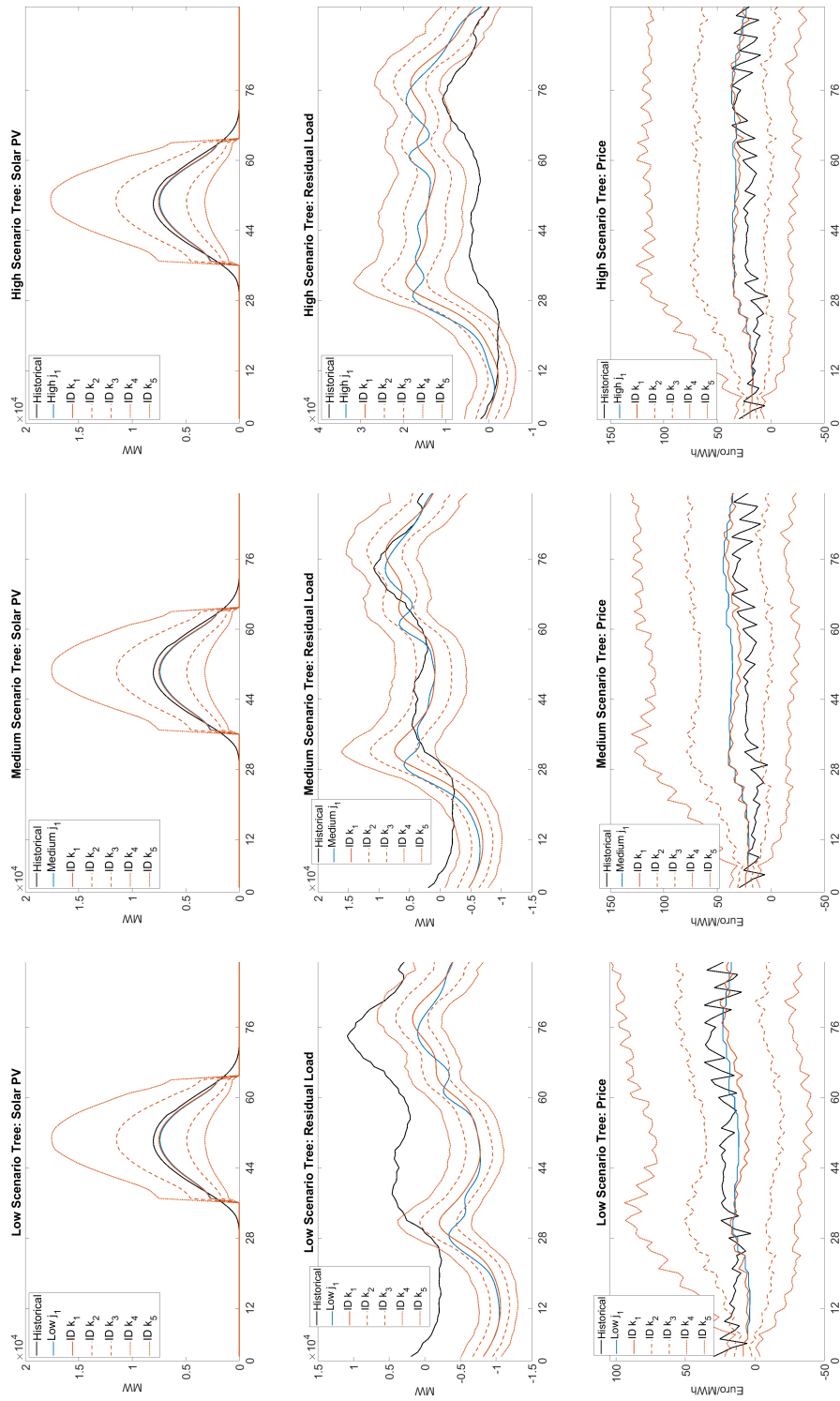


Figure 32: Scenario trees for the representative day-ahead node j_1 and its intraday realizations k : Winter weekend day

A.4 Retailer's trading strategies with increasing solar PV self-generation

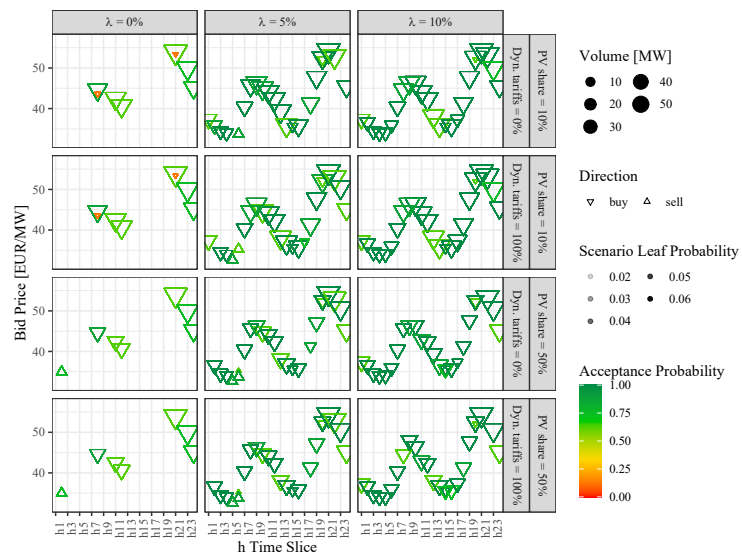


Figure 33: Retailer's day-ahead trading strategy in the summer working day: Medium scenario

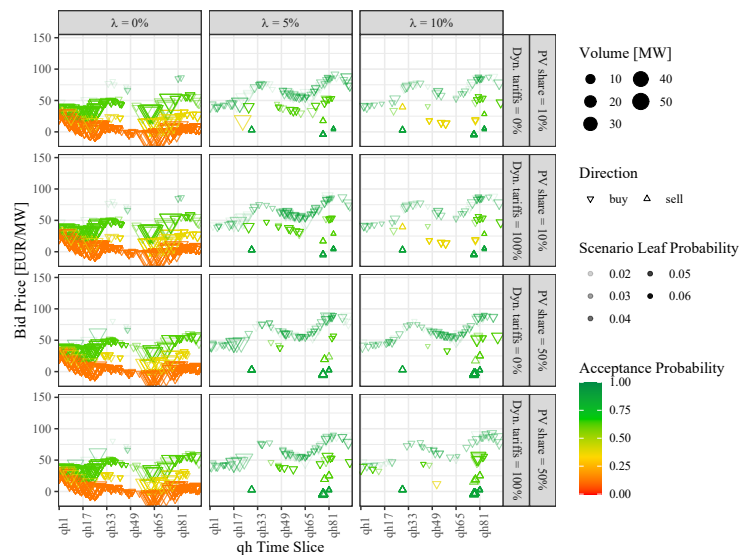


Figure 34: Retailer's intraday trading strategy in the summer working day: Medium scenario

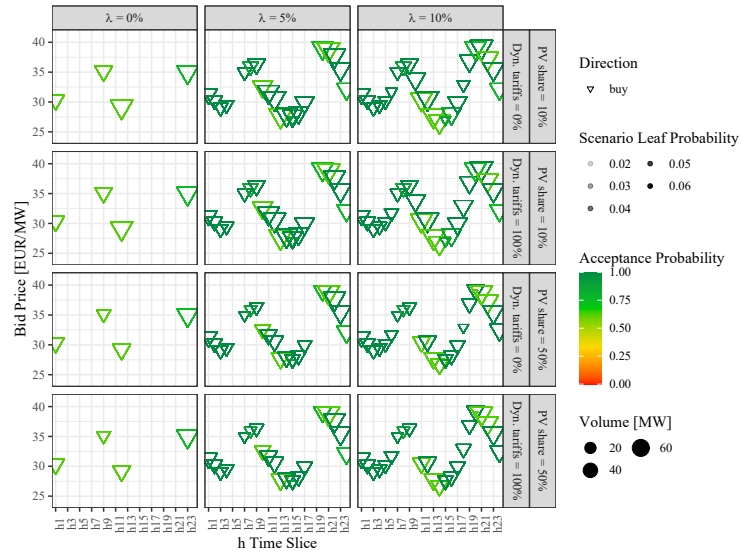


Figure 35: Retailer's day-ahead trading strategy in the summer weekend day: Medium scenario

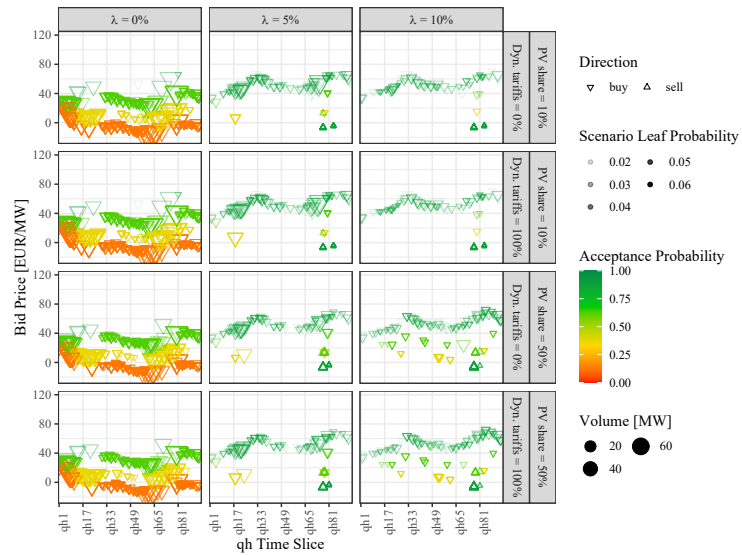


Figure 36: Retailer's intraday trading strategy in the summer weekend day: Medium scenario

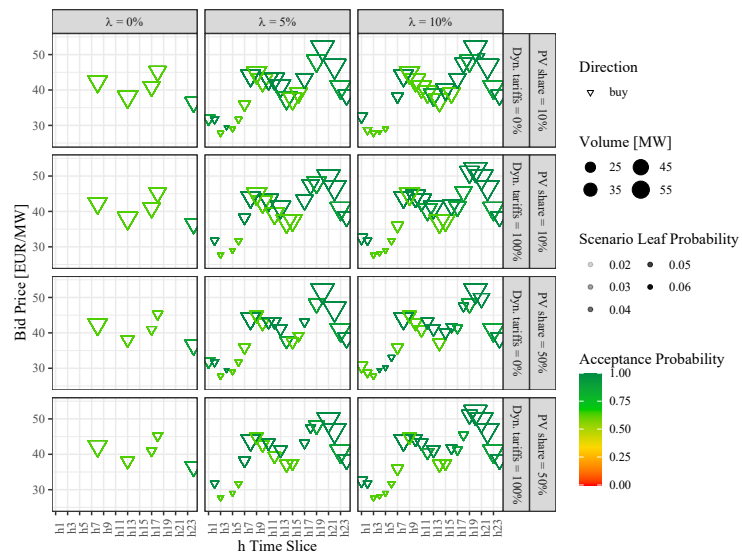


Figure 37: Retailer's day-ahead trading strategy in the transition season working day: Medium scenario

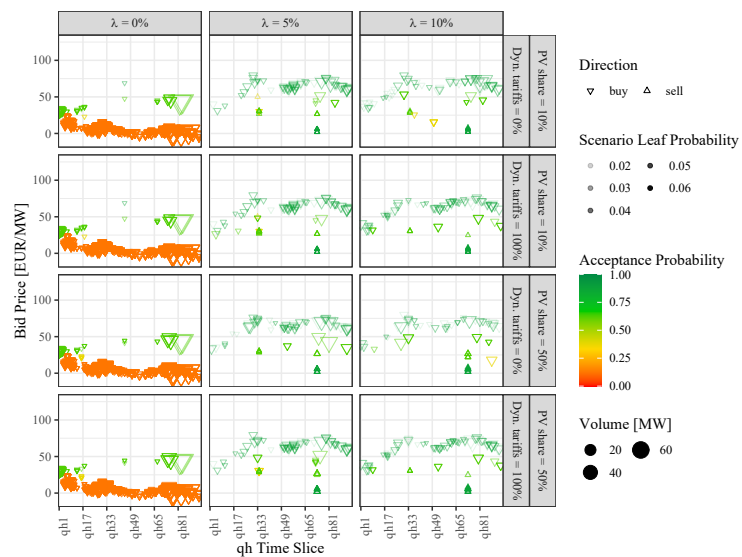


Figure 38: Retailer's intraday trading strategy in the transition season working day: Medium scenario

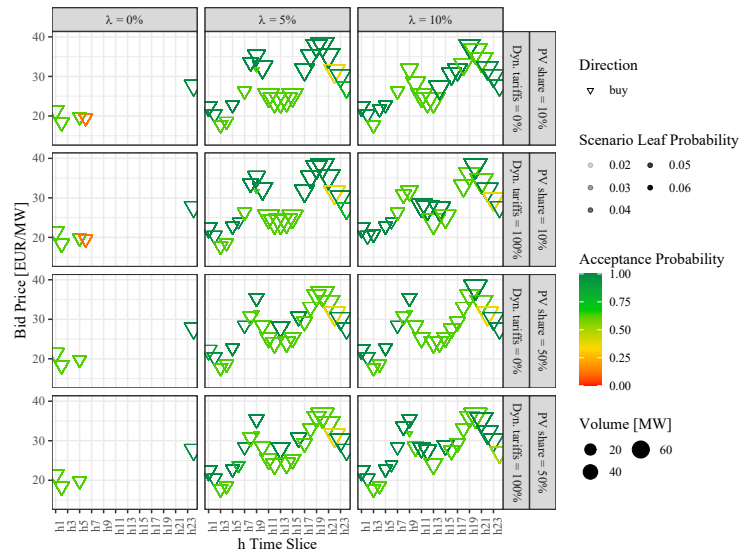


Figure 39: Retailer's day-ahead trading strategy in the transition season weekend day: Medium scenario

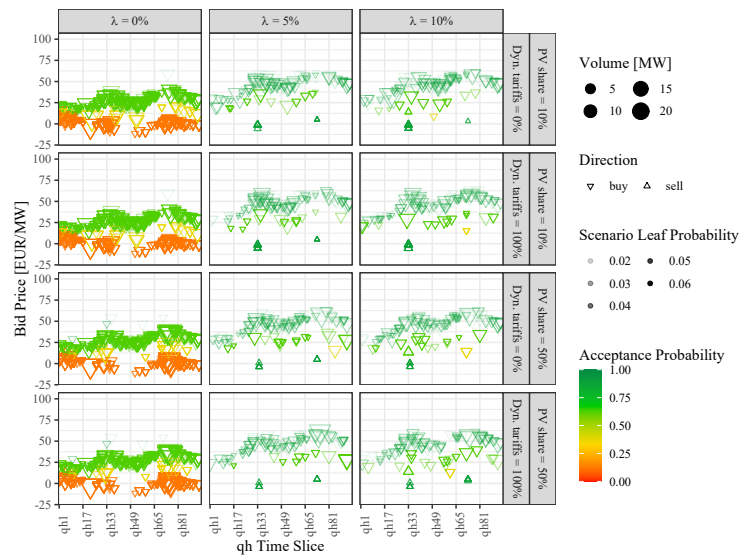


Figure 40: Retailer's intraday trading strategy in the transition season weekend day: Medium scenario

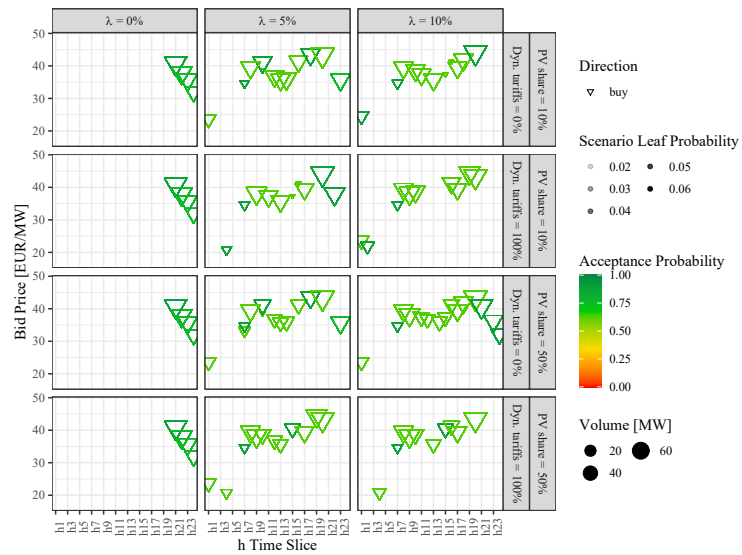


Figure 41: Retailer's day-ahead trading strategy in the winter season working day: Medium scenario

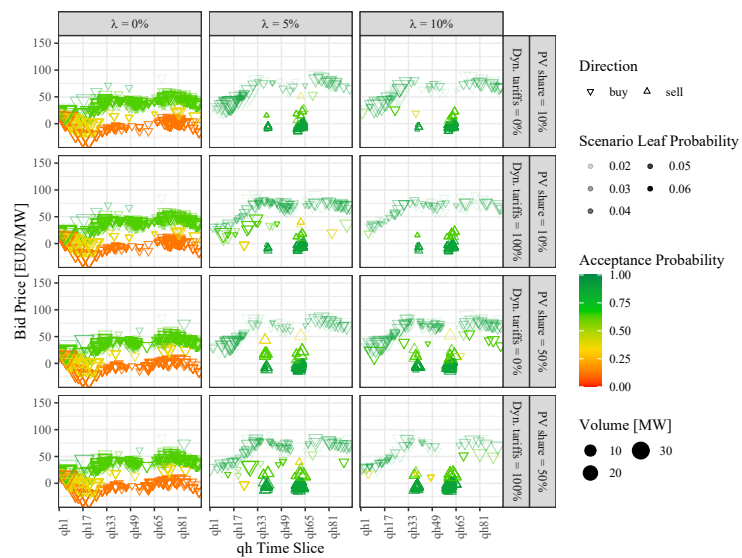


Figure 42: Retailer's intraday trading strategy in the winter season working day: Medium scenario

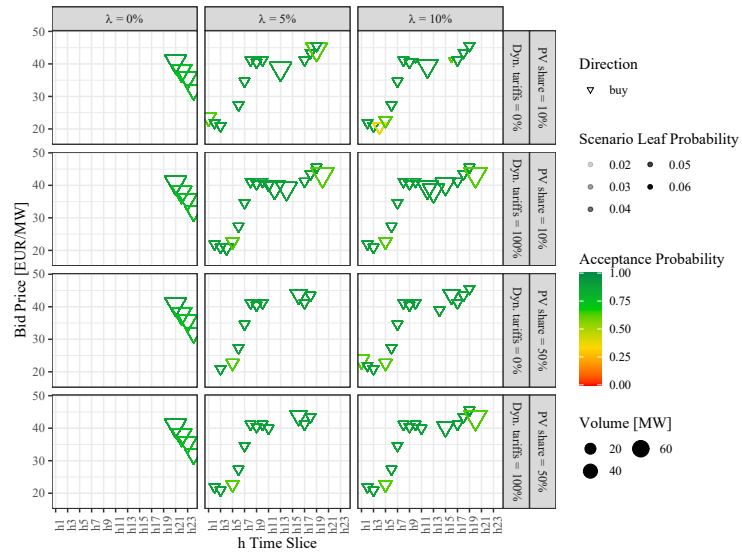


Figure 43: Retailer's day-ahead trading strategy in the winter season weekend day: Medium scenario

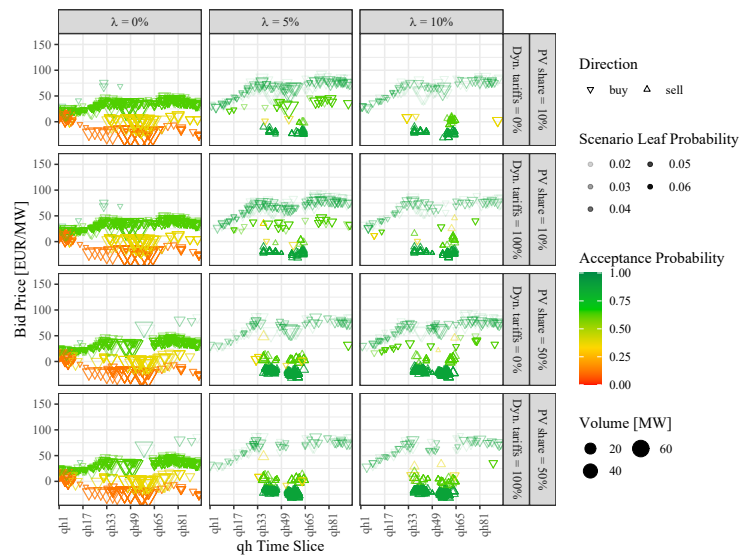


Figure 44: Retailer's intraday trading strategy in the Winter season working day: Medium scenario

A.5 Retailer's portfolio risk management with increasing solar PV self-generation

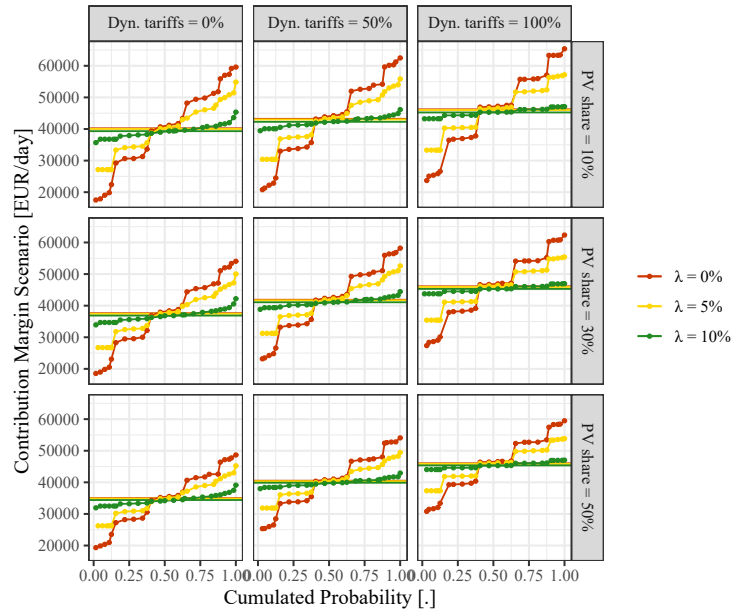


Figure 45: Empirical cumulative distribution functions of contribution margins for the Summer working day: Low scenario

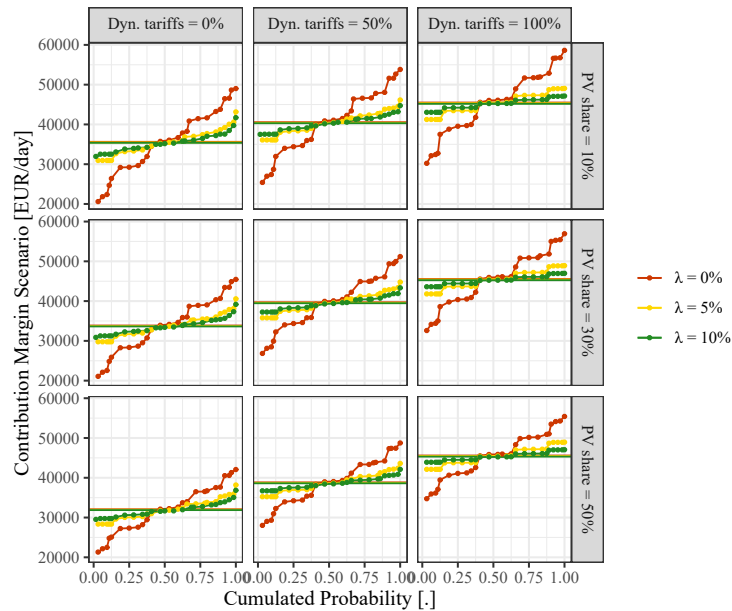


Figure 46: Empirical cumulative distribution functions of contribution margins for the Summer working day: High scenario

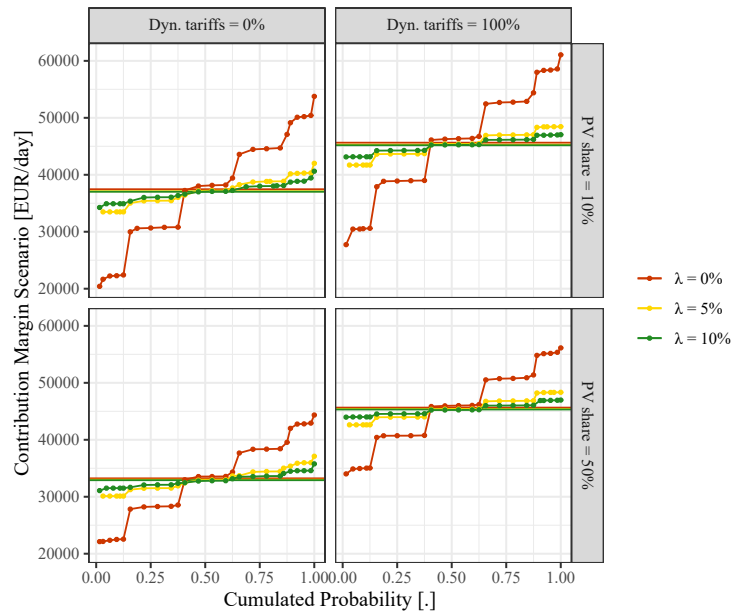


Figure 47: Empirical cumulative distribution functions of contribution margins for the Summer working day: Medium scenario

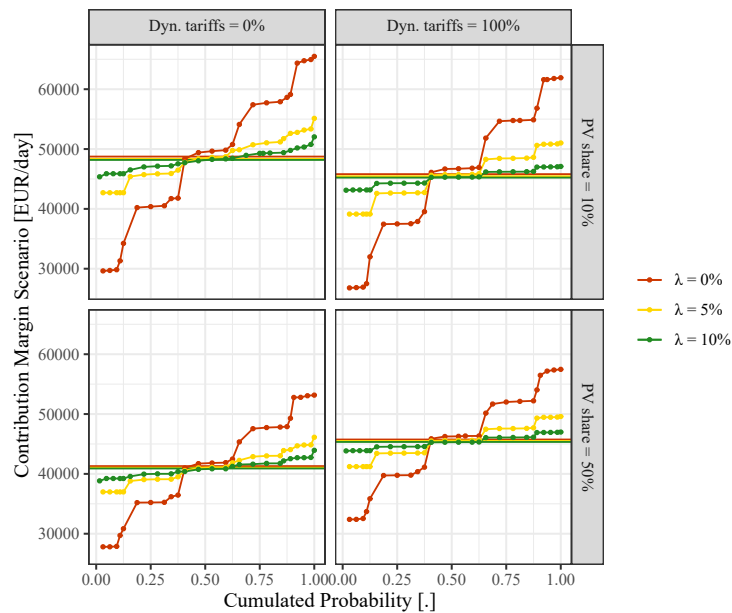


Figure 48: Empirical cumulative distribution functions of contribution margins for the summer weekend day: Medium scenario

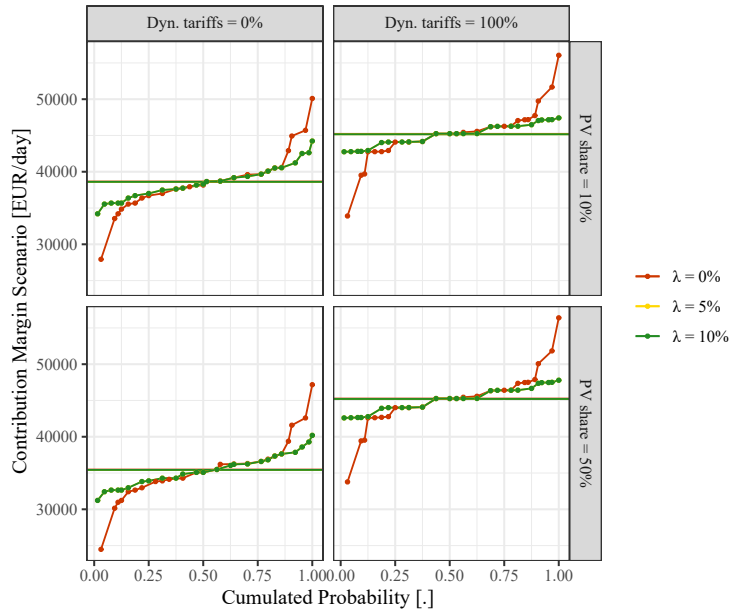


Figure 49: Empirical cumulative distribution functions of contribution margins for the transition season working day: Medium scenario

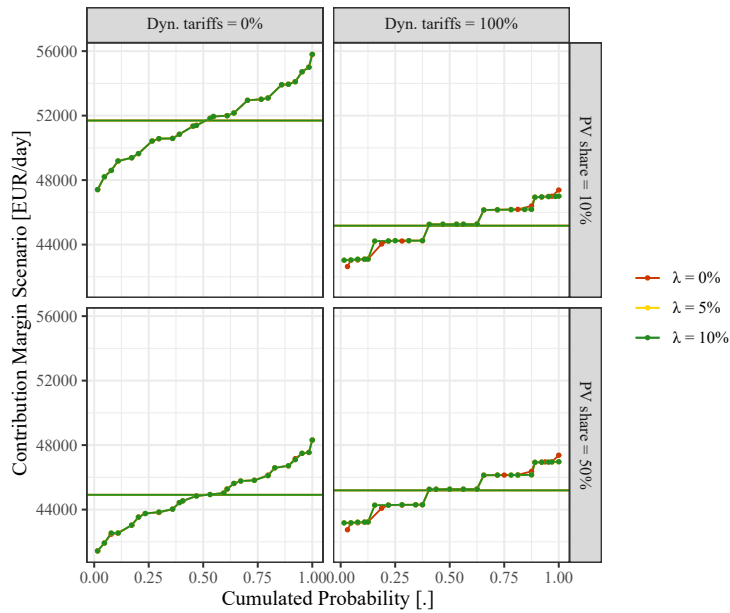


Figure 50: Empirical cumulative distribution functions of contribution margins for the transition season weekend day: Medium scenario

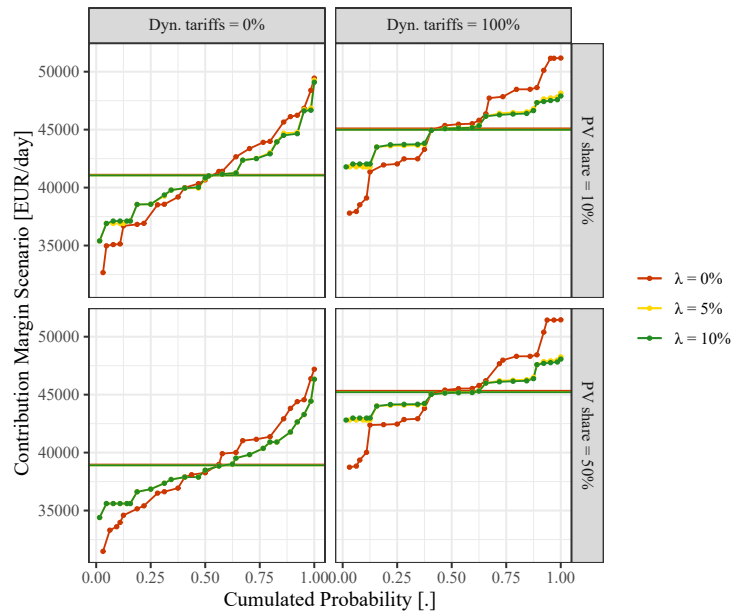


Figure 51: Empirical cumulative distribution functions of contribution margins for the winter working day: Medium scenario

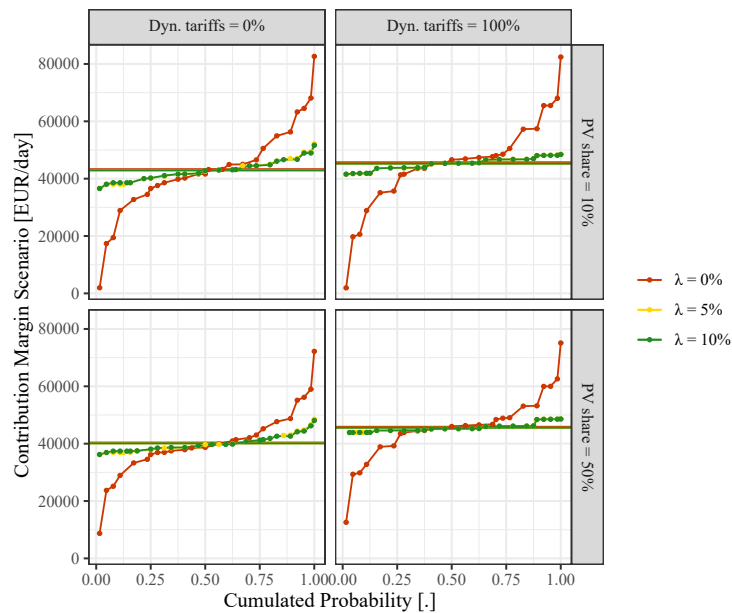


Figure 52: Empirical cumulative distribution functions of contribution margins for the winter weekend day: Medium scenario

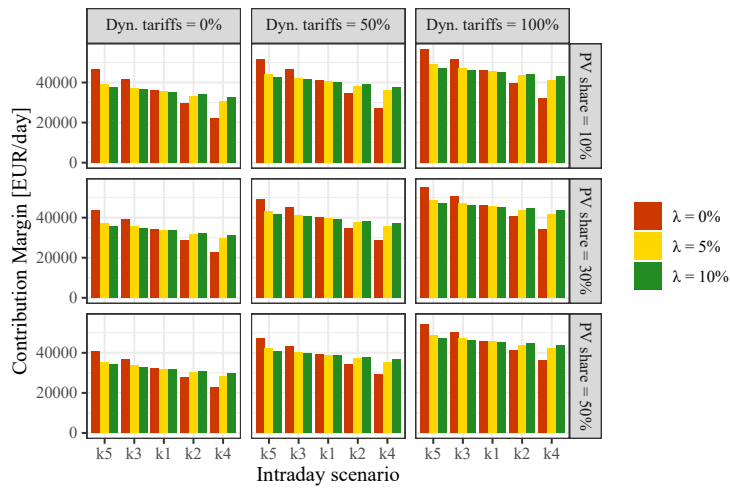


Figure 53: Retailer's contribution margin variability in the intraday market for a summer working day: Low scenario

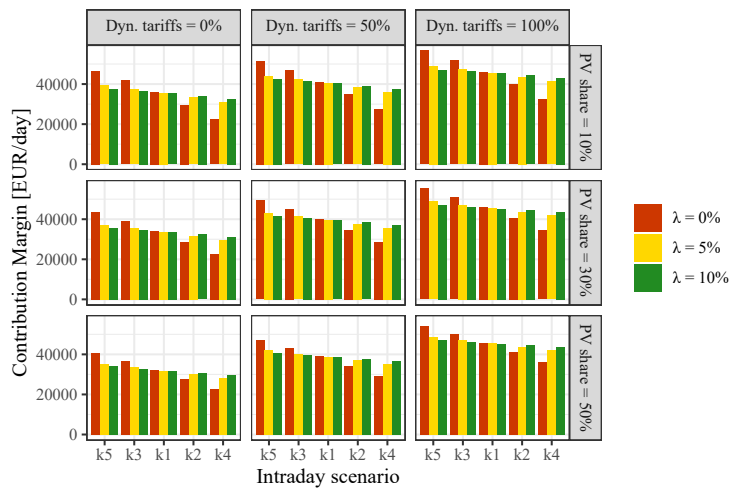


Figure 54: Retailer's contribution margin variability in the intraday market for a summer working day: High scenario

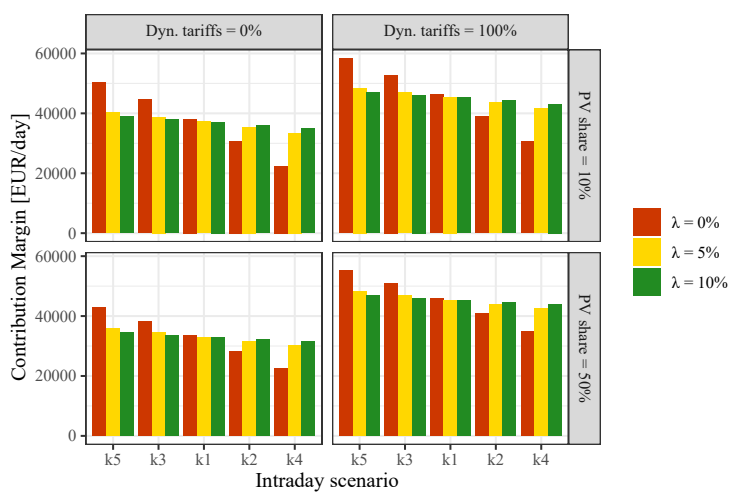


Figure 55: Retailer's contribution margin variability in the intraday market for a summer working day: Medium scenario

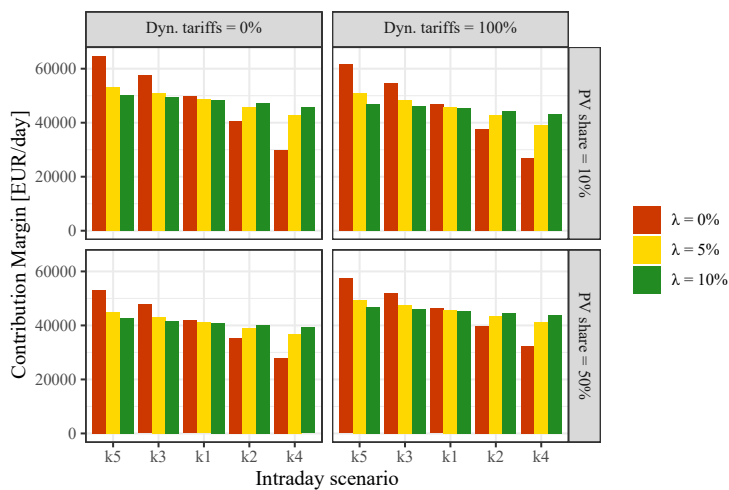


Figure 56: Retailer's contribution margin variability in the intraday market for a summer weekend day: Medium scenario

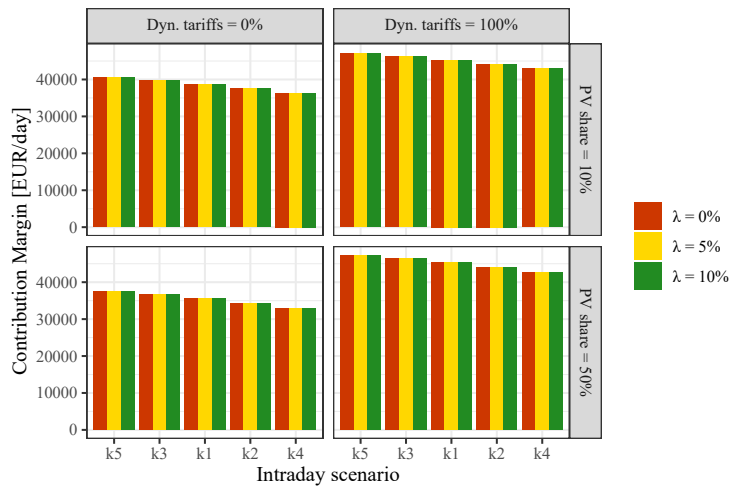


Figure 57: Retailer's contribution margin variability in the intraday market for a transition season working day: Medium scenario

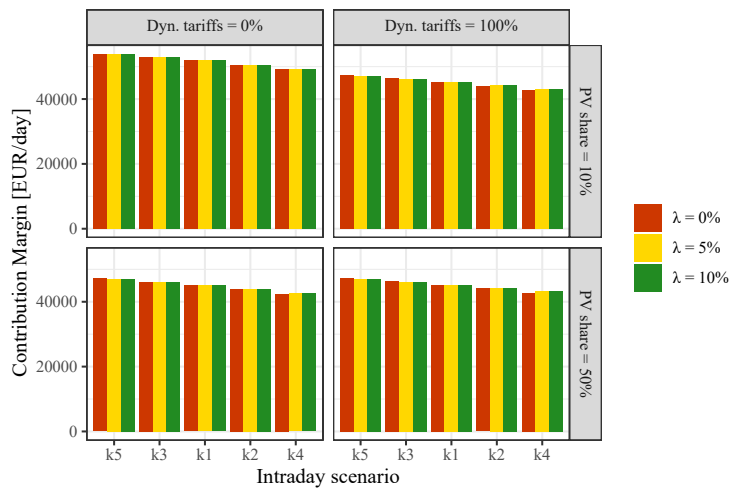


Figure 58: Retailer's contribution margin variability in the intraday market for a transition season weekend day: Medium scenario

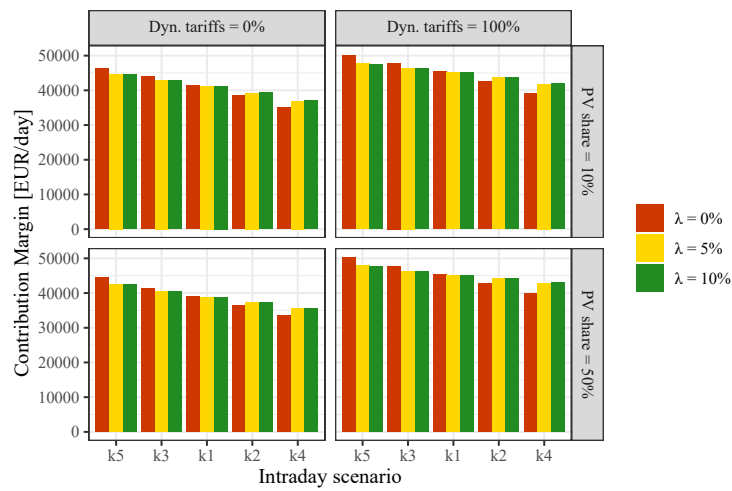


Figure 59: Retailer's contribution margin variability in the intraday market for a winter working day: Medium scenario

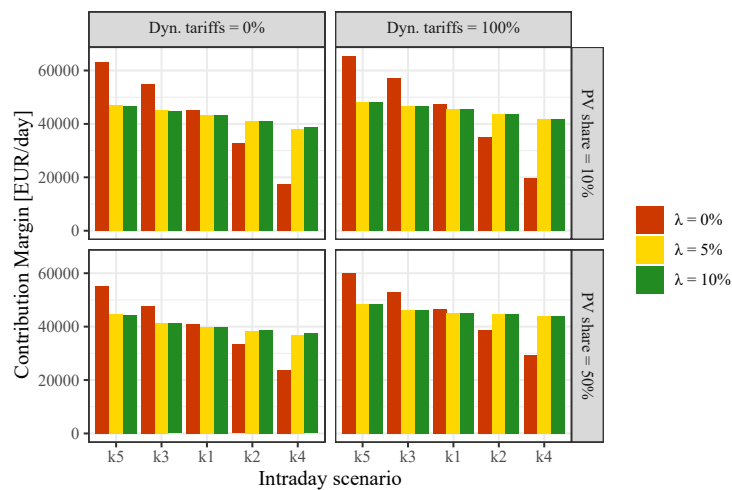


Figure 60: Retailer's contribution margin variability in the intraday market for a winter weekend day: Medium scenario

Paper C

Stochastic optimization of trading strategies in sequential electricity markets

Emil Kraft ^a, Marianna Russo ^{b,c}, Dogan Keles ^d, Valentin Bertsch ^e

^a *Karlsruhe Institute of Technology (KIT), Chair of Energy Economics, Karlsruhe, Germany*

^b *NEOMA Business School, Department of Finance, Mont-Saint-Aignan, France*

^c *Norwegian University of Science and Technology (NTNU), NTNU Business School, Trondheim, Norway*

^d *Technical University of Denmark (DTU), Department of Technology, Management and Economics, Lyngby, Denmark*

^e *Ruhr University Bochum, Chair of Energy Systems and Energy Economics, Bochum, Germany*

Submitted to *European Journal of Operational Research*, published as working paper in the KIT working paper series in production and energy.

Suggested citation:

Kraft, E.; Russo, M.; Keles, D.; Bertsch, V. (2021): Stochastic Optimization of Trading Strategies in Sequential Electricity Markets. In: KIT Working Paper in Production and Energy No. 58, Karlsruhe Institute of Technology (KIT), Karlsruhe. <http://dx.doi.org/10.5445/IR/1000134346>.

Stochastic Optimization of Trading Strategies in Sequential Electricity Markets

Emil Kraft^{*,a}, Marianna Russo^b, Dogan Keles^c, and Valentin Bertsch^d

^aKarlsruhe Institute of Technology, Chair of Energy Economics, Hertzstraße 16, D-76187 Karlsruhe

^bNTNU Business School, Trondheim, Norway

^cTechnical University of Denmark (DTU), Department of Technology, Management and Economics, Lyngby, Denmark

^dChair of Energy Systems and Energy Economics, Ruhr-University Bochum, Bochum, Germany

June 23, 2021

Abstract

Quantity and price risks determine key uncertainties market participants face in electricity markets with increased volatility, for instance due to high shares of renewables. In the time from day-ahead until real-time, there lies a large variation in best available information, such as between forecasts and realizations of uncertain parameters like renewable feed-in and electricity prices. This uncertainty reflects on both the market outcomes and the quantity of renewable generation, making the determination of sound trading strategies across different market segments a complex task.

The scope of the paper is to optimize day-ahead and intraday trading decisions jointly for a portfolio with controllable and volatile renewable generation under consideration of risk. We include a reserve market, a day-ahead market and an intraday market in stochastic modeling and develop a multi-stage stochastic Mixed Integer Linear Program. We assess the profitability as well as the risk exposure, quantified by the conditional value at risk metric, of trading strategies following different risk preferences. We conclude that a risk-neutral trader mainly relies on the opportunity of higher expected profits in intraday trading, whereas risk can be hedged effectively by trading on the day-ahead. Finally, we show that reserve market participation implies various rationales, including the relation of expected reserve prices among each other, the relation of expected reserve prices to spot market prices, as well as the relation of the spot market prices among each other.

Keywords: OR in energy, Electricity markets, Multi-stage stochastic programming, Uncertainty modeling, Risk modeling.

*Corresponding author. E-mail: emil.kraft@kit.edu.

Acknowledgments. The authors acknowledge the financial support of the German Federal Ministry of Education and Research under grant number 03SFK1F0-2 (ENSURE – Neue Energienetzstrukturen für die Energiewende) and of the German Federal Ministry for Economic Affairs and Energy under grant number 03SIN120 (C/sells, in the scope of the SINTEG programme). This work has emanated from Marianna Russo's research time at the Economic and Social Research Institute, Dublin. Marianna Russo acknowledges funding from the ESRI's Energy Policy Research Center and the SFI Energy Systems Integration Partnership Programme (ESIPP) number SFI/15/SPP/E3125. The opinions, findings and conclusions or recommendations expressed in this material are those of the authors and do not necessarily reflect the views of the Energy Policy Research Center and Science Foundation Ireland. All errors remain our own.

1 Introduction

With increasing uncertainties in the energy system in recent years, reserve and spot electricity markets have been moving towards higher granularity and trading decision times appear to move more and more to the short-term and even close to real-time. The increasing shares of weather-dependent volatile renewable generation and the introduction of intraday markets imply many changes in the design of short-term markets, but also in the trading rationales in sequential market structures and the risk exposure of individual market participants. The complexity of trading decisions leads to myriads of possible strategies to bring the flexibility and energy of a power plant portfolio profitably to the electricity markets. Hereby, not only the market segments themselves are subject to uncertainty, but also the relationship and interplay of the market segments need to be considered when deriving trading decisions. Another aspect that is relevant in the course of the energy transition is the actor structure in the energy sector. As more and more small market participants enter the market, that are sensitive to risk but unable to develop sophisticated methods, the demand for insights and approaches to determine sound trading strategies for all market segments increases.

As of today, trading decisions are typically determined with the help of deterministic programming approaches, basic stochastic considerations as well as the gut feeling of traders, and do not consider all market segments as a whole. In the literature, there are several studies that highlight the need to consider different market segments and associated uncertainties in thorough (Boomsma, Juul and Fleten, 2014; Möst and Keles, 2010, e.g.). Yet, due to rising shares of renewables from different sources and market adaptations the relationship and interplay of uncertainties and market prices has become more complex and continues to do so. This requires to extend existing modeling approaches, that consider one or a few sources of uncertainty independently from each other, by including the conditional relations of uncertainties of the relevant parameters, too. (Russo, Kraft, Bertsch and Keles, 2021)

With the proposed approach, we are able to model the uncertainty of the main drivers of power plant portfolios economics at different points in time and to determine sound trading strategies under uncertainty that also take into account the associated risk exposure and attitude. We model the relevant quantity and price risks from the morning of the day ahead until the gate closure of intraday trading and include all key characteristics of the reserve market, the day-ahead spot market as well as the intraday spot market. To estimate and apply the developed models, we provide a case study for the German electricity market design and a renewable generation portfolio consisting of volatile and controllable units.

The results consist on the one hand in a transparent assessment of the expected profits and risks under different trading strategies. In this study, besides the expected value we include risk metrics such as the conditional value at risk into decision-making, as introduced in Conejo, Carrión and Morales (2010). We present efficient frontiers and profit distributions associated with optimal trading decisions. On the other hand, we derive and discuss valuable insights on trading rationales both within and across the market segments. Like that, we provide not only an innovative application of stochastic programming to a complex real-world problem, but also interesting insights for scholars, traders, and ultimately policy makers designing markets for the energy transition.

The remainder of the paper is organized as follows: In Section 2, we discuss approaches in the literature to face the trading problem with stochastic optimization and further specify the research gap. Section 3

presents the considered sequential market setting and key characteristics of the single market segments. In Section 4, we describe the trading problem and develop a methodology to derive optimal trading strategies based on a multi-stage stochastic mixed-integer linear problem. Further, Section 4 includes the stochastic modelling of uncertainties that serves as input for the trading problem. Section 5 applies the developed approach to the case of a power plant portfolio in the German market and discusses results and underlying trading rationales. Finally, Section 6 summarizes the main conclusions for different stakeholder groups and provides an outlook to future developments and applications.

2 Literature Review and Research Gap

Decisions in energy economics are often categorized into strategic (i.e., mostly investment) and operational or short-term decisions. This paper sets a clear focus on short-term decisions. Optimization approaches to provide decision support for short-term decisions of actors in energy economics can be further distinguished into the optimal use of the technical units and the optimal interaction with revenue streams, i.e. the markets for flexibility and energy. As this paper focuses on the European setting of a self-dispatch system with balancing responsible parties (BRP), we will not address ISO optimization approaches, which are deployed mainly in the US (e.g., CAISO in California). We are focusing on approaches from the perspective of individuals.

In the literature, the two short-term optimization problems that are relevant for this paper are, the optimal dispatch problem or unit commitment problem for a power plant portfolio, and the optimal trading problem. However, in most cases these two cannot be separated strictly from each other. Whereas the first describes the problem of delivering a defined schedule of energy or providing a defined flexibility on activation request at minimal cost, the second enhances the scope by taking into account the (expected) market outcomes and optimizing the bids, which lead to the profit-maximizing operation. As the objective function is defined to maximize the contribution margins and as the market commitments are not known *ex ante*, the unit commitment problem is not modeled explicitly but implicitly. Whereas unit commitment rather focuses on technical constraints of the plant or the plant portfolio, the trading problem rather addresses the market operations in more detail.

Obviously, there are many previous works considering the deterministic unit commitment and trading problem. Typically, although technical constraints are non-linear in reality (e.g. efficiency for partial load), the problem is formulated as a Mixed-Integer Linear Program (MILP) to keep the problem mathematically tractable with standard solvers. However, deterministic approaches fail to address for increasing uncertainty and to depict the risk, even more so with rising shares of weather-dependent renewable generation and uncertain market prices. We therefore focus on approaches of stochastic programming. For handling uncertainty, the main stochastic optimization approaches include exact solution methods and approximation techniques (see, e.g., Birge and Louveaux, 2011, for an overview). Zheng, Wang and Liu (2015) provide a review of stochastic optimization approaches for the unit commitment problem and distinguish between stochastic programming, robust programming and (approximate) stochastic dynamic programming. For the literature overview to remain concise, at this point we focus on works that apply stochastic programming approaches to electricity market bidding in sequential market settings and refer to Möst and Keles (2010), Klaboe and Fosso (2013), and Zheng et al. (2015) for more thorough reviews of stochastic modelling in energy economics.

Fleten and Kristoffersen (2007) deploy stochastic programming to determine optimal bidding strategies

for hydropower plants with a cascade structure. Boomsma et al. (2014) model coordinated bidding in electricity spot and balancing power markets in the Nordic market design with the help of a multi-stage stochastic program and compare the risk exposure of different bidding strategies. Ottesen, Tomsgard and Fleten (2018) deploy a multi-stage stochastic program to derive an optimal trading strategy for a portfolio of demand side management units in three market segments: Starting with an option market that is cleared for an entire week, followed by a daily spot market and an hourly flexibility market, the trader faces three possible revenue streams with uncertain prices as in the Nordic market design. Klæboe, Braathen, Eriksrud and Fleten (2019) continue the investigation of coordinated bidding strategies for hydropower plants in the Nordic market with a similar multi-stage stochastic approach.

Plazas, Conejo and Prieto (2005) deploy the case of the Spanish market design to investigate bidding strategies in three market segments of the electricity, aiming at maximizing the expected profit. Pandžić, Morales, Conejo and Kuzle (2013) formulate a multi-stage stochastic problem for offering and operating a virtual power plant in a market setting with spot and balancing market. For the perspective of the operator of a local energy market, Laur, Nieto-Martin, Bunn and Vicente-Pastor (2018) present a multi-stage stochastic approach to procure flexibility services in distribution network and discuss risk implications.

This paper stands in line and pursues similar ideas with the presented papers, although we face a significantly different problem structure. The existing studies do not match the structure of short-term electricity markets and all their relevant design elements that we observe in a real-world market setting as presented in Section 3. For this reason, the study fills this gap by presenting a comprehensive problem description for the trading decisions of a portfolio manager with volatile and controllable renewables and applies it to the case of the German market design. Furthermore, we cover the entire market risk and uncertainties such a portfolio faces in the operations on the short-term markets.

We address these by considering a multi-stage stochastic approach for trading in sequential markets including different temporal resolutions, pay-as-bid and uniform pricing, and high uncertainty of prices and volumes stemming from various sources. The German balancing reserve market in particular is known for hardly explainable prices, supposedly due to a high market concentration. In the past, the design of and actor structure in the reserve markets often led to undesirable and noncompetitive results. Therefore it has been adapted several times in recent years. Several studies deal with these issues and present implications for the development of the market (Ocker and Ehrhart, 2017; Kraft, Keles and Fichtner, 2018, see, e.g.). We refer to Ocker, Ehrhart and Ott (2018) and Kraft, Ocker, Keles and Fichtner (2019) for in-depth analyses of incentives and game-theoretical discussions of the market design.

Further, the need to consider a stochastic approach for trading in sequential markets becomes increasingly important in contexts with rising shares of renewables and increasing uncertainty in spot markets. Forecast errors on the day-ahead are unavoidable and lead to significant price and quantity risks for any market participant. Addressing these adequately in the decision process requires a thorough analysis and modeling of the stochastics and consequently an approach that considers all aspects, the uncertainty and the technical and market constraints. With the approach presented in this paper, we aim at filling this gap in the existing literature.

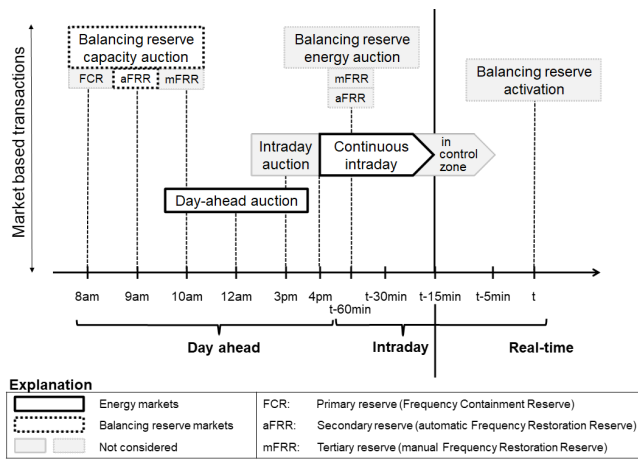


Figure 1: Sequence of markets for electricity and flexibility with gate-closure times in the German market design from November 2020 on. The considered market segments reserve ("aFRR capacity auction"), day-ahead spot market ("Day-ahead auction") and intraday spot market ("Continuous intraday") are marked with the red boxes.

3 Market Description

In European power markets, the products relevant for a power plant portfolio trader can be distinguished into the mere delivery of electricity and the provision of reserve power for the transmission system operator (TSO) to balance the system. Whereas the former is organized in large electricity exchanges and the market design has been harmonized internationally to a large extent, the latter is still organized in distinct national designs. Rising shares of generation by renewable energy sources (RES) led to an increasing relevance of close-to-realtime decisions. This applies not only for reserve products that are procured with shorter lead times, but particularly for the interplay of day-ahead and intraday spot market operations.

The setting that is studied in this paper includes a balancing reserve power market with separate products for positive and negative direction, a day-ahead electricity market, and an intraday electricity market. This threefold organization is typical for European power markets and can be found with small variations in many countries. With regard to the balancing reserve, we focus on the secondary reserve market (i.e., automatic Frequency Restoration Reserve, aFRR) with its lead times and product requirements, the segments for primary and tertiary reserve are left out in this market description to remain concise. For better readability, the term "reserve" is used synonymously with secondary reserve and aFRR in the following. Figure 1 provides an overview over a typical market sequence until real-time and highlights the market segments relevant for this study. To substantiate the products and lead times in a concrete case, we choose the market design setting of Germany. The procurement of reserve products by the TSOs in Germany is organized in a two-stage procedure. The first stage, the so-called capacity market auction for the day ahead, takes place prior to the day-ahead spot market at 9 am and determines the reserve providers for the following day. In this auction, the prequalified reserve providers can place bids consisting of the capacity price (in EUR/MW) and a volume (in MW). Providers are allowed to submit several distinct bids. The 24 hours of the day are split into six time slices consisting of four hours each (0-4, 4-8, ..., 20-24). Further, reserves for the negative (downward

regulation) and the positive (upward regulation) direction are auctioned as separate products. This leads to twelve distinct aFRR auctions each day, which are remunerated according to pay-as-bid pricing. In the second step of reserve procurement, the so-called aFRR energy market auction takes place during the day 45 minutes before the gate closure time of the intraday market, and determines the prices and merit order of activation. The successful bid in the capacity market obliges the trader to trade in the reserve energy market, however also free energy bids are allowed. For the scope of this paper, the aFRR energy market is left out for two reasons. First, the energy price bid can only lead to positive contribution margins if above the variable costs of provision and therefore poses no risk of losses to the portfolio profit. Second and most important, the bid into the energy market can be considered independently from the other trading decisions. For it is rather a complementing element than an opportunity, the aFRR energy market can be neglected.

After the aFRR capacity market, at 12 am the day-ahead spot market auction takes place, in which energy delivery for the next day is traded in hourly resolution with uniform pricing. Subsequently, at 3 pm the intraday auction takes place, in which energy can be traded in quarter-hourly resolution. The intraday market is then open for continuous trading of energy in quarter-hourly products until 30 minutes before delivery¹. To cope with the temporal structure of the rolling gate closure times and respective 96 arrival processes of prices of continuous intraday trading, we require a simplification. In accordance with Ottesen et al. (2018) and Laur et al. (2018) the intraday market is approximated with one hypothetical auction, with the index price ID3 of the trades completed in the last three hours (denoted with p^{ID3}) as representative price for each quarter hour. As p^{ID3} averages completed trades, we handle the hypothetical auction as a uniform pricing auction. This corresponds to modeling the intraday trading as one hypothetical auction with rolling gate closures 30 minutes before the respective delivery. Note that this simplification neglects profit from potential re-positioning in reaction to the volatility of the continuous price process during intraday trading. Further, we assume that the trader acts as a price-taker and is always able to find a counterparty to sell electricity for the p^{ID3} price. With regard to low liquidity this would have been a very strong assumption in the early years of intraday trading. In the meanwhile, however, intraday trading has become sufficiently liquid. For the relatively small trading volumes related to the investigated portfolio and as the scope of the paper is particularly to determine optimal trading strategies on the day ahead, the assumption is considered well reasonable.

In conclusion, the trader faces three markets to be considered: The aFRR capacity market with six four-hour products, the day ahead market with 24 hourly products and the intraday market with 96 quarter-hourly products. Considering both the price uncertainty of the three markets and the volume uncertainty of the renewable generation, the trader faces a complex decision problem with numerous decision variables.

¹Note, that half-hour and hour products are also traded in the intraday market. However, as the 15 minute product is the best approximation for the value of the 15 minutes period if contained within a product with larger resolution, including further product resolutions for intraday trading would not essentially change the trading strategies but result in substitution trades. We do not aspire to optimize for trades across intraday products, but for trading strategies across the considered decision stages. Therefore, this paper focuses on the 15 minute products alone.

Table 1: Overview over information available to the optimization as deterministic or realized information and as stochastic information in form of scenarios.

	Deterministic / realized	Stochastic
Stage 1	<i>deterministic:</i> Expected value RES generation forecast, technical constraints, market constraints	<i>scenarios i:</i> Marginal reserve prices for negative and positive direction
Stage 2	<i>scenarios i:</i> Reserve market result and commitment	<i>scenarios j:</i> Day-ahead RES generation forecast, day-ahead market prices
Stage 3	<i>scenarios j:</i> Day-ahead market result and commitment, day-ahead RES generation forecast	<i>scenarios k:</i> Intraday update RES generation forecast, intraday market prices

4 Methodology

The methodology presented in the following subdivides into the formulation of the optimization problem and the generation of input data by means of stochastic modeling. The optimization is formulated as a mixed-integer linear multi-stage stochastic problem. First, the formulation for a risk-neutral trader is presented. Second, the formulation is extended to a problem that allows for consideration risk-aversion of the trader. After the constraints the optimization is subject to are presented, we finally introduce the modeling and characterization of uncertainties considered in the problem.

4.1 The Trading Problem

For the bidder, the determination of the optimal bids implies both price risks and a quantity risks. The information available to the trader in the optimization problem is summarized in Table 1. Information like the residual load forecast and its updates are not explicitly provided to the problem, but are contained in the price processes as described above. Note further, that logically the stochastic information on later stages is implicitly considered in the decisions of the early stages. The structure of the decisions on the three stages will be explained in more detail in Section 4.2.

4.2 Target Function

We formulate the target for the risk-neutral problem straight forward as maximization of expected contribution margins π throughout the scenarios (i, j, k) in Ω in all market segments and time steps as the revenues (ρ) minus the costs (κ).

$$\max \mathbb{E}_{(i,j,k) \in \Omega}(\pi_{i,j,k}) = \mathbb{E}_{(i,j,k) \in \Omega}(\rho_{i,j,k}) - \mathbb{E}_{(i,j,k) \in \Omega}(\kappa_{i,j,k}) \quad (1)$$

with the expected revenues ρ being the sum of reserve (aFRRpos and aFRRneg) market, day-ahead (DA) market and intraday (ID) market revenues.

$$\mathbb{E}_{(i,j,k) \in \Omega}(\rho_{i,j,k}) = \mathbb{E}_{(i) \in \Omega}(\rho_i^{\text{aFRRpos}}) + \mathbb{E}_{(i) \in \Omega}(\rho_i^{\text{aFRRneg}}) + \mathbb{E}_{(i,j) \in \Omega}(\rho_{i,j}^{\text{DA}}) + \mathbb{E}_{(i,j,k) \in \Omega}(\rho_{i,j,k}^{\text{ID}}) \quad (2)$$

One key challenge in the formulation of the trading problem consists in addressing the reserve market design with its particularities. As pay-as-bid pricing intuitively comes with both the price and the volume as decision variables, an alternative formulation must be deployed for the problem to remain a mixed-integer linear problem (MILP). However, the modelling of uncertainty yields discrete values for reserve prices for positive and negative direction (LP and LN , respectively) for each reserve price scenario i . We therefore define these price levels p_{lp}^{aFRRpos} (p_{ln}^{aFRRneg}) as fixed bidding levels and define only the bid volume $x_{lp,i,ts}^{\text{aFRRpos,bid}}$ ($x_{ln,i,ts}^{\text{aFRRneg,bid}}$) on price level lp (ln) as decision variable for positive (negative) reserve market bidding. In this way, we define a bidding curve with volumes on several price levels to be submitted to each segment of the reserve market.

As we model the uncertainty with a discrete probability space, the trader has no incentive to bid on price levels distinct from the given scenario prices. The eventual acceptance of a bid on price level $lp \in LP$ for the positive reserve product (or on price level $ln \in LN$ for negative reserve) in time slice ts and scenario i is modelled with the help of the binary acceptance parameters $\beta_{lp,i,ts}^{\text{aFRRpos}}$ and $\beta_{ln,i,ts}^{\text{aFRRneg}}$, that translate the marginal prices into acceptance or decline of a bid as described in Equation (51). The resulting expected revenues from the positive reserve market over all time steps and scenarios are then defined as (negative follows analogously):

$$\mathbb{E}_{(i) \in \Omega}(\rho_i^{\text{aFRRpos}}) = \sum_{i=1}^I pr_i \sum_{ts=1}^{TS} \sum_{lp=1}^{LP} \left(\beta_{lp,i,ts}^{\text{pos}} \cdot p_{lp}^{\text{aFRRpos}} \cdot x_{lp,i,ts}^{\text{aFRRpos}} \right) \quad (3)$$

pr_i , pr_j , pr_k denote scenario probabilities for $i \in I$, $j \in J$, and $k \in K$, as described in 4.7. Note, that this formulation takes into account the reserve market to be cleared according to pay-as-bid pricing and the spot market segments according to uniform pricing. The considered price for an accepted bid p_{lp}^{aFRRpos} is therefore indexed with the respective price level and reflects the pay-as-bid pricing.

In contrast, the day-ahead and intraday market are cleared with uniform pricing². Hereby, $p_{j,h}^{\text{DA}}$, $p_{i,j,k,qh}^{\text{ID}}$ denote the prices on the day-ahead and intraday market for the different time steps and scenarios, respectively. The expected revenues on the day-ahead market are defined as the trading volume $x_{i,j,h}^{\text{DA,trade}}$ multiplied by the uniform price $p_{j,h}^{\text{DA}}$ in scenario j , summed up over all hours.

$$\mathbb{E}_{(i,j) \in \Omega}(\rho_{i,j}^{\text{DA}}) = \sum_{i=1}^I pr_i \sum_{j=1}^J pr_j \sum_{h=1}^H p_{j,h}^{\text{DA}} \cdot x_{i,j,h}^{\text{DA,trade}} \quad (4)$$

The day-ahead market is modelled such that the trader submits a bid curve to the market, consisting of volume bids on defined fixed price levels lda . For the evaluation of bidding strategies, we distinguish between bids to sell generation, $x_{i,j,h}^{\text{DA,gen,bid}}$, bids to take a short position (i.e., selling more than is expected to be generated), $x_{i,j,h}^{\text{DA,short,bid}}$, and bids to take a long position (i.e., buying electricity on the day-ahead market), $x_{i,j,h}^{\text{DA,long,bid}}$.

Again, there is no incentive to deviate from the market prices contained in the scenarios j for the day-ahead market decision stage. With the help of the binary parameter $\beta_{lda,j,h}^{\text{DA}}$, denoting the accepted price levels lda of day-ahead market bids for selling electricity in hour h and scenario j , the traded volume is defined as follows. We stress at this point that the trader does not only have the option

²As described in Section 3, we model the intraday auction as an uniform pricing auction with the ID3 price as clearing price.

of purely selling the generation, but also to prepare a good position for potential intraday trading. Thus, both building a short position that exceeds the expected generation and going long (i.e., buying electricity to sell it later and profit from rising prices) is within the trader's action space. The bids to take a long position in the day-ahead market (i.e., buying electricity) have the opposite acceptance structure of selling bids $(1 - \beta_{lda,j,h}^{DA})^3$.

$$x_{i,j,h}^{DA,trade} = x_{i,j,h}^{DA,gen,trade} + x_{i,j,h}^{DA,short,trade} - x_{i,j,h}^{DA,long,trade} \quad (5)$$

with

$$x_{i,j,h}^{DA,gen,trade} = \sum_{lda=1}^{LDA} \beta_{lda,j,h}^{DA} \cdot x_{lda,i,j,h}^{DA,gen,bid} \quad (6)$$

$$x_{i,j,h}^{DA,short,trade} = \sum_{lda=1}^{LDA} \beta_{lda,j,h}^{DA} \cdot x_{lda,i,j,h}^{DA,short,bid} \quad (7)$$

$$x_{i,j,h}^{DA,long,trade} = \sum_{lda=1}^{LDA} (1 - \beta_{lda,j,h}^{DA}) \cdot x_{lda,i,j,h}^{DA,long,bid} \quad (8)$$

However, the long and the short position of the portfolio are constrained to the extent allowed in BRP contracts as will be presented in Equations (23) and (24). The revenues from the intraday market are defined analogously. The factor Δt captures the difference in temporal resolution between hour h and quarter hour qh (i.e. $\Delta t = 0.25$), so that the energy amount equals the integral of the power output.

$$\mathbb{E}_{(i,j,k) \in \Omega}(\rho_{i,j,k}^{ID}) = \sum_{i=1}^I pr_i \sum_{j=1}^J pr_j \sum_{k=1}^K pr_k \sum_{qh=1}^{QH} p_{j,k,qh}^{ID} \cdot x_{i,j,k,qh}^{ID,trade} \cdot \Delta t \quad (9)$$

The realized intraday trades, $x_{i,j,k,qh}^{ID,trade}$, are defined by (10), the intraday trade summands are defined analogously as for the day-ahead market in (6)-(8).

$$x_{i,j,k,qh}^{ID,trade} = x_{i,j,k,qh}^{ID,gen,trade} + x_{i,j,k,qh}^{ID,short,trade} - x_{i,j,k,qh}^{ID,long,trade} \quad (10)$$

The expected costs occurring in each market segment sum up to the total costs. To account for potential active schedule violations in a future application, the term $\kappa_{i,j,k}^{Imb}$ completes the formulation of the trading problem.

$$\begin{aligned} \mathbb{E}_{(i,j,k) \in \Omega}(\kappa_{i,j,k}) &= \mathbb{E}_{(i) \in \Omega}(\kappa_i^{aFRRpos}) + \mathbb{E}_{(i) \in \Omega}(\kappa_i^{aFRRneg}) + \mathbb{E}_{(i,j) \in \Omega}(\kappa_{i,j}^{DA}) \\ &\quad + \mathbb{E}_{(i,j,k) \in \Omega}(\kappa_{i,j,k}^{ID}) + \mathbb{E}_{(i,j,k) \in \Omega}(\kappa_{i,j,k}^{Imb}) \end{aligned} \quad (11)$$

The pure provision of capacity is valued at no costs. For positive reserve (aFRRpos), the reserve activation may lead to additional fuel consumption and thus additional variable costs. On the other hand, an activation of negative reserve (aFRRneg) may lead to fuel savings and thus a reduction of the costs arising from the spot market operation. However, the cost effects of potential reserve

³This formulation implies that in case $p_{j,h}^{DA} = p_{lda,j,h}^{DA}$ a selling bid gets accepted at price level lda , whereas an ask bid is declined. A successful ask bid must be at least one price level above, despite being valued with price level lda . We thereby reflect a certain bid-ask spread and avoid opposite bids that cancel each other out and only inflate trading volumes.

activation can be easily addressed by appropriate energy bids. As the costs of a potential positive reserve activation are independent from the bidding decision on the reserve power market, we consider it reasonable to value them at zero costs. The same applies for the negative reserve.

$$\mathbb{E}_{(i) \in \Omega}(\kappa_i^{\text{aFRRpos}}) = 0 \quad (12)$$

The activation of reserves is not further considered in this paper. The only assumption that needs to be made is that the energy to meet the activation is available for the controllable plants u . The costs for the day-ahead market operation consist of variable costs for the controllable plant u and the renewable source res . The costs for a potential long position are already accounted for in the revenues in Equation (4) and (9).

$$\mathbb{E}_{(i,j) \in \Omega}(\kappa_{i,j}^{\text{DA}}) = \sum_{i=1}^I pr_i \sum_{j=1}^J pr_j \sum_{h=1}^H \left(\sum_{u=1}^U \kappa_u^{\text{var}} \cdot x_{i,j,u,h}^{\text{DA,dispatch,U}} + \sum_{res=1}^{\text{RES}} \kappa_{res}^{\text{var}} \cdot x_{i,j,res,h}^{\text{DA,dispatch,RES}} \right) \quad (13)$$

κ_u^{var} denotes the variable cost of unit u , $x_{i,j,u,h}^{\text{DA,dispatch,U}}$ denotes the energy dispatched (i.e., sold with $x_{lda,i,j,h}^{\text{DA,gen,bid}}$) from unit u on the day-ahead market. The dispatch for renewable source res is defined analogously.

$$\mathbb{E}_{(i,j,k) \in \Omega}(\kappa_{i,j,k}^{\text{ID}}) = \sum_{i=1}^I pr_i \sum_{j=1}^J pr_j \sum_{k=1}^K pr_k \sum_{qh=1}^{\text{QH}} \left(\sum_{u=1}^U c_u^{\text{var}} \cdot x_{i,j,k,u,qh}^{\text{ID,dispatch,U}} + \sum_{res=1}^{\text{RES}} c_{res}^{\text{var}} \cdot x_{i,j,k,res,qh}^{\text{ID,dispatch,RES}} \right) \cdot \Delta t \quad (14)$$

$$\mathbb{E}_{(i,j,k) \in \Omega}(\kappa_{i,j,k}^{\text{Imb}}) = \sum_{i=1}^I pr_i \sum_{j=1}^J pr_j \sum_{k=1}^K pr_k \sum_{qh=1}^{\text{QH}} (x_{i,j,k,qh}^{\text{imb,+}} + x_{i,j,k,qh}^{\text{imb,-}}) \cdot p_{qh}^{\text{imb}} \cdot \Delta t \quad (15)$$

with the absolute value of the energy imbalance $x_{i,j,k,qh}^{\text{imb}}$ denoted by the sum of the positive and negative share ($x_{i,j,k,qh}^{\text{imb,+}} + x_{i,j,k,qh}^{\text{imb,-}}$) valued with the imbalance price p_{qh}^{imb} .⁴ Logically, the imbalance can only either be positive or negative, which is reflected by the constraints (21) and (22) in Section 4.5.

4.3 Consideration of Risk

A major advantage of the stochastic over the deterministic problem formulation consists in the ability of the presented approach to quantify and to take into account risks when determining the trading strategy. Based on theory provided in textbooks such as Conejo et al. (2010) and Birge and Louveaux (2011), we distinguish between risk-neutral decision making and decision making under consideration of risk. Whereas the risk-neutral decision is based solely on the expected value of the profits over all scenarios as presented in (1), a real-world trader most likely will also want to consider the risk exposure related with the trading decision. In order to determine trading decisions with less risk exposure, we therefore introduce risk to our approach. This enables us to make use of the characterization of

⁴As intentional imbalances are prohibited by the up-to-date German BRP contract, $x_{i,j,k,qh}^{\text{imb}}$ is forced to equal zero with a sufficiently large number $BIGM$ as p_{qh}^{imb} . In the presented case study $BIGM$ equals 100,000 EUR/MWh. In the general formulation, p_{qh}^{imb} may be equipped with a close-to-real-time forecast to reflect an expected imbalance price (*reBAP*), if intentional imbalances want to be taken into account in future extensions of the model. However, this exceeds the scope of this paper.

uncertainty, which contains more information than a single figure, such as the expected value, can capture.

In finance literature, the risk exposure is quantified with the help of risk metrics. Commonly used metrics include the variance, the shortfall probability, the expected shortage and as well as value at risk (VaR) and conditional value at risk (CVaR, also referred to as average value at risk or expected shortfall) (Conejo et al., 2010). However, for the trading problem to remain scalable and flexible, the use of a coherent risk metric⁵, particularly one satisfying sub-additivity, is of practical use. As the CVaR meets the properties of coherence, we modify the problem formulation in order to include the CVaR into the target function (adaptation of Conejo et al. (2010)). Further details and the definition of the CVaR and the VaR are provided in Annex A.3.

4.4 Modelling the Conditional Value at Risk

In adaption of Conejo et al. (2010) the target function is augmented by the variable η , that corresponds to the VaR, the parameter α representing the probability level of the VaR and the non-negative continuous variable $s_{i,j,k}$ defined by equation (17) to the maximum of the VaR η minus the contribution margin $\pi_{i,j,k}$ in a scenario and zero. The optimization objective is now the weighted sum of expected value and the CVaR of the contribution margins throughout the scenarios, with $\lambda \in (0, 1)$ as weight in the target function. λ can be referred to as parameter of risk aversion.

$$\max \quad (1 - \lambda) \cdot \mathbb{E}_{(i,j,k) \in \Omega}(\pi_{i,j,k}) + \lambda \cdot \left(\eta - \frac{1}{1 - \alpha} \sum_{i=1}^I pr_i \sum_{j=1}^J pr_j \sum_{k=1}^K pr_k \cdot s_{i,j,k} \right) \quad (16)$$

$$\eta - \pi_{i,j,k} \leq s_{i,j,k} \quad \forall (i, j, k) \in \Omega \quad (17)$$

$$s_{i,j,k} \geq 0 \quad \forall (i, j, k) \in \Omega \quad (18)$$

In the remainder of this paper, sets will be dropped from the notation to remain concise, $\forall (i, j, k) \in \Omega$ is equivalent to $\forall (i, j, k)$, $\forall qh \in QH$ equivalent to $\forall qh$, and so on. The chosen multi-criteria formulation as weighted sum allows us to consider both the expected value of contribution margins and the CVaR at level α . The parameters λ and α will be used in the case study to distinguish between and evaluate different risk strategies. Further, for the interested reader we provide the problem formulation using the VaR as risk metric in Annex A.3.

4.5 Constraints

Besides the aforementioned constraints for modelling the risk, we include constraints from three categories in the problem formulation that will be presented in the subsequent paragraphs. First, several constraints regarding the trading logic, the market design and the market rules need to be considered. Further, the operational constraints of the technical units in the portfolio to fulfill energy delivery and provide the reserve products need to be considered in modelling the trading decision. Hereby, we distinguish between the volatile renewable sources (RES), indexed with *res*, and controllable (renewable) units (e.g., a biogas power plant), indexed with *u*. The third category of constraints comprises

⁵Coherent risk metrics satisfy the conditions of monotonicity, sub-additivity, homogeneity, and translational invariance.

the stochastic programming constraints, in which we summarize the constraints required for the formulation of the multi-stage stochastic problem and further auxiliary constraints.

4.5.1 Market Constraints

The energy balance over the two spot markets (i.e., day-ahead and intraday market) needs to be zero as short- or long-selling beyond the intraday market, i.e. speculating on imbalance prices lower or higher than spot market prices, is prohibited by the market rules. To give the trader the option to close its balance sheet and to deploy bidding strategies between the day-ahead and the intraday stage⁶, the short-selling variables comply with volumes sold but not dispatched in the respective stage and vice versa the long-selling variables comply with the generation volumes not sold or additional energy that is bought on the respective stage. Eventually, the energy schedule needs to be balanced for each qh . In the following, $qh(h)$ denotes the mapping of the quarter hours contained in an hour to the respective hour h (e.g., $qh(1) = \{1, 2, 3, 4\}$). As mentioned earlier, the imbalances (split up in positive and negative part to be able capture the absolute value) $x_{i,j,k,qh}^{\text{imb},+}$ and $x_{i,j,k,qh}^{\text{imb},-}$ enter the target function as positive variables, penalized with BIGM, via equation (15) and are thus forced to equal zero.

$$x_{i,j,h}^{\text{DA,trade}} + x_{i,j,k,qh}^{\text{ID,trade}} + x_{i,j,k,qh}^{\text{imb}} = x_{i,j,h}^{\text{DA,gen,trade}} + x_{i,j,k,qh}^{\text{ID,gen,trade}} \quad \forall(i, j, k), h, qh(h) \quad (19)$$

with

$$x_{i,j,k,qh}^{\text{imb}} = x_{i,j,k,qh}^{\text{imb},+} - x_{i,j,k,qh}^{\text{imb},-} \quad \forall(i, j, k), h, qh(h) \quad (20)$$

For the absolute value consideration of the imbalance volume in (15), a *BIGM* formulation with the auxiliary binary $\delta_{i,j,k,qh}^{\text{imb}}$ leads to the following equations to ensure that $x_{i,j,k,qh}^{\text{imb},+}$ and $x_{i,j,k,qh}^{\text{imb},-}$ are not greater than zero at the same time.

$$x_{i,j,k,qh}^{\text{imb},+} \leq \text{BIGM} \cdot \delta_{i,j,k,qh}^{\text{imb}} \quad \forall(i, j, k), qh \quad (21)$$

$$x_{i,j,k,qh}^{\text{imb},-} \leq \text{BIGM} \cdot (1 - \delta_{i,j,k,qh}^{\text{imb}}) \quad \forall(i, j, k), qh \quad (22)$$

Traders have incentives, if one spot market is dominating the other (e.g. price expectations for the intraday are favorable compared to the day-ahead market), to realize unlimited profit opportunities⁷ of short and long trades between the markets. To account for the trades to be related to the portfolio and not to a purely speculative arbitrage strategy, we introduce volume limits for the short and long position related to the portfolio generation⁸. Equations (23) and (24) limit the short and the long trade volume in the day-ahead market. In consequence, the respective trade volumes are implicitly

⁶According to European Federation of Energy Traders (EFET), not bidding in the forward or day-ahead market in expectation of higher prices in the intraday markets is no capacity withholding and speculation about higher prices in consecutive markets is no market manipulation but a legitimate bidding strategy.

⁷An alternative term sometimes used in this context is arbitrage opportunity. However, we define an arbitrage trade to lead to risk-free profit. As this is not necessarily given, yet the trader might still favor one market expectation over another, we refer to expected profit under risk as profit opportunity.

⁸The up-to-date contracts for balancing responsible parties in Germany provide the regulation that the short or long volume must not exceed a proportion $q^{\text{short/long}}$ of 10 percent of the maximum schedule value of the day. To avoid the maximum operator with decision variables, we consider the sum of the maximum value in the renewable generation forecast and the installed capacity of the controllable plants as approximation for the maximum schedule value of the day instead of $\max_{i,j,k,h,qh(h)}(x_{i,j,h}^{\text{DA,gen,trade}} + x_{i,j,k,qh}^{\text{ID,gen,trade}})$.

limited for the intraday market, too.

$$x_{i,j,h}^{\text{DA,short,trade}} \leq \left(\max_{qh} \left(\sum_{res=1}^{RES} P_{res}^{\text{RES}} \cdot \phi_{qh,res}^{\text{DA}} \right) + \sum_{u=1}^U P_u^{\text{U}} \right) \cdot q^{\text{short}} \quad \forall (i,j), h \quad (23)$$

$$x_{i,j,h}^{\text{DA,long,trade}} \leq \left(\max_{qh} \left(\sum_{res=1}^{RES} P_{res}^{\text{RES}} \cdot \phi_{qh,res}^{\text{DA}} \right) + \sum_{u=1}^U P_u^{\text{U}} \right) \cdot q^{\text{long}} \quad \forall (i,j), h \quad (24)$$

Further, to avoid bids on the same price level that cancel each other out and inflate bidding volumes, Equations (25) and (26) ensure for the day-ahead market that the trader either submits a sell bid or an ask bid on level lda . The analog formulation applies for the intraday market.

$$x_{lda,i,j,h}^{\text{DA,gen,bid}} + x_{lda,i,j,h}^{\text{DA,short,bid}} \leq \text{BIGM} \cdot \delta_{lda,i,j,h}^{\text{DA,ask/sell}} \quad \forall lda, (i,j), h \quad (25)$$

$$x_{lda,i,j,h}^{\text{DA,long,bid}} \leq \text{BIGM} \cdot (1 - \delta_{lda,i,j,h}^{\text{DA,ask/sell}}) \quad \forall lda, (i,j), h \quad (26)$$

Finally, the bids the trader submits to the day-ahead and the intraday market are aggregated for evaluation purposes in the variables $x_{lda,i,j,h}^{\text{DA,bid}}$ and $x_{lid,i,j,k,qh}^{\text{ID,bid}}$ as defined in (27) and (28). These can be interpreted as bid curves submitted to the markets.

$$x_{lda,i,j,h}^{\text{DA,bid}} = x_{lda,i,j,h}^{\text{DA,gen,bid}} + x_{lda,i,j,h}^{\text{DA,short,bid}} - x_{lda,i,j,h}^{\text{DA,long,bid}} \quad (27)$$

$$x_{lid,i,j,k,qh}^{\text{ID,bid}} = x_{lid,i,j,k,qh}^{\text{ID,gen,bid}} + x_{lid,i,j,k,qh}^{\text{ID,short,bid}} - x_{lid,i,j,k,qh}^{\text{ID,long,bid}} \quad (28)$$

4.5.2 Technical Constraints

Several technical constraints need to be respected in the formulation of the bids in order to guarantee the feasibility of the market results for the operation of the plant portfolio. Firstly, the portfolio must be able to provide the reserve commitments, which are defined by the accepted bids for the 4-h-slice ts . As the reserve commitment can be covered by a pool of technical units with any spatial distribution within the market area, each single unit can contribute with its flexibility to reach the market commitment. Thereby, we consider the flexibility contributions of the units to the portfolio to be constant for quarter hours. From technical perspective, we assume reserve provision from both, the units u and the volatile renewable sources res , to be technically feasible⁹. The condition is formulated in (29) for the positive direction, the condition for the negative direction is derived analogously.

$$\sum_{lp=1}^{LP} \beta_{lp,i,ts}^{\text{pos}} \cdot x_{lp,i,ts}^{\text{aFRRpos}} \leq \sum_{res=1}^{RES} x_{i,qh,res}^{\text{aFRRpos,RES}} + \sum_{u=1}^U x_{i,qh,u}^{\text{aFRRpos,U}} \quad \forall ts, qh(ts), i \quad (29)$$

Secondly, the portfolio must fulfill the schedule defined by spot market commitments, which are derived from the accepted bids for each hour in the day-ahead market (and analogously for each quarter hour

⁹Although relatively few capacity of renewable sources is prequalified in today's reserve market, this is caused by rather economical than by technical consideration (see e.g., Brauns, Jansen, Jost, Siefert, Speckmann and Widdel, 2014, for a feasibility study). The main barriers are necessary investments in communication infrastructure and the sheer economics of renewables in providing reserve.

in the intraday market.

$$x_{i,j,h}^{\text{DA,gen,trade}} = \sum_u^U x_{i,j,h,u}^{\text{DA,dispatch,U}} + \sum_{res}^{\text{RES}} x_{i,j,h,res}^{\text{DA,dispatch,RES}} \quad \forall(i, j), h \quad (30)$$

To obtain a feasible dispatch schedule, the minimum load requirement of controllable unit u is modelled with the help of a semi-continuous variable $x_{i,j,k,qh,u}^{\text{dispatch,U}}$ which can only take values that are either 0 or in $[P_u^{\min}, P_u^U]$. As the market constraints distinguish between day-ahead and intraday market dispatch, the overall scheduled dispatch for u is described in (31).

$$x_{i,j,k,qh,u}^{\text{dispatch,U}} = x_{i,j,h,u}^{\text{DA,dispatch,U}} + x_{i,j,k,qh,u}^{\text{ID,dispatch,U}} \quad \forall(i, j, k), h, qh(h), u \quad (31)$$

Thirdly, for a unit u or res to provide negative reserve, it must at least run on that level to be able to decrease the generation. The potential activation of negative reserve capacity must also not violate the minimum load requirement. Likewise, to provide positive reserve, it must at least run on minimum load and a potential activation must not violate the capacity constraint. Equations (32)-(36) formulate these minimum load constraints.

$$x_{i,qh,res}^{\text{aFRRneg,RES}} \leq x_{i,j,k,qh,res}^{\text{dispatch,RES}} \quad \forall(i, j, k), qh, res \quad (32)$$

$$x_{i,j,k,qh,u}^{\text{dispatch,U}} - x_{i,qh,u}^{\text{aFRRneg,U}} \geq P_u^{\min} \cdot \delta_{i,j,k,qh,u}^{\text{aFRRneg,U}} \quad \forall(i, j, k), qh, u \quad (33)$$

$$x_{i,qh,u}^{\text{aFRRneg,U}} \leq \text{BIGM} \cdot \delta_{i,j,k,qh,u}^{\text{aFRRneg,U}} \quad \forall(i, j, k), qh, u \quad (34)$$

$$x_{i,j,k,qh,u}^{\text{dispatch,U}} \geq P_u^{\min} \cdot \delta_{i,j,k,qh,u}^{\text{aFRRpos,U}} \quad \forall(i, j, k), qh, u \quad (35)$$

$$x_{i,qh,u}^{\text{aFRRpos,U}} \leq \text{BIGM} \cdot \delta_{i,j,k,qh,u}^{\text{aFRRpos,U}} \quad \forall(i, j, k), qh, u \quad (36)$$

Fourthly, the provision of positive reserve and the dispatch of a unit u is limited by its nominal capacity P_u^U , leading to capacity constraint (37). Likewise, a unit res is naturally limited by its nominal capacity P_{res}^{RES} derated with the generation forecast $\phi^{\text{DA/ID}} \in [0, 1]$. As described in Section 4.7 we distinguish between the deterministic day-ahead forecast and the scenario-based intraday update. Hereby, to respect the potential downward or upward correction of an intraday forecast update $\phi_{k,qh,res}^{\text{ID}}$ compared to $\phi_{qh,res}^{\text{DA}}$, the possible reserve provision of a renewable unit $x_{i,qh,res}^{\text{aFRRpos,RES}}$ and dispatch must satisfy two capacity constraints (38) and (39). With this formulation, the positive reserve provision is implicitly limited to the minimum out of the day-ahead and the intraday updates of the generation forecast contained in Ω .¹⁰

$$x_{i,qh,u}^{\text{aFRRpos,U}} + x_{i,j,h,u}^{\text{DA,dispatch,U}} + x_{i,j,k,qh,u}^{\text{ID,dispatch,U}} \leq P_u^U \quad \forall(i, j, k, h, qh(h), u) \quad (37)$$

$$x_{i,qh,res}^{\text{aFRRpos,RES}} + x_{i,j,res,h}^{\text{DA,dispatch,RES}} \leq P_{res}^{\text{RES}} \cdot \phi_{qh,res}^{\text{DA}} \quad \forall(i, j), h, qh(h), res \quad (38)$$

$$x_{i,qh,res}^{\text{aFRRpos,RES}} + x_{i,j,h,res}^{\text{DA,dispatch,RES}} + x_{i,j,k,qh,res}^{\text{ID,dispatch,RES}} \leq P_{res}^{\text{RES}} \cdot \phi_{k,qh,res}^{\text{ID}} \quad \forall(i, j, k), h, qh(h), res \quad (39)$$

Further, the fuel storage capability for the dispatchable RES plants onsite (e.g., for a biogas plant) is limited, which leads to a minimum and maximum daily generation $\nu^{\min/\max}$ of unit u as proportion

¹⁰This goes perfectly in line with the feed-in potential based approach to quantify reserve provision potential of volatile renewable sources (Brauns et al., 2014).

of a baseload operation of the installed capacity.

$$|QH| \cdot P_u^U \cdot \nu_u^{\min} \leq \sum_{qh=1}^{QH} x_{i,j,k,qh,u}^{\text{dispatch,U}} \leq |QH| \cdot P_u^U \cdot \nu_u^{\max} \quad \forall (i, j, k), u \quad (40)$$

with $|\cdot|$ as the cardinality of a set.

Finally, each unit u has a limited load change gradient ΔP_u , which needs to be respected to obtain technically feasible results. We consider it to be the same for upward and downward load changes and define it as proportion of the installed capacity P_u^U . At the transition between two quarter hours, load changes can originate from all considered market segments. Therefore, some additional constraints are required. Logically, the maximum possible load changes from all market segments, including potential reserve activation gradients, must comply with the load change gradient of u . To depict the potential reserve activation gradient between two consecutive quarter hours qh and $qh + 1$, the change in the flexibility contribution of u is split into the negative and positive part with positive variables. To model the negative reserve direction, the summands for qh and $qh + 1$ are swapped, leading to (41) and (42).

$$x_{i,qh,u}^{\text{aFRRpos,U}} - x_{i,qh+1,u}^{\text{aFRRpos,U}} = \Delta x_{i,qh,u}^{\text{aFRRpos,U,+}} - \Delta x_{i,qh,u}^{\text{aFRRpos,U,-}} \quad \forall i, qh, u \quad (41)$$

$$x_{i,qh+1,u}^{\text{aFRRneg,U}} - x_{i,qh,u}^{\text{aFRRneg,U}} = \Delta x_{i,qh,u}^{\text{aFRRneg,U,+}} - \Delta x_{i,qh,u}^{\text{aFRRneg,U,-}} \quad \forall i, qh, u \quad (42)$$

Similarly, the spot market schedule changes for u are split with positive variables in upward and downward direction. As for the overall scheduled dispatch in (31), the day-ahead and the intraday market are considered together.

$$x_{i,j,k,qh,u}^{\text{dispatch,U}} - x_{i,j,k,qh+1,u}^{\text{dispatch,U}} = \Delta x_{i,j,k,qh,u}^{\text{spot,U,+}} - \Delta x_{i,j,k,qh,u}^{\text{spot,U,-}} \quad \forall (i, j, k), qh, u \quad (43)$$

To ensure that the changes in market commitments are not simultaneously non-zero, following *BIGM* formulations must hold for all the considered market segments. For conciseness, only the constraints for the changes in spot market commitments are presented. Formulations for the reserve segments follow analogously.

$$\Delta x_{i,j,k,qh,u}^{\text{spot,U,+}} \leq \text{BIGM} \cdot \delta_{i,j,k,qh,u}^{\text{spot,U}} \quad \forall (i, j, k), qh, u \quad (44)$$

$$\Delta x_{i,j,k,qh,u}^{\text{spot,U,-}} \leq \text{BIGM} \cdot (1 - \delta_{i,j,k,qh,u}^{\text{spot,U}}) \quad \forall (i, j, k), qh, u \quad (45)$$

The binary variable $\delta_{i,j,k,qh,u}^{\text{dispatch,U}}$ indicates whether the dispatch changes in upward or downward direction at the transition from qh to $qh + 1$. With (41)-(43), the load change constraint in upward and downward direction for a technical unit u formulates as denoted by (46) and (47). Note, that the chosen formulation with quarter hour resolution of spot market commitments and flexibility contributions to the portfolio's reserve provision implicitly respects the different temporal resolutions of reserve (4h), day-ahead (1h) and intraday (15min) markets. If these were modeled according to the respective product duration, separate cases for (a) the transition to the first quarter hour of a time slice, (b) the transition to the first quarter hour of an hour, and (c) the transition to an intra-hour quarter hour

should be distinguished.

$$x_{i,qh,u}^{\text{aFRRpos,U}} + x_{i,qh,u}^{\text{aFRRneg,U}} + \Delta x_{i,qh,u}^{\text{aFRRpos,U,+}} + \Delta x_{i,qh,u}^{\text{aFRRneg,U,+}} + \Delta x_{i,j,k,qh,u}^{\text{spot,U,+}} - \Delta x_{i,j,k,qh,u}^{\text{spot,U,-}} \leq P_u \cdot \Delta P_u \quad \forall (i, j, k), qh \quad (46)$$

$$x_{i,qh,u}^{\text{aFRRpos,U}} + x_{i,qh,u}^{\text{aFRRneg,U}} + \Delta x_{i,qh,u}^{\text{aFRRpos,U,-}} + \Delta x_{i,qh,u}^{\text{aFRRneg,U,-}} + \Delta x_{i,j,k,qh,u}^{\text{spot,U,-}} - \Delta x_{i,j,k,qh,u}^{\text{spot,U,+}} \leq P_u \cdot \Delta P_u \quad \forall (i, j, k), qh \quad (47)$$

Whereas (37) only considers the sheer capacity of u , (46) and (47) emphasize the value of the flexibility, both in upward and downward direction, and make clear that all market segments are competing for the flexibility of the portfolio. For example, during a scarcity of upward flexibility, a reduction of the spot market dispatch releases upward flexibility to be used for other commitments. It enhances the reserve potential (both positive and negative) and creates the option to increase the positive (decrease the negative) reserve contribution of u to the portfolio's reserve provision. Obviously, it is upon the trader to determine a strategy in which market segments and at which price to allocate the available resources.

4.6 Stochastic Programming Constraints

The problem is formulated as a multi-stage stochastic program. However, for one trading decision with the same information (at the same node of the tree), the decisions have to be consistent for the consecutive stages. Therefore, non-anticipativity constraints for all trading decisions are included in the model formulation according to the information relations: Reserve bids must be consistent throughout all $i \in I$, as well as bids on the day-ahead ($j \in J$) and intraday ($k \in K$) market. With $Ord(\cdot)$ defined as the ordinal number of an element in its set and $|\cdot|$ as the cardinality of the set, we formulate the constraints for the positive reserve (48) and the day-ahead market (49) bids¹¹.

$$x_{lp,i,ts}^{\text{aFRRpos,bid}} = x_{lp,i+1,ts}^{\text{aFRRpos,bid}} \quad \forall lp, \{i \mid Ord(i) < |I|\}, ts \quad (48)$$

$$x_{lda,i,j,h}^{\text{DA,bid}} = x_{lda,i,j+1,h}^{\text{DA,bid}} \quad \forall lda, i, \{j \mid Ord(j) < |J|\}, h \quad (49)$$

4.7 Characterization and Modelling of Uncertainties

For the methodology to deliver meaningful results, it is essential to describe the uncertainty of the real-world problem as accurate as possible. For the sake of computational tractability, we describe the uncertainty as a finite probability space Ω defined by scenarios ω spanning a scenario tree in three stages with scenario branches $i \in I$, $j \in J$, and $k \in K$. The first stage scenario branching, denoted by i , represents the uncertainty of the marginal auction price of the reserve market for the positive and negative product. For our models we use information that is available at 8 am on the day before delivery, one hour before the tender for automatic Frequency Restoration Reserve (aFRR) closes.

As mentioned in Section 2, the reserve market prices cannot be completely explained by fundamental

¹¹Note, that considering only the aggregated bids enables the switch between short volume and dispatch of generation units as scenarios unfold. Formulations for the negative reserve and intraday market bids follow respectively.

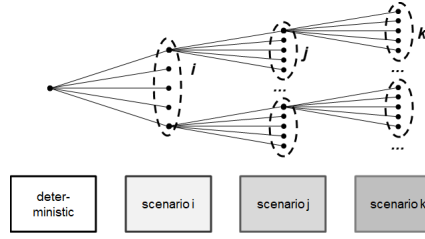


Figure 2: Illustration of the scenario tree with indices i , j and k for the uncertainty considered in the decision stages. The stages correspond to the market segments balancing reserve, day-ahead spot market and intraday spot market.

drivers. This creates a situation where the reserve market prices are subject to an inherent uncertainty, that especially small market participants are exposed to. The marginal reserve prices¹² are modelled with the help of an additive model and a simulation of the stochastic components applying mean-reverting processes with jump regimes, as proposed by Keles, Genoese, Möst and Fichtner (2012) for modeling uncertain prices in electricity markets. The additive model explains the marginal prices $y_{s,w,t}^{\text{reserve}}$ and includes the mean seasonal price for the time slice $\bar{y}_{s,t}^{\text{reserve}}$, the day-ahead PV generation forecast x_t^{PV} , the day-ahead residual load forecast x_t^{RL} , and the price of the previous day's auction for the respective time slice y_{t-6} . Further, weekend days and working days are distinguished with a dummy variable δ_w . Combined with seasonal distinction by winter, summer, and transitional season (i.e., spring and fall)¹³, six logarithmic models are estimated by the following model equation:

$$\log y_{s,w,t}^{\text{reserve}} = c_s + \beta_1 \cdot \log \bar{y}_{s,t}^{\text{reserve}} + \beta_2 \cdot \log x_t^{\text{PV}} + \beta_3 \cdot \log x_t^{\text{RL}} + \beta_4 \cdot \log y_{t-6} + \beta_5 \cdot \delta_w + \beta_6 \cdot \delta_w \cdot \log \bar{y}_{s,t}^{\text{reserve}} + \beta_7 \cdot \delta_w \cdot \log x_t^{\text{PV}} + \beta_8 \cdot \delta_w \cdot \log x_t^{\text{RL}} + \epsilon_t \quad (50)$$

Alternative potential fundamental drivers like carbon emission and fuel prices or derivatives like the clean dark spread¹⁴ have not been found significantly improving the goodness-of-fit of the additive model or suffered from strong multicollinearity and were therefore not further considered. We provide model results for model alternatives including the omitted variables in Table 4 in Annex A.2. Please note, that the seasonal mean $\bar{y}_{s,t}^{\text{reserve}}$ to some extent implicitly captures the price influence of the omitted fundamentals.

The series of stochastic residuals ϵ_t is modelled with the help of a mean-reversion process (Ornstein–Uhlenbeck process, see Uhlenbeck and Ornstein, 1930) and and jump regimes. Regime switching probabilities and calibration of the mean-reversion process are modelled adapting the procedure introduced by Keles et al. (2012). To determine scenarios for the optimization, the obtained stochastic models are simulated 1000 times and reduced by means of k-means clustering. In Annex A.2, more details for the modeling of the reserve prices as well as a validation are provided. For the application in the case study, we use ten scenarios with probability according to the clustering to describe the uncertainty of reserve prices.

¹²Precisely, to obtain a smoother time series, the 90 percent quantiles of the accepted bids in each auction are considered as marginal reserve prices.

¹³Winter: December, January, February; Summer: June, July, August; Transition: rest.

¹⁴The clean dark spread is defined as the difference between the spot market price and the costs for fuel and emission certificates of a hard coal power plant with typical efficiency.

The marginal reserve prices $p_{i,ts}^{\text{reserve,pos}}$ (and $p_{i,ts}^{\text{reserve,neg}}$) determine the acceptance for potential reserve bids on price level lp (and ln) for the positive (and the negative) product in scenario i and time slice ts . For the formulation of the optimization problem, the acceptance of a bid is translated to the binary parameter $\beta_{ln,i,ts}^{\text{pos}}$ as follows (analogously $\beta_{ln,i,ts}^{\text{neg}}$ for the negative product):

$$\beta_{ln,i,ts}^{\text{pos}} = \begin{cases} 1, & \text{if } lp \leq p_{i,ts}^{\text{reserve,pos}} \\ 0, & \text{otherwise.} \end{cases} \quad (51)$$

The second stage scenario branching, denoted by j , depicts the price uncertainty of day-ahead market prices. This uncertainty is on the one hand driven by potential changes in renewable generation and load forecasts between the gate closure of the reserve market (9 am, d-1) and that of the day-ahead spot market (12 am, d-1). On the other hand, a stochastic component for the day-ahead market itself is modelled. Potential changes in residual load forecasts (including the modeling of renewable generation and consecutively residual load) until gate closure of the day-ahead market, influence of forecast changes and stochastic nature of day-ahead market prices, are modelled with a mean-reversion process (Ornstein–Uhlenbeck process, see Uhlenbeck and Ornstein, 1930), provided with the information at 12 am on the day-ahead (d-1). As in this paper a price-taking trader is modelled, the scenarios consist of price levels and respective probabilities.

Analogously to the reserve market, to use the price scenarios in the problem formulation, the price levels are translated into a binary parameter $\beta_{lda,j,h}^{\text{DA}}$ indicating whether a bid on a certain price level lda in hour h is accepted or declined in scenario j . Note, that the second stage is assumed to be independent from the first stage, meaning that the realization of reserve prices (i) has no influence on day-ahead spot market prices.

Based on the second stage the third stage scenario branching, denoted by k , captures an updated renewable generation and load forecast under conditional expectation, resulting in an updated residual load forecast. These are sources of quantity uncertainty and result in a price uncertainty with regard to intraday market prices in the quarter hours qh in the scenario leaves k , reflecting the information uncertainty 60 minutes from real-time.

To thoroughly model the effects as well as the stochastics of changing residual load forecasts on spot market prices, three different sources of uncertainty are distinguished and modeled: the uncertainty of solar generation, the stochastic component of the residual load (to be interpreted as changes in either wind generation or the system load) and the stochastic component of the day-ahead and intraday market themselves. Note, that wind generation as a source of uncertainty is not modeled explicitly. In comparison to the solar generation, that follows a usual daily pattern and can be categorized into levels relatively straight forward, the wind generation does not follow a usual daily pattern but rather day-specific patterns and is therefore difficult to model with the use of a limited number of type days. We therefore include the forecasting uncertainty of wind generation in the model for the residual load uncertainty. Referring to the idea of type days, in this way we consider for the uncertainty of wind generation but relate these to seasonal-average wind days. For deriving trading decisions in real-world applications, we consider it reasonable to include forecasts for the renewable generation and consequently for the residual load on a daily basis into the approach. In particular, this allows to account for day-specific wind patterns and their risk implications.

The modeling of the solar infeed, the residual load, as well as the spot market prices follows the basic

ideas of Keles et al. (2012) and Lingohr and Müller (2019). However, the integrated modeling of mutual dependencies requires an enhanced approach. To capture the character and relations adequately, multivariate mean-reverting processes and stochastic differential equations are estimated based on empirical data and simulated with Monte Carlo. Based on the stochastic simulations, scenarios are derived by k-means clustering, as is presented in further detail in Russo et al. (2021). The stochastic modeling is applied to three seasons (summer, winter, transition) and distinguishes between working and weekend days as well as three levels of residual load (low, medium, high). In total, 18 distinct scenario trees are generated to apply the optimization to the most relevant type days. The transition from stage two to stage three is not assumed to be stage-wise independent, but the presented approach deploys conditional expectations to obtain consistent and arbitrage-free scenarios across the stages. For the case study, five scenarios for the j and k , respectively, are derived with probabilities according to the assumed normal distribution of the σ -ranges¹⁵ in the scenario definition. In the notation, for five scenario leaves, $j1$ is followed by $k1 - k5$, $j2$ by $k2 - k10$, and so on. Analogously to the previous market segments, to use the price scenarios in the problem formulation, the price levels are translated into a binary parameter $\beta_{lid,j,k,qh}^{ID}$ denoting whether a bid on a certain price level lid in quarter hour qh is accepted or declined in scenario j 's follow-up scenario k . Combined with the 10 reserve price scenarios, each of the type days' scenario tree considers 250 possible scenarios to characterize the uncertainty from the day-ahead towards real-time.

An illustrative scenario tree to demonstrate the extent of the price uncertainty in the considered segments and the solar generation uncertainty estimated with the stochastic modeling based on empirical data is provided for the typeday $tra2$ ¹⁶ in the Annex A.2 and A.4 in Figures 14-16.

5 Case Study

In this section, we conduct a case study in which we apply the proposed methodology to an exemplary power plant portfolio in the Germany market design setting. Germany with its high renewable shares, high data availability, and liquid day-ahead and intraday trading is particularly suitable to demonstrate our approach. We present characteristics of optimal bidding strategies under different considerations of risk. To define risk preferences, we enumerate combinations of the parameter α at levels 85%, 90%, and 95% (i.e., consideration of the 15%, 10%, and 5% worst cases) and λ at levels 10%, 25%, and 50% (i.e., the weighting of the CVaR on α -level compared to the expected value of contribution margins). Where necessary, for the results to remain concise, we present mainly the results for the risk strategy with $\alpha = 95\%$ and $\lambda = 50\%$, corresponding to a strong risk aversion. As a benchmark, we present results for the risk-neutral case (i.e., $\lambda = 0\%$). The complete results for the other strategies are provided in the supplementary material.

¹⁵As discussed by Keles (2013) and deployed in adapted manner by Russo et al. (2021), the scenarios are derived from the expected median value of the stochastic simulation by deviating defined multiples of the standard deviation for each time step and type day respectively. To derive five scenarios, the expected median (denoted with $j1$) is complemented by the values $+/ - \sigma$ (denoted with $j2/j3$) and the values $+/ - 2 \cdot \sigma$ (denoted with $j4/j5$) with probabilities according to an assumed Normal distribution. This leads to $pr_j = 0.25$ for $j1$, $j2$, and $j3$, and $pr_j = 0.125$ for $j4$ and $j5$. Same applies for the leaves denoted by k .

¹⁶A working day with medium PV feed-in and medium residual load in the transition season.

5.1 Data and Practical Implications

For Germany, market results of the reserve market are publicly available at regelleistung.net (2021), and for day-ahead market on the ENTSO-E transparency platform (ENTSO-E, 2021). As no historical feed-in forecast data other than the ones from ENTSO-E are available publicly, the generation forecast for the PV plants in the trader’s portfolio are assumed to be perfectly correlated with the system-wide generation forecast, in line with the assumption in Russo and Bertsch (2020). This implies a spatial dispersion of the PV plants that is representative for the overall German PV portfolio¹⁷. Hereby, the stochastic process for the PV intraday forecast update is fed by two inputs to model the information available to the trader as accurate as possible: firstly, the intraday forecast $\phi_{qh,res}^{ID}$ update for the respective renewable plant res and quarter hour qh , provided by ENTSO-E in the morning of the trading day. Secondly, to account for the latest available information at the time of the intraday decision on stage three, the forecast error between the intraday forecast for $qh - 2$ and the (meanwhile available) realisation of $qh - 2$, denoted by $x_{qh-2,res}^{real}$, is considered. Including the latest realised quarter hour $qh - 2$ enables to capture the latest information on PV generation in the decision. We stress at this point, that the difference $(\phi_{qh,res}^{ID} - x_{qh,res}^{real})$ is strongly auto-correlated at a lag of two.

With regard to the price risk, the stochastic price process captures effects of intraday renewable generation and load forecast updates. As mentioned in Section 3, a simplification is applied by taking the price index p^{ID3} (published by EPEX Spot, 2021), the weighted average price of all trades closed in the last three hours before the delivery period. For a more profound representation of continuous intraday price processes and intraday trading strategies, we refer to Kath and Ziel (2018) and Narajewski and Ziel (2020).

The selection of an appropriate recent time horizon of data to estimate the models turns out to be challenging, as both the spot markets and the reserve markets in Germany went through several adjustments in recent years. For the models to provide meaningful scenarios as input for the trading problem, unfortunately a trade-off between the number of observations and the absence of structural changes (e.g., induced by market design adjustments) is necessary.

First and foremost, the reserve market plays a crucial role, as major market design changes were introduced in July 2018, October 2018, July 2019, and November 2020. In July 2018, the temporal resolution and lead times were reduced from weekly off-peak and peak products to 4-hour products that are auctioned on a day-ahead basis. Then, in reaction to strategic bidding and excessive energy price bids, in October 2018 a new scoring rule was introduced calculating a scoring value as linear combination of the capacity price bid and the energy price bid. However, strategic bidding under this scoring rule led to undesirable, security-of-supply-threatening impacts. In July 2019, the market design change was therefore reversed to a capacity-price-based scoring. Since November 2020, a separate auction for balancing energy price bids takes place 60 minutes before real-time, in which also bidders without accepted capacity price bid may participate.

Secondly, due to unwanted ring flows through Poland and the Czech Republic the formerly single market area Austria-Germany was split from October 2018 on. As the market split changed both the demand and the supply structure for the German market participants, price formation on both the day-ahead and the intraday market was affected.

¹⁷However, in the real-world (commercial) application, the availability of the required portfolio-specific forecast data would be no limiting factor.

We therefore use data from the time horizon between July 2019 and the first COVID19-caused lockdown in March 2020 to estimate the stochastic price processes. In this period, we observe stable market circumstances and no structural changes on either the demand or the supply side.

5.2 Composition of Portfolio

The portfolio, for which the presented methodology is particularly relevant, should meet certain characteristics regarding the cost-structure. In order to compete with the reserve market prices, the variable costs of the portfolio should be close to average spot market price levels. Just and Weber (2015) refer to the relation between variable costs and spot market price levels as marginality and distinguish between infra-marginal (i.e., $\kappa^{\text{var}} < p^{\text{spot}}$), marginal (i.e., $\kappa^{\text{var}} = p^{\text{spot}}$) and extra-marginal (i.e., $\kappa^{\text{var}} > p^{\text{spot}}$) power plants. In this terminology, the portfolio should change between being infra-marginal, marginal, and extra-marginal for different time steps and scenarios.

For the case study, we consider a portfolio consisting of a set of electricity-led and thus controllable biogas power plants, and a set of PV plants as volatile renewable source to be suitable to reflect the strengths of the presented approach. Firstly, it depends upon both, the uncertainty of generation quantities (relevant for *res* units) and the uncertainty of price levels (relevant for both *u* and *res* units). Secondly, the variable costs κ_{u1}^{var} are roughly in the range of price variations of the spot markets. Finally, the portfolio is able to provide flexibility in both upward and downward direction or to use the flexibility to profit from spot market prices.

The portfolio for the case study is therefore defined as presented in Table 2. For conciseness, the plants are aggregated and handled as single unit *u1* and *res1*, respectively. The only limitation associated with this is that if multiple smaller units are considered, the minimum load requirement (P_u^{min}) could be handled more flexibly.

Table 2: Composition of plant portfolio and techno-economic parameters for case study.

Parameter	Symbol	Unit	Value
Installed capacity PV generation <i>res1</i>	P_{res1}^{RES}	[MW]	100
Maximum load change of <i>res1</i> within 5 minutes, as share of P_{res1}^{res}	$\Delta P_{res1}^{\text{RES}}$	[-]	1.00
Installed capacity controllable generation <i>u1</i>	P_{u1}^{U}	[MW]	100
Minimum load requirement of <i>u1</i> , as share of P_{u1}^{U}	P_{u1}^{min}	[-]	0.20
Minimum daily generation of <i>u1</i> , as share of baseload operation at P_{u1}^{U}	ν_{u1}^{min}	[-]	0.50
Maximum daily generation of <i>u1</i>	ν_{u1}^{max}	[-]	0.95
Variable costs of <i>u1</i>	κ_{u1}^{var}	[EUR/MWh]	40
Maximum load change of <i>u1</i> within 5 minutes, as share of P_{u1}^{U}	ΔP_{u1}^{U}	[-]	0.50

5.3 Evaluation of Trading Strategies for the Portfolio

As the results for all investigated 18 type days are very extensive, we present the results for an exemplary type day in detail, and based on that we discuss the findings more generally. We present the results for a weekday with a medium level of PV generation and a medium residual load level in the transition season.

Before investigating the decision variables as well as the rationales and characteristics behind the different trading strategies, we first look at the values of the target function and the overall results. To visualize the terms contained in the target function with risk consideration (i.e., expected contribution margins and CVaR), we define the efficient frontier as all combinations of expected contribution margins and CVaR for trading strategies, that were found not to be dominated by another set of decision variables.

Figure 3 presents the efficient frontier plot for all considered combinations of α and λ , as well as for the risk-neutral case. For all investigated CVaR-intervals α , a similar concave pattern can be observed. Obviously, the consideration of risk decreases the expected value of the trading decision, and at the same time with an increasing weight of the risk metric the risk exposure is reduced. Noteworthy, the increase in λ from risk-neutral (0%) to 10% comes with a large impact, likewise the increase from 10% to 25%. In the former, the expected contribution margins decrease considerably (decrease of 1,228-1,903 EUR/day), whereas the CVaR increases strongly (27,763-35,330 EUR/day), indicating a lower risk exposure. In the increase from 10% to 25%, the expected contribution margins decrease stronger (decrease of 5,110-5,659 EUR/day compared to risk-neutral), but yields further benefits with regard to the risk exposure (CVaR increase of 51,000-56,003 EUR/day compared to risk-neutral). However, the increase in λ from 25% to 50% has comparably a small impact. The reduction of the expected contribution margins outweighs the small changes in risk exposure. Overall, a concave shape of the efficient frontier can be observed for all α levels. Table 5 in Annex A provides an overview over the numbers determining the efficient frontier. We stress at this point, that none of the defined and evaluated risk strategies strictly dominates another. In a real-world application, a trader would still be required to choose the risk preference, yet based on information about the opportunities and risks related with the trading decision.

In order to gain insights about the distributional patterns of the contribution margins in the different

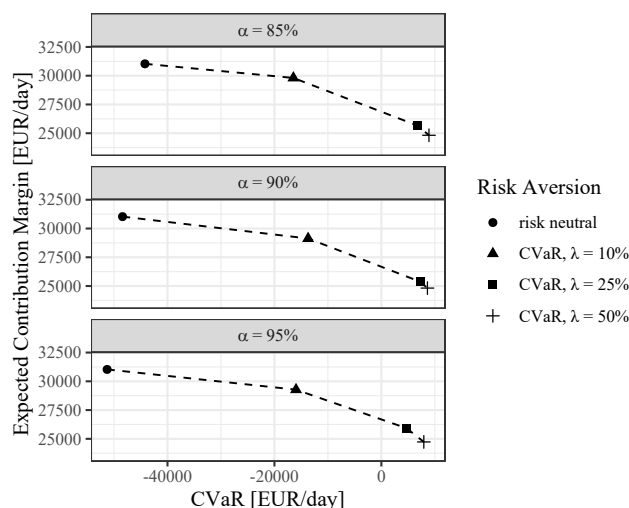


Figure 3: Efficient frontier of trading decisions for different levels of CVaR interval (α) and risk aversion (λ), medium weekday transition season (tra2).

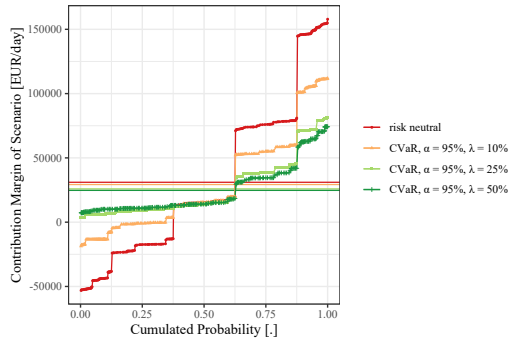


Figure 4: Empirical cumulative distributions of contribution margins throughout scenarios for trading strategies considering the $\alpha = 95\%$ level for the CVaR, medium weekday transition season (tra2).

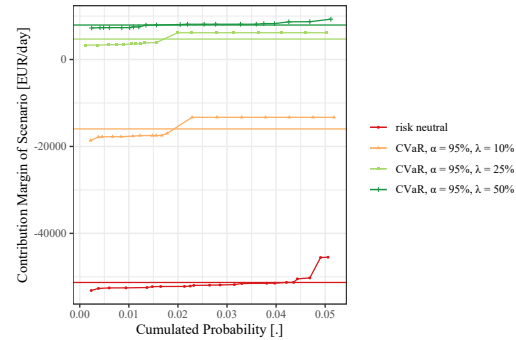


Figure 5: Empirical cumulative distributions of contribution margins in the 5% of worst case scenarios (CVaR range), medium weekday transition season (tra2).

scenarios¹⁸, we arrange the contribution margins in increasing order for each trading strategy. This visualization can be compared to an empirical cumulative distribution function (ECDF) of a distribution and reads as follows: The contribution margin is lower or equal to the value on the vertical axis with the probability level indicated by the horizontal axis. To be able to identify fat tails in the distribution, a second plot zooms into the interval considered for the risk metric CVaR. The expected value of the contribution margin and the CVaR are respectively included into the plots as horizontal lines. Figures 4 and 5 show the ECDF for the strategies with $\alpha=95\%$. One intuitive result derived from the visualization of the risk distribution is that the consideration of risk drastically lowers the spread between the worst and the best cases and thus narrows the distribution, at the expense of a moderate loss in expected contribution margins. Evaluations for the other α -values show analogous patterns.

Investigating the contribution of each market segment to the portfolio's contribution margins in the different scenarios for different trading strategies, we find the main source of risk and the major lever of risk hedging strategies to lie in the spot market decisions, i.e. how to submit bids to the day-ahead and intraday market. To present key differences of risk-neutrality and risk aversion in trading strategies, Figures 6 to 7 show the trader's optimal bids on the day-ahead market and intraday market for the risk-neutral and the strongly risk-averse strategy ($\alpha = 95\%$, $\lambda = 50\%$). As these bids are submitted on the second (day-ahead) and third (intraday) stage of the problem, we summarize the bids for the representative realization $i1$ of the first stage. Note that the actual bids submitted on a stage do not anticipate realized information from later stages and are thus consistent for all j and k for the day-ahead and the intraday market, respectively (see Eq. 48-49).

Figure 6 shows for the risk-neutral day-ahead market bids. The expectation of potentially higher prices in the intraday market yields buying bids, indicating the trader is willing to take a long position. These bids are in the range of the trader's allowed long/short position range (see Eq. (24) and (23)), and are not linked to the portfolio dispatch. The risk-neutral trader seeks to sell the electricity generation on the intraday market, that offers (in expectation) a slightly higher, yet more volatile price level, and even increases a high selling position to sell more volume than the generation capability. On

¹⁸In total, we distinguish 250 scenario leaves with non-equally distributed probabilities. See Section ?? and Annex A.2 for more details on the construction of the trees and probabilities.

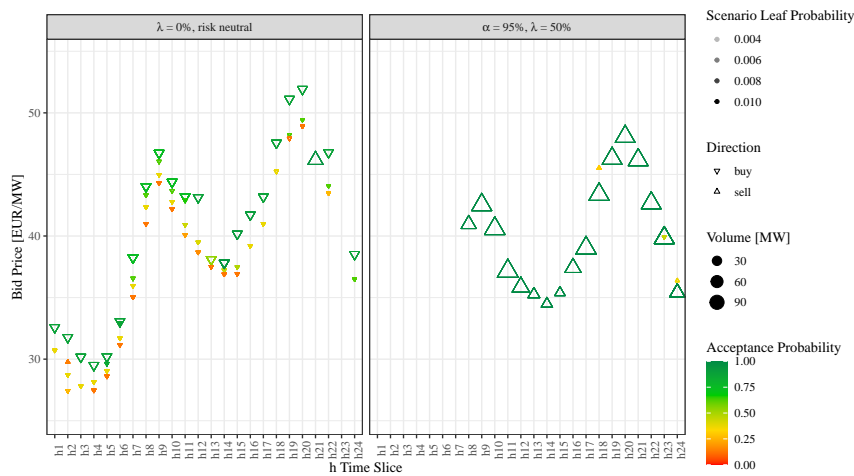


Figure 6: Day-ahead market bids for risk-neutral strategy, medium weekday transition season (tra2). day-ahead market bids for risk-averse strategy ($\alpha = 95\%$, $\lambda = 50\%$), medium weekday transition season (tra2).

the other hand, the risk-averse strategy focuses on reducing the risk exposure early on by selling most of the generation on the day-ahead market at secure yet in expectation slightly lower prices. Notably, the day-ahead trading volumes of the risk-averse trading strategy are considerably higher. Further, the risk-averse strategy contains ask bids on price levels below the variable costs of the dispatchable unit u , allowing to re-buy generation that was sold in the day-ahead market at a higher price. The risk-neutral intraday bids contain less bids to re-position the portfolio, but rely on the (in expectation) higher prices on the intraday market.

The submitted bids on the day-ahead market and the eventual market result determine the position

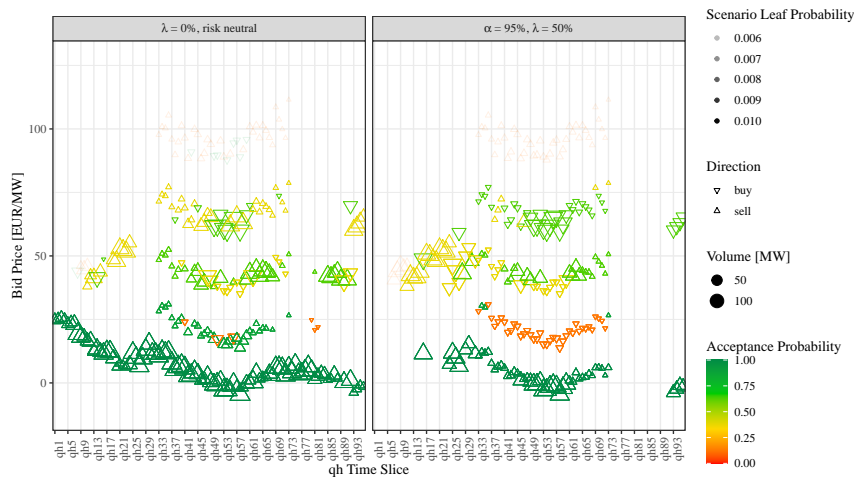


Figure 7: Intraday market bids for risk-neutral strategy, medium weekday transition season (tra2). Intraday market bids for risk-averse strategy ($\alpha = 95\%$, $\lambda = 50\%$), medium weekday transition season (tra2).

of the trader when facing the intraday stage. Figure 7 shows the submitted intraday market bids, that follow the respective day-ahead market bids for the risk-neutral and the risk-averse trading strategy.

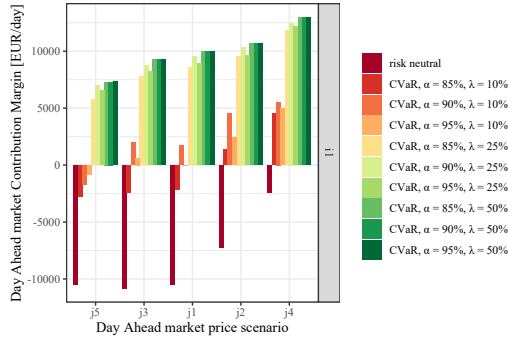


Figure 8: Diagram of contribution margins on the day-ahead market for realizations of scenario j as successor of $i1$ under different risk attitudes.

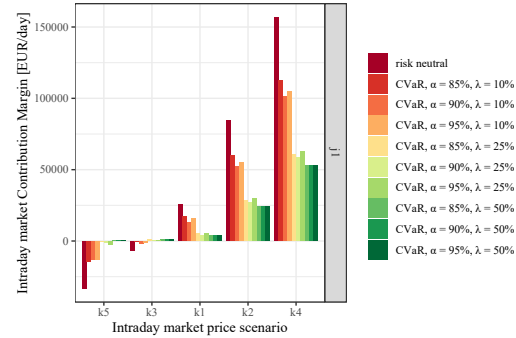


Figure 9: Diagram of contribution margins on the intraday market for realizations of scenario k as successor of $i1$ and $j1$ under different risk attitudes.

It can be observed in the lower string of bids, that driven by the pre-positioning (long position) from the day-ahead market, the risk-neutral strategy mainly consists in selling the electricity at any price on the intraday market. In case the intraday market settles at a higher price level, these bids will be remunerated with the higher price, too, which stands in opposition to bids on the reserve market. It can further be observed, that a considerable amount of bids is placed on price levels, that are linked to a low acceptance probability.

For the representative scenario realizations $i1$ and $j1$, Figures 8 and 9 present the resulting contribution margins from the day-ahead and the intraday market for the considered trading strategies. As discussed before, the risk-averse bids prevent the trader from taking a long position on the day-ahead market and result in profitable sales, which to some extent depends on the realization of j . On the other hand, the risk-neutral ask bids lead to considerable costs (i.e., negative contribution margins), and no positive contribution margins on the day-ahead market. The value of the long position then strongly swings with the realized intraday market scenario, leading to further negative contribution margins if prices are low ($k5$ and $k3$) and to very profitable sales if prices are high ($k2$ and $k4$)¹⁹. Inspecting the successors of the lower ($j3$ and $j5$) and higher ($j2$ and $j4$) day-ahead market price scenarios (see Figure 8) yields the same relations yet differently pronounced. The remaining strategies with a moderate risk-aversion follow a compromise.

The day-ahead bids do not contain ask bids to profit from potentially higher prices in the intraday market, yet a share of the (expected) portfolio generation is offered only at high price levels with low acceptance probabilities on the day-ahead market. Such a mixed bidding behavior allows for both, profiting from secure day-ahead market revenues as well as profiting from higher or lower prices in the intraday market. It avoids excessive ask or sell pressure in the intraday market and provides a balance between the advantages of the day-ahead market (low uncertainty, in expectation lower prices) and the ones of the intraday market (high uncertainty, in expectation higher prices). Whether and which bids are submitted to the reserve market is determined by the opportunities the reserve market and the following spot markets offer and at which costs in terms of operational constraints, such as scheduling restrictions and inflexibility, the reserve can be provided by the portfolio. The

¹⁹Note that the scenarios are not equally probable. As mentioned in Section 4.7, the probability of the moderate scenarios (three scenarios in the center of the plot) is 25% each, and the probability of the outer scenarios is 12.5% each.

opportunities are three-fold: First, the pay-as-bid remuneration opens up a strategy space to decide among different reserve price levels and volumes to bid on them. Hereby, the rationale is to avoid the winner's curse introduced to economic theory by Thaler (1988). Second, the expected level of spot market prices and thus the expected profits require to consider which market is more profitable. Third, the opportunity to profit from price variations between the day-ahead and the intraday spot market by flexibly adjusting to new information.

It therefore occurs, as in the case of the considered typeday *tra2*, that the spot market opportunities dominate the reserve market prices for the positive direction and no bids are submitted to the positive reserve segment. Investigating the economics of the reserve market segments (see Just and Weber, 2008, 2015, for formal descriptions of the interplay between spot and reserve markets), it becomes clear that providing positive reserve competes with spot market operations, whereas providing negative reserve can be considered a complementary element to spot market operations²⁰, and brings only little operational restrictions. A main finding is therefore, that the reserve bids determined with the stochastic optimization differ fundamentally for negative and positive reserve provision.

The bids submitted for the positive reserve, if any are submitted, are placed only on high price levels. In the however unlikely case of a high reserve price scenario, the trader profits from the accepted bid(s). In the case the submitted bids are rejected, the following spot markets offer similar profit opportunities. This rationale is further confirmed by the pay-as-bid remuneration, as it incentivizes riskier reserve market bids. On the other hand, the bids submitted for the negative reserve are not balancing potential reserve market profits with potential spot market profits. The rationale aims at balancing the opportunities among the reserve price levels. Therefore, more diversification in bids and patterns for different risk strategies can be observed. To illustrate this, Figure 19 in the Annex A compares the bids submitted for the time slice 12-16h for the risk-neutral strategy and for a risk-averse strategy. The first observation to note is that the risk aversion leads to a diversification in terms of price levels and aims at securing revenues, whereas the risk-neutral strategy places the reserve bids on a high price level. This can be interpreted as betting on a high price scenario. Secondly, the volume offered in the risk-averse strategy exceeds the volume offered in the risk-neutral strategy, which corresponds to accepting more operational constraints for the spot market decisions. In Annex A.5, we provide additional results, such as the bid curves for all considered risk strategies in time slice 12-16h (Figure 10) and the bids submitted for all time slices of the *tra2* day (Figure 20). To present results for another typeday, we also provide the bids for the negative reserve for a summer weekend day with high residual load (*sum6*, see (Figures 22 and 21)). On this typeday, the diversification of bids is particularly pronounced and underlines the presented findings.

Regarding to the problem size, solver parameters and computational performance, we found the following configuration to be suitable. In its reduced form, the problem for a single type day and risk strategy has 720,000 restrictions (inequality/equality), 560000 variables (230000 binary), and 2,000,000 coefficients. The problem was implemented in GAMS and solved with the CLPEX solver, applying parallel mode with 36 threads and a MIP gap of 0.01. Using a computer equipped with an Intel Xeon Gold 6248R (3.0GHz, 24 Cores, 48 Threads) and 64 GB RAM, the solution time with cold

²⁰This holds for the case that spot prices are higher than the variable costs. For the case that spot prices are below the variable costs, depending on operational restrictions such as minimum fuel consumption, the revenues for providing negative reserve must compensate for the unprofitable spot market operation of the minimum run capacity and the offered reserve volume. However, the revenues for providing of positive reserve must only compensate for the minimum run capacity.

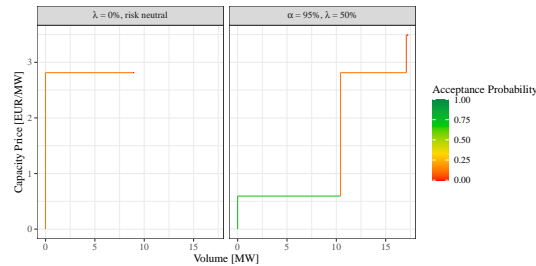


Figure 10: Reserve market (aFRRneg) bids for the time slice 12-16h for the risk-neutral strategy and for a risk-averse strategy ($\alpha = 95\%$, $\lambda = 50\%$), medium weekday transition season (tra2).

start amounts to roughly three hours for a single bidding strategy. However, providing the solver with the solution of a similar strategy (warm start), the solution time can be reduced to below 30 minutes for a single bidding strategy. Further, for days with strictly dominant markets (i.e., the spot market offers higher profit opportunities than the reserve markets), the solver determines within a matter of minutes. Sensitivity runs with only five instead of ten reserve price scenarios reduced computational more than proportionally. Considering the structure of the problem and the curse of dimensionality, this finding is intuitive.

5.4 Discussion

The results presented for the case study and the analysis of underlying bidding rationales allows to derive general conclusions with regard to decisions under uncertainty in the sequential electricity market context. The first conclusion we draw is that trading more and thereby taking a position at an earlier stage can reduce the risk significantly. Intuitively, placing reserve bids at low prices with high acceptance probability and selling generation on the day-ahead market sacrifices profit opportunities but secures revenues early on.

Measures to increase the expected profit and the associated risk exposure include (a) betting on high reserve prices, (b) betting on intraday prices higher than the day-ahead prices (no/few reserve bids, selling offers only at high price levels or even buying to go long on the day-ahead market), and (c) betting on intraday prices lower than the day-ahead prices (no/few reserve bids, selling offers at low price levels or even selling to go short on the day-ahead market). It can be concluded that the intraday market offers the highest risk, but also the highest reward, and that the main task of a trader is to balance these out by participating in all markets.

Therefore, a reasonable strategy appears to determine the operation decision based on the reserve and the day-ahead market results, but to not sell all generation capacity and flexibility on the day-ahead. In that way, one can profit from opportunities of higher or lower prices in the intraday market and the portfolio risk is reasonably hedged. However, the discussion remains without one strictly dominant strategy as this is no one-size-fits-it-all case. The faced uncertainties and the myriads of potential decisions in the markets require a sound decision support.

At this point, we critically reflect that further efforts can improve the developed approach in the future. On the one hand, the neglected reserve market segments as well as activation of reserve energy could be included to the approach. On the other hand, the representation of the intraday market as a single uniform pricing auction neglects arrival processes of prices in continuous trading

and therefore potential re-positioning profits. Finally, trading strategies for larger portfolios with the potential to change market prices should adequately account for the price effects of the submitted bids in each market segment. However, for the purpose of modeling the inter-related uncertainties and trading decisions in a complex setting as presented in this study, these simplifications are considered necessary to remain able to identify the central implications and to keep the model mathematically tractable.

6 Conclusions and Outlook

The developed methodology models the uncertainty related to the trading decisions of a trader on the day-ahead towards real-time on three decision stages (balancing reserve market, day-ahead spot market, intraday spot market) with the help of scenario trees and under conditional expectation. We present a multi-stage stochastic optimization approach that allows to determine optimal bids for the sequence of the reserve market, the day-ahead spot market, and the intraday spot market. Thereby, we consider all market segments that might appear as opportunities to each other.

The approach provides valuable insights with regard to profit distributions under uncertainty and allows for an extension of the target function to include risk. As the characterization of uncertainty contains much more information than a risk-neutral optimization (maximizing the expected value) can capture, we evaluate trading strategies with different risk preferences. An efficient frontier is derived as the set of optimal and non-dominated tuples of expected profit and risk exposure of the considered trading strategies. We discuss trading implications for the individual market segments, but most importantly for their interplay. Amongst others, the results lead to the conclusion that risk-hedging trading strategies prefer securing revenues on earlier stages and thereby being independent of the more volatile prices on the intraday stage. Risk can be effectively reduced by placing reserve bids on lower price levels and selling generation mostly on the day-ahead spot market. However, in that way potentially higher revenues in the reserve market and on the intraday stage are disregarded as they inevitably increase the risk exposure of the revenues. We provide new insights to short-term market decisions under uncertainty, that are interesting for several stakeholder groups, such as traders, policy makers, and research.

Taking the developed approach, next steps could go in the following directions. Firstly, traders may seek the commercial application to a real-world portfolio. This implies using portfolio-specific forecasting information distinct from the overall system renewable generation, and integrating fuel and carbon prices as well as scenario trees on a daily basis instead of using typedays.

Secondly, policy makers may be interested in the individual behavior of participants in short-term markets in extreme events, such as scarcity scenarios that push the system to the limits, or future electricity systems based on renewable generation. Such scenarios are not covered by our data and scope. However, coupling our approach with other electricity market models as well as insights from recent scarcity events (e.g., in France or Texas) offer a solid basis to model these uncertainties and to assess policy implications. Thirdly, electricity storage and sector-coupling with other energy carriers such as hydrogen may be included in the approach, interesting for both traders and scholars. This extension implies a temporal coupling and complicates the determination of optimal bids, particularly if considering reserve energy activation for storages.

Finally, an extension of the presented approach towards investment appraisal based on uncertain revenue streams from multiple markets appears to become more and more relevant. Especially considering the increasing necessity of flexibility and its optimal use for the energy system, all stakeholder groups are interested in methods to assess investment options more sound than based on established valuation approaches.

References

- Birge, J.R., Louveaux, F., 2011. Introduction to stochastic programming. Springer series in operations research and financial engineering. 2. ed. ed., Springer, New York, NY. URL: http://sub-hh.ciando.com/book/?bok_id=320411, doi:10.1007/978-1-4614-0237-4.
- Boomsma, T.K., Juul, N., Fleten, S.E., 2014. Bidding in sequential electricity markets: The Nordic case. *European Journal of Operational Research* 238, 797–809. doi:10.1016/j.ejor.2014.04.027.
- Brauns, S., Jansen, M., Jost, D., Siefert, M., Speckmann, M., Widdel, M., 2014. Regelenergie durch Windkraftanlagen: Abschlussbericht. URL: https://www.iee.fraunhofer.de/content/dam/iwes-neu/energiesystemtechnik/de/Dokumente/Studien-Reports/20140822_Abschlussbericht_rev1.pdf.
- Conejo, A.J., Carrión, M., Morales, J.M., 2010. Decision making under uncertainty in electricity markets. volume 153 of *International series in operations research and management science*. Springer, New York, NY.
- ENTSO-E, 2021. Transparency platform. URL: <https://transparency.entsoe.eu/>.
- EPEX Spot, 2021. Intraday market data. URL: <https://www.epexspot.com/en>.
- Fleten, S.E., Kristoffersen, T.K., 2007. Stochastic programming for optimizing bidding strategies of a Nordic hydropower producer. *European Journal of Operational Research* 181, 916–928. doi:10.1016/j.ejor.2006.08.023.
- investing.com, 2021. Stock market quotes & financial news. URL: <https://www.investing.com/>.
- Just, S., Weber, C., 2008. Pricing of reserves: Valuing system reserve capacity against spot prices in electricity markets. *Energy Economics* 30, 3198–3221. doi:10.1016/j.eneco.2008.05.004.
- Just, S., Weber, C., 2015. Strategic behavior in the German balancing energy mechanism: Incentives, evidence, costs and solutions. *Journal of Regulatory Economics* 48, 218–243. doi:10.1007/s11149-015-9270-6.
- Kath, C., Ziel, F., 2018. The value of forecasts: Quantifying the economic gains of accurate quarter-hourly electricity price forecasts. *Energy Economics* 76, 411–423. URL: <http://arxiv.org/pdf/1811.08604v1>, doi:10.1016/j.eneco.2018.10.005.
- Keles, D., 2013. Uncertainties in energy markets and their consideration in energy storage evaluation. volume 4 of *Produktion und Energie / Karlsruher Institut für Technologie, Institut für Industriebetriebslehre und industrielle Produktion u. Deutsch-Französisches Institut für Umweltforschung*. KIT Scientific Publishing, Karlsruhe.
- Keles, D., Genoese, M., Möst, D., Fichtner, W., 2012. Comparison of extended mean-reversion and time series models for electricity spot price simulation considering negative prices. *Energy Economics* 34, 1012–1032. doi:10.1016/j.eneco.2011.08.012.
- Klaboe, G., Fosso, O.B., 2013. Optimal bidding in sequential physical markets — A literature review and framework discussion, in: 2013 IEEE Grenoble Conference, IEEE. pp. 1–6. doi:10.1109/PTC.2013.6652371.
- Klæboe, G., Braathen, J., Eriksrud, A., Fleten, S.E., 2019. Day-Ahead Market Bidding Taking the Balancing Power Market Into Account. SSRN Electronic Journal doi:10.2139/ssrn.3434318.
- Kraft, E., Keles, D., Fichtner, W., 2018. Analysis of Bidding Strategies in the German Control Reserve Market, in: 2018 15th International Conference on the European Energy Market (EEM), IEEE. pp. 1–6. doi:10.1109/EEM.2018.8469903.

- Kraft, E., Ocker, F., Keles, D., Fichtner, W., 2019. On the Impact of Voluntary Bids in Balancing Reserve Markets, in: 2019 16th International Conference on the European Energy Market (EEM), IEEE. pp. 1–6. doi:10.1109/EEM.2019.8916455.
- Laur, A., Nieto-Martin, J., Bunn, D.W., Vicente-Pastor, A., 2018. Optimal procurement of flexibility services within electricity distribution networks. *European Journal of Operational Research* doi:10.1016/j.ejor.2018.11.031.
- Lingohr, D., Müller, G., 2019. Stochastic modeling of intraday photovoltaic power generation. *Energy Economics* 81, 175–186. doi:10.1016/j.eneco.2019.03.007.
- Möst, D., Keles, D., 2010. A survey of stochastic modelling approaches for liberalised electricity markets. *European Journal of Operational Research* 207, 543–556. doi:10.1016/j.ejor.2009.11.007.
- Narajewski, M., Ziel, F., 2020. Econometric modelling and forecasting of intraday electricity prices. *Journal of Commodity Markets* 19, 100107. doi:10.1016/j.jcomm.2019.100107.
- Ocker, F., Ehrhart, K.M., 2017. The “German Paradox” in the balancing power markets. *Renewable and Sustainable Energy Reviews* 67, 892–898. doi:10.1016/j.rser.2016.09.040.
- Ocker, F., Ehrhart, K.M., Ott, M., 2018. Bidding strategies in Austrian and German balancing power auctions. *Wiley Interdisciplinary Reviews: Energy and Environment* 7, e303. doi:10.1002/wene.303.
- Ottesen, S.Ø., Tomsgard, A., Fleten, S.E., 2018. Multi market bidding strategies for demand side flexibility aggregators in electricity markets. *Energy* 149, 120–134. doi:10.1016/j.energy.2018.01.187.
- Pandžić, H., Morales, J.M., Conejo, A.J., Kuzle, I., 2013. Offering model for a virtual power plant based on stochastic programming. *Applied Energy* 105, 282–292. doi:10.1016/j.apenergy.2012.12.077.
- Plazas, M.A., Conejo, A.J., Prieto, F.J., 2005. Multimarket Optimal Bidding for a Power Producer. *IEEE Transactions on Power Systems* 20, 2041–2050. doi:10.1109/TPWRS.2005.856987.
- regelleistung.net, 2021. Balancing reserve market data. URL: (provided jointly by the German TSOs) <https://www.regelleistung.net/ext/>.
- Russo, M., Bertsch, V., 2020. A looming revolution: Implications of self-generation for the risk exposure of retailers. *Energy Economics* 92, 104970. doi:10.1016/j.eneco.2020.104970.
- Russo, M., Kraft, E., Bertsch, V., Keles, D., 2021. Self-generation and the short-term risk management problem of electricity retailers. URL: www.iip.kit.edu.
- Thaler, R.H., 1988. Anomalies: The winner’s curse. *Journal of Economic Perspectives* 2, 191–202. doi:10.1257/jep.2.1.191.
- Uhlenbeck, G.E., Ornstein, L.S., 1930. On the Theory of the Brownian Motion. *Physical Review* 36, 823–841. doi:10.1103/PhysRev.36.823.
- Zheng, Q.P., Wang, J., Liu, A.L., 2015. Stochastic Optimization for Unit Commitment—A Review. *IEEE Transactions on Power Systems* 30, 1913–1924. doi:10.1109/TPWRS.2014.2355204.

A Annex

Nomenclature

Sets and Indices

H	hours of day
I	scenarios for reserve market
J	scenarios for day-ahead market
K	scenarios for intraday RES generation and intraday market
LDA	levels of price bids for Day-ahead (DA) market
LID	levels of price bids for Intraday (ID) market
LN	levels of capacity price bids for negative reserve (aFR-Rneg)
LP	levels of capacity price bids for positive reserve (aFR-Rpos)
QH	quarter hours of day
$QH(H)$	mapping of quarter hours to respective hours
$QH(TS)$	mapping of quarter hours to respective 4 hour time slices
RES	RES units in plant portfolio
TS	4 hour time slices of day
U	controllable units in plant portfolio

Parameters

α	probability level for VaR and CVaR
β^m	binary acceptance parameter of bids in market $m \in \{\text{aFRRpos}, \text{aFRRneg}, \text{DA}, \text{ID}\}$
κ^{var}	variable costs
λ	risk aversion weight parameter
$\nu^{\text{min/max}}$	minimum/maximum daily generation of controllable unit as share of baseload operation at P^U
$\phi^{\text{DA/ID}}$	day-ahead/intraday renewable generation forecast
$\Delta P^U/\text{RES}$	maximum load change of controllable/renewable unit within reserve activation time as share of P^U/RES
Δt	correction factor between quarter hours and hours
$BIGM$	sufficiently large number, e.g. 100,000
p^{min}	minimum load of controllable unit
p^m	market price of market $m \in \{\text{aFRRpos}, \text{aFRRneg}, \text{DA}, \text{ID}\}$
P^U/RES	nominal capacity of controllable/renewable unit
pr_ω	probability of scenario $\omega \in \{i,j,k\}$
$q^{\text{short/long}}$	maximum short/long position on Day-ahead or Intraday market as proportion of maximum selling volume on spot market

Variables

η	Value-at-Risk (VaR)
--------	---------------------

κ	cost
π	contribution margin
ρ	revenue
$x^{\text{sm,trade}}$	trade volume in spot market $sm \in \{\text{DA}, \text{ID}\}$, negative value represents buy volume
x^{imb}	imbalance volume to be covered by TSO, <i>BIGM</i> formulation to impose zero imbalance

Positive Variables

$\Delta x^{\text{m,U,+/-}}$	upward/downward (+/-) load change of controllable unit in market $m' \in \{\text{aFRRpos}, \text{aFRRneg}, \text{spot}\}$
s	auxiliary variable for <i>CVaR</i> modeling
$x^{\text{m,bid}}$	bid volume on price level in market $m \in \{\text{aFRRpos}, \text{aFRRneg}, \text{DA}, \text{ID}\}$
$x^{\text{rm,U/RES}}$	volume of $rm \in \{\text{aFRRpos}, \text{aFRRneg}\}$ provided by controllable/renewable unit U/RES
$x^{\text{dispatch,U/RES}}$	dispatch volume of controllable/renewable unit
$x^{\text{imb,+/-}}$	absolute value of positive/negative (+/-) imbalance volume
$x^{\text{sm,dispatch,U/RES}}$	dispatch volume of controllable/renewable unit addressed to spot market $sm \in \{\text{DA}, \text{ID}\}$
$x^{\text{sm,gen,bid}}$	sell bid volume for dispatch generation on price level in spot market $sm \in \{\text{DA}, \text{ID}\}$
$x^{\text{sm,gen,trade}}$	sell volume of dispatch generation in spot market $sm \in \{\text{DA}, \text{ID}\}$
$x^{\text{sm,long,bid}}$	ask bid volume on price level in spot market $sm \in \{\text{DA}, \text{ID}\}$ to get a long position
$x^{\text{sm,long,trade}}$	buy volume on market $sm \in \{\text{DA}, \text{ID}\}$ to get a long position
$x^{\text{sm,short,bid}}$	sell bid volume on price level in spot market $sm \in \{\text{DA}, \text{ID}\}$ to get a short position
$x^{\text{sm,short,trade}}$	sell volume on market $sm \in \{\text{DA}, \text{ID}\}$ to get a short position

Binary Variables

$\delta^{\text{sm,ask/sell}}$	auxiliary variable to ensure for one price level in spot market $sm \in \{\text{DA}, \text{ID}\}$ only either an ask or a sell bid
δ^{imb}	auxiliary variable for absolute value of imbalance
$\delta^{\text{m,U}}$	auxiliary variable for (potential) load change in commitment on market $m' \in \{\text{aFRRpos}, \text{aFRRneg}, \text{spot}\}$
$\delta^{\text{rm,U}}$	auxiliary variable for minimum load requirement of controllable unit provision of $rm \in \{\text{aFRRpos}, \text{aFRRneg}\}$
θ	auxiliary variable for <i>VaR</i> modelling

A.1 Highlights

- Application of multi-stage stochastic programming to trading on electricity markets.
- Consideration of expected value and (conditional) value at risk in target function.
- Trading strategies for reserve and spot markets under different risk preferences.
- Risk hedging by trading on the day-ahead, higher expected value on the intraday.
- Discussion of rationales for reserve market participation in a multi-market setting.

A.2 Modelling of Reserve Prices

For each season and reserve direction, a separate model is estimated from empirical data. As an example, Table 3 presents the coefficients, standard error and t-value of the robust estimation for the negative product in the transition season. The standard errors and t-values of all coefficients suggest high significance. The residuals of the estimation ϵ_t are considered as a stochastic process, which consists of three regimes: A base regime as well as a downward and an upward jump regime, with jump regime observations defined as observations more than two standard deviations away from the mean. Figure 11 presents the residuals of the conducted robust estimation for the negative product in the transition season.

Table 4 presents the residual standard errors to compare the used model configuration to less parsimonious ones. It can be observed that the overall model fits support the literature and the hypothesis that reserve prices are not completely explainable by the use of fundamental drivers as the residual standard errors are considerable. Yet, the model fit does not suffer significantly from only considering five explanatory variables (seasonal average, solar generation, residual load, lag 6, and a dummy for the distinction of weekdays and weekends). This observation remains valid for all seasons and both directions. Therefore, the stochastic residuals are estimated based on the parsimonious model configuration presented in Section 4.7.

Besides the distributional also the auto-regressive characteristics need to be modelled for the process to yield sound simulation results. Therefore, an Ornstein-Uhlenbeck process is estimated for the base and the jump regimes. Further, regime switching probabilities are derived from the historical data and used in a simulation of the stochastic residuals. Figure 12 presents the results of one simulation of the residuals.

In total, 1000 stochastic residual time series are simulated. These time series are used in the simulation of the reserve price scenarios for the respective type days. In accordance with Russo et al. (2021), three PV generation and coherent residual load levels are distinguished for each season and type of weekday, resulting in 18 type days in total. The levels of the exogenous variables and the stochastic residuals for the respective type day are fed into the additive model. Note, that the lag y_{t-6} enters the model as exogenous variable. To obtain a steady process with the stochastic components respected for accordingly, therefore the last step consists in simulating 15 days of each day type with the 1000 stochastic residual time series, respectively. Finally, the 1000 observations of the 15th day are clustered with k-means clustering ($k = 10$), to obtain the reserve price scenarios used in the stochastic optimization.

Figures 13 and 14 present the empirically observed values for the transition months and the scenarios derived from the stochastic modeling for the days with medium forecasts for PV generation and residual load. Note, that on the one hand, with variation to low and high levels the reserve price levels become more pronounced. On the other hand, especially days with steep ramps of wind generation are not modelled in the stochastic process but are well contained in the empirical data. The main purpose of the scenario generation is to derive typical days and consistent reserve price patterns. In a real-world application, one would use day-ahead forecasts for the exogenous variables instead of seasonal averages and their variations in upward and downward direction.

Table 3: Coefficients for robust estimation of negative reserve product in transition season. All coefficients are significant.

Coeff.	Value	Std.Error	t-value
c_s	2.250	0.316	7.130
β_1	0.469	0.085	5.550
β_2	-0.066	0.020	-3.355
β_3	-0.628	0.077	-8.195
β_4	0.679	0.016	42.725
β_5	4.508	0.478	9.436
β_6	-0.428	0.146	-2.944
β_7	0.076	0.037	2.056
β_8	-1.169	0.117	-10.001

Table 4: Goodness-of-fit of the additive reserve price models with residual standard error of the robust estimation as a measure for model fit for the used model, alternative 1 (carbon price as additional explanatory variable), alternative 2 (coal price as additional explanatory variable), alternative 3 (clean dark spread as additional explanatory variable), and alternative 4 (carbon price and coal price as additional explanatory variables). No significant improvement of model fit by including additional explanatory variables is observed. Required data for currency exchange rates, carbon and coal prices taken from EPEX Spot (EPEX Spot, 2021) and investing.com (investing.com, 2021).

Season	Direction	Used model	Alt. 1	Alt. 2	Alt. 3	Alt. 4
Winter	negative	0.372	0.356	0.372	0.358	0.383
Transition	negative	0.298	0.301	0.302	0.297	0.297
Summer	negative	0.383	0.390	0.373	0.408	0.372
Winter	positive	0.360	0.356	0.358	0.353	0.353
Transition	positive	0.576	0.563	0.546	0.550	0.560
Summer	positive	0.534	0.536	0.545	0.538	0.520

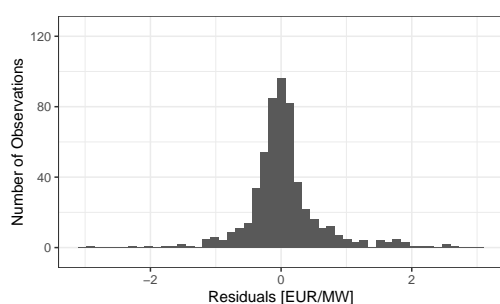


Figure 11: Residuals of the additive model estimation for the negative reserve product and transition season. The center, the outliers in upward direction and the outliers in downward direction are covered by the base regime, the upward jump regime and the downward jump regime, respectively.

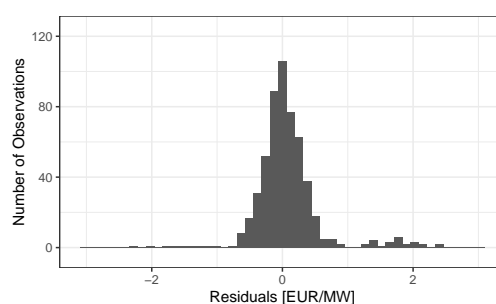


Figure 12: Residuals simulated with the stochastic process for the negative reserve product and transition season. The modeling yields a good fit to the distribution of the residuals in Figure 11. The strict definition of the regimes leads to a slight underrepresentation of values around two standard deviations away from the mean.

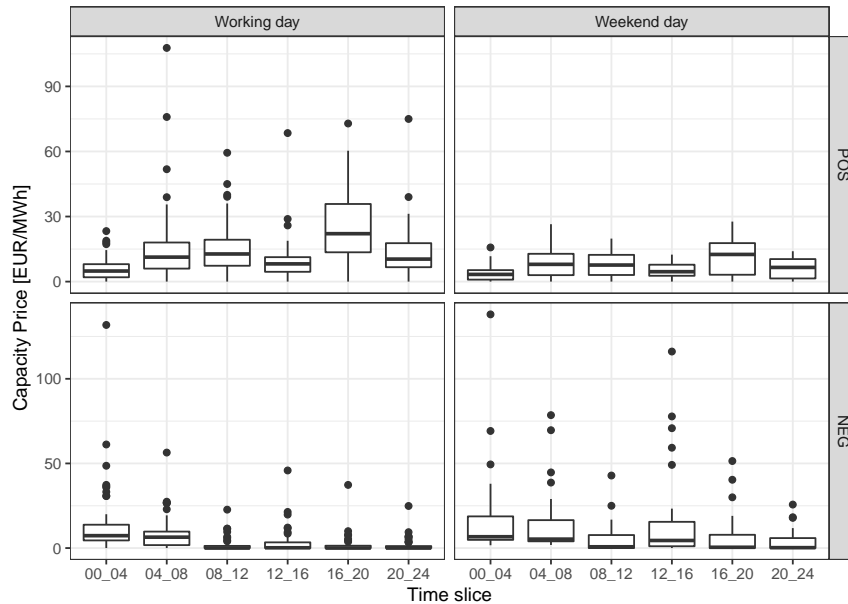


Figure 13: Boxplots of empirical reserve prices in the transition months of 2019, distinguished by reserve product and type of weekday ($n = 1092$).

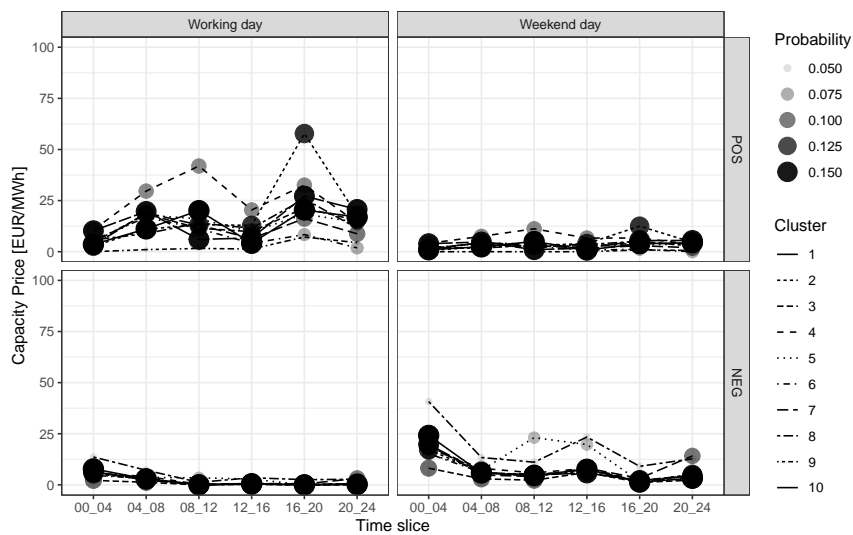


Figure 14: Scenarios derived from the stochastic modelling for the transition season on medium levels of PV generation and residual load, distinguished by reserve product and type of weekday. Reserve price scenarios for typeday *tra2* correspond to the left column.

A.3 Definition and Modelling of Risk

The VaR η is defined as the $(1-\alpha)$ -quantile of the contribution margin distribution, leading to the following definition for a discrete probability distribution:

$$VaR(\alpha, x) = \max \left\{ \eta : P(\omega | f(x, \omega) < \eta) \right\}, \quad \forall \alpha \in (0, 1) \quad (52)$$

with f the distribution of contribution margins, the deterministic parameters x and the stochastic parameters ω in probability space Ω . Including the VaR into the developed approach requires an extension of the model described in the previous sections. However, it is mainly a modification of the target function, two additional sets of constraints and auxiliary variables added to consider for the calculation of the VaR. The target function is augmented by the variable η , that corresponds to the VaR. The target of optimization is now the weighted sum of expected value and the VaR, with $\lambda \in (0, 1)$ as parameter for risk aversion (e.g. $\lambda = 0.2$).

$$\max \quad (1 - \lambda) \cdot \mathbb{E}_{(i,j,k) \in \Omega}(\pi_{i,j,k}) + \lambda \cdot \eta \quad (53)$$

All constraints from above remain unchanged. In addition, the following two constraints are included in the model. Parameter α represents the probability level of the VaR measure (e.g. $\alpha = 0.95$), $\theta_{i,j,k}$ is a binary variable equal to 1 if the contribution margin $\pi_{i,j,k}$ in scenario (i, j, k) is lower than η and equal to 0 otherwise. With the means of 54 and 55, we ensure that with a probability of $1 - \alpha$ percent the contribution margin is lower or equal η .

$$\sum_{i=1}^I pr_i \sum_{j=1}^J pr_j \sum_{k=1}^K pr_k \cdot \theta_{i,j,k} \leq 1 - \alpha \quad (54)$$

$$\eta - \pi_{i,j,k} \leq BIGM \cdot \theta_{i,j,k} \quad \forall (i, j, k) \in \Omega \quad (55)$$

The CVaR is defined as the expected value of the contribution margin in the $(1 - \alpha)$ worst cases of the distribution, or the expected value if the contribution margins fall below η , leading to following definition for a discrete probability distribution:

$$CVaR(\alpha, x) = \max \left\{ \eta - \frac{1}{1 - \alpha} \cdot \mathbb{E}_{\omega \in \Omega} \{ \max\{\eta - f(x, \omega), 0\} \} \right\} \quad (56)$$

with the Value-at-Risk η at α -level ($\alpha \in (0, 1)$), the deterministic parameters x and the stochastic parameters ω in probability space Ω . The main advantage of using the CVaR instead of the VaR, besides the coherence, consists in the consideration of so-called fat-tails in the distribution of contribution margins.

A.4 Exemplary Scenario Tree

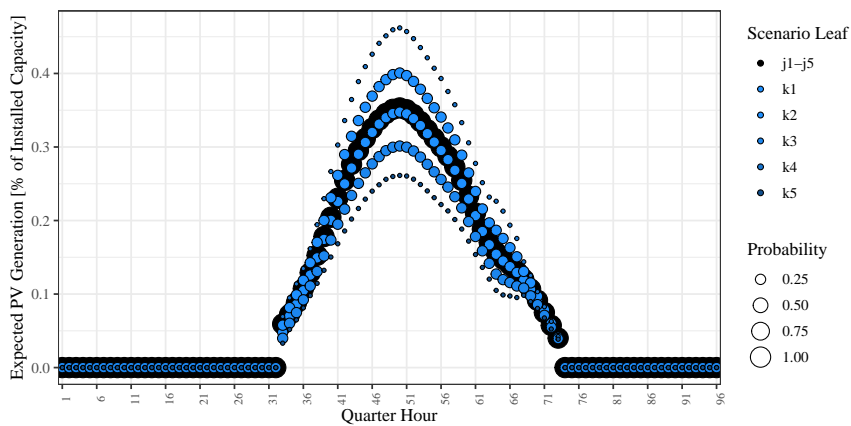


Figure 15: PV generation scenarios derived from the stochastic modelling for the transition season on medium level of PV generation (e.g., *tra2*). The scenario tree captures the daily pattern as well as forecast updates in the intraday stage.

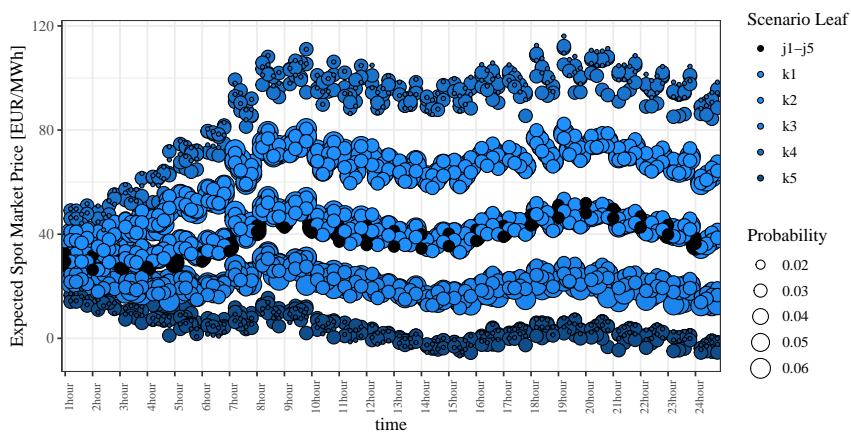


Figure 16: Spot price scenarios derived from the stochastic modelling for the transition season on medium levels of PV generation and residual load. The scenario tree is arbitrage-free and captures the daily pattern as well as the intra-hourly patterns of the quarter-hourly intraday prices.

Table 5: Quantitative results for efficient frontier under different risk aversion levels (λ) and different intervals considered for the risk metric CVaR (α). The columns $\Delta\mathbb{E}(\Pi)$ and ΔCVaR present the differences of the strategies with risk aversion in comparison to the according risk neutral optimization.

Risk metric	α	λ	$\mathbb{E}(\Pi)$	$\Delta\mathbb{E}(\Pi)$	CVaR	ΔCVaR
Unit	[%]	[%]	[EUR/day]	[EUR/day]	[EUR/day]	[EUR/day]
risk neutral	85	0	31033	-	-44220	-
CVaR	85	10	29805	-1228	-16457	27763
CVaR	85	25	25658	-5375	6781	51000
CVaR	85	50	24822	-6210	8897	53116
risk neutral	85	0	31033	-	-48410	-
CVaR	90	10	29130	-1903	-13701	34709
CVaR	90	25	25374	-5659	7259	55668
CVaR	90	50	24821	-6212	8611	57021
risk neutral	85	0	31033	-	-51295	-
CVaR	95	10	29274	-1758	-15965	35330
CVaR	95	25	25922	-5110	4708	56003
CVaR	95	50	24730	-6302	7936	59231

A.5 Additional Results

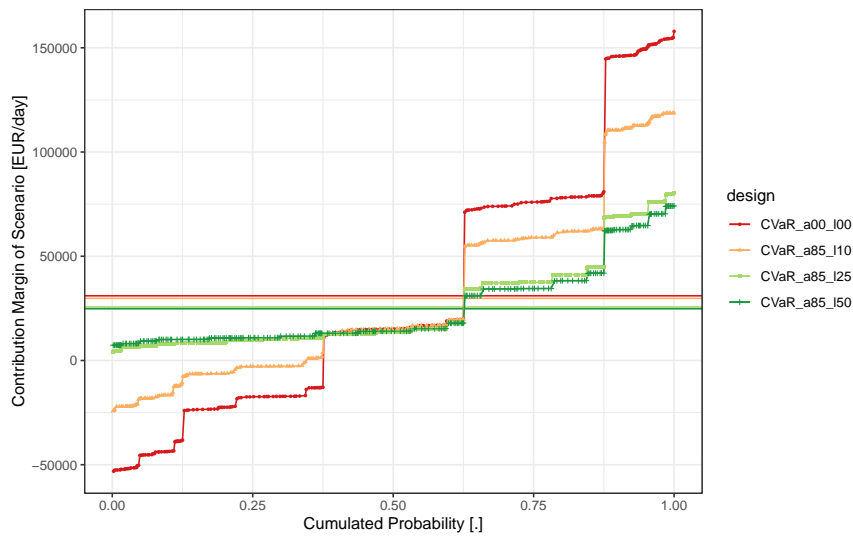


Figure 17: Empirical Cumulative Distributions of Contribution Margins throughout scenarios for trading strategies considering the $\alpha = 85\%$ level for the CVaR, medium weekday transition season (tra2).

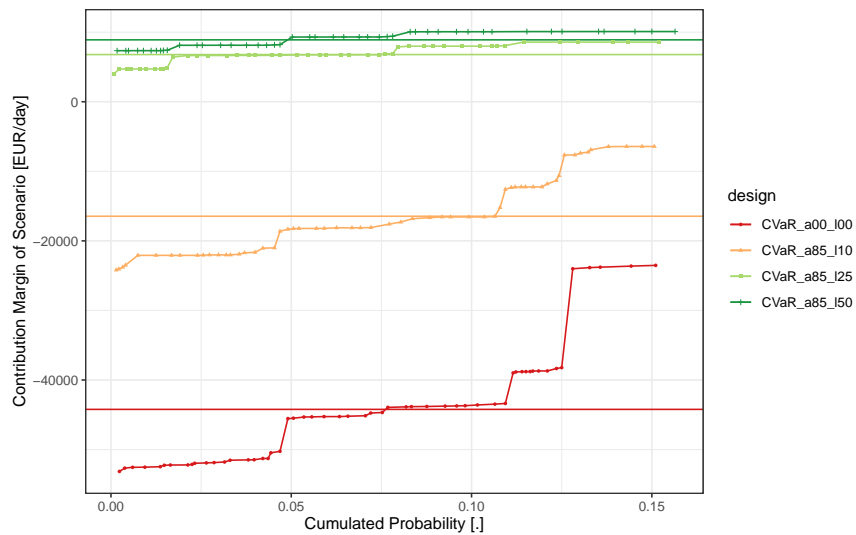


Figure 18: Empirical Cumulative Distributions of Contribution Margins in the 15 % of worst case scenarios (CVaR range), medium weekday transition season (tra2).

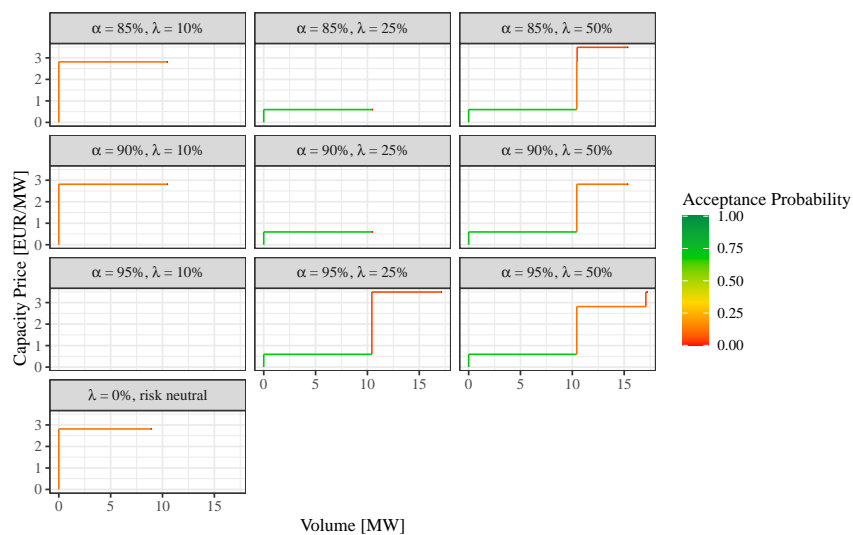


Figure 19: Reserve market (aFRRneg) bid curves for slice 12-16 for different levels of CVaR range (α) and risk aversion (λ), working day with medium residual load, transition season (tra2).

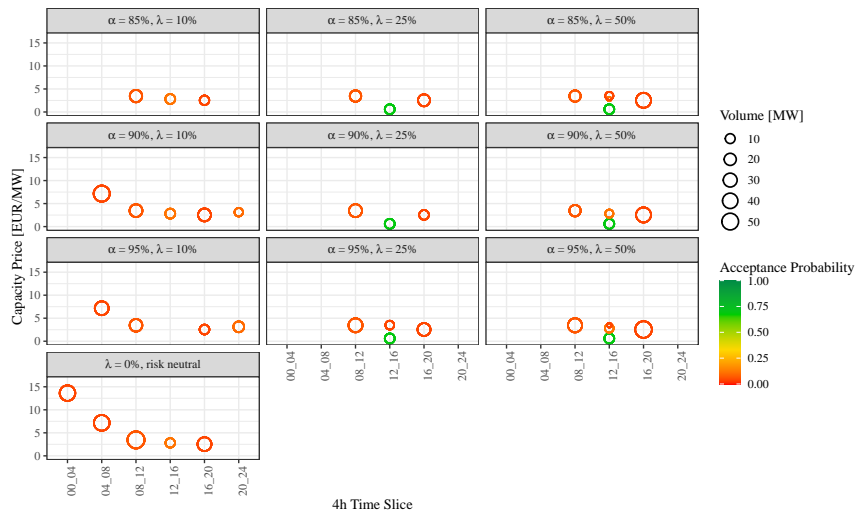


Figure 20: Reserve market (aFRRneg) bids for different levels of CVaR range (α) and risk aversion (λ), working day with medium residual load, transition season (tra2).

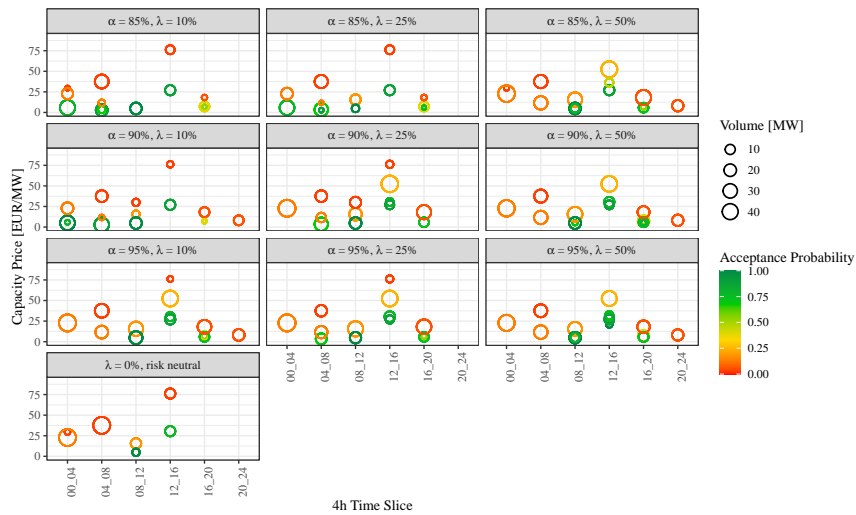


Figure 21: Reserve market (aFRRneg) bids for different levels of CVaR range (α) and risk aversion (λ), weekend day with high residual load, summer season (sum6).

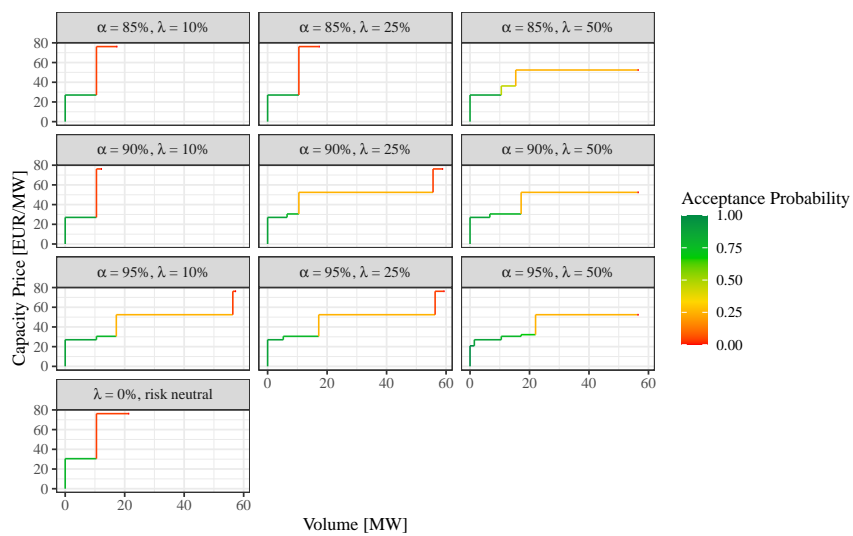


Figure 22: Reserve market (aFRRneg) bid curves for slice 12-16 for different levels of CVaR range (α) and risk aversion (λ), weekend day with high residual load, summer season (sum6).